

CLAY SHALE AND DISCONTINUOUS ROCK MASS STUDIES

being

A FINAL REPORT to the UNITED STATES ARMY

by

P.B. ATTEWELL and R.K. TAYLOR

GRANT NO. DA-ERO-591-72-G0005

REPORT DATED: 20 July 1973.

## CONTENTS

CHAPTER 1	Introduction	p 1.
CHAPTER 2	Slope Profiles in the Kimmeridge Clay, Yorkshire, England.	p 63.
CHAPTER 3	Field and Laboratory Investigations and Analyses pertaining to Chatfield Dam site, Littleton, Colorado.	p 91.
CHAPTER 4	Field and Laboratory Investigations and Analyses pertaining to Bloomington and Savage River (W.Virginia/Maryland) Dam sites with reference also to Curwensville Dam site	p 115.
CHAPTER 5	Mineralogical and Geochemical Study of Cucaracha Clay Shale Samples taken during a Field Investigation in the Panama Canal Zone	p 130.
REFERENCES		p 143.

CHAPTER 1

INTRODUCTION

The first part of this Report is devoted to a summary of the mineralogical, geochemical and technical properties of certain British and N.American clay shales that have been studied by the writers. The former two can be considered as intrinsic material properties which influence the geotechnical response of the shale and which therefore merit quite detailed laboratory and subsequent statistical analysis. It is true, however, that evidence as to the material stability is largely derived from samples that are small compared with the scale of the problem material en masse. As the size of the sample increases, the material stability parameters become more realistic and representative with respect to the problem on account of the increasing presence of macroscopic discontinuities which pervade such shales and which present to the rock mass its lower limiting strength. In any comprehensive stability investigation, therefore, the 'intact' mechanical strength parameters must be considered in the light of additional information concerning the spacial and orientation density distribution of the larger scale discontinuities. This point is also considered in the Report.

Subsequent Chapters are devoted to analyses of specific clay shale situations in Britain, the United States and Central America, the locations being visited by the writers during 1972.

1.1. Definition and nomenclature of weakly-bonded shales

Up to the present time it has proved extremely difficult to provide a comprehensive classification of soils that is acceptable to both the Geologist and to the Engineering Geologist. In fact it has proved impossible to group soils satisfactorily solely on the basis of their geotechnical properties.

Terzaghi (1936) was the first to attempt a classification for

clay soils and he proposed a three-fold division: i) soft intact clays which are free from joints and fissures, ii) stiff intact clays also free from joints and fissures, iii) stiff fissured clays. A consideration of the genetic and compositional characteristics of clays leads to Underwood's (1967) classification. Underwood pointed out that his two major groups of, 'soil-like shale' and 'rock-like shale' were not precise enough for Engineering Geological purposes. Thus he developed a table based on geotechnical properties in order that any clay (or clay-shale) could be evaluated. Bjerrum (1967) based his threefold classification on bond-strength, which he defined as follows: i) overconsolidated clays (i.e. overconsolidated plastic clays with weak or no bonds), ii) clay shales (i.e. overconsolidated plastic clays with well-developed diagenetic bonds) and, iii) shales (i.e. overconsolidated plastic clays with strongly developed diagenetic bonds). In his Rankine lecture (1967), Bjerrum described the Bearpaw shale (one of the North American examples studied in the current work) as, 'a highly overconsolidated clay with strong diagenetic bonds'.

Other terms often encountered in the literature which mean virtually the same as 'weakly bonded shale' are: overconsolidated clay shale (Scott and Brooker 1968), clay shale (Johnson, 1969; Fleming, Spencer and Banks, 1970) and stiff fissured clay (Chandler 1970). Scott and Brooker define an overconsolidated clay shale as: 'A sedimentary deposit composed primarily of silt - and clay-sized particles dominated by members of the montmorillonite group of clay minerals, and these deposits have been subjected to consolidation loads in excess of those provided by present overburden'. A similar definition was proposed by Fleming, Spencer and Banks (1970). They described clay shales as: 'materials of sedimentary origin composed largely of silt- and clay-sized particles, which may or may not be slightly cemented by foreign agents, such as iron oxide, calcite or

silica, and which have been subjected to consolidation loads greatly in excess of their present overburden loads'. However, they go further in explaining the effect of slaking and grain size on these rocks, such that: 'The material is composed principally of clay minerals and pieces of intact material tending to slake when exposed to cyclic wetting and drying'. Materials cemented to the extent that they do not slake when exposed to cyclic wetting and drying are termed siltstone or claystone, depending on particle gradation.

In the absence of a truly definitive classification, the term 'weakly-bonded shale' may be taken to mean an overconsolidated stiff fissured clay with a high proportion of constituent clay minerals.

#### 1.2. Consolidation and diagenetic considerations

In the speciality session No. 10, Mexico City 1969, held to discuss the meaning of the term 'clay-shale', Johnson rightly concluded that in this rather nebulous field, the only feature common to all definitions was the high degree of overconsolidation and all the other chemical and physical alterations which a sediment undergoes after burial. Bjerrum stressed the importance of diagenesis in the development of interparticle bonds within the sediments, and thus it is probably useful at this stage to consider the function that diagenesis plays in the development of a weakly-bonded shale.

The vertical loading of a sediment, as it becomes buried deeper in a sedimentary basin, causes a reduction in pore space which is accompanied by decrease in water content. At the same time, platy minerals begin to re-orientate themselves at right angles to the major principal (vertical) stress. A useful graphical representation of consolidation is provided by Fleming, Spencer and Banks (1970) who have combined graphs by Skempton (1964) and Bjerrum (1967).

Bjerrum's (1967) presentation included the formation of diagenetic

bonds which form during the period from which consolidation has been completed and to when erosion has not yet begun. The time lag between consolidation and erosion may be considerable, minerals having time to recrystallize under suitable temperature gradients, adhesion to be set up, or, for a cementing material to be precipitated in the intergranular spaces. Naturally, the stronger the bonds, the smaller the increase in water content on unloading, because the clay is unable to expand.

A quantitative assessment of the amount of energy taken up by the sediment during consolidation, was given by Brooker (1967). His procedure was to consolidate five remoulded samples of natural clay in a one-dimensional consolidation apparatus. He suggested that the stored energy had three components; i) work expended in consolidation (partially recoverable), ii) elastic deformation (recoverable on release of constraint), iii) work in the formation of diagenetic bonds (partially recoverable depending on the strength of bonds).

The loss in overconsolidation may be complicated by subsequent geological events. In Britain, Jurassic clay-shales are commonly affected by glacial phenomena (Chandler, 1970, 1972), the importance of which have probably been under-estimated in the past. An Upper Jurassic clay-shale which is thought to belong to the Ampthill Clay facies of Corallian age has been investigated in detail in a 60 m deep clay pit of some 14 years standing at Melton (British Grid Ref. SE 973 273; Figure 1.1).

In common with the other Jurassic clays it was deposited under marine conditions and was subject to uplift and erosion at the end of the Kimmeridgian (De Boer et al., 1958). In Albian times, the area was again submerged and remained so until the end of the Cretaceous. A second phase of erosion initiated in Tertiary times has continued until the present day - erosion has thus caused the clay-shale to outcrop under reduced cover.

A total original cover of about 720 m is probably a realistic estimate.

Within the clay-pit excavation, the strata are irregularly folded, the fold amplitudes varying from about 0.5 to 30 m (Plate 1.1.). The irregular distribution of the sharp folds tends to discount a tectonic origin; Kimmeridgian folds are very gentle flexures (De Boer et al 1958). Valley bulging, initiated during the Pleistocene, is a more reasonable cause.

The loss in over-consolidation may well be due in this case to three interacting factors, a) rebound or volume expansion on removal of load (recoverable strain energy), which will also give rise to jointing and fissuring, b) valley bulging, which has certain features in common with Peterson's (1958), 'time rebound', and c) the affinity of certain expandable mixed-layer clay components for water.

The contention which arises from workers such as Bjerrum (1967) and Brooker (1967) is to expand in the vertical direction, the changes in effective vertical stress are larger than those for the effective horizontal stress. Further, clays with strong bonds present considerable expansion; thus the horizontal effective stresses are less than those for weakly-bonded clays. The destruction of bonds, brought about by weathering processes will, therefore, lead to the development of high horizontal stresses in the weathered zone.

In the case of overconsolidated clays, Peterson (1954) shows that in situ horizontal stresses may be 1.5 times the vertical stresses, whilst Skempton (1961), working on the London clay found this ratio to increase from 1.5 at a depth of 100 ft. to 2.5 at 10 ft. Brooker (1967) concluded that clays with lower plasticity gave higher horizontal stresses than those clays with high plasticity.

It should be made clear that the absorption of large amounts of strain energy does not necessarily lead to the formation of strong diagenetic bonds. Bond formation appears to be a function of load duration, mineralogy, and no doubt it will also be under the influence of temperature.

The degree of overconsolidation can best be determined from one-dimensional consolidation tests. Three such tests were performed on specimens from the Melton brick-pit:

Test 1, Sample B<sub>4</sub> from 9.15 m below ground level

Test 2, Sample U<sub>3</sub> from 18.3 m below ground level

Test 3, as 2 but with bedding vertical.

A pre-consolidation load of  $4.0 \text{ kg/cm}^2$  ( $392.4 \text{ kN/m}^2$ ) was determined for sample B<sub>4</sub> and  $0.82 \text{ kg/cm}^2$  ( $80.4 \text{ kN/m}^2$ ) for sample U<sub>3</sub>. The pre-consolidation load equivalent to 610 m of missing Cretaceous is of the order of  $13,800 \text{ kN/m}^2$ . Sixty feet (18.3 m) of Amphill Clay ( $2.08 \text{ Mg/m}^3$  bulk density) represents a normal stress of some  $375 \text{ kN/m}^2$ . Very clearly this material has lost the greater part of its overconsolidation during its complex unloading history. The other specimen from 30 ft (9.15 m i.e. Figure 1.2) is overconsolidated with respect to its present depth within the excavation, but it may well have lost about 97% of its original pre-consolidation load.

It is pertinent to note that the virgin consolidation curves of the two specimens shown on Figure 1.2. run parallel to one another although their bedding planes are at right angles to each other. In line with Fleming, Spencer and Banks (1970) it may well be that the material is beginning to behave isotropically at the higher consolidation pressures, a feature which must be borne in mind when considering anisotropy of  $c'$  and  $\phi'$  shear strength parameters (considered later).

### **1.3. Anisotropy and shear strength of weakly-bonded shales.**

#### **1.3.1. Influence and character of discontinuities.**

Fissures, joints and other planar discontinuities are undoubtedly important in the response of these deposits to internal and external agents. Often they serve as pathways and concentrators for water percolating through the deposit, and thus accelerate the process of weathering and bond destruction. Peterson (1958) concluded that swelling in the Bearpaw shale at damsites in Western Canada was most probably



related to the intensity of slickensides within the deposit.

Skempton (1964) suggested that planar discontinuities acted as stress concentrators within a material, with the possible result of overstressing, and also pointed out that these planes of weakness could well have strengths at or near residual. Probably then, these planes could play a determining role in the progressive failure concept, but Bjerrum (1967) should be noted to the effect that potential failure by a progressive mechanism is not totally dependent on the presence of joints and fissures.

Up to the present time, experimental data has supported the contention that fissures influence peak strength. Skempton and LaRochelle (1965) concluded that peak strength in the London clay could be reduced by up to 30% by the presence of fissures. Both Peterson et al (1960) and Bishop (1966) found that the peak strength in large samples could be as much as 80% lower than the peak strength of small samples, on account of the greater number of fissures present in the former. Fleming, Spencer and Banks (1970) also obtained similar results for large and small samples from stratigraphic equivalents of the Bearpaw in America.

Skempton and Petley (1967) attempted a tentative classification of planar discontinuities and produced a four fold division; 1) Principle displacement shears 2) Relative shear displacements 3) Minor shears, and 4) Joint surfaces.

Group one consisted of landslides, faults and bedding-plane slips where strengths were at or very near residual. Group two were shear surfaces where more than 10 cm. of displacement had taken place. Minor shears made up group three, the criterion being displacement less than one centimetre; in this group the strength can be appreciably higher than residual. Joint surfaces comprised the last group. These features displayed a 'brittle-fracture' texture with little or no relative shear movement. Experimental data on this group implied that vertical joint

formation destroyed cohesion whilst reducing the friction angle  $\phi'$  by only a small amount. However, movements up to 5 mm. in distance were sufficient to produce residual strength conditions and to polish the joints.

Large scale planar discontinuities, as encountered in the field, include bedding planes, faults, unconformities and macrojoint patterns. These well-defined zones of structural weakness in weakly-bonded shale formations may be orientated in such a manner as to control the location of failure surfaces. Fleming, Spencer and Banks (1970) cite numerous examples where these major discontinuities have, in all probability, influenced slope failures in the Upper Cretaceous and Tertiary formations in America.

The directional strength properties of a clay shale are compounded from two physical phenomena. Intrinsic anisotropy is predominantly a function of the platy clay mineral orientation density distribution and by definition a fundamental requirement is that this distribution shall be concentrated in some preferred direction. Natural sedimentation processes satisfy this condition, but in laminated shales a natural fissility may be more a function of fine alternations of mineral species due to cyclic sedimentological regimes. A strain energy approach to the mechanical stability of intrinsically anisotropic fine-grained rocks has been proposed by Attewell and Sandford (1971) and a detailed evaluation of anisotropy with respect to laminae alternations has also been performed in these Laboratories. But, undoubtedly more important in the context of mass stability are the **terminated macroscopic discontinuities** which create planes of mechanical weakness in the mass through their lower shear strength parameters when the mass is required to respond to compressive stresses. Under tensile stress, the weakness of the mass is enhanced.

In any practical analysis, the intrinsic anisotropy problem will tend to be outweighed by the directional significance of the mass discontinuities even when any final failure plane passes through solid rock material. It will therefore be assumed that the discontinuities pose the dominant problem for the purposes of the discussion in this section.

### 1.3.2. Analysis of orientation density distribution of discontinuities

Rock mass stability becomes a problem issue in several areas of ground engineering. The most studied field concerns the stability of natural slopes and cuttings associated with road, river and canal transportation and with open pit workings. Attention here has either been directed towards the physical modelling of rather simplified discontinuous rock situations (for sample, Müller and Hofmann, 1970; Ergun, 1970; Rosenblad, 1970; Brown, 1970), or to theoretical analyses (including finite element - see, for example, Pariseau et al, 1970; Heuze et al 1971; Mahtab and Goodman, 1970; Bhattacharyya and Boshkov, 1970) which either acknowledge or ignore the discontinuous character of the mass, or to geometrical analyses using the stereographic projection (John, 1968, 1970 a, 1970 b; Kuznecov, 1970; Brawner, 1970; Londe et al, 1969), or to the construction of design charts which are based at least in part on an investigation of past failures (Hoek, 1970).

The stability of discontinuous rock in the vicinity of tunnel workings and deep excavations has been only sketchily investigated. In a somewhat similar manner, the competence of dam foundations in such rock - clearly a very important matter - has never been examined systematically; only when a problem has been anticipated has some form of analysis been attempted.

There is therefore a strong case for attempting to develop an analytical technique of universal applicability which, in a numerical way,

assesses the possibility of failure in such rocks and which gives full weighting to the apparent weakness of the discontinuity planes with respect to shear (and the solid elements, which terminate discontinuities, with respect to both shear and tension - see Jennings, 1970). The technique should make no a priori assumptions as to the spacial and orientation density distribution of the discontinuities - any stability analysis must operate on discontinuity data acquired from a geological survey of the rock structure. Furthermore, the technique must acknowledge the essential three-dimensional character of most ground stability situations. This rarely produces a relatively simple three-dimensional failure wedge such as has been popularly analysed by several workers.

A basic requirement involves the geological mapping of discontinuities in terms of their spatial orientation and lengths (for useful contributions on these points see Robertson, 1970; Piteau, 1970), an estimation of the principal stress amplitudes and directions so that the stresses can be resolved normal and parallel to the discontinuities, and an assessment of the shear strength parameters that control the stability. If all this information is available, then it is possible to analyse for stability on the basis of Coulomb-Navier-Mohr theory (see Jaeger and Cook, 1968) provided that data acquired with respect to global space is transformed to principal stress space through a knowledge of the directions in which the principal stresses act. Since there are several variables, the magnitude of none of which is known with any degree of certainty, it has been necessary to program the analysis for a digital computer and, in so doing, it is possible to increment each variable and to explore the sensitivity of each input parameter with negligible effort.

A fundamental requirement is the detailed acquisition of joint orientation data. This is laborious and must be done by hand (an appraisal

of more esoteric, stereoscopic techniques incorporating Fourier transform and spacial filtering methods for the isolation of orientation/linear data tends to rule them out on grounds of expense and information clarity) and inevitably a somewhat pessimistic picture is generated because many of the features are 'excavation induced' and are not likely to be present in the body of the rock where major instability might occur. Yet borehole exploratory methods (for example, see Ruth Terzaghi, 1965) become unreliable for orientations parallel or sub-parallel to the borehole axis. The least unsatisfactory approach would seem to be to measure at available exposures and necessarily taking in induced fractures on the basis of building-in a factor of safety for the discontinuities at depth.

The detailed concepts behind the analysis of discontinuity density distributions and the information presentation in fabric form have been outlined in a paper by Attewell and Woodman (1972). In this paper, it is shown that the standard hand-contouring method is inaccurate and it also indicates a means whereby the shear strain energy input to a rock mass subjected to triaxial stress can be computed and used as a deformability index parameter.

A problem lies in the estimation of the relevant principal stress amplitudes at points of interest. Where the loading is almost entirely generated through external constraints the estimates are seemingly a little more certain than they are when a self loading (e.g. slope or man-made embankment) situation is to be evaluated. Also, when the discontinuities are true joints, and are consequently continuous, the inherent problem is eased. The Monar Dam (arch dam founded on psammitic granulites in Inverness-shire, Scotland) meets these requirements and has been studied quite extensively in this manner, some of the details and analytical procedures having been outlined in the Interim Report. These analyses are not reproduced in this Final Report.

Where discontinuities are terminated by solid elements (viz, a lack of continuity), have a non-uniform distribution, and when a pore water pressure component should be written into the analysis (for example, in the case of a dam foundation), the choice of input parameters becomes much more difficult. Satisfactory specification of the operative stress field is particularly difficult in the case of earth and rockfill dams on such foundations, this problem being considered in a little more detail later in this Report.

Linear measurements in discontinuous rock masses.

Jenning's (1970) approach assumes a prior knowledge of the potential failure plane inclination. He expresses his joint continuity along this plane (line) in terms of the total lengths of discontinuities  $\sum a$  and the total length of solid element interceptors  $\sum b$ . The total line length is clearly  $\sum a + \sum b$  and he expresses a coefficient of continuity of the joints  $k$  as:

$$k = \frac{\sum a}{\sum a + \sum b}$$

A coefficient of discontinuity, representative of the solid element interceptors is:

$$(1 - k) = \frac{\sum b}{\sum a + \sum b}$$

If the overall shear strength parameters (composite joint and solid) are defined as  $c, \phi$ , then

$$\sum b(c_i + \sigma_n \tan \phi_i) + \sum a(c_j + \sigma_n \tan \phi_j) = (\sum a + \sum b) (c + \sigma_n \tan \phi)$$

$$\text{Thus, } c + \sigma_n \tan \phi = (1 - k)(c_i + \sigma_n \tan \phi_i) + k(c_j + \sigma_n \tan \phi_j)$$

(subscripts i and j refer respectively to intact elements and joints). If, with Jennings, we assume the strength of the intact elements to be acquired mainly through the intrinsic cohesion, we can replace the term  $(c_i + \sigma_n \tan \phi_i)$  with the parameter  $s_i$ .

Regrouping terms,

$$c + \sigma_n \tan \phi = \left[ (1 - k) s_i + kc_j \right] + k\sigma_n \tan \phi_j$$

It follows from this that the operative cohesive parameter

$$c = (1 - k)s_i + kc_j \text{ and the friction parameter } \tan \phi = k \tan \phi_j.$$

In his analysis of specific joint intercept patterns, Jennings introduces the concept of tensile failure to supplement planar shear. This required the introduction of shear and tensile continuity coefficients to supplement the earlier coefficients. Such complication may well be justified in the case of relatively simple, well-defined joint intercepting sets, but in situations where the factors possess a quasi-randomness in both orientation and length, the additional sophistication would be largely irrelevant. If we wish to retain the generality of the approach for ground engineering situations other than slopes, and in a three-dimensional setting, orthogonal line scans of fracture spacing would probably be adequate as a first approximation for allocating the most suitable shear strength parameters to the problem in hand. This approach has been adopted for slope situations in clay shales.

#### 1.3.3. Dam foundations in weak and non-continuously jointed material.

Most analytical procedures are directed to the stability of the embankment proper, and although there is usually a quite detailed geological and geotechnical appraisal of the foundation quality during the initial investigation stage, only very rarely in the case of an earth or rockfill embankment is the stability of the foundation investigated directly.\* It is assumed that the strength of the foundation material will not be exceeded by the applied shear stress and it is further tacitly assumed that a soil foundation remains within an elastic behavioural regime during deformation.+ If localised failure should occur - perhaps at points of stress concentration associated with discontinuities - the excessive strain

---

\* Finite element analyses of foundation stresses have been performed by Clough and Woodward (1967).

+ Degree of deformation does not affect the vertical pressure; horizontal pressures reduce with increasing foundation flexibility but they do increase near the toe of the embankment as a result of foundation deformations (results of finite element analyses - Clough and Woodward, 1967).

in such zones will raise a plastic condition and some load-shedding to other adjacent areas that were originally less highly stressed. In theory, therefore, the plastic zones within which limiting shear strength had been achieved could be specified by an iterative numerical technique, and those zones remaining elastically deformed could be determined by difference.

Unfortunately there is no practically acceptable method of plastic analysis applied to this problem, although numerical techniques in continuum mechanics can be used to investigate possible conditions of limiting equilibrium into the plastic state. On the understanding that earth/rockfill gravity dam foundations are unlikely to be over-stressed, the foundation mechanics can be investigated as an elastic problem.

Sherrard et al (1963) have traced some of the earlier attempts at elastic analysis and have pointed out the deficiencies in the approaches. All the analyses have approximated a dam to a triangular elastic wedge on a horizontal foundation, and this was the configuration (with  $3=1$  side slopes) adopted by Bishop (1952) and analysed by relaxation methods. Figure 1.3 reproduces this solution in terms of the distribution of major principal stress and maximum shear stress in the dam itself and in both dam and foundation respectively. The distribution of major principal stress, plotted in terms of the percentage of the overlying embankment weight, indicates that there is little error involved in assuming that the major principal stress is vertical and equal to the embankment weight, the error only increasing directly under the crest of the dam and at the toe. Thus, although there are errors in accepting this latter assumption, in order to avoid computational complexity, it seems reasonable to approximate the two-dimensional principal stress situation acting on any foundation discontinuity as  $\sigma_1$  vertical and  $\sigma_2$  acting in a horizontal plane normal to the axis of the dam. In a three-dimensional analysis of discontinuity stability,  $\sigma_1$  would



still be taken as acting vertically and its amplitude would be the product of the embankment height and the density of the placed fill. At the foundation contact with the fill, the minor principal stress could be approximated to the impounded water pressure and the intermediate principal stress acting along the dam axis could be approximated in amplitude by the summation of the other two principal stresses modified by some constant multiplying factor in order to preserve a plane strain condition within the  $\sigma_1, \sigma_3$  plane (Clough and Woodward, 1967).\*

A condition of stability or instability - is not directly dependent upon the absolute magnitude of the principal stresses but is a function of principal stress and cohesion ratio. However, if a cohesion parameter is to be used in the analysis, the absolute value of cohesion must be normalised to the absolute magnitude of the major principal stress. With respect to this latter, the problem then arises as to what value of density to take into the  $\gamma H$  product. On the upstream side of the dam, a buoyant density should be taken for a height up to top-water-level with the addition of a bulk (dry) density component from top-water-level to crest of the dam. The result of accepting these values would be to create a more nearly hydrostatic state of stress at the base of the dam with little deviatoric component to induce shearing. On the downstream side of the dam a saturated density below top water level could be taken and this together with a dry density up to crest-height would create a strong deviatoric component of stress at the foundation interface. This argument will be used subsequently in this Report for a simple analytical look at Chatfield dam foundation.

#### 1.3.4. Anisotropic shear strength parameters.

In terms of peak strength, planar anisotropy with respect to laminated rocks has been reviewed and investigated by the present writers (Attewell

---

\* Note that any analysis should strictly take account of incremental stress balances during the construction process during progress towards the final equilibrium stage.

and Taylor, 1971). The peak effective strength of weakly-bonded shales such as the Oxford Clay (Parry, 1972) was shown to be as low as  $\phi' = 21.5^\circ$ ,  $c'_p = 20 \text{ kN/m}^2$  when laminations were parallel to the plane of the shear box, or as high as  $\phi' = 33^\circ$ ,  $c'_p = 10 \text{ kN/m}^2$  when the laminations were at right angles to the direction of motion of the box. Slightly lower peak strengths have been obtained for sub-horizontal samples of Oxford Clay from Milton Keynes new town in this laboratory (Table 1.1.) and a similar range (though with generally higher cohesions) was obtained for the Ampthill Clay (visually very similar to the Oxford \*) from Melton clay pit (Figure 1.1).

Anisotropy of  $c'$  and  $\phi'$  for clay-shales is considered to be a macroscale rather than a microscale phenomenon (for example Barden, 1973). Perhaps the most marked feature of Table 1.1 is the fact that  $\phi'_p$  falls from values of over  $30^\circ$  to certain extreme values which are approaching residual. In essence, this behaviour is partly a function of the degree of degradation or weathering (Table 1.1), in that on a weathering scheme such as that of Chandler (1972) all the samples shown on Table 1.1 would fall within Zones II or III. In other words, the clay-shale is fissured and jointed at the best and comprises lithorelicts in an argillaceous matrix at the worst. For the brecciated Zone II Wothorpe borehole material Chandler quotes a  $\phi'_p$  of  $24^\circ$  ( $c'_p = 14 \text{ kN/m}^2$ ), but other samples tested in this laboratory (Table 1.2) imply that that peak  $\phi'$  of other Wothorpe samples can range from  $19^\circ$  to  $31^\circ$ . The Ampthill samples from areas in the clay pit where over-consolidation has largely been lost ( $U_2 \approx U_3$ ), and where the shale has weathered to flakey particles, give  $\phi'_p$  values as high as  $32^\circ$ , but with zero cohesion. In the shear-box, this material is behaving very much as a fragmental material (or an aggregate), which is not at variance with its visual description.

---

\* Liquid Limit = 70 (Oxford Clay)

Liquid Limit = 66-79; mean = 71 (Ampthill Clay).

Triaxial test parameters (Table 1.3) for the Amphill clay-shale show that the cohesion intercept is largely lost in this type of test. Measurements made on failed specimens demonstrated that the failure plane was invariably coincident with a preferred bedding plane.\*

If we are to consider the Amphill strength en masse it is reasonably clear that the maximum peak  $\phi'$  is within the range  $27-32^\circ$  with a minimum peak  $\phi'$  of  $16.5$  to  $17^\circ$ . More typical values within the range  $20$  to  $22.5^\circ$  can reasonably be expected. Because of the orientation of the bedding in response to flexuring it would be unwise to consider  $c'$  as a viable parameter. It is of interest to record that for shallow Kimmeridge clay-shale samples from Pickering the following peak parameters (triaxial) were obtained.

<u>Depth</u> <u>ft.</u>	<u><math>\phi'</math></u> <u>degrees</u>	<u><math>c'</math></u> <u>kN/m<sup>2</sup></u>
5 - 6	14	13.8
10 - 11.5	21.5	67
15 - 16	23	62

Here again, the Zone II type material gives reasonably consistent shear strength parameters, whilst the material at shallow depth which has attained a more fundamental grain size has a  $\phi'$  value which is probably no more than  $4^\circ$  higher than residual (Table 1.2).

For the Amphill clay-shale and the Oxford (Table 1.1),  $\phi'_r$  values in the range  $12^\circ$  to  $15^\circ$  are typical; and such values are in accord with Parry (1972). It will be noted however, that two values are only  $10^\circ$ . Until recently  $\phi'_r$  has been considered to be a constant strength parameter (compare horizontal

---

\* The bedding plane orientations are partly a feature of permafrost effects, mentioned later in the text. The lack of dilation could suggest that some movement might already have taken place in the field during the valley bulging stage.

and vertical samples in Table 1.1. for example). In the shear-box, the Amphill samples did not always approach a residual state due to the presence of projections (hard intact fragments of shale) on the slickensided failure plane. These accretion steps which have been discussed by Norris and Barron (1969), Gay (1970), tended to oppose motion on the shear surface. When such a phenomenon occurred the projections were removed after two or three reversals and the specimen allowed to consolidate.

In reality, particle size and shape is a major control on geotechnical behaviour. Grim (1962) pointed out the influence of grain size on Atterberg limits, in that with a decrease in particle size, the difference between the liquid limit and plastic limit increased. This is reasonable, because it would be expected that smaller particles, having a greater surface area, could retain a greater amount of water. For massive minerals, Kenney (1967) concluded that particle size had little influence on residual strength, but that particle shape did tend to have some effect. Aggregates of rounded particles produced smaller  $\phi'_r$  values than aggregates of sharp edged particles. Kenney concluded that most massive minerals behaved similarly, with  $\phi'_r$  varying from  $29^\circ$  to  $35^\circ$ , dependent on particle shape but independent of particle size.

With clay-shales however, we are considering aggregates of massive and platy minerals, and it is only when these aggregates breakdown to fundamental grains enabling reorientation, that a true residual is attained. This reasoning will be further developed in Chapter 4 in the context of the work by Mesri and Gibala (1971) who found that  $\phi'_r$  for certain Pennsylvanian shales was only  $11^\circ$  for completely disaggregated samples and cut specimens, whilst  $\phi'_r$  attained by shear displacement of the intact material was  $19^\circ$ . Development of a fundamental particle state in nature is very debatable in highly lithified shales (Taylor and Spears, 1970), but there is some evidence from work on the Amphill Clay (reported in this Chapter) that in weakly -

bonded types this state may be more readily attained.

We attempt to show throughout this Report that mineralogy has a very important role in influencing residual strength parameters. Mineralogy can vary dramatically (both vertically and laterally) and such changes may have a major effect on both peak and residual shear strength. Hutchinson (1969) shows that the Lower Gault Clay from Folkestone Warren has peak strength parameters of  $\phi' = 33^\circ$ ,  $c' = 18 \text{ lb/in}^2$  and residual parameters of  $\phi'_r = 12^\circ$ ,  $c'_r = 0$ . In comparison, the Upper Gault, which is lower in montmorillonite but higher in kaolinite, has peak parameters of  $\phi' \approx 53^\circ$ ,  $c' \approx 71 \text{ lb/in}^2$ , with  $\phi'_r$  being  $19^\circ$  ( $c'_r = 0$ ). A block sample of Lower Gault from the same site has been subsequently analysed in Durham. Unlike the original analyses, no free phase montmorillonite was detected (Table 1.4). This may well be caused by variation within the block sample itself. In so far as the Ampthill results are concerned it is significant to record that the sample with a  $\phi'_r$  of 10 degrees is from the upper part of the sequence where quartz is present in low concentration (Table 1.5).

From the above discussion based on experience with British clay-shales it is obvious that shear strength is a function of innumerable variables. However, the influence of mineral components on the short-term and long-term product of degradation will be illustrated by means of the Ampthill clay-shale at Melton clay pit.

#### 1.4. Mineralogical and geochemical aspects in relationship to geotechnical properties.

A simple two-fold division can effectively be applied to the mineralogy of the weakly-bonded shales under consideration. The dominant group comprises the clay minerals with the second group, the massive minerals, usually not exceeding 10% of the total. The latter comprises the non-clay minerals, the most common of which are the quartz, carbonates and feldspar.

There appears to be general agreement that mineralogy does have some role to play in influencing a material's geotechnical properties. However, there is some disagreement over its actual importance.

Grim (1962) noted that pure montmorillonites give the highest liquid limit values and Kenney's data (1967), with values for montmorillonites ranging from 620% to 1995% support this. Even within the montmorillonite group it appears that the exchangeable cation, held within the sheet structure, is significant. Lithium and sodium montmorillonites have greater liquid limits than have calcium or magnesium montmorillonites. A further observation by Grim was that introducing a second mineral, such as kaolinite, into the system in a concentration of 25% greatly reduced a montmorillonite's liquid limit, whilst the introduction of relatively small amounts of montmorillonite into a natural soil raised its liquid limit significantly.

For natural soils (Tourtelot, 1962; Kenney, 1967) there appears to be a general increase in liquid limit as the montmorillonite content in the soil increases (see Figure 1.4.)

The Activity Ratio of a soil, being the ratio of the plasticity index to the clay fraction (as a per cent weight of particles less than 2 mm in size), is a useful method for measuring the tendency of a soil to slake. Extremely fine sands have very low activity ratios (0.05). Clays very rich in kaolinite usually have an activity ratio between 0.20 and 0.10 whilst the value for illitic clays usually approaches 1.0. Bentonites have the highest activity ratio and Kenney (1967) quotes values between 5.8 and 12.0. Similarly, as with liquid limit, the exchangeable cation appears to be important, with sodium montmorillonite giving the highest values. With all the other factors constant, the tendency to slake, or disintegrate, increases as the activity ratio increases.

The ability of a material to absorb strain energy into its bonds is closely related to the degree of slaking that it undergoes on submersion.

Brooker and Ireland (1965) concluded that disintegration, as indicated by slaking, was a function of absorbed strain energy, and they suggested that strain energy was dependent upon clay mineralogy. Replotting their axial strain results against first, the ratio of quartz to total clay minerals, and second the ratio of montmorillonite to massive minerals leads to a tentative conclusion regarding the role of montmorillonite. It would appear that above 10% of the total mineral content, montmorillonite plays an important role in the absorption of strain energy. Further, it is useful to note that montmorillonite has a high capacity for absorbing great amounts of water with the result that montmorillonitic materials expand appreciably upon submersion in water.

Work by Kenney (1967) strongly supports the contention that mineralogy influences the residual shear strength of natural soils. He examined a great variety of monomineralic and multi-mineral component materials, together with a good cross-section of natural soils, including weakly-bonded shales. As mentioned earlier, he obtained  $\phi'_r$  values ranging from  $29^\circ$  to  $35^\circ$  for the massive minerals. There is a general trend, from high  $\phi'_r$  in the massive minerals, through illite \* ( $\phi'_r = 16^\circ$  to  $26^\circ$ ) and kaolinite ( $\phi'_r = 15^\circ$ ) to the montmorillonites ( $\phi'_r$  less than  $15^\circ$ ), which is very similar to trends obtained for variation of liquid limit and activity ratio with mineralogy. From his work on mineral mixtures, Kenney also showed an interesting relationship between  $\phi'_r$  and mineral 'A' content in a mixture of 'A' and quartz. Two different states for illite and montmorillonite arise from the effect of a sodium chloride pore solution. High concentration leads to flocculation, a phenomenon which seems to increase  $\phi'_r$  appreciably when the percentage of quartz is low. The quartz/unflocculated illite and quartz/kaolinite curves are approximately symmetrical whilst the quartz/montmorillonite and quartz/

---

\* These may well be hydro-muscovites, strictly speaking.

flocculated illite curves are strongly asymmetrical. Kenney concludes that the flocculation phenomenon is most probably related to an apparent increase in the ratio of wet clay minerals which flocculate to wet massive minerals, as opposed to the ratios of the two dry weights. On the other hand, the ratio of quartz/kaolinite and quartz/unflocculated illite are almost equal to their dry ratio weights. Plotting three examples of weakly-bonded shales on the graph - the Bearpaw, Pierre, and Cucaracha - shows that these at least tie in quite well with a quartz/sodium montmorillonite mixture indicating that sodium-montmorillonite has a great influence on their strength characteristics.

#### 1.5. Influence of mineralogy on short-term and long-term breakdown.

This aspect has been considered by Taylor and Spears (1970), and in more detail by the present writers (Attewell and Taylor, 1971). However, the rocks previously under investigation were largely highly indurated shales of Carboniferous age. The conclusions reached, however, were that the frequency of small-scale sedimentary structures such as bedding planes, laminations and other existing or potential discontinuities constituted one important control on immediate breakdown. The other two major controls were considered to be air breakage (i.e. capillary pressures developed on desiccation and saturation), and the content of expandable clay-minerals.

In the Ampthill clay-shale, valley bulging has produced superficial folds with consequent bedding plane separation, as well as promoting the opening-up and production of more discontinuities in the vertical plane. Fragmental material (sample CF, Plate 1.2.) with a mineralogy that is not unlike the less weathered parental materials (Table 1.5) is readily formed. Grice (1969) notes that many shales and mudstones disintegrate through a brittle stage into a silty clay. He also states that disintegration can take place at depth due to gentle flexing by tectonism ( in this case, valley bulging).



The slaking behaviour of the - 1/4 in, + 3/16 in B.S. fraction (Taylor and Spears, 1970) helps in the further understanding of the processes involved. The test results (Table 1.6) imply that, as in the Coal Measures shales, the percentage retention in vacuo is greater than the percentage retained in air. Air breakage (capillarity) is obviously an important control on the immediate breakdown of these weakly-bonded shales.

Breakdown is not completely arrested however, which raises the question as to what other mechanism (or mechanisms) are involved. Kennard et al (1967) concluded that solution of calcite cement was the principal cause of disintegration of shales at the Balderhead damsite. Recomputing their  $\text{Ca}^{2+}$  values as calcite suggests that only about 2.4% is present in un-weathered material, and only 0.4% in their slightly weathered shales. Calcite determinations on material used in the slaking tests (Table 1.6) shows no systematic relationship with the degree of breakdown.

On considering the expandable portion of the mixed-layer clay in the slaking test samples it is reasonably clear that this component is a factor which cannot be ignored - the two samples with the highest percentage show the greatest breakdown, the other two showing a much more restricted breakdown behaviour.

The exchangeable cations in the Amphill material point to  $\text{Na}^+$  and  $\text{K}^+$  being minor contributors (Table 5.2, Chapter 5). Comparison with Na-montmorillonite suggests that possibly about 9.0 to 9.5% montmorillonite may be present in the mixed-layer clay component of sample U7. Moreover the figure is unlikely to be more than 2.0 or 3.0 % in B4 and CF.

With respect to the two end-products of weathering (samples CF and CL) it is significant to note that the latter sample contains virtually no calcite and no pyrite (Table 1.5). Calcite is a very soluble carbonate, and moreover, reacts with the sulphuric acid produced by low temperature oxidation of pyrite. The clay-type end-product (CL, Plate 3) was customarily found

in parts of the pit subject to seepages from the overlying Red Chalk. The inference drawn is that unlike the older, indurated shales of the Coal Measures, oxidation of pyrite and solution of calcite with the formation of gypsum may well be a much shorter 'long-term' chemical process. Given sufficient time, therefore, it is not unreasonable to suppose that the initial fragmented clay-shale will ultimately be reduced to a fundamental state comprising a soft plastic clay.

On a comparative basis, hand-vane Cu values show that the fully weathered material beyond the liquid limit ( $\approx$  to CL) are about 21b/in<sup>2</sup>, whereas the more resistant flaky breakdown stage (CF) have Cu values within the range 3 to 6 lb/in<sup>2</sup> (Table 1.7). Using remoulded values as a guide to sensitivity implies that the very wet clay has a sensitivity of 1, compared with about 5 for the clay-shale itself.

#### 1.6. Comparative geochemical and mineralogical investigations (Gt. Britain and N. America)

##### 1.6.1. Introduction.

In order to demonstrate the salient features which differ in British and North American shales investigated by us to date, and before considering specific locations, particularly in the U.S.A., the data contained in Final Report DA-ERO-591-72-G0006 (Attewell and Taylor, 1973), will be drawn upon.

For this project a total of 60 samples (40 from sites in the U.S.A. and 20 from Britain), were analysed for 11 major elements. Geochemical analyses were performed with a Philips PW 1242 Automatic Sequential Analyser X-ray Fluorescence (XRF) machine. Apart from 1 sample from Chatfield Damsite - the clay seam material which is referred to in Chapter 3 - all the remaining N. American samples are detailed in Volume 2, Fleming, Spencer and Banks (1970). Of the British samples it is important to record that unlike the majority of those from N. America the former are generally from shallow depth, and hence are partially weathered in many cases.

They are, however, representative of foundation materials frequently referred to in the geotechnical literature and there is merit in considering the major, important differences between the clay-shales from the two countries. Suffice it to say that minor differences may well be a function of weathering.

Raw data of XRF analyses were processed by standard programs with an IBM 360/67 computer which listed elemental compositions in the combined oxide state (apart from sulphur).

Semi-quantitative mineralogical analyses were obtained using a Philips PW 1130 X-Ray diffractometer (XRD) and in all, 83 samples were examined. The total was made up of 29 N.American and 21 British samples examined in the normal state, and 28 N.American and 5 British samples examined after treatment with Ethylene Glycol solution, a technique used in the identification of expandable clay minerals.

#### 1.6.2. Investigations and results of the N.American samples.

Major element concentrations are given in Table 1.8. whilst Table 1.9 gives mean values and standard deviations for each element. Table 1.10 contains data on the ratios of six relevant oxides to alumina, a technique used in an attempt to reveal trends which can be assigned to clay minerals (e.g. Spears, Taylor and Till, 1971). For this purpose, free quartz as determined by XRD methods is subtracted from the total silica content as obtained by XRF analysis. Ratios of titanium oxide, sulphur, phosphorus pentoxide and manganese oxide against alumina are not included, since these elements are either deemed to be unimportant in clay minerals, or present in such low quantities as to be ineffective with respect to the trends. Table 1.11 and 1.12 comprise the results of semi-quantitative mineralogical analysis, and the mean value and standard deviation for each mineral identified.

Total silica content, excluding two extremely carbonaceous samples (ranges given in this Section automatically exclude these samples), ranges

from a minimum of 55.73 per cent to a maximum of 72.03 per cent (Table 1.8). Undoubtedly, free quartz within the sample exerts a great influence on total silica content, but nevertheless, the total silica values show a high degree of correlation with alumina content, which varies from 12.49 to 19.84 per cent (Table 1.8). The coefficient of positive correlation ( $r$ ) (Table 1.9) between total silica and alumina equals 0.6260, (where  $r = 0.4896$  for 99.9 per cent confidence level - highly significant) reflecting their combination in the sheet silicate minerals.

Total iron oxide (which includes both ferrous and ferric states) varies from 3.36 to 6.93 per cent in all but two carbonaceous samples. Its positive correlation with sulphur, which exceeds the 95 per cent (probably significant) level suggests that most of this iron may be present in the reduced ferrous state, combined with sulphur in the mineral pyrite.

The X-ray identification of pyrite in a number of samples, even though usually in very low concentrations, supports this contention. Most of the samples are from below the depth at which weathering can be expected, so it is unlikely that sulphate minerals play a significant part in geochemical considerations. No sulphates were detected by X-ray diffraction methods.

The calcium and magnesium oxide contents range from 0.26 to 4.32 per cent, and from 1.62 to 3.46 per cent respectively. The highly significant positive correlation between these two elements ( $r = 0.5950$ ) is reflected in the occurrence of carbonate minerals. Values for sodium oxide range from 0.45 to 1.88 per cent, and those for potassium oxide from 0.26 to 3.91 per cent. These two elements show a high degree of negative correlation ( $r$  equalling - 0.5777) and exceeding 99.9 per cent significance, which can be explained by their presence in two important clay minerals, montmorillonite and illite. Potassium is fixed by illites, whereas the most

probable site for most of the Na is in montmorillonite. It is pertinent to note that although the degree of correlation is just below the 95 per cent level for these two clay minerals, it is in fact a negative one ( $r = 0.3739$  for 28 samples, Table 1.9).

Titanium oxide, attributable to the mineral rutile, varies only slightly in concentration which ranges from 0.33 to 0.87 per cent. The majority of manganese oxide concentrations show little variation and all values are less than 0.05 per cent. Phosphorus pentoxide, is probably combined with calcium in the mineral apatite but is present in negligible concentrations reaching a maximum of only 0.22 per cent.

Examination of the data in Tables 1.11 and 1.12 reveals that variation in major element content, and in particular variation in oxide to alumina ratios (Table 1.10) is reflected by a great variation in mineralogy.

Of the massive minerals, quartz varies from zero to 43 per cent, although it was not detected in only two samples. Being the most abundant non-clay mineral it shows high negative correlations (both times exceeding the 98 per cent significance level), with the combined silica to alumina ratios and total clay mineral content. Calcite, a non-detrital mineral by definition, only occurs in four samples, and its measurably high concentration in one Fort Union sample suggests that this is a result of fossil remains. The only other carbonate minerals detected were dolomite and siderite, both showing very low concentrations such that only the former exceeds 1.0 per cent. Pyrite occurs in the Bearpaw formation, but never in high concentrations; in other formations it is relatively rare and in the Pierre samples was not even detected. X-ray diffraction background levels often preclude the detection of pyrite when it is an insignificant constituent.

The name 'shale' implies that clay minerals should be dominant over massive minerals, and this is true for all except one sample. The mean total clay mineral content at 74.31 per cent comprises approximately three-quarters of the total mineral content. In two samples, only clay minerals

were in fact detected whilst another seven contain more than 92% clay minerals. Montmorillonite is the dominant clay mineral present having a mean value of 36.24 per cent and standard deviation of 35.42, the high deviation being accounted for by the fact that the mineral is absent in seven samples whilst exceeding 92.0 per cent of the total in four others. It shows a highly significant correlation, exceeding 98 per cent, with the sodium-to-alumina ratios, whilst having a significant negative correlation with the corresponding potassium ratio (Table 1.12). This suggests that the mineral species is dominantly sodium montmorillonite and the geochemical considerations concerning the Na and K negative correlations for the 40 samples previously discussed would appear to be a logical interpretation. With a mean value of 23.25 per cent, mixed-layer illite-montmorillonite is the second most important clay mineral. Its high negative correlation with montmorillonite (exceeding 99.9 per cent significance), whilst having no correlation of significance to illite, could suggest that it owes its origin to the weathering of montmorillonite at some stage in the latter's history (for example Spears, 1971).

In the Claggett, Pierre and Bearpaw formations, illite is present in minor concentrations and does not exceed 9.0 per cent. However, in the Colorado and Fort Union groups it replaces mixed-layer clay as the most abundant clay mineral. Overall it has a mean of 11.6% and shows a negative correlation, exceeding 95.0 per cent significance, with the sodium oxide to alumina ratio suggesting that sodium is dominantly associated with montmorillonite. Unlike the other three clay minerals, kaolinite never attains great importance in any one sample, even though it is present in all but six samples. It is absent in five out of six of the Pierre samples.

Overall it has a mean value of 2.90 per cent and standard deviation of 2.25. It shows a highly significant positive correlation with illite (exceeding the 99.9% confidence level) and it is interesting to note that they occur together in all except seven cases.

To summarise the mineralogy of the American group it may be said:

- i) The samples contain a high proportion of clay minerals, the major part of which comprises the montmorillonite and mixed-layer illite-montmorillonite.
- ii) Illite and kaolinite occur together but usually only in minor concentrations.
- iii) Quartz is the major massive mineral present and may be accompanied by non-detrital carbonate minerals or pyrite, both of which make up only a very small part of the total content.

#### 1.6.3. Investigations and results of the British samples.

XRF analyses of the British samples are given in Table 1.13, with 1.14 giving the mean and standard deviation for each element or element oxide. Ratios for the relevant six oxides to alumina are given in Table 1.15 whilst Tables 1.14 and 1.16 provide data on the mineralogical analysis and the mean values and standard deviations for each mineral, together with correlation data.

Excluding samples with extremely high calcium concentrations, total silica varies from 45.12 to 55.61 per cent. The good, even distribution is reflected by a mean value of 50.85 per cent, very close to the median value.

Total silica shows no marked positive correlation with alumina but does correlate well with total iron oxide ( $r = 0.4582$ ; greater than 95 per cent, probably-significant level). Again, excluding samples with a high calcium content, alumina varies from 15.66 to 23.20 per cent, the mean at 19.87 per cent reflecting uniform distribution. Calcium displays a highly significant negative correlation with alumina and total iron oxide ( $r$  equalling  $-0.6721$  and  $-0.5949$  respectively; Table 1.14). The former most probably reflects the role of calcite and secondary gypsum (calcium sulphate) as massive minerals reducing the clay mineral content, (e.g. Table 1.16. ). Calcium oxide varies from 1.05 to 16.17 per cent. Despite the common occurrence

---

\* Micaceous minerals (illite plus mixed-layer clay) are shown under the general heading of illite.

of pyrite in the British samples, there is no significant correlation between total iron and sulphur, as was found in the case of the N.American samples.

This is not necessarily surprising in view of the presence of secondary gypsum in the Oxford Clay and Ampthill samples. This secondary mineral can be precipitated from groundwaters at depth (e.g. on the faces of coal cleat: Spears, Taylor and Till, 1971). Chandler (1972) has recently commented on its presence in Upper Lias material at depths which exceed the general depth of weathering. In other words, it may well be transported in advance of weathering and hence will mask geochemical relationships which are a function of primary minerals.

Total iron content ranges from 3.40 to 6.78 per cent, whilst sulphur is only present in relatively low concentrations between 0.65 and 2.80 per cent, the higher concentrations of the latter being related to the occurrence of gypsum (rather than pyrite) in several Oxford Clay and Ampthill samples.

A highly significant negative correlation,  $r = -0.5608$ , exists between the sodium and potassium oxides, but the correlation, although negative, is well below the lower confidence level when the results are rationalised in terms of clay minerals (i.e.  $Al_2O_3$  as denominator). Sodium oxide content varies from 0.10 to 0.68 per cent (Table 1.16) and potassium oxide from 2.53 to 4.15 per cent. There is thus a marked contrast with the American samples (Tables 1.8 and 1.9) where the much higher  $Na_2O$  values are a reflection of montmorillonite content. Titanium oxide, which is attributable to the mineral rutile, only just exceeds 1.07 per cent as a maximum, and phosphorus pentoxide, attributable mainly to apatite, ranges from 0.06 to 0.24 per cent.

Mineralogical investigations revealed that quartz was present in all of the 20 samples examined, the maximum content being 26.0 per cent, the minimum being 3.5 per cent and the mean value being equal to 13.93 per cent.



It is the dominant massive mineral, usually being accompanied in much lower concentrations by carbonate minerals and pyrite. Calcite occurs in all but four samples, and in its highest concentrations reaching 23 per cent. It is controlled in the British sediments by the fossil content. Siderite was detected in only three samples, all from the Lias Clay, and in each case was present in low concentrations not exceeding 3.0 per cent. The Oxford Clay and its variation, the Ampthill Clay, were the only deposits containing gypsum, reaching a maximum content of 8.5 per cent. Pyrite occurs in 14 out of the 20 samples, but again is always an accessory mineral. However, in one of the Kimmeridge Clay samples it does reach a maximum of 11.0 per cent which is high even for marine shales.

The potassium oxide-to-alumina ratio (Table 3.16) displays a highly significant negative correlation,  $r = 0.7515$ , with the total clay mineral content, suggesting that potassic-rich clay minerals (micaceous types) are only present when the total clay mineral content is low. This contention is further supported by the highly significant ~~positive~~ correlation between the sodium-to-potassium ratios and total clay mineral content. Thus it can be inferred that when the clay mineral content is high, sodium is more common in the interlayer positions of the clay sheet silicate structures. Illite displays highly significant negative correlations with both magnesium oxide and total iron oxide ratios to alumina. The strong correlation between magnesium and iron partly explains this. It will be seen from Table 1.4 that vermiculite, which is an Mg-rich clay mineral (often with Fe substitution) has been identified in the Lias and Speeton samples. Parry (1972) records vermiculite in the Oxford Clay from near Bedford. However, in a shallow sample (PAR) from the latter author's collection, there is no obvious vermiculite present. Because this sample is from less than 3 m in depth, the mineral may well have been decomposed 31 during weathering. Vermiculite and expandable smectites (montmorillonites)

are variously recorded in a wide spectrum of British Jurassic and Cretaceous caly-shales (see collation by Perrin, 1971).

It is important to record that mixed-layer clay, which appears as a tail on the low  $2\theta$  side of the  $10\text{ \AA}$  mica reflection, was recorded in all the samples studied in the current work. It accounts for a considerable proportion of the Gault specimen, the Ampthill materials (see Attewell and Taylor, 1972) and samples B604 and B626 (Oxford Clay). Apart from the Ampthill material, very little expansion occurred when the other samples were subjected to glycolation. This could be due to the technique used, but the more likely explanation is that non-expandable mixed-layer clay is not uncommon in these Jurassic and Cretaceous sediments. Brown (1961, p.280) shows that chloritic minerals (Mg-Fe clay minerals) may be a component of mixed-layer species. This particular aspect requires further consideration, and improvement in glycolation techniques are currently being investigated. It is of interest to note that glycolation was successful with the N.American samples and both montmorillonites and mixed-layer mica-montmorillonites were identified and quantitatively differentiated with little trouble from  $10\text{ \AA}$  mica (illite) - see Table 1.11.

The following conclusions can be drawn with respect to the mineralogy of the British samples.

- (1) Total clay content comprises very nearly three-quarters of the total sample.
- (2) Illite first and then kaolinite make up the bulk of the clay mineral content, with expandable clay and mixed-layered clay (with the exception of the Lias and Ampthill Clays respectively) being rare.
- (3) Quartz is almost always the major massive mineral but may share its importance with calcite in one or two cases.
- (4) Siderite and gypsum are absent in all except the Lias and Oxford Clays respectively, whilst pyrite is common in all samples, generally at low concentrations.

#### 1.6.4. Comparison of geochemical means.

Because of the precision of X.R.F. geochemistry it is more realistic to use major elements and not mineralogy for a direct 'mass' comparison of the composition of British and North American weakly-bonded shales. It is pertinent to compare 46 of the latter samples (i.e. selected samples from Fleming *et al.*, 1970 Vol. 2 and Chatfield damsite) with the 20 British samples (Table 1.18).

Although a t-test is simply a comparison of means this type of statistical exercise helps to elucidate major differences which, with the aid of previous mineralogical discussions lends considerable weight to tentative conclusions which have already been drawn.

The higher total silica in the North American sediments is a function of high quartz content, and the Dawson samples (see Chapter 3) included in this current analysis are also high in quartz. If total silica is higher in the North American samples then it is not surprising that alumina (clay minerals) will be lower (Table 1.18). MgO, which has both carbonate and clay-mineral affinities is probably significantly higher in the Upper Cretaceous/Tertiary rocks of N.America, but the other major carbonate oxide (CaO) is higher in the British rocks. The large standard deviation of CaO in the latter case is an expression of its non-uniform distribution in these clay-shales and this is itself a reflection of recrystallised fossil tests in the marine sediments.

Apart from a very small feldspar contribution both  $\text{Na}_2\text{O}$  and  $\text{K}_2\text{O}$  are useful indicators of clay-mineral type. Sodium is at a significantly higher level in the N.American clay-shales whilst  $\text{K}_2\text{O}$  is at a higher level in the British material. However, a more meaningful picture is obtained by rationalizing in terms of  $\text{Al}_2\text{O}_3$  (clay-mineral index) as denominator. In this case the  $\text{Na}_2\text{O}/\text{Al}_2\text{O}_3$  ratio is still higher in the N.American samples (0.08 as opposed to 0.02), but the  $\text{K}_2\text{O}/\text{Al}_2\text{O}_3$  ratio is virtually the same (0.16 N. America; 0.17 Gt. Britain). This would suggest that the mont-

morillonite component in the American shales is responsible for the greater participation of  $\text{Na}^+$  in the clay mineral components of these rocks. In contrast, the  $\text{K}_2\text{O}$  ratios suggest that illitic minerals (including mixed-layer clay) are important in both clay-shale groups, their importance not being restricted to the British shales alone.

$\text{TiO}_2$  is commonly found as rutile inclusions in clay-minerals (see Taylor, 1971) and hence this oxide may well be following clay-mineral content (as shown by  $\text{Al}_2\text{O}_3$  in Table 1.18).

Sulphur is present as both pyrite and gypsum in the British Sediments, whilst the previously mentioned good correlation with  $\text{Fe}_2\text{O}_3$  in the N. American clay-shales implies that it is combined as pyrite (albeit at a very low concentration) in these rocks. It is important to reiterate the fact that secondary gypsum may be precipitated well ahead of the zone of oxidation (weathering) and hence is not necessarily in direct relationship to the clay-shale in which it is found.

In the above analyses the X.R.F. data used are corrected for absorption and normalized to 100 per cent.

#### 1.6.5. General conclusions on comparisons between N.American and British samples.

Detailed examination of Tables 1.8 and 1.16 reveal that apparently minor variations in geochemistry are reflected in comparatively major variations in mineralogy especially within the clay mineral composition between the British and American groups.

The mean value for silica in the N.American group (28 samples) is almost 10.0 per cent higher than the British value. Moreover, the standard deviation of the former is 7.93 and 6.14 for the latter (i.e. for 15 samples). The explanation for this is given by comparing the relative content of free quartz in each group. The difference between the two mean values for free quartz is almost identical to the difference between the two mean values for total silica content; the mean values for

free quartz being 23.19 and 13.93 per cent for N.American and British groups respectively. The inference of this is that approximately the same amounts of combined silica for both groups is being used in the silicate structure of the clay minerals.

Alumina content in the British and N.American groups shows a significant variation. The mean values are 19.87 and 15.06 for British and N. American respectively, both having relatively low standard deviations (Tables 1.16 and 1.9). The result is a considerable difference in the mean values of the silica to alumina ratios, which equals 1.856 for the British and 2.45 for the American. Since total clay contents in both groups are very close to three-quarters of the whole, it follows that there should be a considerable difference in clay mineralogy, as is indeed confirmed by the results of the mineralogical investigation.

Whereas in the American group montmorillonite is the dominant clay mineral, it is replaced in the British group by illite\*, which also appears to be more widespread. Kaolinite is the second major clay mineral species in the British group and occurs in much higher concentrations, and is more widespread than in the American group, whilst kaolinite shows a highly significant positive correlation with illite indicating their occurrence together in the American group. Its role in the British group as a mineral replacing illite is reflected in a highly significant negative correlation. It is also important to note that vermiculite in the British group replaces montmorillonite as the expanding clay mineral type, and further it has a more limited distribution than montmorillonite, being restricted almost entirely to the Lias clay, in the samples investigated.

Quartz is the dominant massive mineral in both the British and N.American groups, although, as already mentioned, it is present in considerably higher concentrations in the latter. This may be partially

---

\* including relatively non-expandable mixed-layer clay.

explained by increased distribution and increased importance of calcite in the British group, possibly a reflection of fossil remains. The other carbonate minerals never achieve any real importance, and in both groups are relatively rare, dolomite not even being detected in the British samples. Pyrite is present in both groups but if anything is more common in the British samples.

The basic differences in the mineralogy of the British and American groups appear to be restricted to the occurrence and importance of different clay minerals in each group. It is well within order, on the basis of Kenney's work (1967), to assume that these variations could result in a difference in behaviour between those two groups in response to geotechnical experimentation.

#### 1.7. Geotechnical investigations of weakly-bonded shales.

##### 1.7.1. N. American material.

With one exception, all geotechnical testing carried out on the American material was performed by the U.S. Army Corps of Engineers in the United States. (only one American sample, from the Dawson formation, was tested in Britain by the writers who determined peak and residual shear strengths, together with Atterberg limits). Table 1.17 shows some geotechnical test results derived by the U.S. Army Corps of Engineers together with results for the appropriate samples which have been analysed for mineralogy and geochemistry at Durham.

Whereas most of the tests were carried out on a restricted number of samples, Atterberg limits were determined for all the 28 samples which have been analysed for mineralogy and geochemistry. Data for Atterberg limits have been supplemented by the results of Tourtelot (1962) and Scott and Brooker (1967), both of whom carried out their own mineralogical determinations.

A total of 19 samples were tested for residual shear strength but use has only been made of 7 results for, as already mentioned, Table 1.17 only includes results for which mineralogical and geochemical data are available. However, as the mean value of  $\phi'_r$  for 7 samples is  $5.14^\circ$  and the mean value

for 18 tests excluding one Fort Union sample is  $5.32^{\circ}$  it would appear that the 7 chosen are fairly representative of the whole. The range of  $\phi'_r$  for the 7 samples is  $3.05^{\circ}$  to  $6.85^{\circ}$ , which compared to Kenney's results for 'clay-shales' is rather low. His values range from a minimum of  $6^{\circ}$  to a very high maximum of  $28^{\circ}$ , and even his pure sodium and calcium montmorillonites show values of  $\phi'_r$  up to  $10^{\circ}$ , the lowest being  $4^{\circ}$ .

The liquid limit values display an extremely large range, from a minimum of 38 to a maximum of 204. Even within each formation there is a considerable range, and even the most consistent set of values (for the Claggett) has a difference of 15 between its maximum and minimum. The mean value of liquid limit for all 28 samples is 93, with a standard deviation of 41.0. As would be expected, the plastic limits are much lower than the liquid limit values but do, nevertheless, show considerable variation for this property, ranging from a minimum of 19 to a maximum of 34. The mean value is 22.5 with a standard deviation of 3. Liquid and plastic limits display a highly significant (exceeding 99.5 per cent confidence level) positive correlation with each other indicating that samples with a high liquid limit usually have a high plastic limit also.

1.7.2. British Material.

Data on peak and residual shear strength for a total of 16 British samples (Table 1.2) have been collated and, of these, 8 were determined in Durham, the remaining 8 being either extracted from the literature or obtained by personal communication with other workers.

Shear strength determinations were carried out in a 6 cm. square shear box at loads of 10, 25 and 40 lbs/in<sup>2</sup> at a displacement rate of .00048 in/min. The four Lias Clay samples, the Kimmeridge Clay sample 13/2, the Oxford Clay sample O.C. and the Speeton Clay samples 1 and 2, were all tested in Durham. Further, the two Oxford Clay samples B62<sub>h</sub> and B60<sub>h</sub>, the Ampthill Clay samples B<sub>h</sub>, U7, and B10, and the Kimmeridge

Clay samples were all tested in the same shear boxes under similar loads. Testing of the Oxford Clay sample, g.c. was tested by Hutchinson(1969).

Peak shear strengths for the British material range from a minimum of  $19^{\circ}$  to a maximum of  $33^{\circ}$ , whereas residual angles range from  $5.0^{\circ}$  to  $18.4^{\circ}$ , the latter having a mean value of  $12.36^{\circ}$  and a standard deviation of  $3.42^{\circ}$ . All of the values for the Lias Clay are below the mean value, the maximum for that material being  $11.3^{\circ}$ . Most of the other clay-shales have  $\phi'_r$  values somewhat above the mean.

Values for  $\phi'_p$  show a considerable degree of variation ranging from a minimum of  $16^{\circ}$  to a maximum of  $33^{\circ}$  with a mean value of  $24.8^{\circ}$ . With the exception of three samples, values of  $\phi'_p$  are considerably higher than the corresponding  $\phi'_r$ , inferring that the material is overconsolidated. The exceptions are: the Oxford Clay sample PAR, the Ampthill Clay sample B4, and the Kimmeridge Clay sample 13/2, the latter having less than  $1^{\circ}$  between peak and residual values.

Liquid and plastic limit results are only available for 8 samples, comprising 4 Lias Clay, one Ampthill Clay, one Kimmeridge Clay and two Speeton Clay samples. With the exception of the Ampthill Clay sample, all values of liquid limit do not exceed 60. The Ampthill clay has a liquid limit of 79 and all other values lie within the range of 49 and 57. The mean value for all liquid limit data is 56.5 with a standard deviation of 8.9. Values for plastic limit range from a minimum of 21 to a maximum of 30 with a mean value of 24 and a standard deviation of 2.7.

Values of  $\tau/\sigma$  (residual conditions) range from a minimum of 0.087 to a maximum of 0.333.

### 1.7.3. Discussion of the results for the British and N.American material.

Comparison of the data on the residual shear strength properties for both the British and American material (Tables 1.17 and 1.2) leads to two important conclusions. First, excluding one result obtained for a



Fort Union sample, the range of  $\phi'_r$  values obtained for the British material is far greater than the range of  $\phi'_r$  values obtained for all of the American material. The range for the American samples is from  $3.05^\circ$  to  $9.7^\circ$ , excluding the unusual maximum of  $24.4^\circ$ , whilst that for the British materials is from  $5.0^\circ$  to  $18.4^\circ$ . The second conclusion is that the mean value of  $\phi'_r$  for the British material is more than twice that value obtained for both the 7 American results and also nineteen of the American results. The mean value for all British results is  $12.36^\circ$  whilst it is  $5.14^\circ$  for the 7 American samples and only  $6.68^\circ$  for all results, including the Fort Union value.

Similar conclusions may also be drawn from comparisons of  $\tau/\sigma$  residual values obtained from British and American material. The ranges are from 0.087 to 0.333 with a mean value of 0.219, whilst the American values (for all except one result) range from 0.054 to 0.171 with a mean value for all results of 0.117.

Values of  $\phi'_p$  for the British and American groups reflect to a lesser extent the conclusions drawn from data on  $\phi'_r$ . The range for all of the American results, excluding the one Fort Union sample which has a peak value of  $29.5^\circ$ , is from a minimum of  $6.9^\circ$  to a maximum of  $19.0^\circ$ , whereas the British material ranges from a minimum of  $16^\circ$  to a maximum of  $33^\circ$ . Similarly, the mean value of  $\phi'_p$  for the British material is almost double that of the American material.

Comparison of data on the liquid and plastic limits of the British and American groups reveals considerable differences between the two. The mean value for the liquid limit of the American material is 93 whilst that for the British at 60 is approximately two-thirds of the American value. Further, the American values display a far greater range, from a minimum of 38 to a maximum of 204 compared with the British group's range of 49 to 79. These differences between the liquid limits of the two groups are also reflected, to a lesser extent, by the plastic limits.

The plastic limits of the American group range from a minimum of 19 to a maximum of 34 with a mean value of 22.5. The British material ranges from a minimum of 21 to a maximum of 30 with a mean value of 24 which in this case is higher than the equivalent value for the American group.

#### 1.8. Correlation and discussion of geological and geotechnical data.

Earlier in the Chapter, a brief summary of the state of knowledge of weakly-bonded shales, from the researches of some other workers, was presented. It has become evident that clay minerals could well play an important role in influencing certain geotechnical parameters, and in particular, the work of Kenney (1967), Scott and Brooker (1968) and Tourtelot (1962) suggested that clay mineral content type almost certainly influenced residual shear strength properties and the liquid limit of natural soils.

In this present Section the contentions held by the authors mentioned above will be tested against the results obtained for the British and American material. In addition, where data are available in the literature, the influence of clay mineralogy on other geotechnical properties, such as axial strain energy take-up and swell pressure, will be tested.

Figure 1.5 displays a plot of liquid limit against the percentage of total clay mineral content in the American samples. The points show a great deal of scattering from what appears to be a general increase in liquid limit as the total clay mineral content increase. Despite this general trend it would be extremely unwise to attempt any linear regression procedure as any 'best-fit' line would be totally unrepresentative of the extreme cases.

By plotting liquid limit against montmorillonite content (Fig.1.6) in the sample the trend is more convincing and although there are fewer points the amount of scatter is reduced. The Figure 1.6 plots can compare

with those in Figure 1.4. These two graphs clearly confirm that as the proportion of montmorillonite increases the liquid limit tends to increase also. Examination of Figure 1.7, a plot of liquid limit against the ratio of montmorillonite content to the massive mineral content, reveals another interesting point. It would appear that the increase in liquid limit is a function of the occurrence of montmorillonite at the expense of the massive minerals in the sample.

Kenney (1967) has already strongly stressed the importance of clay mineral content and clay mineral type on the residual shear strength of both mineral mixtures and natural soils. Figure 1.8 displays a plot of  $\phi'_r$  against the percentage total clay mineral content for a total of 12 American samples, all of which contain more than 50 per cent clay minerals (sensu stricto). From the field of points a general trend can be inferred, such that an increase in clay mineral content of approximately 10 per cent could well lead to a reduction of  $\phi'_r$  of one degree. On the basis of this trend, a minimum value of  $\phi'_r$  for American samples would be in the range of  $3^\circ$  to  $4^\circ$ , when the sample is composed entirely of clay minerals.

The equivalent plot for the British data is given by Figure 1.9 which also displays a similar trend. It is interesting to note that although all 14 points suggest the trend of an increase in total clay mineral content leading to a decrease in  $\phi'_r$ , two Lias samples do not appear to lie within the field of points. Further, all of the Lias samples fall within the same region of high clay mineral and low  $\phi'_r$ .

Figures 1.10 and 1.11 are both plots combining the British and American data. In Figure 1.10,  $\phi'_r$  values are plotted against the percentage total clay mineral content whilst in Figure 1.11,  $\phi'_r$  values are plotted against the ratio of total clay mineral content (logarithmic scale) to massive mineral content. From the first plot, it can be inferred that two trends are present, one lying above the other with a slightly steeper **41** gradient. Both trends suggest that an increase in clay mineral content

leads to a decrease in  $\phi'_r$ , the amount of decrease being subject to the trend to which the mineral belongs. The Lias material, (denoted by the symbol  $\star$  Figure 1.10) appears to span the two fields, with two points plotting with the steeper trend, composed entirely of British material, whilst the other two plot within the lower gradient trend which contains all of the American material. Moreover, 10 out of the 12 samples in the 'British' trend contain no detectable expandable clay mineral\*, whilst 13 out of the 14 samples in the 'American' trend do contain expandable clay mineral (denoted by the symbol  $\dashv$ ). Thus it may be concluded that the presence of an expandable clay mineral, namely montmorillonite, for the American material, has the effect of lowering the overall values of  $\phi'_r$ , but an increase in total clay mineral content also leads to a decrease in  $\phi'_r$  as borne out by both trends. The Lias material, which contains an expandable clay mineral (probably vermiculite), appears to be transitional between the British and American groups and, in a similar way to montmorillonite, the vermiculite may lead to an overall reduction in  $\phi'_r$ .

Figure 1.11, the plot of  $\phi'_r$  against the log of the ratio of total clay minerals to massive minerals for both British and American data, displays the two trends even clearer than in Figure 1.10. The conclusions drawn for Figure 1.10 are also pertinent here.

In examining the effect of the expandable clay minerals alone, it must be remembered that, from the conclusions drawn for Figures 1.10 and 1.11, non-expandable clay minerals do exert some influence on  $\phi'_r$  and so, in effect, the values of  $\phi'_r$  are not entirely a result of montmorillonite content. Figure 1.12 is a plot of  $\phi'_r$  against expandable clay minerals in the British and American materials combined. The fields of points display an approximate trend such that as the percentage of expandable clay

---

\* Mixed-layer clay is, however, common.

minerals increases so the value of  $\phi'_r$  decreases. Unfortunately, the majority of the samples contain less than 40 per cent of expandable clay minerals and the 'sensitivity' of  $\phi'_r$  to these component materials is apparently reduced for low concentrations. Before any firm conclusions can be drawn from Figure 1.12, samples with a greater range of expandable clay to massive mineral ratios require analysing.

TABLE 1.1. Direct Shear Box Results.

Sample	Initial moisture content %	Bulk Density lb/ft. <sup>3</sup>	Normal pressure lb/in. <sup>2</sup>	Peak shear strength lb/in. <sup>2</sup>	Residual shear strength lb/in. <sup>2</sup>	Brittleness Index %	$\phi'$ degrees	$c'$ lb/in. <sup>2</sup>	$\phi'$ degrees	$c'$ lb/in. <sup>2</sup>
U2	27		10	7.6	4.5	40.7				
U2	30		13.2	6.9	4.0	42.0				
U2	28	123	25.7	14.8	5.0	66.2	32	0	13.5	0.9
U2	26		25.7	15.6	-	-				
U2	27		38.2	24.6	11.5	53.3				
U9	-		13.2	11.4	-	-				
U9		120	20	15.7	-	-				
U9			38.2	23.1	-	-	22.5	5.9	-	-
B10		123	30	14.7	-	-				
B10			40	22.9	-	-				
U1N	27	123	10	10.1	2.5	75.2				
U6N	28	123	20	14.6	3.0	79.5				
U7N	-	125	30	20.3	7.5	63.1	27.0	5.6	14.0	-1.0
U7N	-		20	18.1	3.0	83.4				(0)
B4	25		10	10.2	2.5	75.5				
B4	24	130	20	12.2	4.0	67.2	16.5	6.9	14.0	0
B4	23		30	16.2	7.5	53.7				
B4N	23		40	23.6	-	-				
B4N	22	128	4.9	2.1	-	-	30.5	-1.0		
B4N	24		35	18.1	-	-		(0)		
U12	29	121	10	5.9	2.5	57.6				
U14	43	115	20	6.3	3.0	52.4	16.5	2.0	10	0
U14	41		30	11.9	6.0	49.6				

TABLE 1.1 cont.....

Sample	Initial moisture content %	Bulk Density lb/ft. <sup>3</sup>	Normal pressure lb/in. <sup>2</sup>	Peak shear strength lb/in. <sup>2</sup>	Residual shear strength lb/in. <sup>2</sup>	Brittleness Index*	$\phi'$ degrees	$c'$ lb/in. <sup>2</sup>	$\phi'$ degrees	$c'$ lb/in. <sup>2</sup>
<u>Composite for sub-horizontal specimens</u>										
<u>Oxford Clay</u>										
S2A			10	6.21	3.48	43.9				
S2B			25	15.44	4.86	68.5	28.0	1.16	14	0.27
S2C			40	22.45	10.82	51.8				
S3A			10	6.18	3.38	45.3				
S3B			25	13.34	6.90	48.3	18.0	3.77	13	1.02
S3C			40	16.36	10.34	36.8				
S1A			10	6.25	3.25	48.0				
S1B			25	12.11	6.82	43.7				
S1C			40	18.10	7.00	61.3	24	1.62	10	1.45
S1C'			40	21.00	11.02	47.5				
S4A			10	8.77	2.86	67.4				
S4B			25	13.08	6.86	47.6	28	1.97	15	0.19
S4C			40	25.26	10.88	56.9				

\* Brittleness Index =  $\frac{\text{Maximum shear stress} - \text{Residual shear stress}}{\text{Maximum shear stress}}$

N : Samples with bedding normal to shear plane

Note: Parameters by least squares regression

TABLE 1.2.

Geotechnical results for British material.

<u>Sample</u>	<u>Liquid limit</u>	<u>Plastic limit</u>	$\frac{\sigma'_p}{p}$	$\frac{\sigma'_r}{r}$	$\frac{\tau}{\sigma}$
Lias 1	57	23	23	11.3	0.207
2	55	26	31	9.5	0.167
3	57	25	19	6.5 - 7.0	0.113
4	52	24	22.5	5.0 - 7.0	0.087
B626			24	11.0	0.194
Oxford B604			28	15.0	0.268
PAR			21.5	17	0.306
Amphill B4	79	30	16.5	14	0.249
U7			27	14	0.249
B10			22.5	13.5	0.231
Kimmeridge 13/2	53	21	19.75	18.4	0.333
JLS			22.9	10	0.176
Lower Gault GC			33	12	0.176
Speeton SPC 1.	50	22	33	14	0.249
2.	49	22	29	13	0.231



TABLE 1.3.

Triaxial test (consolidated-drained) results.

Sample	Initial Moisture Content %	Bulk Density lb/ft. <sup>3</sup>	Cell Pressure lb/in. <sup>2</sup>	Stress difference lb/in. <sup>2</sup>	Linear strain at failure %	Volumetric strain at failure %	$\phi'$ degrees	$c'$ lb/in. <sup>2</sup>
B4	25	124	15	17.26	2.4	- 0.37	20	0.5
B4	24	124	30	30.30	4.9	- 0.31		
B4	23	125	45	51.75	6.2	- 0.43		
B4	25	125	60	64.75	6.1	- 1.03		
B10	26	125	15	13.85	1.7	- 0.24	17	0.75
B10	25	126	30	29.22	2.9	- 0.30		
B10	25	129	45	40.80	4.1	- 0.60		
B10	24	126	60	53.06	6.2	- 0.31		

TABLE 1.4 British Mineralogy (X-Ray diffraction)

<u>Depth</u>	<u>Sample</u>		<u>Total Clay</u>	<u>Mont/ Verm.</u>	<u>Illite &amp; Mixed-layer</u>	<u>Kaol.</u>	<u>Qtz.</u>	<u>Calc.</u>	<u>Gyp.</u>	<u>Siderite</u>	<u>Pyrite</u>	<u>TC/MASS</u>
	Lias Clay	1	86.5	10	47	29.5	8.5	5		4.1	3.5	6.10
		2	84	12	48	24	12	2.5		2	2.1	5.25
		3	76	8	42	26	10.5	4.5		1.5	5.8	3.16
		4	88.5	22	43	23.5	11	2.5			5.5	7.69
		5	96.5	18	52	27	3.5					27.57
29'-30.5'		6	89		53	36	8				3	8.09
13'-14.5'		7	78.5	20	30	28.5	15.5				6	3.65
9'-10.5'		8	93	25	55	23.0	6					13.28
4-4.5 m	Oxford Clay B604		73.5		57	16.5	22.5	3			6.8	2.77
4 - 5 m	B626		62.5		55	7.5	19.5	2			4.6	1.66
3 m	PAR		50		44	6	26	23	5			1.00
14 m	Amphill "	U1	77		61	16	15	1.5	5		1.5	3.34
9 m		B4	70		41.5	28.5	20.5		8.5		1.0	2.33
7 - 8 m		U7	74		44.5	29.5	11	8.5	5.5		1.0	2.84
5 m		B10	70		43	30.5	7.5	10.5	7.5		1.0	2.33
near surface	Kimmeridge "	JLS	81.5		68	13.5	15	5				4.40
7 - 7.5 m		13/2	58		53	5	12	10			11	1.38
near surface	Gault Clay		75		59.5	15.5	20	5 *				3.00
1 m	Speeton Clay 2		82	Trace	69	13	11.5	6.5				4.55

-40-

48

\* chemical analyses suggest that calcite is a major component in this material.

TABLE 1.5.  
MINERALOGY.

MAIN COMPONENTS OTHER THAN CLAY MINERALS  
(to nearest 0.5%)

SAMPLE	For horizon see Fig. 1.1.				Weathered materials	
	U1	B4	U7	B10	CF	CL
QUARTZ	15.0	20.5	11.0	7.5	8.5	10.0
PYRITE	1.5	1.0	1.0	1.0	1.0	0.0
GYPSUM <sup>(1)</sup>	5.0 <sup>(2)</sup>	8.5	5.5	7.5	8.0	5.0
CALCITE	1.5	0.0	8.5	10.5	7.0	0.5
	23.0	30.0	26.0	30.0	24.5	15.5

(1) From chemical analyses

(2) By X-ray diffraction

CLAY MINERAL PERCENTAGES

TOTAL	77.0	70.0	74.0	70.0	75.5	84.5
KAOLINITE <sup>(3)</sup>	16.0	28.5	29.5	30.5	32.0	23.0
10 Å ILLITE and MIXED-LAYER CLAY	61.0	41.5	44.5	43.0	43.5	61.5

(3) By subtraction

SHAPE FACTOR<sup>(4)</sup>

10 Å MINERALS	1.49	0.90	2.08	1.50	2.20	2.50
---------------	------	------	------	------	------	------

(4) Ratio width at half peak height  
to peak height.

TABLE 1.6.

SLAKING TEST RESULTS.

Sample	% retained on No.14 B.S. sieve	% retained in vacuo	% calcite in samples	Ratio expandable mixed-layer clay: mixed-layer com- ponent.
U7	53.8 53.1	88.6	11.9	12.5
B4	51.0	88.4	1.3	18.5
B10	72.0	86.0	11.0	negligible
CF	91.7	96.0	7.2	negligible

Aggregate (intact fragments) passing 1/4 in. sieve  
and retained on 3/16 in. B.S. sieve.

TABLE 1.7.

PILCON HAND VANE VALUES.

	<u>Cohesion</u>	
35° - 40° slope in fresh clay-shale	15 lb/in. <sup>2</sup>	103 kN/m <sup>2</sup>
42° " " " " "	10 "	69 "
Weathered, <u>in situ</u>	10 "	69 "
Fresh wet shaly clay	9 "	62 "
Weathered, undisturbed	8 "	55 "
Soft failed mass	7 "	48 "
Soft clay aggregate	6 "	41 "
Mud flow	2 "	14 "

TABLE 1.8 Geochemistry - N. American material

Sample	SiO <sub>2</sub>	Al <sub>2</sub> O <sub>3</sub>	Total iron oxide	MgO	CaO	Na <sub>2</sub> O	K <sub>2</sub> O	TiO <sub>2</sub>	MnO	S	P <sub>2</sub> O <sub>5</sub>	Total
Dawson	70.21	16.73	4.17	1.29	1.30	0.43	1.22	0.73	0.15	0.78	0.08	97.11
Claggett	1 60.13	14.01	5.48	3.21	2.02	1.35	2.58	0.75	0.03	1.05	0.16	90.55
	2 57.20	17.16	6.53	3.19	1.00	3.25	0.49	0.64	0.02	0.32	0.04	89.86
	3 61.24	15.12	5.07	2.75	2.57	2.51	2.49	0.79	0.03	1.14	0.11	93.84
	4 59.38	15.53	6.92	2.59	1.09	1.41	2.70	0.82	0.04	0.66	0.13	91.27
	5 58.85	15.88	6.89	2.35	1.06	1.77	2.65	0.83	0.04	1.37	0.12	91.79
	6 60.02	15.84	6.93	2.16	1.09	1.43	2.47	0.75	0.06	0.93	0.16	91.85
	7 60.97	16.58	6.67	2.15	0.65	1.49	2.41	0.80	0.06	0.99	0.11	92.89
	8 66.21	14.20	4.70	2.44	1.21	1.63	2.05	0.64	0.06	0.94	0.12	94.22
	9 24.30	5.24	2.12	1.04	0.73	2.61	0.00	0.49	0.06	0.01	0.12	36.72
	10 57.96	17.38	6.16	2.51	0.94	2.22	0.61	0.81	0.06	0.94	0.09	89.69
Pierre	1 61.47	13.87	5.58	2.57	1.75	1.37	3.10	0.70	0.16	0.58	0.10	91.25
	2 62.47	13.34	5.25	2.38	1.92	1.31	2.96	0.68	0.09	0.77	0.10	90.27
	3 64.25	14.89	3.85	2.84	1.63	1.35	1.25	0.59	0.03	0.29	0.05	91.02
	4 56.39	15.80	6.03	1.85	2.47	0.90	3.69	0.74	0.36	1.85	0.23	90.29
	5 60.84	13.77	6.40	2.42	1.23	1.38	2.85	0.71	0.15	0.26	0.09	90.10
	6 56.91	16.10	4.93	1.94	2.41	0.88	3.84	0.75	1.08	0.74	0.17	89.75
	7 69.61	14.02	4.96	2.45	0.83	0.84	2.56	0.59	0.06	0.00	0.08	96.01
	8 59.15	17.69	5.61	1.89	0.60	0.81	3.91	0.69	0.06	0.95	0.14	91.49
Bearpaw	1 60.84	15.96	6.00	2.09	0.87	1.33	3.49	0.81	0.05	0.97	0.12	92.51
	2 63.03	15.39	5.48	1.96	0.70	1.57	2.85	0.79	0.03	1.14	0.08	93.02
	3 63.08	15.20	5.26	2.05	0.70	1.8	2.67	0.77	0.03	0.96	0.08	92.58
	4 63.51	15.06	5.03	1.93	0.83	1.77	2.59	0.75	0.03	1.18	0.08	92.74
	5 60.20	15.72	6.15	2.19	1.10	1.88	2.98	0.78	0.04	0.85	0.09	90.98
	6 59.27	15.11	6.26	2.70	1.33	1.88	2.80	0.81	0.04	0.76	0.09	91.05
	7 62.71	15.21	5.55	2.05	0.70	1.77	2.61	0.78	0.03	0.99	0.08	92.54
	8 62.43	16.16	5.73	1.99	0.85	1.48	2.80	0.70	0.06	0.72	0.11	93.03

TABLE 1.8 cont....

<u>Samples</u>	<u>SiO<sub>2</sub></u>	<u>Al<sub>2</sub>O<sub>3</sub></u>	<u>Total iron oxide</u>	<u>MgO</u>	<u>CaO</u>	<u>Na<sub>2</sub>O</u>	<u>K<sub>2</sub>O</u>	<u>TiO<sub>2</sub></u>	<u>MnO</u>	<u>S</u>	<u>P<sub>2</sub>O<sub>5</sub></u>	<u>Total</u>
Colorado 1	65.36	14.11	3.79	2.28	1.40	1.25	2.76	0.73	0.03	1.64	0.16	95.51
2	55.73	19.84	4.57	3.44	1.81	3.41	1.25	0.72	0.03	0.57	0.15	91.52
3	63.67	14.53	4.12	2.63	1.99	1.81	2.31	0.69	0.03	1.44	0.15	93.35
4	62.63	18.02	3.90	1.73	0.55	0.84	3.64	0.87	0.02	0.51	0.13	92.85
5	65.12	16.62	3.70	1.74	0.42	0.87	3.43	0.84	0.02	0.58	0.16	93.50
6	68.71	18.46	3.44	1.62	0.26	0.62	0.26	0.85	0.06	0.52	0.13	94.92
Fort Union 1	56.78	14.34	6.10	3.27	3.76	0.59	3.24	0.76	0.09	0.31	0.13	89.71
2	64.02	16.96	3.52	2.34	0.61	0.45	3.39	0.72	0.03	0.13	0.02	92.17
3	60.14	13.24	5.55	3.46	2.41	0.56	3.88	0.65	0.09	0.25	0.09	89.89
4	59.85	18.06	5.05	2.56	0.61	1.47	3.54	0.85	0.04	0.22	0.15	92.40
5	60.60	17.01	6.35	2.02	0.54	1.47	3.42	0.82	0.03	0.05	0.99	92.40
6	64.20	12.49	3.36	3.24	4.32	0.84	2.60	0.56	0.06	0.20	0.18	89.05
7	34.10	5.99	7.09	1.16	0.93	0.97	2.24	0.33	0.06	7.76	0.10	61.03

Table 1.9

Significance of major element correlations in N. American samples

	<u>Total SiO<sub>2</sub></u>	<u>Al<sub>2</sub>O<sub>3</sub></u>	<u>Total Iron</u>	<u>MgO</u>	<u>CaO</u>	<u>Na<sub>2</sub>O</u>	<u>K<sub>2</sub>O</u>	<u>TiO<sub>2</sub></u>	<u>MnO</u>	<u>S</u>	<u>P<sub>2</sub>O<sub>5</sub></u>
Mean	60.071	15.005	5.268	2.327	1.332	1.455	2.594	0.721	0.085	0.870	0.137
S.Dev.	7.930	2.711	1.170	0.558	0.868	0.657	0.961	0.111	0.169	1.190	0.142
Var.	62.879	7.347	1.368	0.311	0.753	0.432	0.923	0.012	0.029	1.417	0.020
SiO <sub>2</sub>		→99.9%		→95%				→95%		→95%	
Al <sub>2</sub> O <sub>3</sub>								→99.9%		→95%	
Total Iron					→99.9%						
MgO											
CaO											
Na <sub>2</sub>							→99.9%				
K <sub>2</sub> O										→95%	
TiO <sub>2</sub>											
MnO											
S											
P <sub>2</sub> O <sub>5</sub>											

TABLE 1.10 Oxide/Alumina ratios in N.American samples

Ratios		SiO <sub>2</sub>	Na <sub>2</sub> O	K <sub>2</sub> O	Na <sub>2</sub> O	MgO	Fe <sub>2</sub> O <sub>3</sub>	CaO	MnO
		Al <sub>2</sub> O <sub>3</sub>	Al <sub>2</sub> O <sub>3</sub>	Al <sub>2</sub> O <sub>3</sub>	Al <sub>2</sub> O <sub>3</sub>	Al <sub>2</sub> O <sub>3</sub>	Al <sub>2</sub> O <sub>3</sub>	Al <sub>2</sub> O <sub>3</sub>	Al <sub>2</sub> O <sub>3</sub>
Claggett	1	2.0485	0.0963	0.1841	0.5232	0.2291	0.3911	0.1441	0.0021
	2	3.333	0.1893	0.0285	6.6326	0.1858	0.3805	0.0582	0.1165
	3	1.4841	0.1693	0.1646	1.0281	0.1818	0.3353	0.1699	0.0019
	4	1.7823	0.0907	0.1738	0.5662	0.1667	0.4455	0.0701	0.0025
	5	1.9238	0.1114	0.1668	0.6679	0.0667	0.4338	0.0667	0.0025
Pierre	1	2.7159	0.0987	0.2235	0.4419	0.1852	0.4023	0.1261	0.0115
	2	3.4865	0.0982	0.2218	0.4425	0.1784	0.3935	0.1439	0.0067
	3	4.2075	0.0906	0.0839	1.0800	0.1907	0.2585	0.1094	0.0020
	4	3.0816	0.0569	0.2335	0.2439	0.1170	0.3816	0.1563	0.0227
	5	2.2396	0.1002	0.2069	0.4842	0.1757	0.4647	0.0893	0.0108
	6	2.4726	0.0546	0.2385	0.2291	0.1204	0.3062	0.1496	0.0670
Bearpaw	1	2.1578	0.0833	0.2186	0.3810	0.1309	0.3759	0.0545	0.0031
	2	2.4450	0.1020	0.1851	0.5508	0.1273	0.3560	0.0454	0.0019
	3	2.9197	0.1171	0.1756	0.6666	0.1348	0.3460	0.0460	0.0019
	4	1.9926	0.1175	0.1719	0.6833	0.1281	0.3339	0.0551	0.0019
	5	2.8244	0.1195	0.1895	0.6308	0.1393	0.3912	0.1195	0.0025
	6	2.8239	0.0880	0.1853	0.6714	0.1786	0.4142	0.1244	0.0026
	7	2.2360	0.0499	0.1715	0.6781	0.1347	0.3648	0.0499	0.0019
Colorado	1	1.5705	0.0885	0.1956	0.4528	0.1615	0.2686	0.0992	0.0021
	22	2.8089	0.1718	0.0630	2.7280	0.1733	0.2303	0.0912	0.0015
	3	2.4893	0.1220	0.1589	0.7835	0.1810	0.2835	0.1369	0.0020
	4	1.6600	0.0465	0.2018	0.2397	0.0959	0.2163	0.0305	0.0011
	5	2.1552	0.0523	0.2063	0.2536	0.1046	0.2226	0.0252	0.0012
Fort Union	1	3.0166	0.0410	0.2253	0.1820	0.2273	0.4450	0.2614	0.0062
	2	1.7287	0.0265	0.1998	0.1327	0.1379	0.2075	0.0359	0.0017
	3	1.7477	0.0422	0.2930	0.1443	0.2613	0.4191	0.1820	0.0067
	4	2.6661	0.0813	0.1960	0.4152	0.1417	0.2796	0.0337	0.0022
	5	2.4162	0.0864	0.2010	0.4298	0.1187	0.3733	0.0317	0.0017



TABLE 1.11 Detailed Mineralogy of N. American specimens

Sample	Montmorillonite %	Mixed layer mont- morillonite-illite %	Illite %	Kaolinite %	Total Clay %	Quartz %	Calcite %	Dolomite %	Siderite %	Pyrite %
<u>Claggett</u>										
DH1 U1	56.0		3.3	2.1	61.4	32.6	2.7	3.3		
DH1 U20	98.0 *		2.0		100.0					
DH1 U57	56.0			1.8	57.8	38.8		1.3		2.1
DH2 U3	61.5 +11	"	3.0	3.8	68.3	31.7				
DH2 U14	65.6			6.1	71.7	28.3				
<u>Pierre</u>										
DH1 U2	71.0+		5.0		76.0	23.8		0.1	0.1	
DH1 U10	80.6+"	"	3.5		84.1	15.9				
DH1 U20	98.4*				98.4	1.6				
DH1 U23	92.4*				92.4	7.6				
DH1 U32		61.9		2.1	64.0	36.0				
DH2 U4		79.9			79.9	19.1				
<u>Bearpaw</u>										
DH1 U2		61.4	9.0	3.2	73.6	26.4				
DH1 U6	62.4+"	"	7.0	2.1	71.5	25.4				3.1
DH1 U17	76.2		2.5	2.6	81.3	18.7				
DH1 U20	10.0	52.6		1.2	63.8	33.5				2.7
DH1 U46	66.3+"	"	2.0	3.1	71.4	16.6		0.1		1.9
DH2 U5		79.9	1.5	2.0	83.4	16.6		0.1		
DH2 U14	60.3+		7.0	4.0	71.3	28.7				0.1
<u>Colorado</u>										
DH1 U5	25.0	15.4	11.0	2.0	53.4	43.2		0.1		
DH1 U6	58.2		37.0	4.8	100.0	0.1				
DH1 U7	57.6+		13.8	Trace	71.4	27.5	1.1	0.5		
DH1 U25		13.1	50.0	6.2	69.3	30.7				0.1
DH1 U29		7.9	55.0	7.8	70.7	29.3				
<u>Fort Union</u>										
DH1 U5	27.1		36.8	7.2	71.7	13.4	15.5			
DH1 U10	"	32.0"	30.0	3.3	65.3	34.7				
DH1 U12		2.8	33.6	4.7	41.4	37.0	18.5	3.4		
DH1 U17		68.3	15.0	5.0	88.3	11.7				
DH1 U22	20.0	"	47.0+"	4.8	80.5	19.5				

\* well ordered (high crystallinity)

+ poorly crystalline

" including mixed layer clay

TABLE 1.12 Significance of N. American sample mineralogy

	<u>SIAL</u>	<u>NAAL</u>	<u>KAL</u>	<u>NAK</u>	<u>MGAL</u>	<u>FEAL</u>	<u>CAAL</u>	<u>MNAL</u>	<u>TCML</u>	<u>KAOL</u>	<u>MONT</u>	<u>ILLI</u>
MEAN	2.445	0.093	0.185	0.797	0.157	0.347	0.104	0.010	74.336	2.898	36.243	11.643
SDEV	0.630	0.039	0.052	1.219	0.042	0.074	0.060	0.025	13.530	2.246	35.424	16.110
VAR	0.397	0.002	0.003	1.487	0.002	0.005	0.004	0.001	183.073	5.046	254.886	259.525
	<u>MXCM</u>	<u>QUTZ</u>	<u>TCQZ</u>	<u>LLIM</u>	<u>PLIM</u>							
MEAN	23.250	23.193	12.427	93.000	22.464							
SDEV	29.685	11.610	26.655	41.192	3.343							
VAR	881.190	134.795	710.494	696.786	11.177							

Correlation Matrix.

	<u>SIAL</u>	<u>NAAL</u>	<u>KAL</u>	<u>NAK</u>	<u>MGAL</u>	<u>FEAL</u>	<u>CAAL</u>	<u>MNAL</u>	<u>TCML</u>	<u>KAOL</u>	<u>MONT</u>	<u>ILL</u>
SIAL												
NAAL												
KAL												
NAK												
MGAL												
FEAL												
CAAL												
MNAL												
TCML												
KAOL												
MONT												
ILLI												
MXCM												
QUTZ												
TCQZ												
ILLIM												
PLIM												

TABLE 1.13 Geochemistry - British material

Sample		SiO <sub>2</sub>	Al <sub>2</sub> O <sub>3</sub>	Total iron	MgO	CaO	Na <sub>2</sub> O	K <sub>2</sub> O	TiO <sub>2</sub>	MnO	S	P <sub>2</sub> O <sub>5</sub>	Total
Lias Clay	1	52.07	20.66	6.19	2.03	3.80	0.56	3.13	0.96	0.03	1.29	0.22	90.94
	2	52.01	21.00	6.58	2.11	3.22	0.40	3.14	0.98	0.03	0.91	0.20	90.57
	3	51.46	21.42	6.70	2.17	3.41	0.45	3.11	0.95	0.03	1.47	0.20	91.37
	4	52.08	22.04	5.94	2.08	2.78	0.38	3.13	0.96	0.02	2.17	0.13	91.72
	5	47.82	22.96	6.41	1.73	1.57	0.52	3.14	1.04	0.15	2.80	0.14	88.28
Oxford Clay	B626	54.93	19.07	4.60	1.72	3.75	0.27	3.19	0.95	0.02	2.03	0.16	90.69
	B624	54.83	18.06	4.77	1.68	4.29	0.33	3.25	0.90	0.02	2.57	0.11	90.81
Pur	PAR	45.73	13.00	3.40	1.32	12.18	0.19	2.53	0.62	0.06	0.65	0.19	79.86
	OC1	54.65	17.24	5.66	1.83	15.44	0.29	2.82	1.07	0.08	0.74	0.24	
	OC2	50.32	21.60	4.35	0.95	5.18	0.43	2.98	0.86	0.16	1.04	0.14	88.07
Amphill Clay	B4	55.62	20.09	6.78	2.20	1.05	0.27	4.15	0.95	0.02	2.52	0.06	93.72
	U7	47.70	17.75	5.52	2.10	6.40	0.36	3.58	0.83	0.02	1.94	0.11	86.31
	B10	45.12	18.19	5.17	2.09	7.96	0.11	3.57	0.75	0.04	2.27	0.09	85.34
	AC7	48.11	18.61	6.18	2.08	5.16	0.10	3.69	0.85	0.03	2.30	0.08	87.19
Kimmeridge Clay	13/2	51.06	15.66	5.36	2.03	9.95	0.03	3.75	0.72	0.04	1.53	0.12	90.26
	JLS	50.32	21.60	4.35	0.95	5.18	0.43	2.98	0.86	0.16	1.04	0.14	88.00
Gault Clay (lower)		41.49	16.84	3.60	1.58	16.17	0.51	3.20	0.57	0.12	1.06	0.13	85.27
Speeton Clay	1	48.91	20.61	5.49	1.27	3.27	0.51	3.18	0.79	0.15	1.32	0.10	83.59
	2	50.63	23.20	6.47	1.33	2.53	0.68	3.22	1.02	0.14	1.48	0.09	90.79
	3	50.06	24.28	5.90	1.24	1.44	0.49	3.12	1.05	0.17	0.87	0.09	88.72

TABLE 1.14 Significance of major element correlations in British samples

	Total SiO <sub>2</sub>	Al <sub>2</sub> O <sub>3</sub>	Total iron	MgO	CaO	Na <sub>2</sub> O	K <sub>2</sub> O	TiO <sub>2</sub>	MnO	S	P <sub>2</sub> O <sub>5</sub>
MEAN	50.851	19.868	5.735	1.802	5.060	0.364	3.352	0.899	0.061	1.659	0.130
SDEV	3.738	2.318	0.915	0.362	4.359	0.166	0.384	0.121	0.063	0.626	0.051
VAR	13.970	5.373	0.838	0.131	19.002	0.027	0.147	0.015	0.004	0.392	0.003

Correlation matrix

SiO <sub>2</sub>	+>95%							+>95%			
Al <sub>2</sub> O <sub>3</sub>				->95%		+>95%		+>95%	+>95%		
Tot.Fe.				->95%				+>95%			
MgO						->95%	+>95%		->99.9%		
CaO								->95%			
Na <sub>2</sub> O							->95%		+>95%		
K <sub>2</sub> O									->95%		
TiO <sub>2</sub>											->95%
Mn											
S											
P <sub>2</sub> O <sub>5</sub>											

TABLE 1.15 Alumino ratios : British material.

<u>Sample</u>		Combined $\frac{\text{SiO}_2}{\text{Al}_2\text{O}_3}$	$\frac{\text{Fe}_2\text{O}_3}{\text{Al}_2\text{O}_3}$	$\frac{\text{MgO}}{\text{Al}_2\text{O}_3}$	$\frac{\text{CaO}}{\text{Al}_2\text{O}_3}$	$\frac{\text{Na}_2\text{O}}{\text{Al}_2\text{O}_3}$	$\frac{\text{K}_2\text{O}}{\text{Al}_2\text{O}_3}$	$\frac{\text{Na}_2\text{O}}{\text{K}_2\text{O}}$
Lias Clay	1	2.10	0.29	0.09	0.18	0.02	0.15	0.17
	2	1.90	0.31	0.10	0.15	0.01	0.14	0.12
	3	1.89	0.31	0.10	0.16	0.21	0.15	0.14
	4	1.86	0.27	0.09	0.13	0.02	0.14	0.12
	5	1.93	0.28	0.08	0.07	0.02	0.14	0.17
Oxford Clay	B626	1.86	0.24	0.09	0.20	0.01	0.17	0.08
	B604	1.79	0.26	0.09	0.25	0.02	0.18	0.10
	PAR	1.51	0.26	0.10	0.93	0.01	0.19	0.07
Amphill Clay	B4	1.75	0.34	0.11	0.05	0.01	0.21	0.06
	U7	2.07	0.31	0.12	0.36	0.02	0.20	0.10
	B10	2.01	0.28	0.11	0.44	0.01	0.20	0.03
Kimmeridge Clay	13/2	2.49	0.34	0.13	0.64	0.00	0.24	0.01
	JLS	1.64	0.20	0.04	0.24	0.02	0.14	0.14
Gault Clay (lower)		1.28	0.21	0.09	0.96	0.03	0.19	0.16
Speetch Clay 2		1.82	0.27	0.06	0.06	0.02	0.15	0.16

TABLE 1.16 Significance of British sample mineralogy

	<u>SIAL</u>	<u>FEAL</u>	<u>MGAL</u>	<u>CAAL</u>	<u>NAAL</u>	<u>KAL</u>	<u>NAK</u>	<u>TCML</u>	<u>M/V</u>	<u>ILL</u>	<u>KAOL</u>	<u>QTZ</u>	<u>TCMA</u>
MEAN	1.855	0.278	0.093	0.321	0.029	0.173	0.109	75.333	4.667	51.100	19.700	13.933	5.089
SDEV	0.263	0.040	0.021	0.288	0.049	0.030	0.049	11.902	7.254	38.785	8.854	6.137	6.275
VAR	0.069	0.002	0.000	0.083	0.002	0.001	0.002	141.655	52.622	77.173	78.393	37.662	39.377

Correlation Matrix

	<u>Combined SIAL</u>	<u>FEAL</u>	<u>MGAL</u>	<u>CAAL</u>	<u>NAAL</u>	<u>KAL</u>	<u>NAK</u>	<u>TCML</u>	<u>M/V</u>	<u>ILL</u>	<u>KAOL</u>	<u>QTZ</u>	<u>TCMA</u>
SIAL		+ > 95%										95%	
FEAL			+ > 95%							- > 95%			
MGAL						+ > 95%	- > 95%			- > 95%			
CAAL						+ > 95%		- > 95%					
NAAL													
KAL							- > 99.9%	- > 95%	- > 95%				
NAK								+ > 95%					
TCML									+ > 95%		+ > 95%	- > 95%	+ > 95%
M/V										+ > 95%		- > 95%	+ > 95%
ILL											- > 95%		
KAOL												- > 95%	
QTZ													- > 95%
TCMA													

Samples correlated:

LC1	B626	KC 13/2 and JLS	SC11
2	604	GC	OC PAR
3		B4	
4		U7	
5		AC U7	
		AC B10	

TABLE 1.17 Geotechnical data on N.American material.

Sample		Liquid Limit	Plastic Limit	$\frac{w_p}{L}$	$\frac{w}{L}$	Swell pressure tons per sq.ft.	q <sub>ult</sub> tons per sq. ft.
Laggett	1	62	20	-	-	-	2.91
	2	107	26	-	-	-	-
	3	92	19	-	-	-	-
	4	72	22	-	-	3.3 4.5	-
	5	93	22	-	-	-	2.37
Pierre	1	162	28	-	-	3.4 4.5	-
	2	145	26	-	-	-	-
	3	143	34	5.1 4.5	0.089 0.079	12.5 13.6	-
	4	204	29	4.1 4.0	0.072 0.070	-	-
	5	55	20	-	-	-	-
Bearpaw	6	67	20	-	-	-	17
	1	56	21	7.1 5.9	0.124 0.104	-	-
	2	85	20	-	-	-	-
	3	101	21	5.7 5.3	0.100 0.092	-	-
	4	81	21	5.5 4.9	0.096 0.086	15.9 20.4	-
Colorado	5	108	23	-	-	-	40
	6	104	23	-	-	-	-
	7	105	21	-	-	-	68
	1	81	21	6.7 7.0	0.122 0.118	-	-
	2	54	20	-	-	-	37
Fort Union	3	171	24	-	-	5.7 6.8	-
	4	40	20	-	-	-	-
	5	38	19	-	-	-	-
	1	68	22	-	-	-	-
	2	59	20	-	-	4.4 5.4	-
Lawson	3	52	22	-	-	-	10.5
	4	66	23	-	-	-	15.2
	5	133	22	3.3 2.8	0.057 0.048	-	-
	U22	55	22	7	-	-	-
	U15	53	22	8	-	-	-
	U17	65	24	6	-	-	-
	U25	65	21	5	-	-	-
	U10	60	22	6	-	-	-
	U 7	60	25	6	-	-	-

TABLE 1.18.

Students' t test; comparison of British and N.American samples geochemistry

corrected and normalized X.R.F. elements and element oxides

Element Oxide	<u>Gt. Britain (29 samples)</u>		<u>N.America (46 samples)</u>		<u>t value</u>	<u>Significance</u>
	<u>Mean</u>	<u>Standard Deviation</u>	<u>Mean</u>	<u>Standard Deviation</u>		
Total $\text{SiO}_2$	56.39	2.59	67.00	2.56	15.1783	Different at 99.9% level
$\text{Al}_2\text{O}_3$	22.11	2.97	17.60	1.99	7.1146	Different at 99.9% level
$\text{Fe}_2\text{O}_3$	6.13	1.01	5.55	1.20	1.8561	Not significantly different
$\text{MgO}$	1.93	0.44	2.35	0.75	2.2911	Different at 95% level
$\text{CaO}$	6.37	4.99	1.49	0.90	6.2980	Different at 99.9% level
$\text{Na}_2\text{O}$	0.41	0.19	1.41	0.78	5.5217	Different at 99.9% level
$\text{K}_2\text{O}$	3.65	0.39	2.73	0.97	4.0044	Different at 99.9% level
$\text{TiO}_2$	0.99	0.13	0.80	0.08	7.4598	Different at 99.9% level
$\text{MnO}$	0.08	0.07	0.11	0.18	0.6118	Not significantly different
$\text{S}$	1.80	0.73	0.83	0.43	6.6170	Different at 99.9% level
$\text{P}_2\text{O}_5$	0.15	0.01	0.30	0.32	1.9250	Not significantly different

99.9% confidence level = highly significant

99% " " = significant

95% " " = probably significant

North American samples

Claggett - 9 samples      Colorado - 6 samples  
 Pierre - 8 samples      Dawson - 9 samples (C,D,E,F,G,J,K,L,M)  
 Bearpaw - 8 samples      Fort Union - 6 samples

British Samples

Gault Clay - 1 sample      Ampthill Clay - 4 samples  
 Speeton Clay - 3 samples      Oxford Clay - 5 samples  
 Kimmeridge Clay - 2 samples      Upper Lias - 5 samples



## CHAPTER 2. SLOPE PROFILES IN THE KIMMERIDGE CLAY, YORKSHIRE, ENGLAND.

### 2.1. Introduction:

As part of the general clay shale study, some detailed attention was directed towards the Kimmeridge Clay exposures in Yorkshire, England. The mineralogy and geochemistry of the Clay has been outlined and its geotechnical properties considered elsewhere in this present Report. In this Section, attention will be directed less towards possible mass instability of the material but rather towards the degradational influence of time upon slope profile development.

The Kimmeridge Clay in the Vale of Pickering, Yorkshire, forms the ceiling of the Jurassic rocks in both Lincolnshire and Yorkshire, reaching a maximum thickness of 400 ft (Wilson, 1948). Generally, the clays and shales are poorly fossiliferous and are overlain by alluvium and glacial deposits, while isolated patches of the Clay resting on the Upper Carboniferous Grit border the alluvium along the northern fringe of the Vale.

Exposures at outcrop are rare, scattered and except on the coast, incomplete. Kimmeridge Clay exposures of any size occur as isolated hills rising out of the alluvial plain, two of the principal ones being Golden Hill and Marton Hill near the village of Marton (British Ordnance Survey map number S.E.78,S.W. Grid reference 735 833), 4 miles south east of Kirby Moorside (Figure 2.1). The exposure at Marton Hill (Figure 2.2) is known locally as 'Fox Holes' and is of Lower Kimmeridge age (Eudox US zone). The other exposure (Figure 2.3) at Golden Hill is of Upper Kimmeridge age (Pectinatites Zone). Blue clays and shales with septaria comprise the Lower Kimmeridge and on the whole it is much lighter in colour and not so finely laminated as the beds above. The Upper Kimmeridge consists of alternations of finely-laminated, dark bituminous and lighter shale with harder brown-coloured bands. In physical appearance, the clay shales studied at Golden Hill vary from a stiff to a very stiff Terzaghi

and Peck (1967) classification and from olive-grey, finely grained mudstones to a brittle, pale-yellow-brown, finely laminated iron-stained limestone. At Fox Holes, the clay shales are mainly soft-to-brittle medium and dark-grey, calcareous, often carbonaceous, in places fissile, mudstone with some very hard ironstone bands. The clay weathers to small iron-stained, disaggregated brittle platelets, similar to one of the Amphill clay-shale degradation products (sample CF) mentioned earlier in the Report.

There is a history of clay-shale extraction and slope profile change over the years in the two areas. This information will be used subsequently in this Report.

## 2.2. Jointing in the Kimmeridge Clay.

Kimmeridge Clay is regularly jointed in a continuous manner (see Plate 2.1.) and even where the clay is substantially weathered at Fox Holes, the joints are still prominent. Two major orthogonal and near-vertical joint trends in directions NW-SE and NE-SW are highlighted by computer analysis and these directions are wholly consistent with the joint trends in the Lower Lias beach platform in Robin Hood's Bay (see Figure 2.1 and Attewell and Taylor, 1970). The verticality of the joints (the term 'joint' being descriptive of a 'continuous parallel group of discontinuities along which there has been little or no movement) and a very shallow bedding dip means that the jointing is always normal to the bedding.

Inspection of the joint surfaces indicated that they were basically smooth although they did intersect numerous linear bedding discontinuities displaced from each other by an average of 0.2 cm. Although the jointing was essentially linear, the joint surfaces were sometimes 'wavy' and some large arcuate joints were observed. Open joints, up to 3 in. wide, sometimes contained a clayey gauge and there was some evidence of free water on the joint surfaces.

The discontinuities in these two shales were subjected to a detailed measurement program and were subsequently analysed for stability.

### 2.3. Slope Design criteria.

The discontinuous character of the Kimmeridge Clay, its low intrinsic strength with respect to rock, and its other geotechnical and geochemical properties imply that it will fall quite satisfactorily under the heading of 'clay-shale'. Lane (1969) has acknowledged the geotechnically intermediate stance with respect to strength of a clay-shale and that geologically it should have a structure, and accept joints, faults and other defects. He notes that it should be fissile and stratified and yet respond very much like a hard clay in a soil test. The term 'weakly-bonded shale' is probably compatible with the overconsolidated clay shale of Scott and Brooker (1968), the clay shale of Johnson (1969) and of Fleming et al (1970) and the stiff, fissured clay of Chandler (1970).

Excavated slope stability can be assessed for practical purposes with respect to three limiting conditions:-

- (i) Initial or construction conditions,
- (ii) Intermediate conditions,
- (iii) Long-term, essentially residual strength, conditions.

In Figure 2.4, the numerical symbols are:

- 1 = Unknown history subsequent to major geological unloading
- 2 = Initial or construction condition (based on in situ tests)
- 3 = Intermediate condition (based on empirical observations)
- 4 = Long term conditions (based on residual shear tests)

The first condition involves a consideration of the mass-strength of the clay-shale, which implies a knowledge of both spacial distributions and orientations of pre-existing planes of weakness and the shear resistance which can be mobilised on those planes. Since in some cases the relaxed stress differences may be high, the possibility for shearing through solid clay elements exists and this consequently involves knowledge also of intrinsic strength. The in-situ mass shearing resistance is influenced by joints, fissures, fissility, faulting and the re-orientation of clay minerals along surfaces of

previous movement. It is generally accepted that mass-shearing resistance cannot be determined from tests on small samples recovered from conventional borings and so large scale field in-situ tests are required to include the effects of joints and other discontinuous features.

During the intermediate condition (3) the strength of the clay may be decreasing with time because of:-

a) Softening effects associated with the opening of joints and faults:

Before excavation the clay is rigid and the fissures (small, quasi-randomly distributed and orientated discontinuities) are closed. The reduction of stress during excavation permits an expansion of the clay, and some of the (optimally orientated) fissures open. Any water can then enter and soften the clay adjoining these fissures. Unequal swelling produces new fissures until the larger, intact pieces disintegrate, and the mass is transformed into a soft matrix containing hard cores. This change in state may not necessarily be abrupt but may be represented by a progressive decrease in softening with distance into the solid element. A slide occurs as soon as the shearing resistance of the weathered clay becomes too small to counteract the forces of gravity. Most slides of this type occur along toe circles involving a relatively shallow body of soil, because the shearing resistance of the clay increases rapidly with increasing distance below the exposed surface.

b) Swelling of the material from stress-relief and the slaking effects of expandable clay-minerals: On account of the large changes in volume associated with the unloading of poorly-bonded clay-shales under conditions of no lateral strain, they become the seat of severe horizontal residual stresses. As has been indicated previously the ratio between the horizontal and the vertical normal stresses increases while the overburden is being gradually removed. Even in less heavily pre-consolidated clay deposits the ratio may approach the coefficient ( $K_p$ ) of passive pressure of the clay (Skepton, 1961; Terzaghi, 1961).

These stresses can contribute to the mechanical disintegration of the shales adjacent to the slopes of river-valleys or behind man-made cuts.

c) Progressive failure.<sup>1.</sup>

Initial or construction stability.

Most failures of excavated slopes in clay-shale occur during the construction period. This point is certainly borne out at Golden Hill where over-steepening of the face during excavation work has resulted in several large-scale movements of material from the face into the excavation.

Terzaghi and Peck (1967) maintain that because of the low permeability<sup>2.</sup> of poorly bonded clay-shales at all depths below their present surface, failures of newly-cut slopes take place under  $\phi \rightarrow 0$  conditions. In this case, the shearing resistance ( $\tau$ )  $\rightarrow$  cohesion ( $c$ ), and is approximately equal to half the unconfined compressive strength of the material. ( $\tau \approx c \approx \frac{1}{2} q_u$ ).

As emphasised by Bhatia (1969) the importance of bedding and dip on slope stability should not be overlooked. He has stated that the effect of bedding plane inclination can result in the strength being only 30-40% of the strength that would normally be determined in the laboratory.

On the south side of Golden Hill excavation the clay-shale dips gently into the excavation. Conversely, on the north side the shales dip gently away from the excavation. It is the south face of the excavation where much of the movement has taken place. This is attributed to an initial over-steepening of the face (a stress-release factor) and to the unfavourable dip of the strata into the excavation (a gravitational factor, being largely a function of the friction of one block against another).

It would appear that failure immediately after excavation is presaged by the initiation of tension gashes parallel to the excavated face. Relics

---

1. See discussion later

2. Rowe (1972) quotes figures for the permeability of the Kimmeridge Clay at Waddeston, Buckinghamshire, England of  $10^{-12}$  to  $10^{-10}$  m/sec. at depths of between 5 - 10 m.

of these have been found at both Golden Hill and Fox Holes excavations, together with more recent ones developing, presumably, prior to failure of the newly excavated face to the left of the entrance on the south side of the pit at Golden Hill. (See Figure 2.3)

Intermediate and long-term stability.

Lane (1969) has proposed that a strength decrease in clay-shales subsequent to excavation could possibly be avoided by designing for a long-term strength substantially below the peak strength, but well above the residual strength. As a basis for selecting such a strength, he has suggested that it be the stress at which the deviator stress in a triaxial compression test departs from the initial linear portion of the stress-strain deformation curve. By restricting the designing stress to such a value, he maintains that irreversible or progressive failure effects might be either minimized or eliminated, thereby preventing continuous failure surfaces from ultimately developing, after having first reached the peak strength in progressive failure type action.

On the other hand, Morgenstern (1969) has cited a slope failure in London Clay that occurred after 30-40 years; this presumably would not have occurred if the concept proposed by Lane was applicable.

Lane (1969) has also pointed out the importance of weathering or softening effects working down from the surface, and how the strength would decrease with time from this effect. Johnson (1969) has commented on the extreme lack of data relating to strength decrease of clay shales with time, despite the evidence that this occurs. Skempton (1969) for example has analysed the cohesive value of the London Clay along eight first time slides and has shown that cohesion progressively decreases with increased time (see Figure 2.5). Morgenstern (1969) has cited data from stability studies in the London Clay, and maintains that, for periods of about 100 years, stability could be estimated on the basis of  $c' = 0$ ,  $\phi' = \phi'$  peak from drained shear tests provided that residual conditions had not developed through appropriate displacements along pre-existing planes of weakness. Such an argument should be restricted to

London Clay and not be applied to clay-shales in general.

#### 2.4. Shear Strength determination in the Kimmeridge Clay.

It is well known that heavily over-consolidated clays and clay shales are likely to exhibit high peak strengths even when tested under fully-drained conditions because of their strong inter-particle bonds. Of interest also in an evaluation of the mechanics of progressive slope modification is the residual strength approached after relatively large shear displacements involving localized bond destruction and particle re-orientation along the shear plane. 12 inch square shear box tests were performed on samples of Kimmeridge Clay following consolidation for 2 days at a particular value of normal pressure  $\sigma_n$ . Reversed shear was continued until a constant value of shear stress was achieved, at which stage  $\sigma_n$  was increased to some value  $\sigma'_{n2}$  until further displacement produced a further constant value of shear resistance along the shear plane. Pre-loading was then continued to a third stage.

A plot of  $\sigma'_n$  versus  $|\tau|$  gave a  $\phi'_r$  angle of  $10^\circ$  for the Kimmeridge Clay, with a  $c'_r$  of  $14 \text{ kN/m}^2$  ( $2.03 \text{ lb/in}^2$ ). If, on the other hand,  $c'_r$  was taken to be zero, a linear regression analysis on the data produced a  $\phi'_r$  angle of  $16^\circ$ . This may be a more realistic residual angle in that the undisturbed material could be regarded as being essentially an aggregate with little inter-unit bonding. Evidence also from the basic shear stress - displacement curves indicated a continuing increase in shear strength along the shear plane at the termination of box travel and it should be remembered that ring shear experimental evidence suggests a very large displacement requirement (of the order of 1 metre or more - c.f. maximum travel on the 12 inch shear box of 2.54 cm.) before a true residual condition is achieved. On this basis, the  $\phi'_r$  angle of  $16^\circ$  can be regarded as an absolute maximum residual.

Skempton and Hutchinson (1969) suggest, when designing slopes in stiff fissured clays on a long-term basis, applying a time-dependent reduction factor ( $r$ ) in conjunction with  $c'$  and  $\phi'$  (peak strength parameters, drained).

When designing on a short term basis they advocate the application of a reduction factor for fissures (f), plus a reduction factor (x) for the rate of testing, anisotropy and so on to  $c_u$  (peak strength parameters, undrained).

Iverson (1969) advocates a more empirical approach to slope design based mainly on geological defects determined either from test pits and/or observations in the area. If no obvious geological defects are apparent, then the problem of selecting a basis for design would hinge to some extent on the importance of the excavation together with a value for the peak strength with a factor of safety or some value between the peak strength and the residual.

Hardy (1969) objects to any suggestion that a residual strength concept be used in the design of slopes in clay shale unless, for example, the swelling behaviour of the shale is considered explicitly.

To some extent, much may be gained by incorporating all or most of these concepts in any design problem, but very often a shortage of time or money or both precludes a comprehensive analysis of the problem at hand.

Probably the best practical approach is to examine both natural and excavated slope angles in various rock, clay or soil types and to incorporate these results into the design analysis, especially on a long-term basis.

## 2.5. Slope angle measurement.

"The inclination at which a slope in nature finally becomes stable against any form of landsliding is known as its angle of ultimate stability. This angle depends upon the properties of the clay and the climate and ground water conditions, and in general it can be determined with accuracy only from field observations." (Skempton 1969).

Because clay shales will weather - at least superficially - within a relatively short time, they experience progressive failure, or creep, receding primarily by intermittent sliding and thereby becoming progressively flatter. As the slope angle decreases, the average shearing stresses also decrease along potential surfaces of sliding. Ultimately, slopes are reduced to 1



vertical on 10 horizontal ( $6^{\circ}$ ), or even less (Terzaghi and Peck, 1967).

An important point when considering the time factor with respect to excavations is the nature of the material forming the excavated slopes. Muller (1964) maintains that "the permissible angle of the slope, as well as the slope stability, are a function of time". Relative to the average life of, for example, open pits, time-dependent deformations of hard rocks are significant. Soft rocks such as shale, mudstone and other types of argillaceous materials, however, can undergo magnitudes of deformation which can lead to failure within periods much shorter than the economic life of the excavated slope. Sometimes, such failures may develop within days.

It has been possible, therefore, to observe and record a wide range of slope angles at both Golden Hill and Fox Holes excavations, even though the maximum age difference between slopes is only 18 years. Slopes in harder rocks, which are less susceptible to the weakening effects of weathering, or the physical breakdown phenomenon of capillarity (Taylor and Spears, 1970) would show markedly less slope angle differentiation within much longer periods of time.

The various slope angles for both Golden Hill and Fox Holes excavations in the Kimmeridge Clay are tabulated below and are profiled in Figures 2.6 to 2.9 inclusive.

Table 2.1 - Slope angle-age analysis for Golden Hill and Fox Holes

Excavations, Marton, Yorks., England.

Age of the slope	Mean slope(1) angle (A)	Mean slope angle (B)	Age difference (Years)	Mean slope angle difference (A)	Mean slope angle difference (B)
1. Freshly excavated face(1 month)	67.5	70.5	1-2 (2)	2.5°	1.5°
2. 2 years	65	69	2-3 (6)	13.0°	28°
3. 8 years	59, 49, 48 52	43, 47, 33 41	3-4 (10)	14.5°	8°
4. 18 years	33.5, 42 42.5, 32 37.5	40.5, 30 26, 34 33	1-4 (18)	30.0°	37.5°

Mean slope angle (A) computed by summing angles at breaks of slopes (1) and dividing by the number of breaks.

Mean slope angle (B) computed by drawing a line from crest to base and measuring the angle so formed.

Plotting the ratio of age (in months) to height (in metres) against mean slope angle produces graphs of the forms shown in Figures 2.10 and 2.11.

In Figure 2.10 the mean slope angle (A)<sup>1</sup> has been plotted to produce a good linear correlation between the two variables.

---

1. See footnote under Table 2.1 for explanation.

From the plot (Figure 2.11) of mean slope angle (B)<sup>1</sup> it is clear that a linear relationship no longer holds and that the slope angle tends to be stabilising at around 30° independent of the slope age : height parameter. This latter point is not really acceptable and will be considered again a little later.

Reference to Table 2.1 in column 5, 6 for mean slope angle difference (A) shows that slope angle differences are approximately proportional to constant differences in age throughout 18 years. But using mean slope angle (B) it can be demonstrated that 75% of all slope degradation processes over 18 years have been effected within 8 years (45% of the time).

It is reasonable to expect a marked decrease in slope angle in the few years immediately after excavation as a result of the unstable nature of the slope. This would then be followed by a gradual tailing-off in latter years as the slope approaches its angle of stability in a less dynamic fashion.

The logic of this argument may be tested in another way. Suppose that the relationship between the X(mean slope angle) and Y ( $\frac{\text{age}}{\text{height}}$ ) variables were linear. By extrapolating the line in Figure 2.11 backwards to meet the Y axis, it will then be possible to calculate an approximate age for any given slope of known height (in the Kimmeridge Clay).<sup>2</sup>

Assume that a slope of height 5 m. has a mean slope angle (A) = 15; then from the graph, Y = 60; the age of the slope in months is given by

$$\frac{x}{5} = 60 = \frac{300}{12} \text{ years} = 25 \text{ years.}$$

---

1. see footnote under Table 2.1 for example.

2. This presupposes comparisons between slopes in regions of similar climates, etc.

It seems unlikely that a slope (in Kimmeridge Clay) would attain its angle of ultimate stability<sup>1</sup> after only 25 years, for after 18 years its mean slope angle (A) is still only 37.5 (see Table 2.1). This would indicate an unlikely 20° decrease in slope angle after only another 7 years.

However, by extrapolating the curve as drawn in Figure 2.11 back to meet the Y axis, a similar analysis provides an approximate age of 63 years (on the basis of mean slope angle (B)) for a 5m. slope at 15°. This is, in all probability, a far more realistic value.<sup>2</sup>

Hutchinson (1957) and Skempton and Delory (1967) have analysed several naturally occurring inland and coastal slopes in London Clay with regard to their age/angle relationships. Their results demonstrate a general tendency for inclination to decrease with increasing orders of magnitude of time, and they conclude that angles of ultimate stability can be correlated with residual strength. Unfortunately, there seems to be no similar quantification of the age/height/slope angle parameters for slopes in clay shales although Banks (1972) has recently published plots of slope height against slope angle for several N.American clay-shale formations. Unfortunately, except perhaps for the Bearpaw and Pierre formations, no useful relationships emerge and even with these two formations there seems to be a tendency for the height of the slope to increase with the cotangent of the slope angle. This is contrary to what might logically be expected.

Slope data for the Kimmeridge clay have been plotted in a similar manner in Figure 2.12 and although the maximum slope heights are at least an order of magnitude less than those considered by Banks, op cit they do

---

1. Angle of ultimate stability here taken as  $\phi'r$  (see discussion later)

2. A 10m. slope at 10° would have an approximate age of 200 years.

present a much more logical picture. The consensus of evidence implies that as the slope height decreases, the cotangent of the slope angle increases out of proportion and that a slope angle of  $15^{\circ}$  (8L, 18L, 18TE) is very close to the residual condition determined experimentally.

For other work on slope angle-slope height relationships, reference can be made to Hoek (1970), and the work of Shuk (1955), Kley and Lutton (1967) and Lutton (1970) provide a qualitative indication of typical slope height-slope angle relationships but which are of limited value in the quantitative design of slopes.

## 2.6. The stability angle in design criteria.

Skempton (1969) has pointed out that the prediction of an angle of ultimate stability is a difficult matter, since it depends on a rather exact knowledge of piezometric conditions and soil properties at shallow depths. This is why the angle is best determined from field observations. On the other hand, an approximate quantitative explanation of the stable angle can be derived.

Using the Skempton and Delory (1957) analysis for planar slides in infinite slopes, a stable slope angle,  $\beta$ , may be computed for a factor of safety of unity using the standard equation:-

$$F = \frac{c' + z \cos^2 (\delta - m\gamma_w) \tan \phi'}{\gamma z \sin \beta \cos \beta}$$

where F = factor of safety against sliding

Z = an average distance from the top of the slope to the plane of sliding.

m = height of water table above the plane of sliding.

This analysis makes no allowance for fluctuations in the water table, nor does it allow for a progressive decrease in the strength of clay shales, for example, with time. In other words, a stable angle after 10 years may not be a stable angle after 20 years.

For the field area studied, it is proposed that a long-term slope design could be based to a significant extent on the prediction of the stable angle after  $x$  years using a graph of the form shown in Figure 2.11. This method ensures that correct piezometric and other conditions apply, for the date is derived from the field measurements of actual stability situation at various periods of time.

On a short-term basis, Skempton and Hutchinson (1969) recommend, for cuttings in jointed clays, ignoring  $c'$  and using  $\phi'$ . Additional data on both highly weathered and moderately weathered samples of Kimmeridge Clay from Pickering indicate a  $\phi'$  of  $22^\circ$  and a  $c' = 64.5 \text{ kN/m}^2 (9.35 \text{ lb/in}^2)^1$ .

If a cutting is made in a highly jointed clay one line of approach would be to treat the mass medium essentially as an aggregate possessing little or no cohesion even if laboratory tests on intact specimens of the clay indicate a quite high cohesive value and if logic suggests that any failure plane will cut both along and across discontinuities. It is hoped subsequently to demonstrate the applicability of these assumptions to the Golden Hill/Fox Holes area.

## 2.7. Computer aided slope stability analysis.

Conventional analytical methods used in slope stability computations invoke no kinematical considerations regarding soil behaviour, and the shape of the potential slip surface must be assumed unless constrained by bedding or other structural features. However, it is commonly assumed in the analysis of slope stability problems that the shape of the slip surface below is circular. The choice of a circular slip surface is usually justified on the grounds that the computations are made simpler (Morgenstern and Price, 1965).

Field observations at Golden Hill and Fox Holes excavations indicate that slope failure has followed an approximately circular arc pattern, although in some instances planar failure may have taken place where unfavourable dips occur.

Failure seems to have been proved by the appearance of tension gashes approximately  $1\frac{1}{2}$  m. from the face. The depths of these tension gashes are not great, in most instances only  $\frac{1}{2}$  m. or so. They are believed to be relatively dry, even after periods of prolonged rainfall.

On the basis of these field observations, a computer-aided slope stability analysis based on the Bishop Simplified approach has been used to determine minimum factors of safety against circular arc failure for various  $c'$  and  $\phi'$  parameters for an 8-years slope at Fox Holes.

A given failure surface is located by specifying the co-ordinates of the circle centre and the real or imaginary failure line to which the circle must be tangential. The failure line is chosen depending on the nature of the slope profile and the soil parameters. According to Capper and Cassie (1957), when  $i$  (the slope angle) is  $53^\circ$  and  $\phi$  is zero or very small, the most dangerous circle passes below the toe. The centre of this circle is considered to be situated vertically above the mid-point of the slope.

The depth of the arc of rupture is generally governed by the presence of rock or other firm material at a certain depth below the foot of the slope. This is quite important, for when choosing a failure line to which all subsequent failure circles would be tangential, it should be realised that a potentially more dangerous circle may exist which passes below the toe.

For the data at hand, the most critical circle is assumed to pass through the toe of the slope.

A given failure surface is located by stipulating the co-ordinates of the circle centre and the failure line to which the circle must be

tangential. The computer is instructed to step the position of the circle centre in a defined way and to carry out the calculation for the new circle (still tangential to the same failure line). This procedure may be carried out a large number of times and therefore various factors of safety are calculated for a large number of circles, in order to define the locus of the minimum factor of safety which is a function of the input rock parameters.

It was also considered worthwhile to appraise the influence of a water table in the slope upon the factor of safety against arc failure.

Construction of a parabolic phreatic surface, according to Casagrande (1937), requires the location of a parabolic point B (this approximately represents the level of saturation, or the water-table.

This value is an unknown quantity for the particular slopes being analysed, seepage at the toe of the slopes (after heavy rainfall) being the only water observed. The parabolic point B has, therefore, been assumed and the basic parabola constructed according to a set geometrical technique (see Figure 2.13).

The computer analysis was carried out for an 8-years slope at Fox Holes using various  $c'$  and  $\phi'$  parameters. The resultant minimum factors of safety determined by the program are tabulated below:-

Cohesion $\text{kN/m}^2 (\text{lb/in}^2)$	Angle of internal friction $\phi^\circ$	minimum f/s		% difference
		with $\nabla$	without $\nabla$	
34 (5.0)	15	1.116	1.167	4.38
69 (10.0)	10	1.693	1.734	2.36
69 (10.0)	20	1.977	2.057	3.89

Table 2.2. Minimum factors of safety for various  $c'$ ,  $\phi'$  values with and without a water table ( $\nabla$ ) 8 - years slope at Fox Holes.



As would be expected, the lowest factors of safety are those associated with the lowest value of  $c'$  and  $\phi'$ . By increasing the value of  $c'$  by 100% and that of  $\phi'$  by  $5^\circ$  ( $15^\circ$  to  $20^\circ$ ), the minimum factor of safety is correspondingly increased by 43.25% (1.167 to 2.057). The same procedure applied with a water-table ( $\nabla$ ) gives an increase of 43.5% (1.116 to 1.977).

The influence of  $\phi'$  on the factor of safety is shown by keeping  $c'$  constant (at  $69 \text{ kN/m}^2$ ) and then by computing a minimum F/S for both  $\phi = 10^\circ$  and  $20^\circ$ . Results indicate that an increase of  $5^\circ$  in  $\phi'$  gives an increase of 14.5% in the minimum factor of safety (1.693 to 1.977). With a water-table, the increase is 15.7% (1.734 to 2.057).

Surprisingly, however, the difference that a water-table exerts upon the minimum factor of safety for similar  $c'$  and  $\phi'$  parameters is only 3.54%.

A plot of  $\frac{c'}{F}$  versus  $\frac{\phi'}{F}$  gives two straight lines of the form shown in Figure 2.14. By extrapolating the lines to meet the x and y axes, it is possible to find maximum values for  $c'$  and  $\phi'$  assuming a factor of safety of unity. Values obtained by this method are:-

$c' = 47.8 \text{ kN/m}^2$	$(6.85 \text{ lb/in}^2)$	)
$\phi' = 37.6^\circ$		)
	with a water-table	)
$c' = 48.4 \text{ kN/m}^2$	$(7.0 \text{ lb/in}^2)$	)
$\phi' = 32.5^\circ$		)
	without a water-table	)

(In many respects the trend shown here is comparable to that which is evident when comparing Mohr's circles for both the undrained and drained conditions, that is, an increase in  $\phi'$  and a decrease in  $c'$  on an effective stress basis over the equivalent drained parameters.)

Mean values for both  $c'$  and  $\phi'$  (with and without a water-table condition) are readily obtained from the graph:-

$\bar{c}'$	=	23.9 kN/m <sup>2</sup> (3.43 lb/in <sup>2</sup> )	}	with water-table
$\bar{\phi}'$	=	18.8°		
$\bar{c}'$	=	24.2 kN/m <sup>2</sup> (3.5 lb/in <sup>2</sup> )	}	without water-table
$\bar{\phi}'$	=	16.25°		

By inserting these values back into the program, a minimum factor of safety = 1.0 should result.

For  $c' = 24.2 \text{ kN/m}^2$ ,  $\phi' = 16.25^\circ$  the resulting minimum  $F/S = 0.94$ .

For  $c' = 48.4 \text{ kN/m}^2$ ,  $\phi' = 0^\circ$ , the minimum  $F/S = 1.0006$ .

By feeding various other parameters back into the program it would be possible to explore progressively all qualities of agreement. An apparently large discrepancy in the estimated  $F/S = 1.0$  may result from even only very small variations in both  $c'$  and  $\phi'$  due to extrapolation on the basis of thinness of results near the x and y axes. Further work would be needed to obtain factors of safety for high  $\phi'$  and low  $c'$  and vice versa in order to eliminate any error when putting a straight line through the points. Indeed, the relationship  $\frac{\phi'}{F}$ ,  $\frac{c'}{F}$  may not be linear, and only apparently so within certain limits.

It is of some interest to note that for a factor of safety of unity, the  $c'$  and  $\phi'$  parameters are not unlike the proposed residual values for this material as discussed earlier.

## 2.8. Stability analysis on orientation density distribution of discontinuities.

Detailed discontinuity surveys were performed on the excavation faces at Golden Hill and Fox Holes using the line scan technique and subsequently

analysing the data as per Attewell and Woodman (1972). Orientation data can be evaluated on the basis of an area normalisation where the area to be scanned for data points is a function of the data point density (usually inversely proportional) or the scan area can be prescribed and the distribution function for the data points can be weighted by a factor that is inversely proportional to the product of the sample density and the scan area (this latter is usually chosen through convention to be 0.01, or 1 per cent). For a small number of data points, the choice from the two options can have a considerable influence on the final density presentation of the data. In general, the former (area normalisation) produces more statistically-acceptable results for a more nearly uniform discontinuity orientation distribution (near-spherical fabric symmetry) than for a highly concentrated distribution, and vice versa. Since the exposures in the Kimmeridge Clay presented evidence of discrete jointing leading to high discontinuity concentrations, the results from this part of the work were plotted by the computer on the basis of the latter criterion, viz, n% per 1% area.

As a result of the discontinuity orientation analysis, the poles to the major joint sets in the Kimmeridge Clay were shown to be orientated N75E and N167E and to lie vertically. At the former orientation, the maximum joint concentrations are 21% per 1% area while at the latter orientation they just achieved a maximum of 13% per 1% area.

In order to assess the shear response of the discontinuities, a number of normalized stresses and discontinuity shear strength parameters were applied to different discontinuity scan traverses, both length-standardised and un-standardised. All the stereograms are not presented in this Report on account of the number that was actually produced and their total bulk. The conditions set out in Table 2.3 were, however, specifically considered for this report.

In Table 2.3., the series of  $c$ ,  $\phi$  shear strength parameters is terminated in the final column with the actual values determined experimentally. It can be seen that under the range of stress combinations considered, the Golden Hill slope is quite stable with respect to any possible shear movement. On the other hand, the 15 m. high Fox Holes slopes are just prone to possible shear failure at the lower principal stress ratios, and it is of interest to observe that the north face is more vulnerable (higher anisotropic index due to a higher orientation density distribution of discontinuities aligned for shear failure) than the east or west faces.

A more detailed appraisal of the results as summarized in Table 2.3 indicates the great significance of relatively small levels of cohesion when the discontinuities are subjected to triaxial stress differences. For example, in the first row of Table 2.3. (Golden Hill, 6 m. slope) compare the anisotropic index values for the conditions  $\phi = 15$ ,  $c = 5 \text{ lb/in}^2$ ;  $\phi = 0$ ,  $c = 5 \text{ lb/in}^2$ ; and  $\phi = 15$ ,  $c = 0$ . In the first case, there is no shear at all. In the second case, the removal of all frictional restraint, but with the retention of the  $5 \text{ lb/in}^2$  cohesion leads to only a relatively small amount of shear strain energy (0.1444 units) in the clay shale. On the other hand, if the cohesive component is lost and a friction angle of  $15^\circ$  is required, there is quite a high strain energy of shear movement in the clay shale (8.2818 units). These conclusions can be confirmed - and others derived with respect to the stress ratio and shear strength parameter interplay - through a close examination of Table 2.3.

For the computer runs from which Table 2.3. has been compiled, the the principal stress ratios have been input on a logical but quasi-arbitrary magnitude basis. It is more logical to assume - and any numerical (for example, finite element) analysis shows - that the magnitude of the principal stress ratios changes as a function of position within the mass and particularly with respect to location along a slope failure plane.

It is therefore very necessary to increment this ratio through a wide range since by so doing it might be possible to suggest where a large scale shear failure is actually initiated within the slope. It is accepted that shear failure is not a phenomenon that develops contemporaneously at all points along a failure surface - slight shear movement at a critical point in an over-consolidated clay sufficient to take the shear strength just beyond peak would suggest a temporary decrease in pore water pressure and an associated migration of pore water from adjacent elements to the point in question (Henkel, 1956; Bishop, 1971). If the stability of the discontinuous material is less critical with respect to  $\phi$  than with respect to  $c$ , then the overstressing on an element-to element basis along the eventual failure surface will be facilitated and the total failure accelerated in time. Acceleration will, in fact, result from progressive shear displacements nucleating from the initially over-stressed source, the greater the displacement the more the shear strength reduction towards a local residual state and hence the more rapidly will total shear failure be mobilized through 'strength shedding' to contiguous discontinuities.

A detailed discussion of the practical failure mechanics is beyond the scope of this Report since it involves, for example, strength interactions between discontinuities and bounded intact clay elements. Statistical knowledge of discontinuity orientation density distributions is of vital importance in the progress towards the solution of such a multi-variable problem, but until the implied spacial density distribution solution is forthcoming the problem can be described - and a total solution prescribed - only incompletely.

A further routine matter concerns the influence of the intermediate principal stress. It has been shown (Attewell and Woodman, 1972) that  $\sigma_2$  is quite critical with respect to a shearstrain energy criterion and yet, in earlier analysis, it has been specified arbitrarily as  $0.5 \sigma_1$ . If a plane strain condition is to be valid (and this is implied in most two-dimensional analyses) then, for a more logical approach and with a Poisson's ratio of

0.5, the intermediate principal stress parameter should be input to any analysis as one half the sum of the other two principal stresses. This operation has been performed on the Fox Holes west and east face data and the shear strain energy parameters plotted in three ways in Figures 2.15, 2.16 and 2.17.

The isotropic parameter is exclusively stress controlled and reflects the balance of deforming shear stress to restricting shear stress. It is independent of fabric and its amplitude is a function solely of the three principal stresses and the shear strength parameters. In contrast, the anisotropic parameter is controlled by the nature of the fabric topography within the 'failure' window. At the present time, shear strain energy levels are computed numerically. Ideally, one would wish to describe the discontinuity orientation distribution by means of a series of associated Legendre polynomials but where, as is generally the case, there is little or no fabric symmetry this approach becomes virtually intractable.

It is probably most useful, as an aid to interpretation, to regard the projected 'failure' window as a step function operating upon the fabric having certain numerical characteristics as a function of location within the window. There should be regular, monotonical changes in the isotropic parameter as a function of the shear stress-strength balance, as shown in Figure 2.16. On the other hand, local but intense discontinuity orientation concentrations create temporary surges in the anisotropic parameter as the isotropic window expands or contracts through them. However, since the window has a smoothing capacity with respect to any non-isotropic fabric (noting, of course, that this capacity is a function of the stress-strength balance) the anisotropic parameter will usually plot quite smoothly against the principal stress ratio. Perturbations on this smoothness, if increasing the anisotropic shear strain energy, represent regions of steep fabric topography which could exert a particular control on structural stability with respect to shear.

Reference to Figure 2.15 will indicate that such a condition arises under

plane strain conditions for a principal stress ratio  $\sigma_3/\sigma_1$  of 0.125 and that the magnitude of the effect is conditioned by the  $c, \phi$  shear strength parameters of the discontinuities (note that there is a visible distortion due to the log scale). The significance of this particular ratio is also, of course, a consequence of the principal stress directions as applied to the discontinuity fabric; had the slope face (and hence the principal stress orientations for the same magnitudes) been orientated differently then, depending again on the steepness of the fabric topography in other regions of the projection, anisotropic shear strain energy criticality could develop at a different  $\sigma_3/\sigma_1$  ratio.

Although the anisotropic shear strain energy is the important parameter controlling facility for failure, it is generally useful to normalize it to the isotropic parameter in order to produce a 'danger' index.\* There are two consequences of this operation. First the shear strain energy acquired through potential discontinuity movements is stabilized to some level which is independent of fabric while remaining directly tied to the stress-strength balance; the resultant dimensionless parameter thereby serves as an index upon which comparisons between different discontinuity fabrics subjected to the same ranges of deforming stress systems can be built. Second, there is a distinct practical advantage in that, whereas there develops a very wide numerical range of both anisotropic and isotropic strain energies through the application of a spectrum of principal stress ratios, the normalization process usually reduces this range to the extent

---

\* The inverse ratio  $I/A$  can be regarded as a 'safety' index, but the resultant high orders of magnitude (high degrees of safety) require a log-linear plot (the same argument can be applied to the  $A/I$  index but the points of high safety plot in this case at the ordinate axis origin).

that the inter-relationships between all the major variables can be expressed graphically on linear-linear scales.

In Figure 2.17. the Anisotropic Shear Strain Energy Index (ASSEI)  $A/I$  is shown, for the present fabric, to increase with decreasing  $\sigma_3/\sigma_1$ . The fact, for example, that ASSEI increases through an increasing range of discontinuity shear strength is an expression of increasing discontinuity orientation concentration as the failure window ( effective shear stress  $> 0$ ) condenses solely under  $c, \phi$  control towards a situation of total discontinuity stability. In all such stability problems it is the influence of the stress balance - increasing  $c, \phi$  and reducing  $\sigma_2/\sigma_1, \sigma_3/\sigma_1$  or reducing  $c, \phi$  and increasing  $\sigma_2/\sigma_1, \sigma_3/\sigma_1$  - that can generate a specific anisotropic and isotropic parameter.



TABLE 2.3.

Discontinuity Analyses of the Kimmeridge Clay Slopes, Yorkshire, England.

Reproduced from  
best available copy.

	Input stress	Shear strength parameters and Shear Strain Energy Indices							
		$\phi = 15^\circ$	$c = 5 \text{ lb/in}^2$	$\phi = 10^\circ$	$c = 10 \text{ lb/in}^2$	$\phi = 20^\circ$	$c = 10 \text{ lb/in}^2$	$\phi = 0^\circ$	$c = 5 \text{ lb/in}^2$
		A	I	A	I	A	I	A	I
Golden Hill 6 m. high slope	$\sigma_1$ vertical	0	0	0	0	0	0	0.1444	2.0673
	$\sigma_2$ 0.5 E-W								
	$\sigma_3$ 0.2 N-S								
	$\sigma_1$ vertical	0.0024	0.0228	0	0	0	0	0.4199	5.7010
	$\sigma_2$ 0.5 E-W								
	$\sigma_3$ 0.1 N-S								
	$\sigma_1$ vertical	0.0299	0.2541	0	0	0	0	0.6362	8.4156
	$\sigma_2$ 0.5 E-W								
	$\sigma_3$ 0.05 N-S								
Fox Moles 15 m. high slope north face	$\sigma_1$ vertical	0.5349	4.1343	0.0466	0.4681	0	0	5.6521	42.6821
	$\sigma_2$ 0.5 E-W								
	$\sigma_3$ 0.2 N-S								
	$\sigma_1$ vertical	2.1195	11.8246	0.3039	2.8361	0.0170	0.1159	11.0827	60.2886
	$\sigma_2$ 0.5 E-W								
	$\sigma_3$ 0.1 N-S								
	$\sigma_1$ vertical	4.0957	17.7786	0.5641	5.1037	0.0938	0.6488	14.9869	70.7755
	$\sigma_2$ 0.5 E-W								
	$\sigma_3$ 0.05 N-S								

# Discontinuity Analyses of the Kimmeridge Clay Slopes, Yorkshire, England.

[illegible]

TABLE 2.3. cont....

Discontinuity Analyses of the Kimmeridge Clay Slopes, Yorkshire, England.

Input stress	Shear Strength Parameters and Shear Strain Energy Indices								
	$\phi = 15^\circ$	$c = 51\text{lb/in}^2$	$\phi = 10^\circ$	$c = 10\text{ lb/in}^2$	$\phi = 20^\circ$	$c = 101\text{lb/in}^2$	$\phi = 0^\circ$	$c = 51\text{lb/in}^2$	
	A	I	A	I	A	I	A	I	
$\sigma_1$ vertical $\sigma_2$ 0.5 N-S $\sigma_3$ 0.2 E-W	0.4555	4.1344	0.0077	0.4683	0	0	5.8952	42.6857	
$\sigma_1$ vertical $\sigma_2$ 0.5 N-S $\sigma_3$ 0.1 E-W	2.4382	11.8269	0.1419	2.8351	0.0034	0.1161	11.6543	60.2886	-89-
$\sigma_1$ vertical $\sigma_2$ 0.5 N-S $\sigma_3$ 0.05 E-W	4.8273	17.7736	0.3558	5.1039	0.0523	0.6494	15.7701	70.7745	

Location - Fox Holes 15 m. high slope, west (and east) face.

TABLE 2.3. cont.....

Discontinuity Analyses of the Kimmeridge Clay Slopes, Yorkshire, England.

<u>Input Stress</u>	Shear Strength Parameters and Shear Strain Energy Indices											
	$\phi = 0^\circ$	$c = 10 \text{ lb/in}^2$	$\phi = 5^\circ$	$c = 0$	$\phi = 10^\circ$	$c = 0$	$\phi = 15^\circ$	$c = 0$	$\phi = 20^\circ$	$c = 0$	$\phi = 22^\circ$	$c = 9.35 \text{ lb/in}^2$
	A	I	A	I	A	I	A	I	A	I	A	I
$\sigma_1$ vertical	0.2611	7.9404	26.4565	81.6346	16.5600	50.8369	9.7279	28.9100	5.1710	14.7865	0	0
$\sigma_2$ 0.5 N-S												
$\sigma_3$ 0.2 E-W												
$\sigma_1$ vertical	0.8074	15.2083	42.4927	109.4229	31.3706	75.7758	22.9082	50.3006	16.4137	32.0445	0.0046	0.1118
$\sigma_2$ 0.5 N-S												
$\sigma_3$ 0.1 E-W												
$\sigma_1$ vertical	1.3519	19.9965	52.3337	125.4432	42.0110	90.6713	32.1822	63.7571	25.2113	43.7818	0.0689	0.6660
$\sigma_2$ 0.5 N-S												
$\sigma_3$ 0.05 E-W												

Location - Fox Holes 15 m. high slope, west (and east) face.

CHAPTER 3

FIELD AND LABORATORY INVESTIGATIONS AND  
ANALYSES PERTAINING TO CHATFIELD DAMSITE, LITTLETON,  
COLORADO.

3.1 Introduction.

This site was visited in July 1972 and discontinuity measurements were carried out within the Spillway excavations for a subsequent study of foundation mass stability which is discussed later in the Chapter.

A 20 ft. high vertical section of the Dawson Formation was sampled in the vicinity of Borehole DH 174 (D.M. NO. PC-24 Vol. I, 1968.) Subsequent geochemical and mineralogical work was carried out on these 'silty' clay-shale samples which were taken at 1 ft. intervals (Table 3.2, samples 1-19). A sample of channel sandstone (very dense semi-lithified sand) was also taken at this location (sample 21). At the eastern end of the northern wall of the spillway, ironstaining was pronounced well below the upper limit of the Dawson. The nature of this phenomenon was uncertain so it was decided to sample these measures for further chemical and mineralogical consideration (Table 3.3, samples A to O).

Although in the context of mass stability the precise nature and classification of discontinuities is not important, it did seem logical to sample the more unusual 'soft seams', which are tentatively concluded to be a shear feature induced within the Dawson during the evolution of the Rocky Mountains. Mechanical and mineralogical work carried out on this material, together with shear-box tests and limit determinations carried out on in situ block samples is also reported upon. Cross-correlations between mineralogy on the one hand and limits and

residual shear strength on the other hand imply that this type of approach may well prove useful in ascertaining the likely behaviour of other clay-shale formations.

Visits were also made to the proposed Bear Creek damsite but sensible strata sampling and discontinuity measurements were precluded by topography and the nature of the surface weathering. A sample of Laramie clay-shale was taken from just below the sandstone contact with the Arapahoe Formation. The mineralogical analyses are included for comparison with the Dawson.

### 3.2. Mineralogy, Chemistry and Geotechnical evaluations.

The mineralogical analyses were carried out on a quantitative basis in that calibration curves are available for the minerals detected. The nature of the montmorillonite in these rocks enabled this mineral to be estimated from curves constructed from well-known bentonites. Glycolation enabled at least partial differentiation of montmorillonite, mixed-layer clay and illite to be made.

The computerised X-ray fluorescence output for major elements and element oxides is conveniently expressed in this Report in absolute terms (100% - (organic carbon +  $\text{CO}_2$  +  $\text{H}_2\text{O}$ )). For direct statistical comparisons however, (e.g. Students'  $t$  test) the normalized results used have been corrected for absorption.

#### 3.2.1 Mineralogy and geochemistry of the Dawson sections.

##### a) Samples 1 to 19.

\* Table 3.2 shows that the section in the vicinity of DH 174 is probably more silty than the borehole record would suggest. The minimum quartz percentage is 36 whilst the upper limit is 60.

A consideration of the clay mineralogy on its own merits infers that much of the clay mineral suite comprises pure phase montmorillonite which is commonly associated with mixed-layer illite-montmorillonite. The trend (double arrow) is for the montmorillonite component to be dominant. There is the possibility that mixed-layer clay could increase in the more weathered sections, but as iron staining could be detected in all samples bar 1 to 3 and oxides such as CaO which are susceptible to leaching show no marked decrease in the upper, very silty and more permeable materials, this possibility is unlikely.

The overall identification is very similar to that of H.A. Tourtelot (D.M. NO PC-24 Vol. II, Plate 189). Compared with the latter analyses, the illite content in the sections analysed in Durham would appear to be lower and the presence of chlorite is debateable. However, these are very minor points.

The chemical analyses (Table 3.1, without absorption correction) are marked by a high total silica content (quartz plus silica combined dominantly in the clay minerals). Potassium is low compared with illite-rich Pennsylvanian sediments of the British Coal Measures, and in any case some of the  $K_2O$  is combined in trace feldspars.

If we consider selected oxide/alumina ratios (Figure 3.1) certain variations which are probably attributable to the dominant clay mineral, montmorillonite, are apparent. The total silica ratio is, of course, a reflection of quartz and combined silica. Quartz does not vary considerably within the section except in the upper part (e.g. Sample 19, Table 3.2). It is not unreasonable, therefore, to regard the total  $SiO_2$ /alumina ratio as being symptomatic of clay mineral variations. Montmorillonite\* has a high combined  $SiO_2$ /alumina ratio (see Grim 1968, p. 578), whereas mixed-layer clays have a somewhat lower ratio and kaolinite has a very low ratio indeed.

---

\* Montmorillonite around 2.6 to 3.0; Fithian illite about 1.98; Kaolinite about 1.2

Calcite is present in detectable quantities in the upper part of the section (Table 3.2), but otherwise can be assigned to the clay minerals. On Figure 3.1 there is a quite surprising compatibility between the  $\text{SiO}_2$  and  $\text{CaO}$  profiles. This infers that  $\text{Ca}^{2+}$  may well be following combined silica and there is good reason to accept this argument because  $\text{Ca}^{2+}$  is regarded as the dominant ion in the Dawson at Chatfield (D.M.No. PC-24, Vol.II, Plate 195, 1968). It can also be seen from Figure 3.1 that as the  $\text{SiO}_2$  and  $\text{CaO}$  ratios fall, there is a tendency for the  $\text{K}_2\text{O}$ /alumina ratio to increase (although it remains relatively constant in the upper part of the section). This again might imply that illite and/or mixed-layer clay increases slightly when montmorillonite decreases. The sodium ratio shows no systematic variations which can be readily attributable to the clay minerals. Generally  $\text{Na}^+$  is not present in particularly high concentrations in these sediments.

The Laramie shale from Bear Creek would appear to be similar to the Chatfield material and here again the sample taken demonstrates the care with which the term clay-shale should be used. It is distinctly silty material although this is not particularly obvious in the field.

The channel 'sandstone' (sample 21, Table 3.2) is strictly a very dense, weakly lithified sand. It is high in quartz and is devoid of montmorillonite, although mixed-layer clay is the dominant clay mineral phase. In this material feldspars are still present in small percentages. Mineralogically there is little difference between this sediment type and a bed described as 'siltstone' in the ironstained section of the north wall of the Spillway (Tables 3.2 and 3.3).

b) Ironstaining in the Dawson Formation.

Ferruginous staining some 13 ft. below the exposed top of the Dawson Formation was very pronounced at the eastern end of the north wall of the Spillway (in the vicinity of borehole DH 240).



The zone affected was about 6 ft. in thickness and was sampled by Mr. K.C. Schulte. The descriptions of the samples taken are given in Table 3.3, together with the ratio  $\text{Fe}_2\text{O}_3/\text{FeO}$ . Of the samples collected, C to O were chemically analysed in Durham and certain of these results have already been used for comparison of British and North American clay-shales (Table 1.13).

Representative samples were also analysed mineralogically (Table 3.2). It is pertinent that the shale (sensu stricto) is mineralogically similar to the other sequence just considered, but in the current section the Dawson is coarsening downwards, i.e. samples N and O (Table 3.2) are very high in quartz.

We will first of all compare this section with the previous sequence by comparing the means of the 13 samples C to O with those of samples 1 to 19 (Table 3.4). The Students' t test carried out on the corrected and normalized data highlights a number of interesting features:

- i) The  $\text{Fe}_2\text{O}_3$  content of the 'ironstained' sequence is significantly lower than that of the other sequence.
- ii) Calcium and Magnesium are significantly higher in the section near DH 174 and so is  $\text{K}_2\text{O}$ . This might imply a higher degree of leaching in the ironstained section but this cannot be verified because of the probability of differences in original composition and rock type. Original differences are more likely because  $\text{Na}_2\text{O}$  would also be subject to leaching but this oxide is higher in the 'ironstained' sequence.
- iii) Sulphur which is only present in very small amounts in both sequences is significantly higher in the 'ironstained' measures. This element is probably present as pyrite (up to about 2% by weight) and is again highly susceptible to oxidation.

The  $\text{Fe}_2\text{O}_3$  figures shown on Table 3.3 indicate that total iron is not substantially more concentrated in the ironstained zone than in the

surrounding rocks. Percolation by groundwaters (possibly a past water table level) has apparently caused more ferric iron to be precipitated on the surfaces of the shale fragments.

Ferric iron in these clay-shales is derived from ferrous minerals. The fact that pyrite is not a prime source would suggest that siderite ( $\text{FeCO}_3$ ) is the other most likely source. In this context, the latter mineral was identified in one sample (Table 3.2). We have commonly noted that partially oxidised siderite is masked by the resulting limonite and therefore is not easily identified in rocks subject to oxidation.

In rocks which contain pyrite, objections can be raised against using  $\text{Fe}_2\text{O}_3/\text{FeO}$  ratios as an oxidation index (See Taylor and Spears, 1973). In the current 'ironstained' section the pyrite content is low and relatively constant (Table 3.3).. Although pyrite iron will be expressed as  $\text{Fe}_2\text{O}_3$  and not FeO it will consequently have a negligible effect in the present exercise.

The ferric/ferrous ratios shown on Table 3.3 do lend credence to the contention that the degree of oxidation is generally higher in the iron-stained zone than in the immediately adjacent samples.

### 3.2.2 Soft seams (Clay seams).

Very soft horizons were encountered at various depths in some of the boreholes during the damsite investigation (Design Memorandum No. PC-24, Vol. I). In the Weir excavations, these seams were being identified, flagged and photographed during the period of our visit. They appeared to vary in thickness from 'paper thin' to more complex zones over 0.5 ft. in thickness. Within the Dawson clay-shale (and its more silty variations, though not in the dense weakly cemented sands ('sandstone')), the soft seams appeared to occur at any horizon and individual ones could be traced over distances of tens of feet.

Of greater importance, however, is the fact that an individual seam

would change horizon and many were flexed and overfolded to form complex configurations. Discussions held with Corps of Engineer geologists and members of the U.S.G.S. (together with field visits) implied that, within a mile or so from the damsite, the Dawson Formation is upturned as a result of the later stages of the uplift of the Rocky Mountains. In contrast, steep dips and major faulting is not a feature of the damsite itself.

Because soft seams appear physically to be comprised of 'rock flour' and have been considered to be planar (near horizontal), non-slickensided features they have been designated in the past as bedding-plane relief joints produced by erosional unloading. The over-folding of the seams examined on site would suggest that they may well be a restricted bedding-plane slip phenomenon which occurred while the clay-shales were still plastic. A second phase which would accommodate the compressive stresses during the later uplift of the mountain belt would sensibly result in flexuring and overfolding of the seams. Being extensively discontinuous and filled with highly comminuted sediment there seems no good reason why they should not have remained as channels for later groundwater entrainment after lithification of the Dawson clay-shales.

The question posed was whether the composition of the soft seams was the same as the parent rock, that is, has the 'gouge material' been derived from the rock through which the seams pass?

A 12 in x 12 in x 6 in block sample from the Southern end of the Weir, which trends in a direction N  $37^{\circ}$  W, was forwarded to Durham for examination. In the middle of the block was a zone of paper thin clay layers striking at N  $45^{\circ}$  E and dipping at  $12^{\circ}$  North East. The lower part of the block (below the clay seam zone) comprised crushed shale, whilst the upper part was essentially intact.

### 3.2.1. Laboratory Tests.

97

The block was orientated in a 12 in x 12 in reversing shear box such that

the clay zone was more or less contiguous with the plane of the shear. The sample was then consolidated and sheared at a normal load of  $68.89 \text{ k N/m}^2$  to a total displacement  $0.27 \text{ m}$ . The normal pressure was then increased to  $133.69 \text{ kN/m}^2$  and the sample sheared for a further displacement of  $0.40 \text{ m}$ . The cycle was then repeated at a normal pressure of  $267.18 \text{ kN/m}^2$  to a further  $0.27 \text{ m}$  displacement, the rate of strain in all cases being  $0.000048 \text{ in/min}$ . The total shear displacement was therefore  $0.94 \text{ m}$ .

A computer print-out  $\tau/\sigma'$  versus displacement for the highest normal stress used (Figure 3.2.) shows the residual characteristics of the sample. For comparison is shown a typical set of curves for a fine-grained Coal Measures colliery discard (Figure 3.3). This latter Figure shows characteristic particle reorientation peaks which occur when the material is close to residual. The post-orientation rising stress seen in the latter Figure for the last four runs is a function of the shear-box, in that the leading edge of the box is at that stage shearing the large-scale ridge and furrow slicks which are a feature of the ultimate shear plane. For the Dawson clay seam (Figure 3.2), the slickensides were not as pronounced (possibly a function of the small grain size) and no distinct particle re-orientation peaks are present. That the slickensides are not very pronounced in the laboratory could imply that this was originally the case in the field when the clay gouge was derived - and hence their non-recognition as a shear phenomenon.

The residual plot (Figure 3.4.) highlights yet another feature. At the lowest normal stress it can be seen that the initial peak strength is little different from the residual. In other words, the clay seam would appear to be essentially at its residual strength. It is difficult to contemplate the importance of residual however, in that clay seams are an integral part of the rock mass and the fact that they are folded mitigates against failure occurring along a discrete clay seam 'path', except perhaps locally.

Table 3.5 is a comparison of the chemistry and mineralogy of the clay seam and the immediately adjacent strata from the sample block. Major element geochemistry is a more sensitive technique for monitoring changes than is quantitative x-ray diffraction. The striking feature of the material above the soft seam and the clay seam itself is the similarity in major elements. The differences between the upper two units and the lower sample are not major ones. Total  $\text{SiO}_2$  comprises free silica (quartz) and the silica combined in the clay minerals. In the upper part of the block there is slightly more free silica than in the soft seam, which implies that the combined  $\text{SiO}_2$ /alumina ratio for the soft seam is higher than that of the overlying and underlying specimens. Cations such as  $\text{Na}_2\text{O}$  and  $\text{K}_2\text{O}$  which in these sediments can be attributed almost entirely to the clay minerals, have a somewhat enhanced ratio to alumina in so far as the soft seam is concerned.

The clay minerals and quartz contents confirm the very similar composition of the over-lying clay-shale and the soft seam; the results for the underlying material point to differences being minor ones. The total major element content, X-ray diffraction evidence and slightly enhanced  $\text{Fe}_2\text{O}_3$  content of the lower section infers that there is a small siderite (carbonate) contribution in this part of the clay-shale block.

It can be seen (Table 3.5), that the consistency limits of the soft seam and the 'parental' rock are virtually the same. The general conclusion drawn from the analysis and the limits is that the soft seam 'flour' is in fact derived from the Dawson shale-type rocks.

### 3.2.3. Other shear-box tests.

Two other 12 in. square blocks of undisturbed, slickensided silty shale from the Weir section adjacent to sampling area (1 to 19, Table 3.1) were forwarded to Durham. Although one of these samples (block b) had burst open in transit, the other (block a) was intact. Because there was

insufficient material on which to conduct large size peak shear strength tests, block a was used for small size shear-box peak and ultimate\* strength tests (3in x 3in x 1in shear-box samples). The rate of shear displacement was 0.00048 in/minute, the mean dry density of the specimens was 123.6 lb/ft<sup>3</sup>, and the bulk density being 128.3 lb/ft<sup>3</sup>. The quartz content of these samples was 45%, so confirming that the material sampled was a very silty horizon of the Dawson formation.

---

\* (ultimate is defined as the shear stress value after 0.5 in. horizontal shear displacement (see Design Memorandum No. PC-24, Vol. II, 1968)).

---

The liquid limits were quite high (51% block a, 48% block b), but only marginally greater than a number of specimens featured on Plate 185 of Design Memorandum No. PC-24, Vol. II. The plastic limits (20%) are not unlike other silty Dawson specimens.

The results of the shear-tests (Figure 3.5) imply that  $\phi'$  peak is of the order of  $34^\circ$  (statistical) and that  $\phi'_{ult}$  is between  $20^\circ$  and  $24.5^\circ$ . The statistical fit for the Mohr envelope suggests that  $c'$  in both cases is around 1.25 lb/in<sup>2</sup>, but the test carried out at the lowest possible normal pressure is not incompatible with a curved envelope (i.e.  $c'$  possibly = 0). Compared with the wide spectrum of results assimilated by the Corps of Engineers (Plate 187) it is clear that the peak and ultimate  $\phi'$  values conform to the silty shale/siltstone bracket ( $\phi'_p = 27$  to  $37.7^\circ$ ,  $\phi'_{ult} = 22.8$  to  $32.6^\circ$ ). This is in accord with the visual description of the undisturbed blocks and their quartz content (also samples 1 to 19, Table 3.2).

#### 3.2.4 Correlations.

Plates 185 and 186 (D.M. No. PC-24, Vol. II, 1968) show generally that reciprocal relationships exist between moisture content and liquid limit on the one hand and  $\phi'_p$  and  $\phi'_{ult}$  on the other hand. In Final Report

(DA-ERO-594-72-G0006, April, 1973) we show that inverse trend relationships exist between  $\phi'_r$  and specific mineralogical components in British and American clay-shale rock types. Moreover in this current report (Figure 4.12) it is concluded that the negative correlation of  $\phi'_r$  and the logarithm of the quartz/total clay minerals ratio is statistically valid. Although limited in number there are proximate mineralogical analyses for certain Dawson shale samples tested in direct shear. It is of interest to see that for this material  $\phi'_r$  falls as the total clay minerals to quartz ratio increases (Figure 3.6)). Similarly, the influence of expandable minerals (montmorillonite and mixed-layer clay) are again an important control on  $\phi'_r$  - the latter decreases as the specific clay minerals to quartz ratio increases (Figure 3.6). With a larger number of results, it is probable that the relationship would be a log-linear function. Unlike Kenney's (1967) conclusions, it has been shown by Fleming, Spencer and Banks (1970) that  $\phi'_r$  may to some extent be related to the liquid limit of the shale. Figure 3.6 does suggest that in the case of Chatfield, the Dawson Formation limits increase as  $\phi'_r$  decreases. Here again, (Figure 3.7) limits may well reflect the mineralogy fairly closely\*, but as mentioned in the Interim Report (31-5-72) the method of preparation (crushing or ultrasonic disaggregation) may affect the actual values obtained. However, their usefulness as an index of engineering behaviour on a comparative basis within a sequence was also mentioned previously, and this is substantiated by the Chatfield results.

---

\* Ratios of platy to equant habit minerals (i.e. clay minerals to quartz) would appear to give the best mineralogical correlation with limits. A log-linear relationship is suggested by the distributions shown. Results computed from Tables 3.2. and 3.6. and D.M. No. PC-2b, Vol. II, 1968, Plate 189.

### 3.3 Discontinuity fabrics in the Dawson.

A few discontinuity measurements were taken in the silty measures of the Dawson at the damsite by the Resident Geologist. The discontinuities were identified as slickensides and fractures and although their numbers were too few to ensure that the orientation density distributions remain meaningful, it was thought worthwhile to reproduce the fabrics in Figures 3.8 to 3.11 inclusive. Density distributions are reproduced as  $n\%$  per cent per  $1\%$  area as equal area, upper hemisphere projections. Letters A through N denote  $11\%$  through  $24\%$ , the obliques / indicating  $> 24\%$  per  $1\%$  area. The extremely high concentrations are, of course, a function of the paucity of data from which the densities are compounded. In general, the evidence suggests that at the spillway, the inclined slickensides could be affected with respect to shear by any imposed stress system, while the horizontal and sub-horizontal fractures are less significant with respect to shear failure. Figure 3.10 also indicates that the slickensides at the weir section are dominantly inclined and as such might be required to mobilize their shear strength under strong stress differences.

In their site measurements, the present authors did not attempt to differentiate between fractures (in the sense of a predominantly tensile structural feature) and slickensided shear discontinuities. Measurements were taken at the spillway (Figure 3.12) and weir (Figure 3.13), both sets of measurements indicating that a lower degree of significance should be allocated to any horizontal discontinuities. Major concentrations at the spillway appear to dip at about  $50^\circ$  in a direction slightly east of north-east while the major concentrations at the weir dip vertically and are aligned along north-south and east-west axes. Compounded orientation density distributions from both areas are shown in Figure 3.14.

With the availability of this discontinuity data and shear strength



parameters for Dawson material it seemed appropriate to perform a rapid investigation of discontinuity stability under two possible stress systems that might be imposed at the dam foundation when the Lake has been fully established. From the Corps Design Memorandum No.PC-24, the following information has been accessed for computer input:

- i) Dam alignment (N. 108°E)
- ii) Maximum height of embankment (142 ft. over South Platte River Channel)
- iii) Head of water fully impounded (115 ft. allowing 27 ft. for a full pool below crest of dam)
- iv) Density of fill (Plate 200 - Corps D.M.No.PC-24)

Type	In situ weight lb/ft <sup>3</sup>	saturated weight lb/ft <sup>3</sup>	submerged weight lb/ft <sup>3</sup>
Impervious	120.0	126.0	63.6
Random	120.0	126.0	63.6
Pervious	130.0	136.0	73.6
Dawson	120.0	126.0	63.6

- v) Foundation strength (Plate 187/8 - Corps D.M.No.PC24).

Description	$\phi_p$	$C_p$
a) In lieu of Dawson 'S' strength	15°	0
b) Minimum for clay shale	19.8°	0
c) Boundary, clay-shale-silty shale & siltstone	27°	0
d) Boundary, silty shale & siltstone - sandy shale & siltstone	37.7°	0
e) Maximum, sandy shale and sandstone	42°	0
f) Weathered sandstone	21°	0

Foundation strength (additional to Corps D.M. No. FC-24)

<u>description</u>	<u><math>\phi</math></u>	<u><math>c</math></u>
g) Slicked lean of fat clay shale (Banks, in 17th Symposium on Rock Mechanics Illinois, 1974)	$4.5^{\circ}(r)$	0
h) Dawson clay seam - present authors' tests at Durham University.	$8.5^{\circ}$	393 lb/ft <sup>2</sup>
i) Dawson silty clay-shale from weir- present authors' tests at Durham University.	$24^{\circ}(\text{ult.})$	185 lb/ft <sup>2</sup>

The two simple stress systems used in the stability analysis have been calculated for possible upstream and downstream face conditions of the dam. In both cases, the major principal stress has been assumed to act vertically downwards and to be imposed in the former case by a buoyant fill density to top-water-level plus a dry density from top-water-level to dam crest and in the latter case by a saturated density from top-water-level plus again a dry density to crest. This is taken as an intermediate downstream case for analysis. If the core is leaky, then it could be argued that the same conditions should be input as for the upstream face. If significant flow through the core is inhibited, then an extreme dry density case might be considered. In both cases, for equilibrium, a maximum water pressure is assumed to act hydrostatically at foundation level and thereby to provide the minor principal pressure component. The intermediate principal stress is assumed to act along the line of the dam and, for a condition of plane strain within a section normal to the line, to take an amplitude equal to half the sum of the other two principal stresses.

The results of the stability analysis are tabulated over and are

discussed subsequently:

Table 3.7 Stability analysis on measured discontinuities in the Dawson at Chatfield Dam foundation.

Position	Strength Parameters			Figure Number	Shear Strain Energy Parameter		Shear Strain Energy Index I/A
	No.	$\phi$	c		Anisotropic	Isotropic	
Upstream	1.(V)a	15°p	0	3.15	3.3384	3.9490	1.1829
"	1.(V)b	19.8°p	0	3.16	0.4180	0.5838	1.3966
"	1.(V)c	27°p	0	-	0	0	0
"	1.(V)d	37.7°p	0	-	0	0	0
"	1.(V)e	42°p	0	-	0	0	0
"	1.(V)f	21°p	0	3.17	0.1800	0.2775	1.5417
"	1.(V)g	4.5°r	0	3.18	32.0298	36.2529	1.1318
"	1.(V)h	8.5°	3931lb/ft <sup>2</sup>	3.19	11.1563	12.6203	1.1312
"	1.(V)i	24°ult	1851lb/ft <sup>2</sup>	3.20	0.0001	0.0003	3.000
Downstream	2.(V)a	15°p	0	-	0	0	0
"	2.(V)b	19.8°p	0	-	0	0	0
"	2.(V)c	27°p	0	-	0	0	0
"	2.(V)d	37.7°p	0	-	0	0	0
"	2.(V)e	42°p	0	-	0	0	0
"	2.(V)f	21°p	0	-	0	0	0
"	2.(V)g	4.5°r	0	3.21	3.1449	3.6444	1.1588
"	2.(V)h	8.5°	3931lb/ft <sup>2</sup>	-	0	0	0
"	2.(V)i	24°ult	1851lb/ft <sup>2</sup>	-	0	0	0

In the discontinuity fabrics Figures 3.15 to 3.21, X at north and Y at west define axes north-south and east-west respectively (the third-Z-axis is overprinted by character P). P,Q,R define the axes of major, intermediate and minor principal stress. The plus (+) characters delimit stable and potentially unstable areas in global and principal stress space (note that the

nature of any stress space can be identified by the requirement that a principal stress axis P,Q,R must be in stable space). Direction cosine matrix:

$$\begin{array}{ccc} a_{11} & a_{12} & a_{13} \\ a_{21} & a_{22} & a_{23} \\ a_{31} & a_{32} & a_{33} \end{array}$$

referring principal stress to global axes: is bracketed beneath the discontinuity fabric together with the normalized stresses, normalized cohesion parameter and  $\tan \phi$ . The Anisotropic and Isotropic shear strain energy unit values as proposed and defined by Attewell and Woodman (1972) produce a shear strain energy index for the stressed material which is unique for the particular discontinuity suite matched to a particular triad of orthogonal stresses. Shear strain energy values are the summation of all the individual shear strain energies along each discontinuity, the influence of the sampling density being largely offset by the available normalisation to an isotropic shear strain energy value (a unity probability density distribution of discontinuities over the sphere of projection).

It must be emphasised at this stage, and when discussing the stability fabrics, that the indication of a failure regime does not mean that failure will necessarily occur. It simply implies, through the relationship between the projected potential failure areas and the probability density distribution of the discontinuity orientations within those areas, that shear movement could take place along such discontinuities given that the principal stress ratios and their directions of action as applied to the problem are valid and that the compounded shear can only be accommodated through free boundary displacement - such a displacement facility being available.

The stability fabrics in Figures 3.15, 3.16, 3.17, indicate that, in the absence of any cohesion mobilisation, failure becomes increasingly less likely in the formation with respect to an upstream stress condition as the

friction angle exceeds  $21^{\circ}$ . Potential fail orientations are easily identified through the condition that the principal stress axes, P, Q, R can of course, by definition, never accept any normal shear stress and their presence therefore indicates a safe area or areas on the projection. However, Figures 3.15, 3.16, 3.17 suggest that the clay shale and weathered sandstone horizons could be suspect if the stress input conditions used in the analysis are realistic. Inevitably, through similar reasoning, Banks' (1971) residual friction condition for slicked lean or fat clay shale (Figure 3.18) could be problematical with respect to shear failure. The Durham shear strength parameters for the Dawson clay seam are insufficiently high to preclude shear failure (Figure 3.19) and it can also be seen that there is still a failure possibility (Figure 3.20) for the silty clay with the Durham shear strength parameters of  $24^{\circ}$  ultimate friction angle and  $185 \text{ lb/ft}^2$  cohesion.

From Table 3.7 it can be seen that with respect to the proposed but simplified downstream stress conditions, only Banks' op cit very low residual friction condition ( $2.(V)g$ ; Figure 3.21) could create any problems, but here the anisotropic strain energy parameter is an order of magnitude down on the equivalent parameter for the upstream side of the dam (Table 3.7 1.(V)g.). Since the dam foundation comprises a whole suite of rock types, it could be totally unrealistic to select quite arbitrarily this single lithologic type as a source for any concern unless it could be demonstrated quite unambiguously that its presence was widespread over the foundation area.

It is clear from the fabric analysis that the upstream side of the core could impose rather more searching stress differences upon any foundation discontinuities but since equilibrium conditions must be maintained across the dam as an entity, the stability of the structural foundation is only really as strong as its weakest portion.

There are adequate references in the literature to the fact that the strength of a fissured material is a function of the strength of the fissures themselves. If this strength is to be taken fully into account it can only be assessed in the context of a three-dimensional analysis. It is totally inadequate to present planar discontinuities as line features which are required to respond to a two-dimensional stress input. These analyses on Chatfield Dam have acknowledged the importance of the intermediate principal stress in such problems and as demonstrated mathematically by Attewell and Woodman (1972).

TABLE 3.1.

CHEMISTRY CHATFIELD SAMPLES (Borehole DH 174 vicinity)

OXIDE SAMPLE	SiO <sub>2</sub>	Al <sub>2</sub> O <sub>3</sub>	Fe <sub>2</sub> O <sub>3</sub>	MgO	CaO	Na <sub>2</sub> O	K <sub>2</sub> O	TiO <sub>2</sub>	S	P <sub>2</sub> O <sub>5</sub>	TOTAL
1 *	65.33	16.07	3.85	1.50	1.42	0.13	2.14	0.64	0	0.06	91.16
2	61.29	16.55	5.47	1.61	1.53	0.14	2.14	0.68	0	0.07	89.49
3	67.85	14.95	3.82	1.34	1.31	0.20	1.82	0.64	0	0.06	91.98
4	67.29	15.04	4.42	1.37	1.40	0.14	1.64	0.65	0	0.06	92.03
5	67.60	14.10	3.87	1.26	2.52	0.08	1.44	0.62	0	0.04	91.53
6	64.63	15.99	5.48	1.39	1.31	0.12	1.33	0.72	0	0.06	91.03
7	66.68	15.63	3.98	1.36	1.20	0.12	1.37	0.73	0	0.06	91.13
8	72.29	13.65	3.57	1.06	1.01	0.12	1.31	0.68	0	0.06	93.75
9	68.74	14.87	3.84	0.98	1.37	0.11	1.41	0.66	0.17	0.07	92.22
10	73.00	12.71	3.31	1.16	1.06	0.15	2.12	0.53	0	0.14	94.19
11	62.58	16.33	5.99	1.35	1.24	0.15	2.00	0.66	0	0.06	90.36
12	62.13	16.67	5.48	1.42	1.31	0.13	1.75	0.70	0	0.06	89.64
13	64.36	16.12	4.73	1.34	1.24	0.13	1.71	0.70	0	0.06	90.38
14	62.74	16.82	4.77	1.45	1.20	0.23	2.00	0.72	0	0.06	90.00
15	63.33	17.06	4.73	1.45	1.19	0.13	2.04	0.72	0	0.07	90.71
16	62.11	16.72	3.94	1.83	2.15	0.11	2.48	0.69	0	0.11	90.14
17	67.36	14.98	3.28	1.56	1.43	0.15	2.25	0.60	0	0.09	91.70
18	68.44	14.21	3.36	1.38	1.62	0.12	2.48	0.57	0	0.11	92.29
19 +	74.39	11.28	2.93	1.18	2.02	0.28	2.03	0.46	0	0.09	94.65

\* Base of section (Elevation 5470 ft.)

+ Top of section (Elevation 5450 ft.)

MINERALOGY OF SECTIONS SAMPLED.

<u>Sample</u>	<u>Quartz</u>	<u>Kaolinite</u>	<u>Illite</u>	<u>Mixed-layer clay.</u>	<u>Montmorillonite</u>	<u>Potassium Feldspar</u>	<u>Carbonate.</u>
Laramie * (Bear Creek)	45	4	5		46		
21 (sandstone)	80	5		10-15		5	
19	60	4		40-50		Trace	Trace (calcite)
16	45	4	← 10 →		40		2 (calcite)
14	36	3		← 60 →			
13	42.5	3			53	Trace	
7	41	5		← 51 →		Trace	
5	45	1-2		← 53 →		Trace	
3	46	4		Trace	50	Trace	
1	39.5	5	← Trace →		55	Trace	
c	52	8			40	Trace	
F	43	9	10		40	Trace	2-5 (siderite)
J	46	4			50		
N	82	Trace		18		Trace	
O	72			28		Trace	

\* surface location from just below sandstone contact with the Arapahoe.

Note: Double arrow points to dominant clay mineral contributor.



TABLE 3.3

Ironstained section - North Wall of Spillway (Sta. 8+22<sup>57</sup> Lt)

Sample	Depth, ft.	Elevation ft.	Sulphur, $\text{Fe}_2\text{O}_3$ % by wt.	$\text{Fe}_2\text{O}_3$ % by wt.	$\text{Fe}_2\text{O}_3$ / $\text{FeO}$ ratio.	Description.
A	0	5398.5	(dominantly as pyrite)			Clay-shale, silty
B	1.5					" " "
C	3.0		0.80	4.05	1.88	" " "
D	4.5					" " "
E	6.0		0.78	4.83	1.73	Clay-shale, fat
F	7.5		0.77	4.65	1.44	Clay-shale, silty
G	9.0		0.79	4.42	1.44	" " "
H	11.0		0.78	2.03	1.31	Siltstone
I	13.0		0.76	2.18	1.67	"
J	15.0		0.80	3.43	1.68	Clay-shale, silty
K	17.0		0.78	4.50	1.70	" " slightly silty.
L	19.0		0.76	5.21	1.89	Clay-shale, fat to silty.
M	21.0		0.83	3.65	1.73	Clay-shale, slightly silty.
N	22.0		0.79	2.20	1.68	Siltstone
O	24.0	5374.6	0.74	1.62	1.62	Siltstone, sandy.

IRONSTAINING

TABLE 3.1

Dawson Formation, Geochemical comparisons (corrected and normalized).

Section in vicinity of DH 17 <sup>h</sup> (19 samples)			Section in vicinity of DH240 (13 samples)		t value	significance
	Mean weight per cent	Standard Deviation	Mean weight per cent	Standard Deviation		
Total SiO <sub>2</sub>	72.32	2.77	74.47	6.10	1.3050	N.S.D.
Al <sub>2</sub> O <sub>3</sub>	16.55	1.72	16.37	3.46	0.1796	"
Fe <sub>2</sub> O <sub>3</sub>	4.24	0.92	3.38	1.19	2.2138	D 95%
MgO	1.23	0.34	0.89	0.42	2.3951	D 95%
CaO	2.63	1.11	1.06	0.40	4.7509	D 99.9%
Na <sub>2</sub> O	0.14	0.05	0.57	0.56	3.2179	D 99%
K <sub>2</sub> O	2.24	0.36	1.76	0.50	3.0542	D 99%
TiO <sub>2</sub>	0.69	0.07	0.61	0.14	1.9667	N.S.D.
S	0.05	0.10	0.81	0.05	23.8095	D 99.9%
P <sub>2</sub> O <sub>5</sub>	0.08	0.06	0.06	0.05	0.7013	N.S.D.

N.S.D. = Not significantly different.

D = Significantly different at - 95%, 99%, 99.9% confidence levels.

Major element geochemistry, mineralogy and limits for 'soft seam'  
and adjacent strata.

X.R.F. Analyses (weight percentages)

	Total <u>SiO<sub>2</sub></u>	<u>Al<sub>2</sub>O<sub>3</sub></u>	<u>Fe<sub>2</sub>O<sub>3</sub></u>	<u>MgO</u>	<u>CaO</u>	<u>Na<sub>2</sub>O</u>	<u>K<sub>2</sub>O</u>	<u>TiO<sub>2</sub></u>	<u>MnO</u>	<u>S</u>	<u>P<sub>2</sub>O<sub>5</sub></u>	<u>Total</u>
Above soft seam	67.82	17.21	4.60	1.56	1.26	0.40	1.19	0.78	0.15	0.77	0.09	95.84
Soft seam	70.21	16.73	4.47	1.29	1.30	0.43	1.22	0.73	0.15	0.78	0.08	97.11
Below soft seam	60.28	18.65	5.98	1.70	1.56	0.37	1.15	0.88	0.16	0.77	0.09	91.60

X-ray diffraction (Principal components), weight percentages.

	<u>Montmorillonite (dominant)</u> <u>and mixed-layer clay.</u>	<u>Kaolinite</u>	<u>Quartz</u>
Above soft seam	57	3	40
Soft seam	60	3	37
Below soft seam	69	3	28
	<u>Liquid limit</u>	<u>Plastic limit</u>	<u>Plasticity Index</u>
Composite sample (excluding soft seam)	54	24	30
Soft seam	54	22	32

TABLE 7.6.

LIQUID AND PLASTIC LIMITS.

<u>SAMPLE</u>	<u>LIQUID LIMIT %</u>	<u>PLASTIC LIMIT %</u>	<u>PLASTICITY INDEX.</u>
U 7	60	25	35
U10	60	22	38
U15	53	22	31
U17	66	23	43
U22	55	22	33
U25	65	21	44
15 *	57	23	34
13	58	31	27
7	51	24	27
5	44	24	20
1	44	24	20
F	55	27	28

DESIGN  
MEMORANDUM II  
Plate 189

\* Chemically identical to sample 14

CHAPTER 4.                    FIELD AND LABORATORY INVESTIGATIONS AND  
ANALYSES PERTAINING TO BLOOMINGTON AND SAVAGE RIVER  
(W.VIRGINIA/MARYLAND) DAMSITES WITH REFERENCE ALSO  
TO CURWENSVILLE DAMSITE.

4.1 Introduction.

The following damsites were visited in June 1972 at the tail-end of the floods in Pennsylvania and W. Virginia:

- a) CURWENSVILLE on the West Branch of the Susquehanna River, Pennsylvania.
- b) SAVAGE RIVER, West Virginia.
- c) BLOOMINGTON, on the North Branch of the Potomac River at the State line between Garrett County, Maryland. and Mineral County, West Virginia.

4.1.1. Curwensville: Unfortunately, due to Corps of Engineers personnel problems as a result of the floods, we were unaccompanied during most of this period. Thunderstorms and heavy rain precluded much useful work being carried out at the Curwensville site. Moreover, strip mining exposures suitable for discontinuity measurements appeared to us to be few in number. However, the systematic joints recorded implies that a principal ESE-WNW set exists, with a minor set at right angles. Systematic joints (see Nickelsen and Hough, 1967) are planar or very slightly curvi-linear joints which cut completely through the rock units. They appeared to be essentially vertical. It had previously been brought to our attention that the Lower Killanning underclay had proved troublesome under certain part construction conditions. Consequently we collected a sample of what we believe to be this horizon from strip mine workings near the right abutment of the dam. 115  
Mineralogical and geochemical considerations of this material are included in Section 4.2.

4.1.2. Savage River: Discontinuity measurements were carried out in the vicinity of the Savage River dam and reservoir. Generally, the interbedded Mississippian limestone and dark red flaggy sandstones which dip at  $12^{\circ}$  in an apparent direction downstream at the dam-site are far stronger rocks than the seatearths, shales/mudstones and siltstones of the Pennsylvanian at Curwensville or Bloomington. In other words, they are unlikely to pose a stability problem. For comparative mineralogical and chemical purposes both limestone and sandstone samples (used as rock-fill in the dam) were collected for analysis.

An orientation density distribution diagram of joint discontinuities in the dark red sandstone on the north bank of the river (Figure 4.1.) suggests a dominance of discontinuities dipping at about  $80^{\circ}$  WSW and striking at about  $N165^{\circ}$ E. There is a further trend of almost vertical discontinuities striking  $N105^{\circ}$ E and a minor trend dipping at about  $85^{\circ}$  WNW and striking at  $N15^{\circ}$ E. An indication of the orientations of partings in the siltstone and shale on the south bank of the Savage River is given in Figure 4.2, and this projection generally confirms the discontinuity trends on the north bank. The fabric diagram compounded from the discontinuities on both banks is shown in Figure 4.3.

4.1.3. Bloomington: Discontinuity measurements were carried out in Pennsylvanian brown, flaggy sandstones and siltstones outcropping on Route 135 - to the West of Bloomington dam-site. The discontinuity plots in Figure 4.4 show two near-orthogonal concentrations, one dipping at about  $85^{\circ}$ SSW and striking  $N120^{\circ}$ E and the other more dominant concentration dipping at just over  $80^{\circ}$ NW and striking  $N35^{\circ}$ E. When compounded with the total Savage River discontinuities in Figure 4.5, the dominant strike trend becomes more north-south with the steep  $80^{\circ}$  dips being retained. At the dam-site itself, measurements were made (Figure 4.6) in the siltstones and shales

between the overlying Buffalo Sandstone and Lower Mahoning Sandstone of the Pennsylvanian Conemaugh series (Units 6A to 6I, Design Memorandum No.8, Part I, Bloomington Reservoir). Measurements were also taken (Figure 4.7) in the Lr. Mahoning Sandstone (Unit 7) and in the immediately underlying silty shales (Figure 4.8) (Unit 7A). All discontinuity measurements relate to the right abutment. Mr. Richard Royer (Baltimore District, Corps of Engineers) discussed the reservoir proposals in detail and demonstrated the rock types in the field and from core samples. Because there are a number of differences in the terminology of carboniferous rocks appertaining to Britain and North America it was agreed that two very different non-weathered claystone samples would be forwarded to Durham for mineralogical analyses. (Unit 6CD, 53.5 to 54.0 ft. Bh. 182; Unit 4J, 29.5 to 30.0 ft. Bh 198).

From Figure 4.6, it will be seen that the dominant discontinuity concentration in the claystone dips at about  $65^{\circ}$  just to the east of north and strikes at  $N100^{\circ}E$ , with a sub-dominant concentration dipping almost vertically and striking at  $N30^{\circ}E$ . The latter concentration is clearly compatible with the major concentration recorded in the road cutting to the west of the damsite, but the dominant concentration in Figure 4.6 is consistent in strike with the sub-dominant trend in the sandstone on the north bank of Savage River, although the concentrated average dip at about  $65^{\circ}NNE$  is  $20^{\circ}$  less severe than at Savage River.

Discontinuities in the Lower Mahoning sandstone have a strong preferred orientation, dipping vertically and striking E-W (see Figure 4.7). The apparent lack of consistency with the fabric in Figure 4.6 is not carried over to Figure 4.8, the dominant concentration in the latter fabric reflecting that in Figure 4.6. There is, however, in Figure 4.8 an additional concentration of discontinuities dipping due east at about  $20^{\circ}$  and striking N-S. All the damsite discontinuities are compounded in the Figure 4.9 fabric to produce a maximum concentration of discontinuities of 11% per 1% area dipping at  $60^{\circ}$  to the north and striking at  $N105^{\circ}E$ . There is also some

evidence of a sub-dominant concentration (maximum of 8% per 1% area) of vertical discontinuities striking E-W. Finally, a composite fabric (Figure 4.10) for the discontinuities surveyed over the whole of the Bloomington area (including the ~~dam~~site) confirms a preferred discontinuity dip of  $60^{\circ}$  at a full dip direction of  $15^{\circ}$  E of N (via a maximum concentration of 7% per 1% area).

The above fabric diagrams, and particularly those referred to the ~~dam~~site itself can be compared with the fabric in Figure 4.11. In this case, joint data acquired for the appropriate Corps Memorandum have been processed in the same manner as for the earlier fabrics, and it will be noted that there is little compatibility between Figure 4.11 and, for example, Figure 4.9, except for the fact that a generally steeply dipping discontinuity field for most azimuthal directions is confirmed. The number of data points upon which both fabrics are constructed is almost the same (84 and 85) and the maximum concentration in both cases is 11% per 1% area. The main concentration in the Corps data is, however, a preferred, near-vertical discontinuity dip at a strike of about  $N110^{\circ}$  E compared with the writers' preferred northerly dip of about  $60^{\circ}$  at about the same strike angle. Since the main concentration in the Corps data is more nearly tending towards a southerly dip, the differences in the two fabrics cannot be accounted for solely by possible errors in angular dip measurements.

Joint strikes as measured by both Corps personnel and by the present writers are entirely compatible with the joint strikes in the coal seams measured in the Appalachian Plateau in Pennsylvania by Nickelson and Hough (1967, plate 2). The orthogonal joint set depicted by Nickelson and Hough op.cit. is indicated much more firmly on the processed Corps data (Figure 4.11) than on the fabric compounded by the present writers from all their ~~dam~~site data (Figure 4.10). Corps data suggests a second concentration of joints dipping S-E at about  $85^{\circ}$  and striking at  $N25^{\circ}$  E. This concentration, at 10%



per 1% area, is only 1% per 1% area less than the amplitude of the dominant concentration. At a similar strike, the secondary concentration of discontinuities in Figure 4.9 is limited to a maximum of 5% per 1% area.

The apparent discrepancy between the orientation densities determined by the Corps and by the present writers is almost certainly related to the geographical position of the data acquisition and to geological structure at the damsite. At the point of interest, the Potomac River flows in a broad synclinal basin which generally follows the gently down-plunging axis of the George's Creek syncline. The dam is located on the left flank and close to the axial plane of the Potomac Syncline (see Plate 5 of the Corps Design Memorandum). Since the Potomac axial plane passes approximately to the right of the dam, the beds are nearly flat on the right abutment but have about 3% plunge on the left abutment. The present writers had the benefit of measuring discontinuities within exposed measures near to the right abutment that would not have been accessible to Nickelsen and Hough, op.cit. nor to the Corps personnel prior to their report preparation. It would seem that the dip of the measures just off the axis of the anticline is responsible for the swing of the jointing dip along the axis of the dam.

No detailed stability analysis on these discontinuities has been attempted for two reasons. First, the foundation strata to the dam, although of varying lithologies, are basically strong. Second, since the line of the dam at 13° E of N is in the plane of maximum concentration full dip (data from both the Corps and the present authors), there would be no question of shear instability along discontinuities even under conditions of vertical stress much greater than will actually be applied to the foundation at maximum construction height (about 296 ft. above the stream bed at the centre line).

#### 4.2 Mineralogy/geochemistry.

All the Pennsylvanian rock types examined in the field are very similar

in lithology to their British equivalents. However, in so far as the clay-shales (claystones) are concerned, the intensity of slickensiding would appear to be greater than in the British equivalents. This is undoubtedly a function of the degree of folding i.e. the tectonic setting of the Appalachians. In terms of Bloomington, Unit 6 CD is highly slickensided claystone, whereas Unit 4 J is very similar to British non-marine shales of Pennsylvanian age.

From Design Memorandum No.8, Part 1 it is clear that the mineralogy of the Pennsylvanian shales and siltstones is similar to British equivalents:- quartz, illite, kaolinite, minor or moderate amounts of mixed-layer clay, minor chlorite and occasional feldspar.

Table 4.1 is a semi-quantitative analysis of all the samples mentioned in the Introduction. Unit 4J was recorded as a soft grey claystone in the borehole log and this is substantiated by its lower quartz content than Unit 6 CD. Alumina ( $\text{Al}_2\text{O}_3$ ), which can be attributed to the clay minerals almost entirely, is somewhat higher in the latter sample (Table 4.2) and this is borne out by the clay minerals total of Table 4.1 \*. The non-detrital iron carbonate, siderite, which is resistant to chemical weathering, is concentrated at a relatively high level in sample 4J. This again is confirmed by the  $\text{Fe}_2\text{O}_3$  values (Table 4.2), particularly when oxides are normalized in terms of alumina. Some of the  $\text{Fe}_2\text{O}_3$  and MgO must be attributed to minor chlorite in Unit 4J, but the higher CaO/Alumina ratio in this sample is almost certainly a function of carbonate affinities.

It can be seen (Table 4.1) that illite plus mixed-layer clay are the dominant clay minerals in all the samples considered in this study (Table 4.1)

---

\* Quantitative estimates of clay minerals are correct within  $\pm 10\%$  (e.g. Reeves 1971). The totals in Table 4.1, which exclude organic carbon and trace minerals such as rutile do not consequently sum to 100%.

On an X-ray diffraction chart, mixed-layer clay occurs as a 'tail' on the low 2 $\theta$  side of the 10A<sup>0</sup> mica reflection. If running conditions are fixed (degrees per minute and amplitude) then the width at half peak height to peak height ratio of the 10A<sup>0</sup> mica reflection can be used to monitor changes in micaceous minerals. For example, a muscovite of high crystallinity from Miami gave a shape factor of 0.0001, whereas the A.P.I. reference Morris illite which contains mixed-layer clay, has a ratio of 0.134 (Taylor 1971). Marine shale from Tinsley Park, Sheffield, England gave a ratio of 0.213 to 0.215 and dark shales from the same horizon (but from a different location) gave ratios ranging from 0.100 to 0.141 (Table 4.1). Similarly in the un-burnt Yorkshire Main Colliery Spoil Heap which comprises dominantly shales and mudstones with minor siltstone, the shape factor is 0.171. Hence, rocks containing micaceous minerals of high crystallinity (e.g. muscovite or hydromuscovite) have a low ratio, whilst those with a higher concentration of mixed-layer clay have a higher ratio.

The two shales from Bloomington have a relatively high shape factor compared with the Savage River sandstone, which has a lower content of illite (strictly speaking, hydromuscovite). It is of interest to record the ? Lower Kittanning underclay which is relatively rich in quartz, has an illite shape factor which is again indicative of hydromuscovite. It is somewhat paradoxical that the latter underclay should have posed problems because mixed-layer clay is the usual source of trouble, being commonly composed of expanding interstratified illite-montmorillonite. The slaking characteristics of the Bloomington shales and mudstones are therefore not unexpected on this score alone.

The K<sub>2</sub>O/alumina ratios for the shales and siltstones are an expression of illite content and mica crystallinity. Thus the illite (mica) in Unit 4J which has a lower mixed-layer content than 6 CD (see shape factors, Table 4.1) has a higher K<sub>2</sub>O/Al<sub>2</sub>O<sub>3</sub> ratio. The ratio of Unit 6CD (Bloomington) is not

unlike that of illite-rich British Coal Measures shales (colliery tips, Table 4.2 \*). The higher  $K_2O$ /Alumina ratio for the Savage River sandstone reflects the higher crystallinity of the mica which is present in a lower concentration than at Bloomington.

It is important to note that the kaolinite (the second most common clay mineral)+ in the Bloomington samples is a disordered type. Alternatively, the clay platelets may be of very small grain size, but this is unlikely because kaolinite is usually of larger grain size than fine-grained illite (see Grim, 1968). Apart from certain underclays, the kaolinite in the British Coal Measures is usually reasonably well-ordered, so this feature may be one aspect of the mineralogy which is different in the two countries - more samples require analysing if this possibility is to be verified. In rocks of Pennsylvanian age,  $Na_2O$  is usually a component of micaceous minerals (including mixed-layer clay). The Savage River sandstone \*\*has a higher ratio than Bloomington because it contains a small percentage of alkali feldspar as well. Similarly, the same applies to the British Coal Measures types (Table 4.2.), because siltstones and sandstones are also present to some extent in spoil-bank materials.

---

\* The 68 samples from British Colliery tips give a good indication of the composition of Coal Measures shale-type rocks in Britain.

+ For currently exploitable coals in Britain 'inert' kaolinite is dominant in the associated rocks of the Northern coalfields. In the Midlands and the Southern coalfields micaceous minerals (including mixed-layer clay) are dominant (Taylor and Spears, 1970).

\*\* This rock type is marginally a siltstone using the British Coal Measures classification of Elliott and Strauss (1970) which is based on quartz content (sandstone > 50%; siltstone 20-50%; mudstone < 20%). Very few geologists however, would classify the two Bloomington samples (Table 4.1) as siltstones.

In general, the similarities in chemistry between the Bloomington specimens and the British Coal Measures are quite marked and it now remains to comment on the Savage River specimens.

Thin sections of the limestone were observed under the microscope. The limestone is comprised mainly of fragmental calcitic shell debris and is therefore classified as a shelly limestone. Free silica (quartz) and clay minerals (probably mica - see  $K_2O/Al_2O_3$  ratio, Table 4.2) are present in very small percentages. Recasting the CaO (Table 4.2) as calcite implies that this rock comprises about 76% calcite.

In contrast, the sandstone has a small calcite contribution. Its red colour is not obvious from the mineralogy because neither hematite nor limonite could be detected by X-ray diffraction. The  $Fe_2O_3$  figure (Table 4.2.) implies that a relatively small amount of ferric mineral is present. Work on other rocks such as slate (for example Attewell and Taylor, 1968) has shown that a very small percentage of hematite is sufficient to give a distinct dark red colour. Similarly, recent work on our colliery tips (Taylor 1973) shows that with low-grade combustion the hematite derived by oxidation of ferrous minerals is finely divided amorphous material, somewhat similar to that found in tropical red soils. This latter type of poorly crystalline hematite would not be detected by X-ray diffraction. It is, therefore, very probable that the small amount of ? hematite or limonite in the Savage River sandstone may be symptomatic of the climatic conditions of the original source area which provided the arenaceous sediment.

#### 4.3. Mechanical characteristics.

The Design Memoranda for Curwensville (No. 8) and Bloomington (No.8, Part I) record very little mechanical data which are applicable to the shale-type rocks themselves. However, certain germane implications do arise and these tend to highlight the many problems pertaining to indurated clay shales.

Invariably, the inherent discontinuities preclude shear tests being carried out on large size specimens. Hence, many results concerning shales in the literature are derived from tests carried out on small intact specimens. At the other end of the spectrum, shales that can be extruded to form small triaxial specimens are commonly very weathered; consequently they show many similarities with sediments. The peak strengths recorded by Mesri and Gibala, (1971) were obtained from non-standard rotary core sized specimens (3 in. long x  $1\frac{1}{2}$  in. diameter). The latter size is however, compatible with specimens extruded for soils work. The peak shear strengths given by the latter authors are possibly those applicable to the shale in a partly weathered condition. In contrast, the unconfined tests carried out on Curwensville material give near-origin high  $\phi$  values which can be expected for rocks with a very high compressive to tensile strength ratio. It is unlikely that these particular Curwensville values are in essence greatly different from the effective stress parameters obtained for similar rock types from the British Coal Measures (Table 4.3). This behaviour represents one extreme, the other being the very low  $\phi_r'$  values which Mesri and Gibala (1971) obtained for pre-cut Pennsylvanian shales and completely remoulded shale sediment.

The intact siltstones are quartz-rich, but with a reduction in this mineral and hence increase in clay minerals, the ability to store strain energy (Price 1959) is reduced and the mudstones (in particular fissile shales) are progressively more jointed and fissured. Their shear strength characteristics are therefore more in keeping with fragmental shales (e.g. the Curwensville Strip Mine waste, Bloomington unprocessed weathered rock, and British colliery tips). The  $\phi'$  range is undoubtedly a function of the argillaceous content.

The next stage in the breakdown towards a fundamental grain size is probably conducive to a fall-off in  $\phi$  to within the range of residual values that are customarily associated with shale-type rocks (compare Bloomington

weathered shale, Misri and Gibala (1971) and McKechnie Thomson and Rodin 1972 - Table 3).

The pre-cut and remoulded residual value of Misri and Gibala (1971) implies that this is the true residual for the fundamental particles on the shear plane are no longer aggregated and hence constrained. However, the shear displacement (comminution process) necessary to reduce a shale to this condition from an initial discontinuous mass would currently seem to be very many tens of metres (based on large-scale shear box tests). The importance of chemical weathering necessarily must be entered as another variable which may accelerate the process, but chemical weathering is a function of climatic conditions.

For clay-shales of Pennsylvanian age it would, therefore, seem reasonable to suggest that a maximum peak  $\phi'$  value of around  $45^\circ$  could be assigned to the more silty types in the discontinuous mass, whereas at the other end of the scale a peak  $\phi'$  of around  $25^\circ$  is not unlikely. Curvature of a Mohr envelope may quite easily result in both values being attributed to the same rock type, but for the usual range of structural loads (e.g. earth-dams) it is feasible to take a normal stress level applicable to the problem in question and rotate the Mohr envelope so that  $c'=0$  (see McKechnie Thomson and Rodin, 1972).

Figure 4.12 (Taylor 1971), shows that  $\phi'_r$  as conventionally determined within the stress range 10 to 40 lb/in<sup>2</sup>, correlates with the quartz/clay minerals ratio (a log-linear relationship). The results shown are for weak rocks in various stages of weathering and some sandstone, siltstone and shale samples were pre-cut. In view of the previous discussion it may well be that the statistical 'best fit' may include residuals in the conventional sense and others in the 'sediment' sense of Misri and Gibala (1971). One could, therefore, pre-suppose that intense weathering could result in a residual somewhat lower than that obtained in the laboratory from an intact core, The quartz

to clay minerals ratio applicable to Figure 4.12 is determined from the integrated area of quartz  $d = 4.26 \text{ \AA}$  to that of the  $7\text{\AA}$  plus  $10\text{\AA}$  clay minerals peaks on the X-ray diffraction chart. Applying this technique to the Bloomington specimens of Table 4.1 suggests that  $\phi'_r$  is around 20 to 21 degrees. Remembering the limitations of the method, this is not greatly different from the Bloomington weathered shale (Table 4.3, shear box). It is therefore of interest to speculate that these latter weathered shales may be close to their residual strength.



TABLE 4.1.

MINERALOGY - X-ray diffraction (semi-quantitative).

	<u>Quartz</u>	<u>Illite &amp; Mixed-layer Clay</u>	<u>Kaolinite</u>	<u>Chlorite</u>	<u>Siderite</u>	<u>Feldspar</u>	<u>Illite shape factor</u>
<u>BLOOMINGTON</u>							
Unit 4J Bh198 *	21	50	6	4	9		0.240
Unit 6CD Bh182 *	31	54	12		Trace		0.268
<u>SAVAGE RIVER</u>							
Sandstone	50	39	4	2	5 (calcite)	Trace	0.164
<u>CURWENSVILLE</u>							
Lr. Kittanning seatearth	33.5	51	16				0.059
<u>Mansfield Cyclothem, Wales, Nr. Rotherham, Yorkshire, England.</u>							
Mudstone							0.073
Dk. shale (5 samples)							0.120
<u>Yorkshire Main Colliery tip</u>							range 0.100 to 0.141
Unburnt shales and silty mudstones (13 samples)							0.171

\* Limits for crushed shale  
Unit 4J LL = 22 PL = 16  
Unit 6CD LL = 24 PL = 16

TABLE 4.2

Major element geochemistry (wt. percentage.)

	SiO <sub>2</sub>	Al <sub>2</sub> O <sub>3</sub>	Fe <sub>2</sub> O <sub>3</sub>	MgO	CaO	Na <sub>2</sub> O	K <sub>2</sub> O	TiO <sub>2</sub>	S	P <sub>2</sub> O <sub>5</sub>	Total
<u>BLOOMINGTON</u>											
1) Unit 4J Sh198	53.16	19.68	12.51	1.86	1.60	0.08	4.25	0.86	0.00	0.30	94.3
2) Unit 6CD Sh 182	55.76	25.67	3.27	0.92	0.65	0.21	4.16	1.16	0.00	0.03	91.83
<u>SAVAGE RIVER</u>											
3) Siltstone/sandstone	56.96	13.72	5.01	2.75	5.54	0.48	3.23	0.74	0.00	0.14	88.57
4) Limestone	14.55	1.59	0.68	0.23	42.99	0.01	0.47	0.11	0.00	0.00	60.63
5) <u>BRITISH COAL MEASURES</u> <u>COLLIERY TIPS (68)</u>	46.29	19.68	5.42	1.02	0.75	0.41	3.38	0.87	0.98*	0.19	78.99
Standard deviation	7.98	2.67	2.77	0.35	0.74	0.20	0.56	0.10	0.73	0.28	

100% - total

\* Organic carbon,  
CO<sub>2</sub> and H<sub>2</sub>O\* occurring as  
pyrite (from the  
coal) or as  
sulphate (ex-  
oxidation processes)Ratios (÷ Al<sub>2</sub>O<sub>3</sub>)

	SiO <sub>2</sub>	Fe <sub>2</sub> O <sub>3</sub>	MgO	CaO	Na <sub>2</sub> O	K <sub>2</sub> O	Na <sub>2</sub> O/K <sub>2</sub> O
1)	2.70	0.64	0.09	0.08	0.004	0.22	0.019
2)	2.17	0.13	0.04	0.03	0.008	0.16	0.050
3)	4.15	0.37	0.20	0.40	0.035	0.24	0.149
4)	9.15	0.43	0.14	27.04	0.006	0.30	0.021
5)	2.35	0.28	0.05	0.04	0.021	0.17	0.121

TABLE 4.3

	<u>Undrained</u>		<u>Triaxial</u>		<u>Shear-box</u>		<u>Shear-box</u>		
	LL %	PL %	$\phi_u$ degrees	Cu T/ft <sup>2</sup>	$\phi'_p$ degrees	C' <sub>p</sub> lb/in <sup>2</sup>	$\phi'_p$ degrees	C' <sub>p</sub> lb/in <sup>2</sup>	$\phi'_r$ degrees
Grey shale									
<u>Caseyville</u> <u>Formation</u>	37	22			29-32		29	38	19 11 *
(Mesri & Gibala 1971)									
Curwensville							26-38.5	0	
D.M.No.8							35-39	0	
Plate 8-24									
<u>Strip Mine Waste</u>									
Curwensville									
<u>?underclay</u> (Table 3)			28.3	6.25					
Carbonaceous			81.5	7.5					
<u>Siltstone</u> (Table 3)			81.7	1.83					
Bloomington									
TP-C, CH-48	44	21	4.5	1.2	15.5	0	17.7-18		
DM.No.8			8.5	0.6					
Part I									
<u>Weathered</u> <u>Shale</u>									
Bloomington	28	21			38	0			
Unprocessed	to	to							
<u>Weathered</u> <u>Rock</u>	31	20							
(Plate 41)									
Range for									
<u>British Colliery</u> <u>tips.</u>					25-40	0			17.5-22.0 (McKechnie Thomson & Rodin 1972)
<u>weathered shale</u> <u>and mudstone</u>	39	26			28.5	1.39			
Gt.Britain	to	to							
(Spears & Taylor, 1972)	49	30							
<u>Siltstone(lower)</u>							(1)*		
Gt.Britain	30	19			77.5	58.58	28.0		
low confining	to	to					(2)*		
pressures	35	28					35.0		
high confining									
pressures									
(Spears & Taylor, 1972)					34.0	2000			

129

\* pre-cut and remoulded samples (1) saturated (2) non-saturated

CHAPTER 5.

MINERALOGICAL AND GEOCHEMICAL STUDY OF CUCARACHA  
CLAY SHALE SAMPLES TAKEN DURING A FIELD INVESTIGATION  
IN THE PANAMA CANAL ZONE.

5.1 Introduction.

In mid-December, 1971, six horizons of the unstable Cucaracha formation were sampled. Three of the horizons sampled are designated Lower Cucaracha, being an embankment exposure (devoid of vegetation) just to the north-west of the East Culebra extension slide (Old Station 1769 E). The other three samples (designated Upper Cucaracha) were from Cerro Escobar hill (Old Station 1830, traverse at right angles to Canal), which is capped by basalt.

All the specimens were of slickensided and fissured 'clay-shale' type, the descriptions being as follows:

<u>Sample</u>	<u>Description*</u>	<u>Location</u>
3 Up.Cucaracha	Purple-red shaly mudstone with sharp upper boundary: fissured.	Cerro Escobar (30 ft. below basalt)
2 Up. Cucaracha	Grey-green silty mudstone; fissured and slickensided (mammoth remains(phosphatic) on surface of outcrop)	Cerro Escobar (100 ft. from highway)
1 Up. Cucaracha	Greenish-grey shaly mudstone; heavily slickensided.	Cerro Escobar (50-60 ft. from highway)
A1 Lr.Cucaracha (orientated specimen)	Mottled grey-brown heavily slickensided shale: clay ironstone nodules lying on surface of exposure.	N.W. of extension slide (elevation 190 ft.)
B1 (orientated) B2 (disturbed) Lr.Cucaracha	Green grey heavily slickensided shale with iron-staining.	N.W. of extension slide, 8 ft. vertically below A1
C1 & C2 (orientated) Lr.Cucaracha	Grey slickensided and fissured silty shale, Specimen C1 more iron-stained than C2.	20 ft. above conglomerate band.

\* colour after oven drying.

According to Mr. R.H. Stewart (P.C.C.) locations A,B and C were close to a fault. The dip of the strata as measured in the field however, was 2 to 5° East. It is also worth noting that the Cucaracha clay-shale materials of Miocene age are notorious for their slaking behaviour in water and their low residual shear strength ( $\phi'_r = 7.12^\circ \pm 1.52^\circ$ , 15 results; c.f peak  $\phi' = 18.86^\circ \pm 4.85^\circ$ ,  $c'_p = 29.00 \pm 35.22 \text{ kN/m}^2$ , 7 results).

The purpose of the current report is to record the mineralogical and geochemical characteristics of the horizons sampled and to place these findings in the context of previous work (summarized by Lutten and Banks, 1970).

#### 5.2. Mineralogical and chemical methods.

Representative sub-samples of all horizons were analysed in a Philips PW 1212 X-ray fluorescence spectograph, using previously wet analysed standards which closely bracket the unknowns. Computer processing allows standards to be selected so that the calibration between them and the unknowns is such that the ultimate analyses attain a very high degree of precision. Major elements, and elements expressed as oxides (Table 5.1), are on a water-free, carbon dioxide-free and organic carbon-free basis.

Early work (e.g. MacDonald, 1915) implied that the clay minerals of the Cucaracha were dominated by the mineral chlorite. In more recent times, however, it has been eminently clear that montmorillonite is the major clay mineral present. Because the exchangeable cations associated with the smectite group of minerals have an important bearing on their behaviour it was decided to determine exchangeable Na, K, Ca and Mg. using the ammonium acetate (see Spears, 1973 for details of the method currently adopted), Cation exchange capacities are given in Table 5.2.

A Philips PW 1130 3 Kw X-ray machine (Fe filtered, Co radiation) was used to identify the minerals present in the samples and to assess quantitatively quartz, carbonates and clay minerals, (Table 5.3). Additional techniques such as progressive hydration, glycolation, acid dissolution and heat treatment were used in an attempt to identify clay mineral species in more detail.

### 5.3. Thin sections and X-ray texture goniometry.

From the orientated, undisturbed samples it was only possible to impregnate one specimen (sample C.2) using Carbowax 6000. Other impregnating techniques were also tried (see Attewell and Taylor, 1971), but unfortunately rapid slaking precluded the making up of either thin sections or X-ray goniometer disc specimens. The thin sections and X-ray texture specimens from C.2 were cut orthogonally and aligned with respect to magnetic north. The former were examined optically in detail and the latter processed using a Philips texture-goniometer used in conjunction with a PW 1310 2 kW diffractometer (see Attewell and Taylor, 1971, for details).

Because montmorillonite is unsuitable for X-ray texture work (the main reflection having a Bragg angle which is lower than those conventionally resolved) it was necessary to scan the  $7\text{\AA}^0$  kaolinite/chlorite peak. The texture output did not reveal any strong preferred orientation and although the clay minerals are exceedingly fine-grained and at the limit of optical resolution the same conclusion can be drawn from the thin sections. Several striking textural features could be elucidated from the thin sections and because they may well have a bearing on the subsequent behaviour of these rocks, they will be considered prior to the mineralogy and chemistry.

#### 5.3.1. Thin Section observations.

It is accepted that the Cucaracha source materials were volcanic in origin (e.g. Thompson, 1947). Occasional angular, very cloudy rock fragments up to 3.5 mm. in size, may well represent degraded parental material. Of more

importance, however, are more rounded (often pseudomorphic) fragments of similar size which are optically identical to the ground mass clay. In other words, there is some evidence that this lower Cucaracha shale has itself been re-worked after deposition, possibly in an environment not unlike that postulated for seatearths, or underclays (see Moore, 1968 p.120). Although the interconnected curvilinear slickensides of the Cucaracha are not unlike those developed at some horizons in seatearths, there is a marked absence of rootlets in the Cucaracha, so any analogy is by no means direct.

Another important feature mentioned by Mead and MacDonald (1924) concerns the discontinuities in the rock. Evidence that there was an early phase of shrinkage (presumably after the shale had been re-worked) is seen from the fact that secondary clay mineral growths occur around some of the included fragments. Optically, these secondary clay minerals are micaceous in character, but the fact that micaceous minerals were not identified by X.R.D. and are therefore below the level of detection by X-ray diffraction implies that on a weight percentage basis they are present in very low concentrations indeed. Other ragged discontinuities (probably shrinkage cracks) which in places appear to grade into slickensides are an interesting phenomenon on their own merits.

Sample C.2 contains myriads of spherulitic siderite ( $\text{Fe CO}_3$ ) bodies, most of which are nucleated around a chlorite grain. These spherulitic bodies (of 0.1 mm. average diameter) tend to concentrate, particularly along the ragged discontinuities. It is generally accepted that siderite is an early diagenetic carbonate, so the above relationship suggests that the shrinkage discontinuities pre-date the formation of siderite, and hence the discontinuities themselves must represent a very early sedimentological feature. The probable inter-relationship of the shrinkage discontinuities and the slickensides could well imply that the former would be subject to shear stresses under a rapidly accumulating over-load and slickensiding would be induced. i.e. the slickensides being developed from the earlier shrinkage cracks.

In preparing the thin sections it is very clear that, under conditions of desiccation, discontinuities around the rock fragment inclusions, together with the inherent shrinkage cracks and the slickensides open up, thus reducing the mass strength. A similar situation can be envisaged in the field.

Amongst the minerals identified as relatively rare constituents under the microscope were plagioclase feldspars, chlorite, ? feldspathoids and strained quartz grains up to 0.03 mm. in size. Most of the quartz content (see Table 6.3) must therefore be of clay-grade size.

#### 5.4. Chemical and mineralogical considerations.

From Tables 5.1, 5.2 and 5.3, certain features of the sediments can be elucidated.

1. In the first instance it is pertinent to note the quartz is present at quite a high level in all samples, except for sample 3. Sample 2 and horizon C should perhaps be regarded as siltstones from their quartz content.
2. The principal clay mineral present is montmorillonite (Table 5.3). However, the areal ratios of montmorillonite/boehmite (Table 5.3b) are not in direct proportion to the amount of montmorillonite computed by subtraction of the other principal mineral components from 100%. This could infer that the composition of the montmorillonite may be variable.

Cation exchange capacities (CEC) recorded in Table 5.2 show that Ca is the dominant exchangeable cation present in all horizons. In the Interim Report (31.5.72), exchangeable Ca was considered to be unreliable in the Ampthill sediments (Gt. Britain) because of interference by carbonates and sulphates. With the Cucaracha formation, however, Ca, Mg, Mg carbonate is only present to a marked degree in sample 1 and from Table 5.1 (sulphur values) it is clear that sulphates will be absent in virtually all horizons. The sulphur that is present in two samples can be more readily attributable to organic carbon and pyrite. Hence, apart from sample 1 the exchangeable Ca is of significance. The interim Report showed that exchangeable Na could be



closely related to montmorillonite in the Wyoming bentonite and the Stafford tonstein (see Table 5.2 f and c). The maximum amount of Na-montmorillonite in the mixed-layer clay component of the Amphill was believed to be less than 10 per cent. On the other hand, the Wyoming bentonite is dominantly a Na-montmorillonite and the Stafford tonstein contain 70 per cent mixed-layer clay which comprises 65 per cent mica and 35 per cent montmorillonite. The slaking behaviour and swell pressures obtained for the Stafford tonstein are not inconsistent with a Na-montmorillonite component.

Exchangeable Na in these Cucaracha samples is only of significant interest in horizon 1 for which the  $15 \text{ \AA}^0$  monmorillonite peak area to  $6.18 \text{ \AA}^0$  boehmite area ratio is low compared with, say, sample 2 which contains about the same proportion of the mineral by subtraction.

Based on the behaviour of this clay mineral on treatment (Table 5.3 c) and the exchangeable cations, there is strong evidence that the Cucaracha contains dominantly Ca-montmorillonite with a subsidiary Na-rich interstratification. It should be borne in mind, however, that Na-saturated montmorillonite may expand in water to such an extent that it dissociates into platelets which are of the same order of thickness as the unit cell ( $10 \text{ \AA}^0$ ) (see Gillott, 1968).

From sample 3, quartz was deducted from the total  $\text{SiO}_2$  (see Table 5.1 and 5.3) and after making allowance for the Kaolinite present, the chemistry was re-computed after Nagelschmidt (1938) in order to derive a proximate chemical formula for the montmorillonite component. The resulting formula ( $\text{Si}_{3.44} \text{ Al}_{1.73} \text{ Fe}_{0.76} \text{ Mg}_{0.18} \text{ O}_{11}$ ) would imply that on Nagelschmidt's ternary plot the mineral corresponds closely to a beidellite.

3) Of all the areas along the canal which have been limed it is unlikely that this could apply to the area from which samples A to C were taken.

Lime treatment in the field may provide a means of stabilizing Na-montmorillonite by C E C , but any major policy involving this technique should now be carefully considered in view of the dominance of Ca as the exchangeable cation, at least in the near-surface zone samples examined.

It has been mentioned that a remote possibility exists that areas like Cerro Escobar may have already been limed (exchangeable Na possibly having already been replaced), but this could always be checked.

4) A  $7A^{\circ}$  mineral which appears to be highly disordered with a broad, ragged, two-tailed reflection is thought to be kaolinite rather than chlorite. We know from microscopic examination that chlorite is present. However, the following points mitigate against chlorite as being the second most important mineral in these samples: i) no  $14A^{\circ}$  X-ray reflection was recorded, ii) heat treatment results in the disappearance of the  $7A^{\circ}$  reflection (a positive kaolinite test), iii) warming sample 3 in dilute HCl at  $80^{\circ}\text{C}$  overnight did not reduce the 7A reflection significantly (see Brown, 1961 re. tests pertaining to chlorite of poor crystallinity).

5) Siderite and calcite have been recorded as non-detrital minerals present at two horizons. The chemistry (Table 5.1 b) infers that the 'calcite' may be a slightly more complex Ca,Fe, Mg, Mn carbonate. The slightly enhanced  $P_2O_5$  figure for this horizon is indicative of a phosphatic mineral (? organic affinities), which would mean only about 1.6% by weight if the mineral is hydroxyapatite.

6) It will be recalled that sample 3 horizon is purple-red in colour. There is no evidence from the chemistry (Table 5.1) of any leaching, so a penecontemporaneous buried soil origin (Mead and MacDonald, 1924) is unlikely. The enhanced  $Fe_2O_3$  value of sample 3 and the colour may well

imply the presence of very finely divided haematite. A very small amount of this mineral will produce the colour effect. The proximity of the overlying basalt is a more reasonable source for early oxidising effects (see Lutton and Banks, 1970).

The above appraisal should be read in conjunction with Table B3, Lutton and Banks, 1970, which summarizes earlier mineralogical work.

It was mentioned in the interim report (with respect to the British Upper Jurassic Ampthill Clay) that exchangeable Mg. values for marine shales are generally higher than those of non-marine shales. Lutton and Banks (1970) refer to the Culebra formation in terms of marine deposition, with the Cucaracha being generally non-marine. The higher Mg C.E.C. of the Lower Cucaracha could imply that these beds have quasi-marine affinities, and comparison with Culebra sediments would be of interest.

#### 5.5. Comparison of the chemistry of the Cucaracha with N.American and British Clay-shales.

Although the Student's - t test is a comparison of sample means and does not take into account variance, it is of interest to compare Cucaracha samples with Up. Cretaceous/Tertiary samples from the U.S.A. and with the Jurassic-Cretaceous specimens from Britain. Chemistry is more sensitive than mineralogy in such circumstances so the comparisons are made on this basis (Table 5.4).

The general conclusion is that there is a greater difference between the Cucaracha and the N.American chemistry than there is between the former, and the older British clay-shales. Careful examination of the values are necessary to bring out the general trends. The elevated quartz contents of N.American samples are referred to elsewhere in the Report and this feature is brought out by the total  $\text{SiO}_2$  means (Table 5.4). In terms of specific clay minerals, the mica-rich British shales are highlighted by  $\text{K}_2\text{O}$  comparisons. However, although  $\text{Na}_2\text{O}$  in the Cucaracha and British shales is not significantly different; the clay mineral types in which this element is found are different (montmorillonite in the former, dominantly micaceous minerals in the latter).<sup>137</sup>

The fact that the N.American shales have a higher (significantly different)  $\text{Na}_2\text{O}$  mean than the Cucaracha is pertinent. The general conclusion has already been drawn that the montmorillonite in the Cucaracha is dominantly a Ca-rich variety and tentative backing evidence is, therefore, provided by comparison with the N.American rocks which also contain montmorillonite. The latter rocks have a significantly higher  $\text{Na}_2\text{O}$  mean (Table 5.4).

#### 5.6. Atterberg Limits.

Published Atterberg limits for the Cucaracha show that there may be quite large variations from sample to sample. With the remaining material, it was possible to determine limits for Sample B1 and a mixture of samples 1 and 2 (Table 5.5). Sample B1 with an overall high clay content has elevated limits, whilst the combined sample with a much lower clay content (higher quartz and carbonate values) shows significantly lower limits.

TABLE 5.1.

a) Chemical Analyses Wt.%

Sample	<u>SiO<sub>2</sub></u>	<u>Al<sub>2</sub>O<sub>3</sub></u>	<u>Fe<sub>2</sub>O<sub>3</sub></u>	<u>MgO</u>	<u>CaO</u>	<u>Na<sub>2</sub>O</u>	<u>K<sub>2</sub>O</u>	<u>TiO<sub>2</sub></u>	<u>MnO</u>	<u>S</u>	<u>P<sub>2</sub>O<sub>5</sub></u>	<u>Total.</u>
3	48.88	19.97	11.08	1.34	2.01	0.24	0.41	0.93	0.05	0.00	0.05	84.96
2	60.06	16.09	8.03	1.58	2.01	0.26	0.15	1.21	0.08	0.25	0.05	89.76
1	44.07	14.16	7.52	1.31	12.47	0.07	0.41	0.73	0.57	0.00	0.69	82.63
A1	54.83	18.50	9.08	1.76	1.40	0.32	0.73	1.13	0.02	0.00	0.04	87.81
B1	54.33	18.66	9.13	1.70	1.41	0.37	0.72	1.14	0.01	0.00	0.03	87.50
C2	51.43	16.63	12.42	1.74	2.27	0.16	0.74	1.50	0.20	0.15	0.13	87.37

CO<sub>2</sub> = 6.14%, organic C = 0.05%, H<sub>2</sub>O = and - = 6.44% (by deduction from 100%)

b) Using alumina (Al<sub>2</sub>O<sub>3</sub>) as denominator (i.e. in terms of clay mineral content)

Sample	<u>Total SiO<sub>2</sub></u>	<u>Fe<sub>2</sub>O<sub>3</sub></u>	<u>MgO</u>	<u>CaO</u>	<u>Na<sub>2</sub>O</u>	<u>K<sub>2</sub>O</u>	<u>MnO</u>
3	2.96	0.491	0.095	0.076	0.017	0.039	0.001
2	2.91	0.489	0.091	0.076	0.020	0.039	0.001
1	3.09	0.747	0.105	0.137	0.010	0.044	0.012
A1	3.11	0.531	0.093	0.881	0.005	0.029	0.040
B1	3.73	0.499	0.098	0.125	0.016	0.009	0.005
C2	2.45	0.555	0.067	0.101	0.012	0.021	0.003

TABLE 5.2.

Cation Exchange Capacities (C.E.C. in m.eq/100g.)

a) Panama

<u>Sample</u>	<u>Na</u>	<u>K</u>	<u>Ca</u>	<u>Mg.</u>
3	4.8	1.2	48.1	5.9
2	2.1	4.3	42.7	11.5
1	10.8	4.4.	100.7	7.2
A1	3.1	1.3	34.9	14.4
B1	0.4	1.2	47.6	17.9
C2	2.2	1.3	30.1	17.0

b) Amphill Clay

B4	1.5	1.7	30.3	22.4
U7	5.2	2.2	116.8	14.4
CF	1.3	1.7	102.4	6.3

c) Stafford tonstein (mudstone, ex-volcanic fall-out)

14.2	4.9	6.1	2.5
------	-----	-----	-----

d) Coal Measures Marine shale (LS 24)

1.6	1.1	3.6	12.9
-----	-----	-----	------

e) Harvey seatearth (Coal Measures)

5.3	2.8	3.9	1.2
-----	-----	-----	-----

f) Wyoming Bentonite (1)

54.0	-*	11.0	15.0
------	----	------	------

g) Kaolinite (1)

-*	-*	0.5	0.4
----	----	-----	-----

\* below detection level

(1) Carroll and Starkey (1958).

TABLE 5.3.

X-ray Diffraction data.

a) Mineralogical Suite.

<u>Sample</u>	<u>Quartz</u>	<u>Kaolinite/Chlorite</u>	<u>Montmorillonite*</u>	<u>Carbonate</u>	<u>Plagioclase Feldspar</u>
3	7.0	10.2	82.8		-
2	38.7	3.5	57.8		? trace
1	20.0	5.0	56.0	19.0 calcite	Present = 5%
B1	15.8	9.0	75.2		? Trace
C1	31.0	19.0	50.0		Present = 5%
C2				16.18(1) siderite	

\* subtraction of total major components from 100%

(1) Re-calculated from chemical analyses

b) Montmorillonite/boehmite 6.18 Å<sup>0</sup> ratios.

<u>Sample</u>	<u>3</u>	<u>2</u>	<u>1</u>	<u>B1</u>	<u>C1</u>
	6.40	9.60	3.02	6.61	7.16

c) Treatments (Montmorillonite)

<u>Sample</u>	<u>Treatment</u>	<u>d Å Spacings</u> <sup>0</sup>	<u>Remarks</u>
3	Ethylene Glycol.	17.25	Expansion from 15.0 Å <sup>0</sup>
3	Air dry	15.09	
3	Heated at 100°C 1 hour	13.10	
3	Saturated in water overnight.	19.36 Å <sup>0</sup>	? some Na montmorillonite.

TABLE 5.4.

Comparison of chemical means (Student's -t test) of Cucaracha with

N. American and British samples (data normalized to 100%)

	<u>Means</u>			<u>Means</u>		
	<u>Cucaracha</u>	<u>U.S.A.</u>	<u>Significance</u>	<u>Cucaracha</u>	<u>Gt. Britain</u>	<u>Significance</u>
SiO <sub>2</sub>	60.26	67.00	Different 99.9%	60.26	56.39	Different 98%
Al <sub>2</sub> O <sub>3</sub>	20.02	17.60	Different 99%	20.02	22.11	Not sig.diff.
Fe <sub>2</sub> O <sub>3</sub>	11.03	5.55	Different 99.9%	11.03	6.13	Different 99.9%
MgO	1.81	2.35	Not sig.diff.	1.81	1.93	Not sig.diff.
CaO	4.27	1.49	Different 99%	4.27	6.37	Not sig.diff.
Na <sub>2</sub> O	0.27	1.41	Different 99%	0.27	0.41	Not sig.diff.
K <sub>2</sub> O	0.61	2.73	Different 99.9%	0.61	3.65	Different 99.9%
TiO <sub>2</sub>	1.28	0.80	Different 99.9%	1.28	0.99	Different 99%
MnO	0.19	0.11	Not sig. diff.	0.19	0.08	Not sig. diff.
S	0.08	0.83	Different 99.9%	0.08	1.80	Different 99.9%
P <sub>2</sub> O <sub>5</sub>	0.20	0.30	Not sig.diff.	0.20	0.15	Not sig. diff.

Panama (Cucaracha) = 6 samples

U.S.A. = 46 samples

G.B. = 20 samples

TABLE 5.5.Liquid and Plastic Limits (Air dried material)

	<u>Liquid Limit</u>	<u>Plastic Limit</u>	<u>Plasticity Index</u>
Sample B1 (Lr. Cucaracha)	108	50	58
Combined samples 1 & 2 (Up. Cucaracha)	61	29	32



REFERENCES

- Attewell, P.B. and Sandford, M.R. (1971), 'On an energy criterion of failure for intrinsically anisotropic rock', Symposium of the International Society of Rock Mechanics, Paper 11-4, Nancy, France.
- Attewell, P.B. and Taylor, R.K. (1968), 'A Microtextural Interpretation of a Welsh Slate', Int. J. Rock Mech. Min. Sci., Vol. 6, pp 423-438.
- Attewell, P.B. and Taylor, R.K. (1971), 'Jointing in Robin Hood's Bay, North Yorkshire Coast, England.' Int. J. Rock Mech. Min. Sci., Vol. 8 pp 477-481.
- Attewell, P.B. and Taylor, R.K. (1971), 'Investigations, tests and experiments on the mechanical strength and breakdown characteristics of certain overconsolidated clay shales.' Interim and Final Reports on DA-ERO-S91-70-G0002 to European Research Office, U.S. Army.
- Attewell, P.B. and Taylor, R.K. (1972), 'Clay shale and discontinuous rock mass studies.' Interim Report DA-ERO-591-72-G0005 to European Research Office, U.S. Army, 31st May.
- Attewell, P.B. and Taylor, R.K. (1973), 'Geochemical, mineralogical and geotechnical comparisons between some N.American and some British clay shales.' Final Report DA-ERO-591-72-G0006 to European Research Office, U.S. Army, 8 April.
- Attewell, P.B. and Woodman, J.P. (1972), 'Stability of Discontinuous Rock Masses under Polyaxial Stress Systems, Stability of Rock Slopes, 13th Symp. on Rock Mechanics, Univ. of Illinois, U.S.A. 1971, pp 665-683.
- Banks, D.C. (1972), 'Study of clay shale slopes; 'Stability of Rock Slopes,' 13th Symp. on Rock Mech., Univ. of Illinois, 1971, Ed. E.J. Cording, Publ. A.S.C.E., pp 303-328.
- Barden, L. (1973), Reply: 'The Influence of Structure on Deformation and Failure in Clay Soil', Géotechnique, Vol. 23, pp 130-131.

- Bhatia, H.S. (1969), in: 'Engineering Properties and Behaviour of Clay-Shales.' (Reporter: S.J. Johnson) 7th Int. Conf. Soil Mech. Found. Engineering, Mexico City, Vol. 3, pp 483-488.
- Bhattacharyya, K.K. and Boshkov, S.H. (1970), 'Determination of the Stresses and the Displacements in Slopes by the Finite Element Method,' Proc. 2nd Congress, Int. Soc. for Rock Mechanics, Belgrade, Vol. 3 pp 339-344.
- Bishop, A.W. (1952), 'The stability of earth dams', Ph.D. thesis, Imperial College, London, England.
- Bishop, A.W. (1966), 'The strength of soils as engineering materials.' Géotechnique, Vol. 16, pp 91-128.
- Bishop, A.W. (1971), 'The influence of progressive failure on the choice of the method of stability analysis.' Géotechnique, Vol. 21, No. 2, pp 168-172.
- Bjerrum, L. (1967), 'Mechanism of progressive failure in slopes of over-consolidated plastic clays and clay-shales.' Proc. A.S.C.E. (J. Soil Mech. & Found. Div.), Vol. 93, SM5, pp 1-49.
- Brawner, C.O. (1970), 'Stability Investigations of Rock Slopes in Canadian Mining Projects,' Proc. 2nd Int. Congress, Int. Soc. for Rock Mechanics, Vol. 3, pp 317-327.
- Brooker, E.W. (1967), 'Strain energy and behaviour of overconsolidated soils.' Canadian Geotechnical Journal, Vol 2, pp 326-333.
- Brooker, E.W. and Ireland, H.O. (1965), 'Earth pressures at rest; related to stress history.' Canadian Geotechnical Journal, Vol. 2, pp 1-15. **144**
- Brown, E.T. (1970), 'Modes of Failure in Jointed Rock Masses.' Proc. 2nd Congress Int. Soc. for Rock Mechanics, Belgrade, Vol. 2, pp 293-298.

- Brown, G. (1961), 'The X-ray identification of crystal structures of clay minerals.' Mineralogical Society, London, 544 p.
- Capper, P.L. and Cassie, W.E. (1957), 'The Mechanics of Engineering Soils.' Publ. E. and F.N. Spon. 2nd Edition.
- Carroll, D. and Starkey, H.C. (1958), 'Effect of Seawater on Clay Minerals.' Proc. 7th National Conference on Clays and Clay Minerals. Pergamon Press, 80-101.
- Casagrande, A. (1937), 'Seepage through Earth Dams.' New England Water Works Association, Vol. 51, No. 2.
- Chandler, R.J. (1970), 'Shallow slab slide in the Lias Clay near Uppingham, Rutland.' Géotechnique, Vol. 20, pp 253-260.
- Chandler, R.J. (1970), 'Solifluction on low-angled slopes in Northamptonshire.' Quarterly Journal of Engineering Geology, Vol. 3, pp 65-69.
- Chandler, R.J. (1972), 'Lias Clay: weathering processes and their effect on shear strength.' Geotechnique, Vol. 22 pp 403-431.
- Clough, R.W. and Woodward, R.J. (1967), 'Analysis of embankment stresses and deformations.' Journ. of Soil Mechanics and Foundations Div., A.S.C.E., Vol. 93, No. SM4, pp 529-549.
- De Boer, G., Neale, J.W. and Penny, L.F. (1958), 'A guide to the geology of the area between Market Weighton and the Humber.' Proc. Yorks. Geol. Soc., Vol. 31, pp 157-209.
- Elliott, R.E. and Strauss, P.G. (1970), 'A Classification of Coal Measures Rocks Based on Quartz Content.' Compte.Rendu 6 e Congrès Intern.Strat. Géol. Carbonif., Sheffield, 1967, Vol. 2 pp 715-724.
- Ergün, I. (1970), 'Stress Distribution in Jointed Media' Proc. 2nd Congress Int. Soc. for Rock Mechanics, Belgrade, Vol. 1 pp 497-507.
- Fleming, R.W., Spencer, G.S. and Banks (1970), 'Empirical study of behaviour of clay shale slopes.' N.C.G. Technical Report No. 15 (2 Vols.), U.S. Army Engineer Nuclear Cratering Group, Livermore, Calif.
- Gay, N.C. (1970), 'The formation of step structures on slickensided shear surfaces.' J. Geol., Vol. 78, pp 523-532.

- Gillot, J.E. (1968), 'Clay in Engineering Geology', Elsevier Publ. Co., 296 p.
- Grice, R.H. (1969), 'Test procedures for the susceptibility of shale to weathering'. In: Johnson, S.J. (Reporter), 'Engineering properties and behaviour of clay-shales'. Speciality Session No.10. Proc. 7th Int. Conf. Soil Mech., Mexico City, Vol. 3 p.884
- Grim, R.E. (1962), 'Applied clay mineralogy'. McGraw Hill Book Co., Inc. New York.
- Grim, R.E. (1968), 'Clay Mineralogy', McGraw-Hill, New York, 596 p.
- Hardy, R.M. (1969), In: 'Engineering Properties and Behaviour of Clay-Shales' (Reporter: S.J. Johnson). 7th Int. Conf. Soil Mech. Found. Engineering, Mexico City, Vol. 3, pp 483-488.
- Henkel, D.J. (1972), 'The relevance of laboratory-measured parameters in field studies. Stress strain behaviour of soils.' Rowe Memorial Symp. Ed. R.H.G.Parry, Pub. Foulis, pp 669-675.
- Heuze, F.E., Goodman, R.E. and Bornstein, A. (1971), "Numerical Analyses of Deformability Tests in Jointed Rock - 'Joint Perturbation' and 'No Tension' Finite Element Solutions:" 2nd Int. Cong., Int. Soc. of Rock Mechanics, Belgrade, Vol. 3, pp.13-24.
- Hoek, E. (1970), 'Estimating the stability of Excavated Slopes in Opencast Mines.' Sect. A: Min. Industry Trans. Inst. Min. Metal., Vol. 79, pp 109-132.
- Hutchinson, J.N. (1967), 'The Free Degradation of London Clay Cliffs.' Proc. Geotechnical Conf., Oslo, Vol. 1, pp 113-118.
- Hutchinson, J.N. (1969), 'A Re-consideration of Coastal Landslides at Folkestone Warren, Kent.' Géotechnique, Vol. 19, pp.6-38.
- Iverson, N.L. (1969), In: 'Engineering Properties and Behaviour of Clay-Shales.' (Reporter: S.J. Johnson). 7th Int. Conf. Soil Mech. Found. Engineering, Mexico City, Vol. 3, pp 483-488.
- Jaeger, J.C. and Cook, N.G.W. (1968), 'Fundamentals of Rock Mechanics,' Methuen, London, 513 p.

- Jennings, J.E. (1970) 'A Mathematical Theory for the Calculation of the Stability of Slopes in Open Cast Mines, Planning Open Pit Mines , Symposium Johannesburg, Ed. P.W.J. van Rensburg, Publ. A.A. Balkema, Cape Town, pp 87-102.
- John, K.W. (1968), 'Graphical Stability Analysis of Slopes in Jointed Rock.' J. Soil Mechanics and Foundations Div., A.S.C.E. Vol. 94, pp 497-526.
- John , K.W. (1970a) 'Engineering Analyses of Three Dimensional Stability Problems Utilizing the Reference Hemisphere.' Proc. 2nd Congress, Int. Soc. for Rock Mechanics, Belgrade, Vol. 3, pp 385-391.
- John ,K.W. (1970 b) 'Three Dimensional Stability Analyses of Slopes in Jointed Rock, Planning Open Pit Mines, Symposium, Johannesburg, Ed. P.W.J. Rensburg, Publ. A.A. Balkema, Cape Town, pp 87-102.
- Johnson, S.J. (1969), 'Engineering properties and behaviour of clay-shales,' Speciality Session 10, Proc. 7th Int. Conf. Soil Mechanics Found. Engineering, Mexico City, Vol. 3, pp 483-488.
- Kennard, M.F., Knill, J.L. and Vaughan, P.R., (1967), 'The geotechnical properties and behaviour of Carboniferous Shale at Balderhead Dam.' Q. Jl Engng Geol. Vol 1 pp 3-24.
- Kenney, T.C. (1967), 'The influence of mineral composition on the residual strength of natural soils.' Proc. Geotechnical Conf., Oslo, Vol. 1 pp 123-129.
- Kenney, T.C., Moum, J. and Berre, T. (1967), 'An Experimental Study of Bonds in a Natural Clay.' Proc. Oslo Geotech. Conf., Vol. 1 , pp 65-69.
- Kley, R.J. and Lutton, R.J. (1967), 'A study of selected rock excavations , as related to large nuclear craters,' PNE 5010, U.S. Army Engineer Nuclear Cratering Group, Livermore, Calif., U.S.A.
- Kuznecov, G.N. (1970), 'Graphische Methode zur Ermittlung der Grenzzustände des inhomogenen, Klüftigen Gebirgskörpers' Rock Mechanics, Vol. 2 pp 75-92.

- Lane, K.S., (1969), In: 'Engineering Properties and Behaviour of Clay-Shales.'  
7th Int. Conf. Soil Mech. Found. Engineering. (Reporter:S.J.Johnson),  
vol. 3, pp 483-488.
- Londe, P. Vigier, G. and Vormeringer, R. (1969), 'Stability of Rock Slopes,  
a Three-Dimensional Study,' J. Soil Mech. and Foundations Div., A.S.C.E.  
Vol. 95 (SM1), pp 235-262.
- Lutton, R.J. (1970), 'Fractures and failure mechanics in loess and  
applications to rock mechanics.' U.S. Waterways Experiment Station -  
Research Report S-69-1Aug.1969.
- Lutton, R.J. and Banks, D.C. (1970), 'Study of Clay Shale Slopes Along the  
Panama Canal,' Report 1 East Culebra and West Culebra Slides and the  
Model Slope. Technical Report S-70-9 U.S. Army Engineer Waterways  
Experiment Station, Vicksburg, Mississippi, 285 pp
- MacDonald, D.F. (1915), 'Some Engineering Problems of the Panama Canal  
in their Relation to Geology and Topography,' U.S. Bureau of Mines  
Bulletin 86, 86 pp.
- McKechnie Thomson, G and Rodin, S. (1972), 'Colliery Spoil Tips - After  
Aberfan' Proc. Instn Civ. Engrs. Paper 7522, 1972, 59 p.
- Mahtab, M.A. and Goodman, R.E. (1970), 'Three Dimensional Finite Element  
Analysis of Jointed Rock Slopes,' Proc. 2nd Congress, Int. Soc. for Rock  
Mechanics, Belgrade, Vol. 3, pp 353-360.
- Mead, W.J. and MacDonald, D.F. (1924), 'Chemical and Physical Condition of the  
Cucaracha, the Chief Sliding Formation,' in Report of the Committee of the  
National Academy of Sciences on Panama Canal Slides, National Academy  
of Sciences Memoirs, Vol. 18, pp 53-67.
- Mesri, G and Gibala, R. (1972), 'Engineering Properties of a Pennsylvanian  
Shale', Stability of Rock Slopes, 13th Symposium on Rock Mechanics,  
University of Illinois, Aug./Sept. 1971, Ed. E.J. Cording, Publ. American  
Society of Civil Engineers, pp 57-75.

- Moore, L.R. (1968), 'Some sediments closely associated with Coal Seams.'  
Coal and Coal-Bearing Strata. (eds Murchison and Westoll), Oliver and  
Boyd, Edinburgh, pp 105-123.
- Morgenstern, N.R. (1969), 'Shear Strength of Stiff Clay.' Proc.  
Geotechnical Conf., Oslo, Vol. 2, pp 59-69.
- Morgenstern, N.R. and Price, V.E. (1965), 'The Analysis of the Stability  
of General Slip Surfaces,' Géotechnique, Vol. 15, pp 79-93.
- Müller, L. (1964), 'The rock slide in the Vajont Valley,' Rock Mechanics  
and Engineering Geology, Vol. 2, pp 148-212.
- Müller, L. and Hofmann, H. (1970), 'Selection, Compilation and Assessment  
of Geological Data for the Slope Problem', Planning Open Pit Mines,  
Symposium, Johannesburg, Ed. P.W.J. van Rensburg, Publu. A.A. Balkema,  
Cape Town, pp 153-170.
- Nickelson, R.P. and Hough, Van Ness D. (1967), 'Jointing in the Appalachian  
Plateau of Pennsylvania,' Bull. Geol. Soc. of America, Vol. 78,  
pp 609-630.
- Pariseau, W.G., Voight, B. and Dahl, H.D. (1970), 'Finite Element Analyses  
of Elastic-Plastic problems in the Mechanics of Geologic Media; An  
Overview, Proc. 2nd Congress Int. Soc. for Rock Mechanics, Belgrade, Vol.2  
pp 311-323.
- Parry, R.H.G. (1972), 'Some Properties of Heavily Over-Consolidated Oxford  
Clay at a Site near Bedford.' Géotechnique, Vol. 22, pp 485-507.
- Perrin, R.M.S. (1971), 'The Clay Mineralogy of British Sediments.'  
Mineralogical Soc. (Clay Mins. Group), London, 247 p.
- Peterson, R. (1954), 'Studies of Bearpaw Shale at damsite in Saskatchewan.'  
Proc. of the American Society of Civil Engrs, Separate No. 476, Vol. 80,  
New York.
- Peterson, R. (1958), 'Rebound in the Bearpaw Shale, Western Canada,'  
Bull. Geol. Soc. Am. Vol. 69, pp 1113-1124.

- Peterson, R., Jaspar, J.L., Rivard, P.J. and Iverson, N.L. (1960),  
'Limitations of laboratory shear strength in evaluating stability  
of highly plastic clays,' A.S.C.E. Research Conference on Shear  
Strength of Cohesive Soils., Boulder, Colo. p. 765.
- Piteau, D.R. (1970), 'Geological Factors Significant to the Stability  
of Slopes cut in Rock, Planning Open Pit Mines, Symposium, Johannesburg,  
Ed. P.W.J. van Rensburg, Publ. A.A.Balkema, Cape Town, pp 33-53.
- Price, N.J. (1959), 'Mechanics of Jointing in Rocks,' Geol. Mag. vol 96,  
pp 149-167.
- Reeves, M.J. (1971), 'Geochemistry - Mineralogy of British Carboniferous  
Seatearths from Northern Coalfields,' Ph.D. Thesis, University of  
Durham, England.
- Robertson, A.Macly (1970), The Interpretation of Geological Factors for  
use in Slope Theory, Planning Open Pit Mines, Symposium, Johannesburg,  
Ed. P.W.J. van Rensburg, Publ. A.A.Balkema, Cape Town, pp 55-71.
- Rosenblad, J.L. (1970), 'Failure Modes of Models of Jointed Rock Masses,'  
Proc. Int. Congress, Int. Soc. for Rock Mechanics, Belgrade, Vol. 2 pp 75-81.
- Rowe, P.W. (1972), 'The relevance of soil fabric to site investigation  
practice,' 12th Rankine Lecture, Géotechnique, Vol. 22, No. 2., pp 193-300.
- Scott, J.S. and Brooker, E.W. (1968), 'Geological and engineering aspects  
of Upper Cretaceous shales in Western Canada,' Paper 66-37, Geological  
Survey of Canada, Department of Energy, Mines and Resources, Ottawa.
- Sherard, J.L., Woodward, R.J., Gizienki, S.F. and Clevenger, W.A. (1963),  
'Earth and Earth-Rock Dams,' John Wiley and Sons Inc., New York, 725 p.
- Shuk, T. (1970), 'Optimization of slopes designed in rock', Proc. 2nd  
Congress, Int. Soc. Rock Mechanics, Vol. 3, pp 275-280.
- Skempton, A.W. (1961), 'Horizontal stresses in overconsolidated Eocene  
Clay,' Proc. 5th Int. Conf. on Soil Mechanics and Found. Engineering,  
Vol. 1, p.351., Paris, France.



- Skempton, A.W. (1964), 'Long-term stability of clay slopes.' *Géotechnique*, Vol. 14, pp 77-101.
- Skempton, A.W. (1970), 'First Time Slides in Overconsolidated Clays,' *Géotechnique*, Vol. 20, pp 320-324.
- Skempton, A.W. and Delory, F.A. (1967), 'Stability of Natural Slopes in London Clay,' *Proc. 4th Int. Conf. Soil Mech. (London)*, Vo. 2, pp 378-381.
- Skempton, A.W. and Hutchinson, J.N. (1969), 'Stability of natural slopes and embankment foundations,' *State of the Art Volume, 7th Int. Conf. Soil Mech. Found. Engineering, Mexico City*, pp 291-340.
- Skempton, A.W. and La Rochelle, P. (1965), 'The Bradwell slip; a short-term failure in London Clay,' *Géotechnique*, Vol. 15. pp 221-242.
- Skempton, A.W. and Petley, D.J. (1967), 'The strength along structural discontinuities in stiff clays,' *Proc. Geotechnical Conf., Oslo*, Vol.II, pp 3-20.
- Spears, D.A. (1971), 'The mineralogy of the Stafford Tonstein,' *Proc. of the Yorkshire Geological Society*, Vol. 38, pp 497-516.
- Spears, D.A. (1973), 'Relationship between Exchangeable Cations and Palaeosalinity,' *Geochimica et Cosmochimica Acta*, Vol. 37, pp 77-85.
- Spears, D.A. Taylor, R.K., and Till, R. (1971), 'A Mineralogical investigation of a spoil heap at Yorkshire Main Colliery.' *Quarterly Journal of Engineering Geology*. Vol. 3, pp 239-252.
- Spears, D.A. and Taylor, R.K. (1972), 'The influence of weathering on the composition and engineering properties of in-situ Coal Measures Rocks.' *Int. J. Rock.Mech. Min. Sci.*, Vol. 9 pp 729-756.
- Taylor, R.K. (1971), 'The Petrography of the Mansfield Marine Band Cyclothem at Tinsley Park, Sheffield,' *Proc. Yorks. Geol. Soc.*, Vol. 38, pp 299-328.
- Taylor, R.K. (1973), 'Compositional and Geotechnical Characteristics of a 100-year old Spoil Heap.' *Trans. Instn. Min. and Metall. (Section A: Mining Industry.)* Vol. 82, pp. 1-14.

- Taylor, R.K. and Spears, D.A., (1970), 'The breakdown of British Coal Measures Rocks.' Int. J. Rock Mech. Min. Sci., Vol. 7, pp 481-501.
- Taylor, R.K. and Spears, D.A. (1973), Discussion: 'Lias Clay - Weathering Processes and their Effect on Shear Strength.' by Chandler, R.J., (1972). Géotechnique, Vol. 23 pp 132-133.
- Terzaghi, K. (1936), 'Stability of slopes in natural clay,' Proc. 1st International Conf. on Soil Mech. and Found. Engng. Vol. 1, pp 161-165.
- Terzaghi, K. and Peck, R.B. (1967), 'Soil Mechanics in Engineering practice,' John Wiley & Sons., New York, 729 pp.
- Terzaghi, R.D. (1965), 'Sources of Error in Joint Surveys,' Géotechnique Vol. 15, pp 287-303.
- Thompson, T.F. (1947), 'Origin, Nature and Engineering Significance of the Slickensides in the Cucaracha Clay Shales,' Isthmian Canal Studies Memorandum 245, Panama Canal Company, Diablo Heights, Canal Zone.
- Tourtelot, H.A. (1962), 'Preliminary investigation of the geologic setting and chemical composition of the Pierre Shale, Great Plains Region.' U.S.G.S. Professional Paper 390, Washington, D.C.
- Underwood, L.B. (1967), 'Classification and identification of shales,' Journ. Soil Mechn. and Found. Div., A.S.C.E., Vol. 93, No. SM6, pp 97-116.
- Wilson, V. (1948), 'East Yorkshire and Lincolnshire,' Mem. Geol. Survey U.K. H.M.S.O., London.

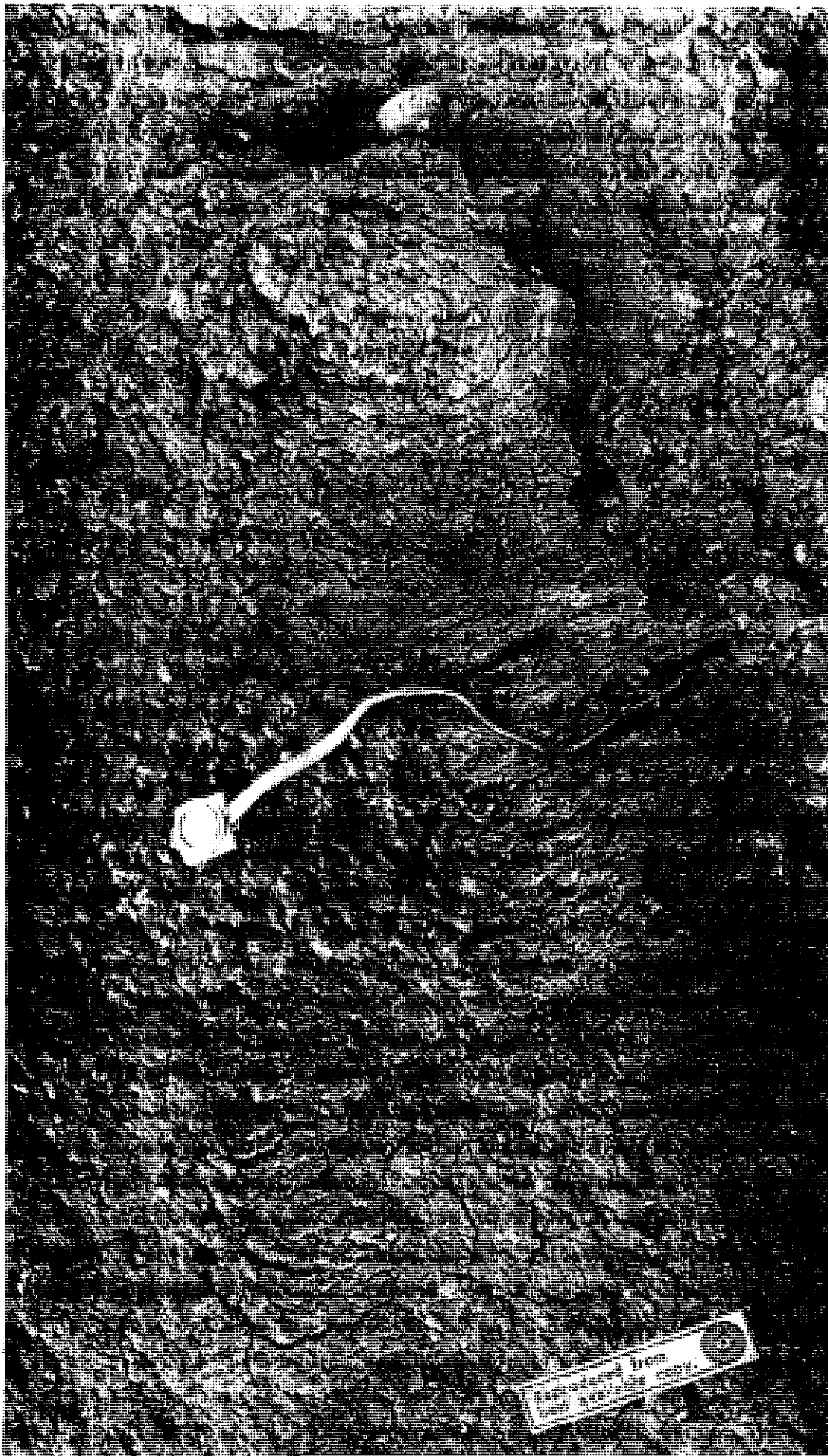


PLATE 1.2

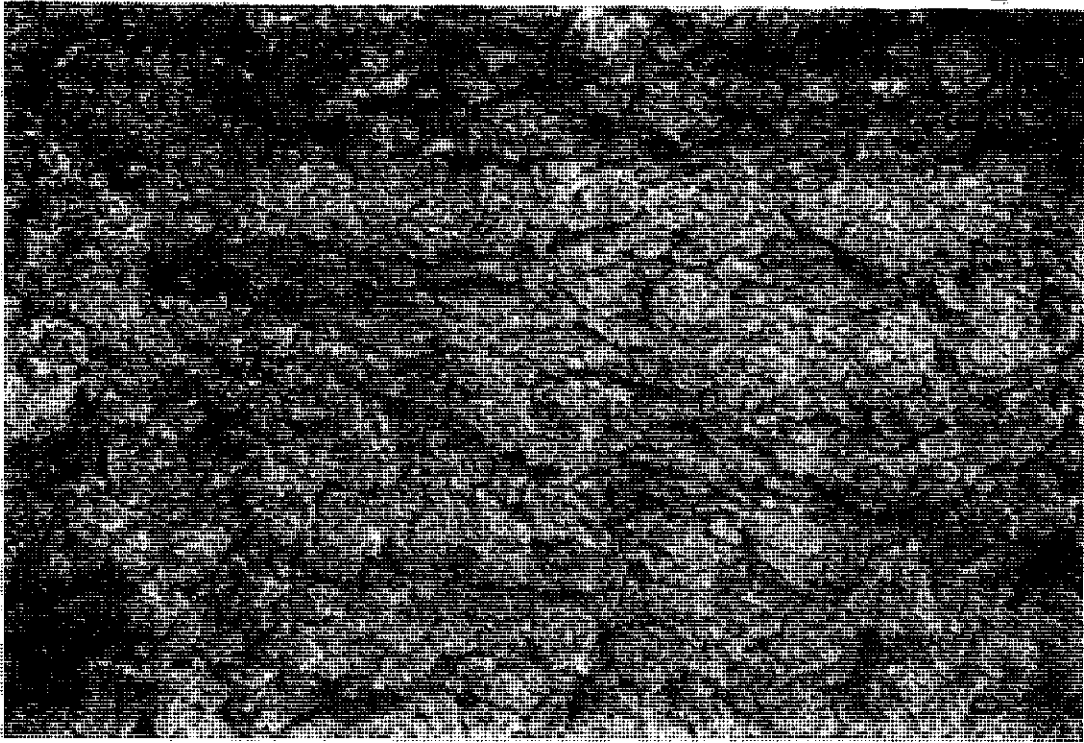


PLATE 1.3



Reproduced from  
best available copy.





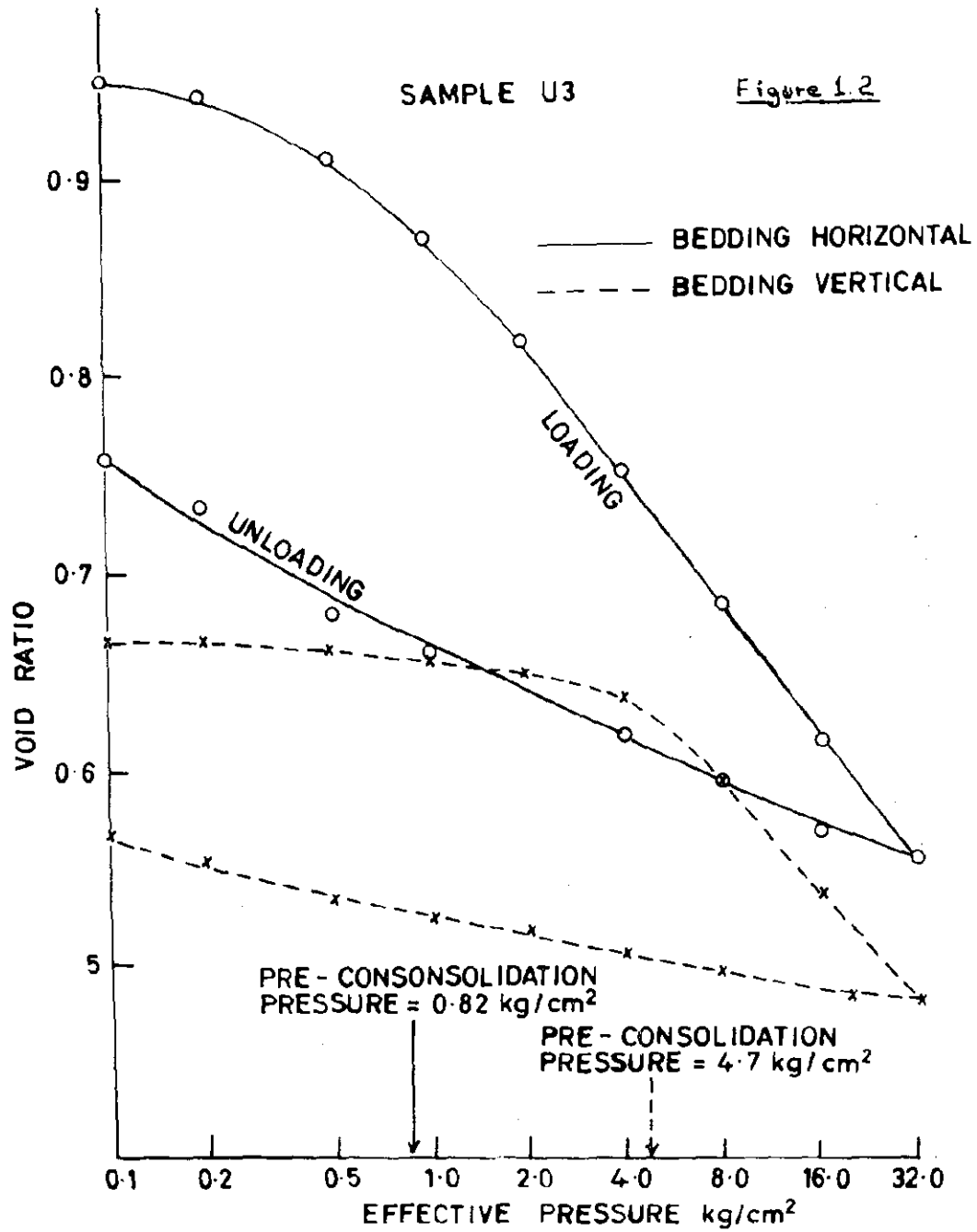


Figure 1.3. Possible distributions of major principal stress and shear stress at an earth-dam foundation  
 (note that  $\sigma_1$  is normalised to the overburden pressure at a particular point in the dam and not to overburden pressure at crest height).

Distribution of  $\frac{\tau_{\max}}{\gamma H}$  { — Relaxation solution (Bishop, 1952)  
 - - Jurgenson solution

Distribution of  $\frac{\sigma_1}{\gamma h}$  - - - -

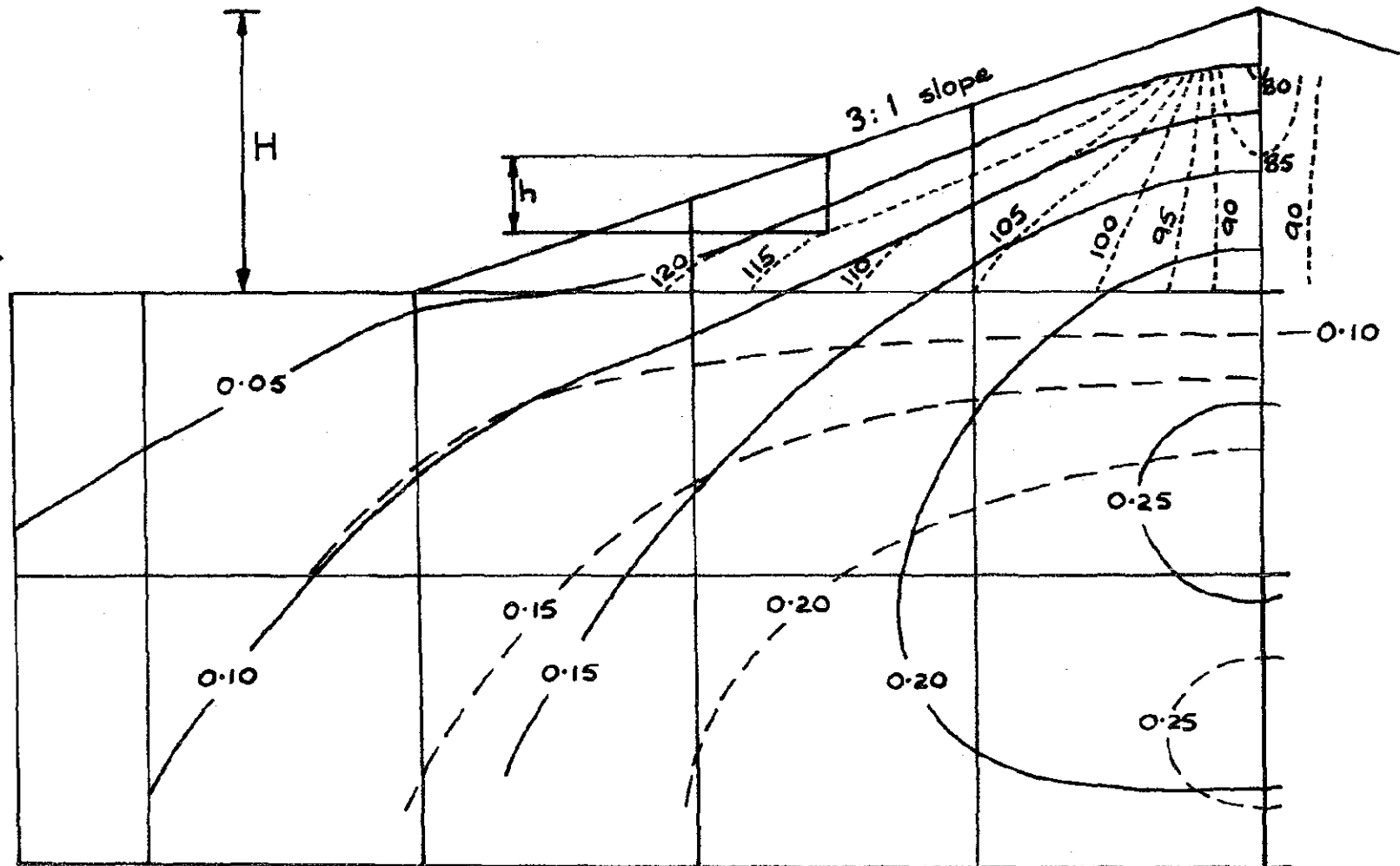


Figure 1.4. Influence of  
montmorillonite percentage  
on liquid limit - N.American  
samples

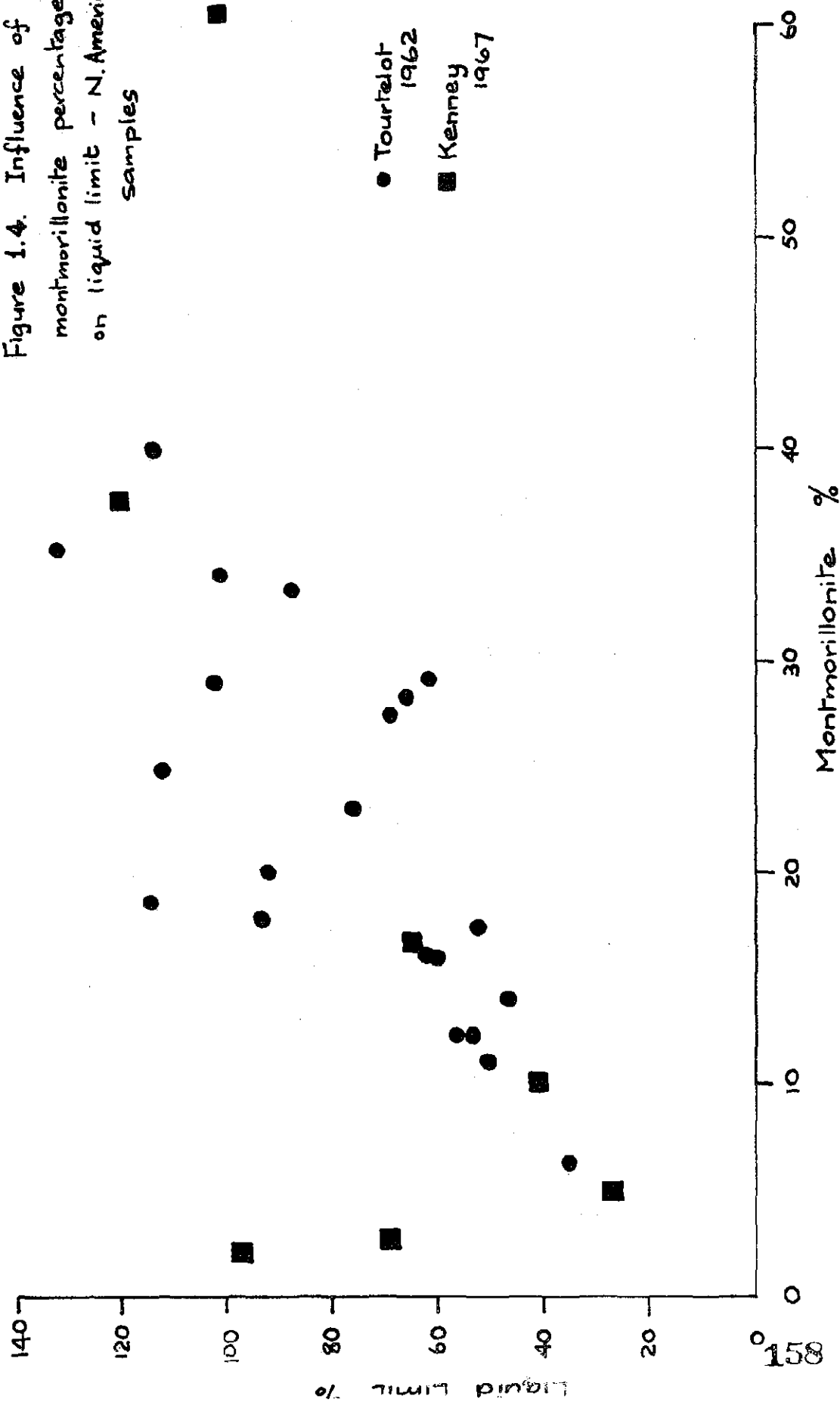




Figure 1.5 Influence of clay mineral  
percentage upon the liquid limit -  
N. American samples

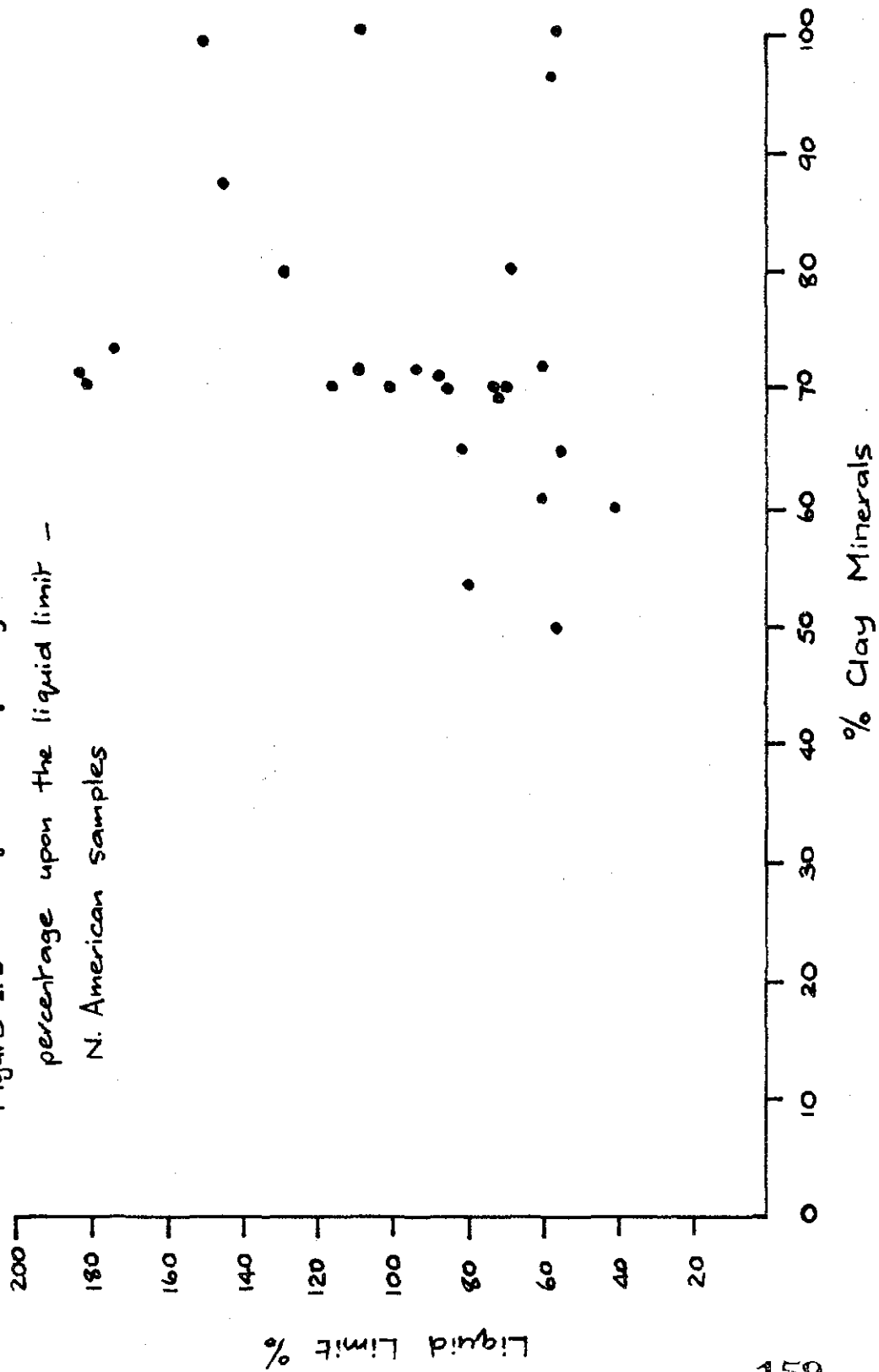
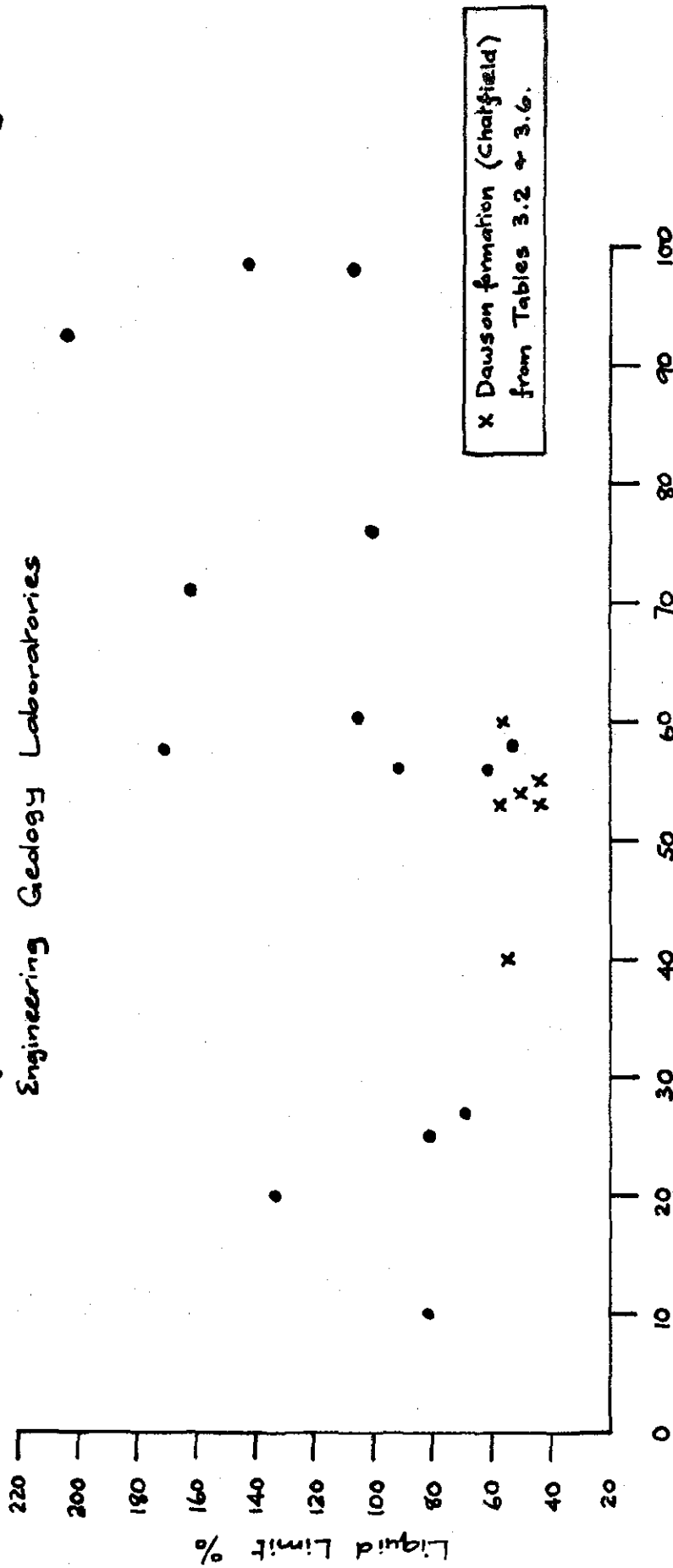


Figure 1.6. Influence of montmorillonite percentage on the liquid limit of the N. American samples tested in the Durham University Engineering Geology Laboratories



160

\* Well crystallised (based on shape of XRD peaks)

Figure 1.7. Influence of the ratio of montmorillonite to massive minerals in N. American material upon the liquid limit

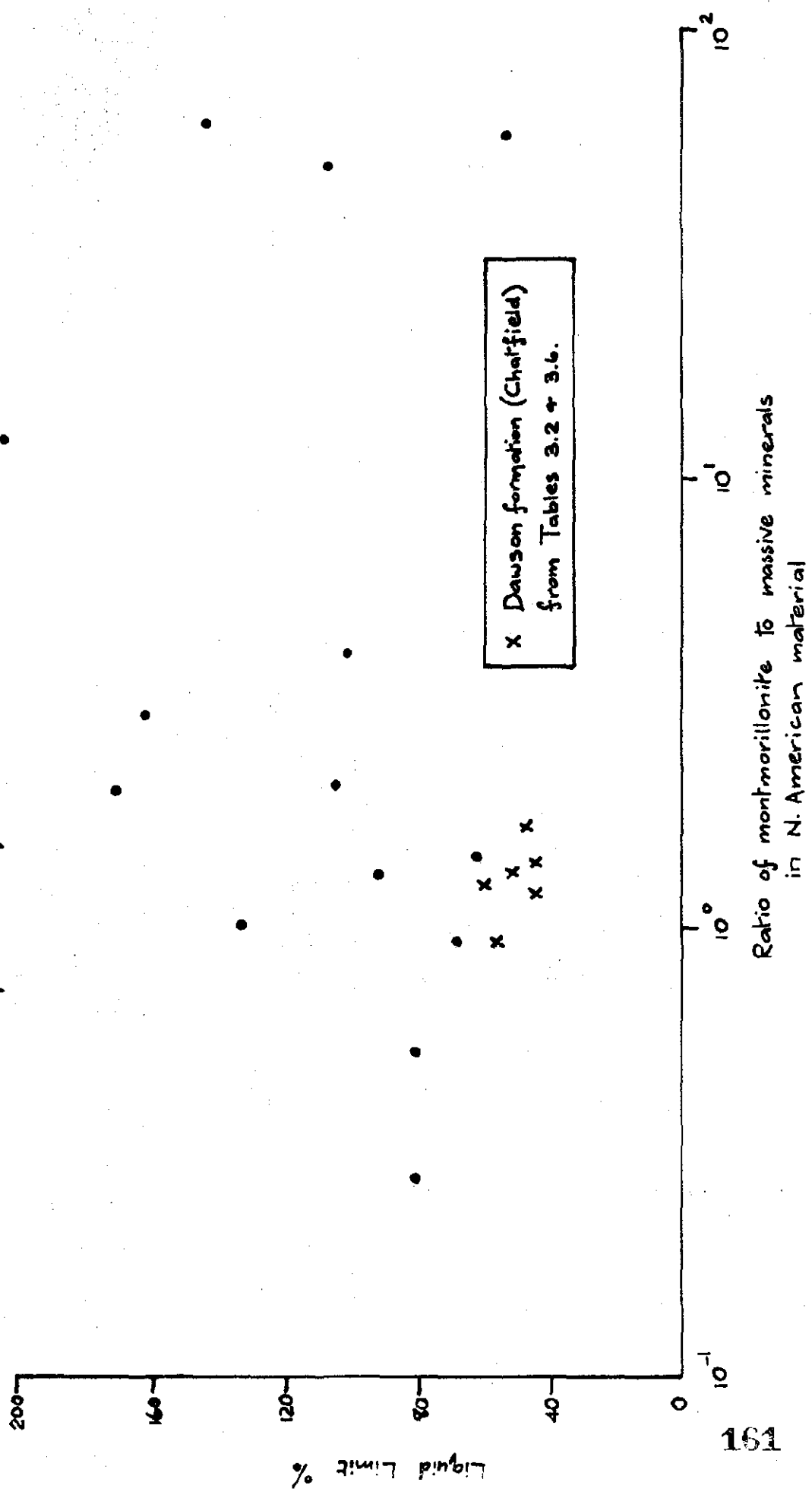


Figure 1.8a. Influence of montmorillonite and total clay mineral content upon the effective residual friction angle in N. American samples

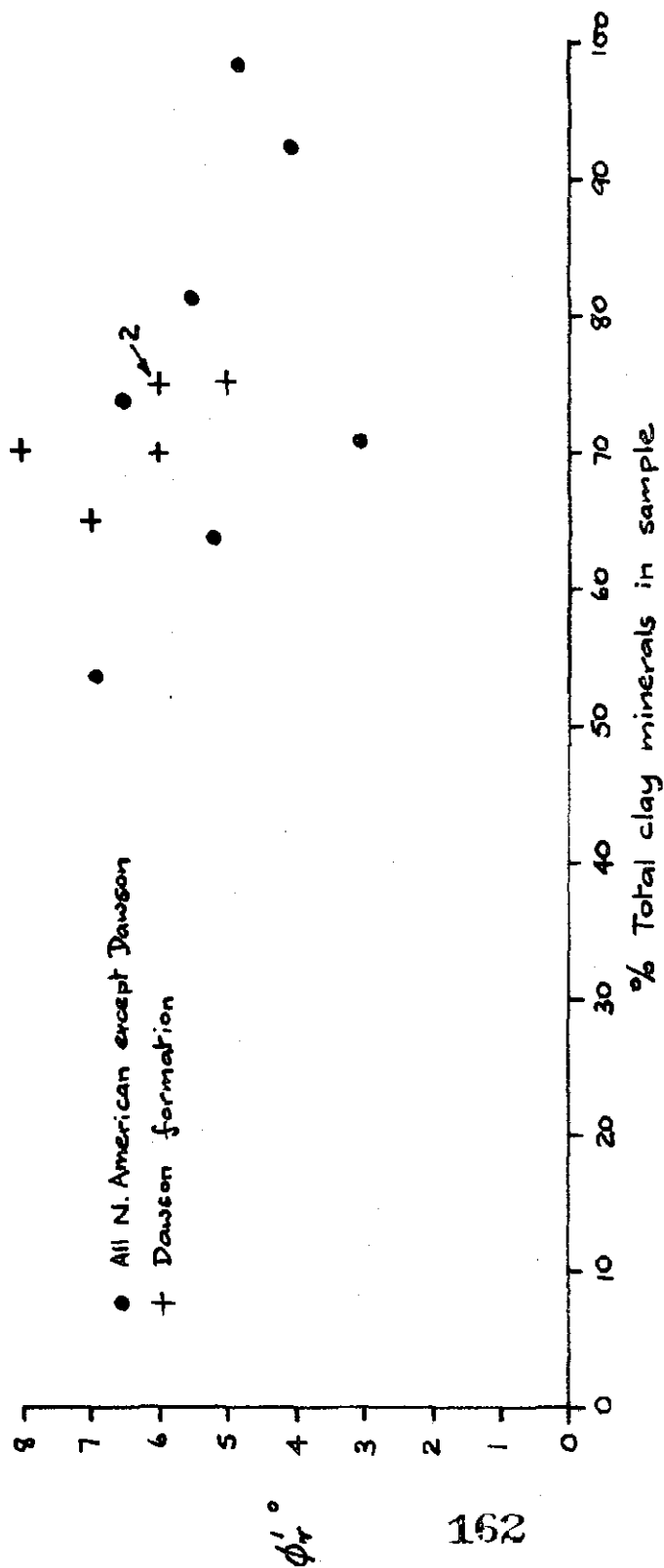
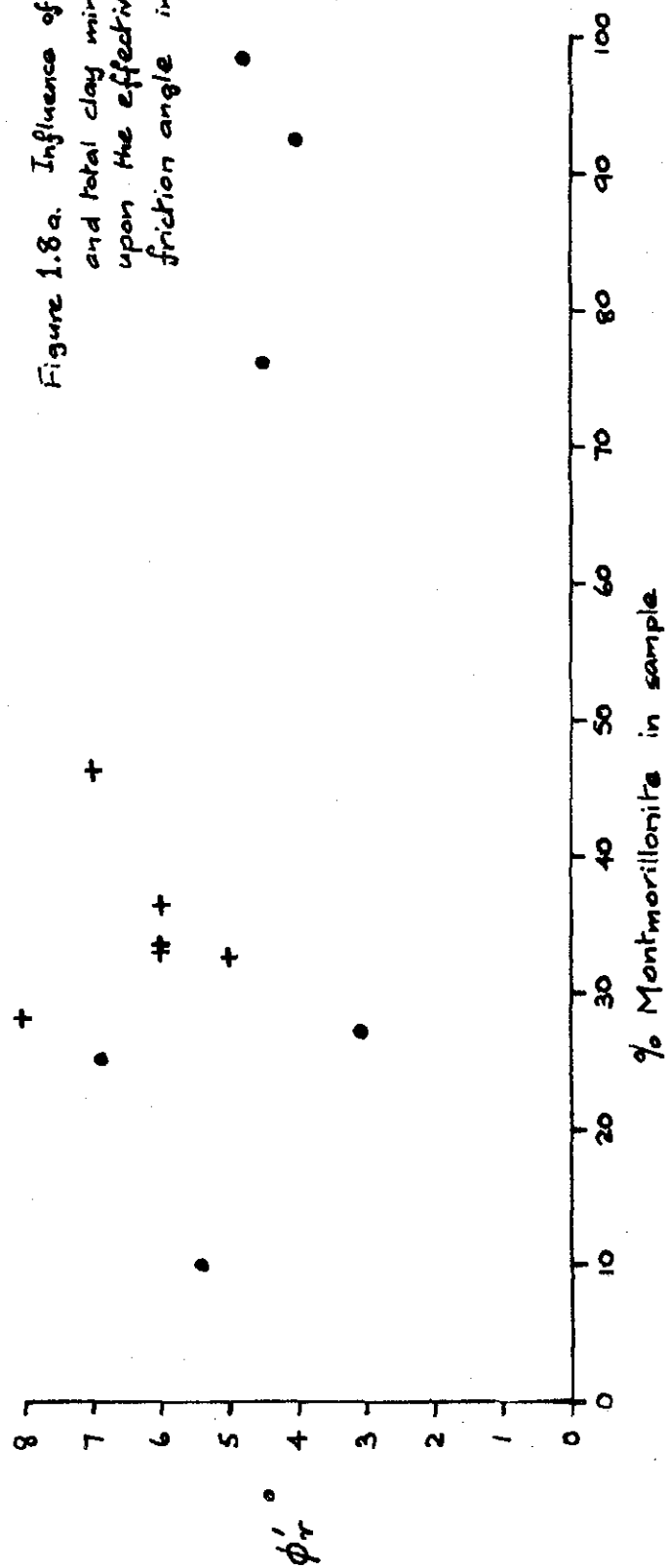


Figure 1.8b. Influence of montmorillonite and total clay content upon the effective residual friction angle - N. American samples

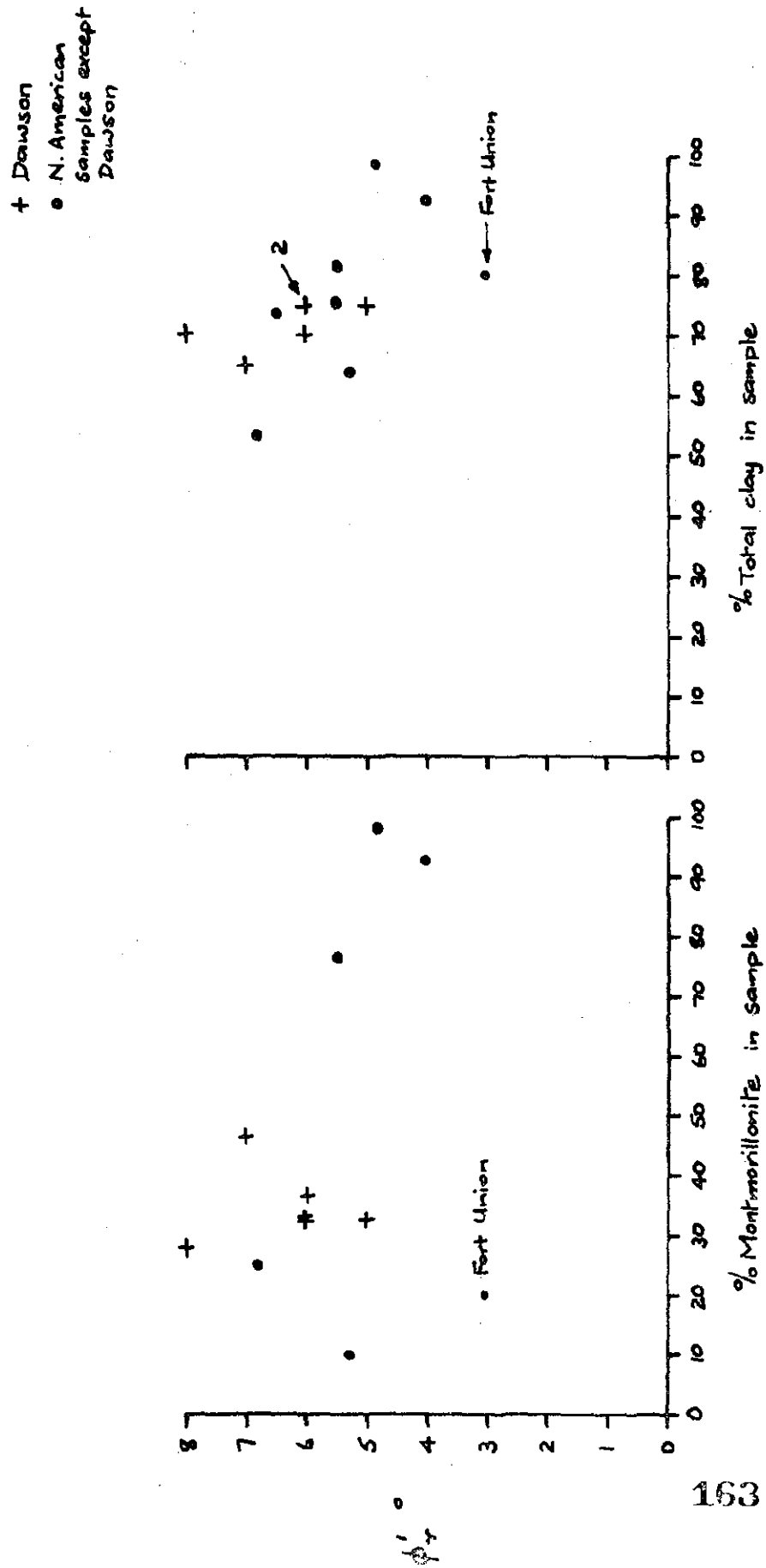


Figure 1.4 Influence of total clay and total clay-to-massive minerals ratio upon the effective residual friction angle in some stiff British clays

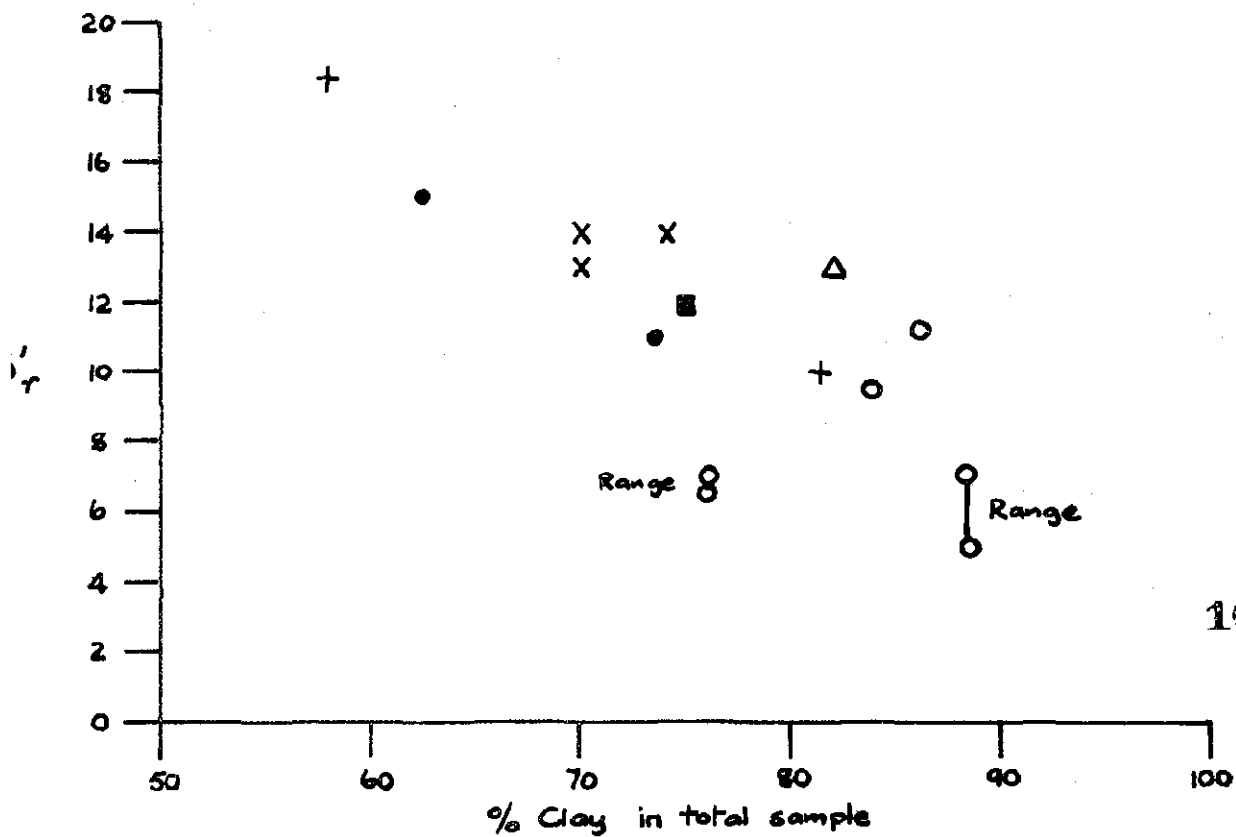
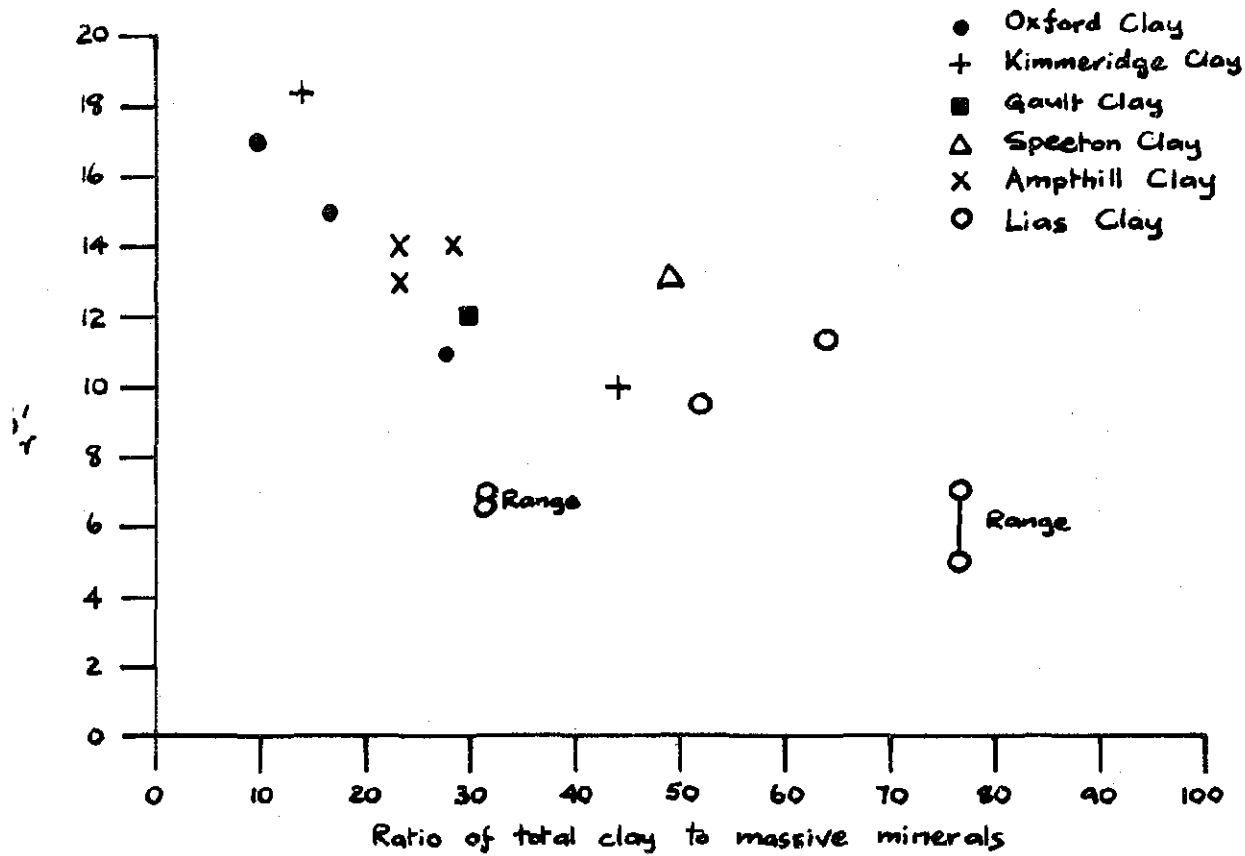


Figure 1.10. Influence of clay mineral percentage upon the effective residual friction angle in both British and N. American samples.

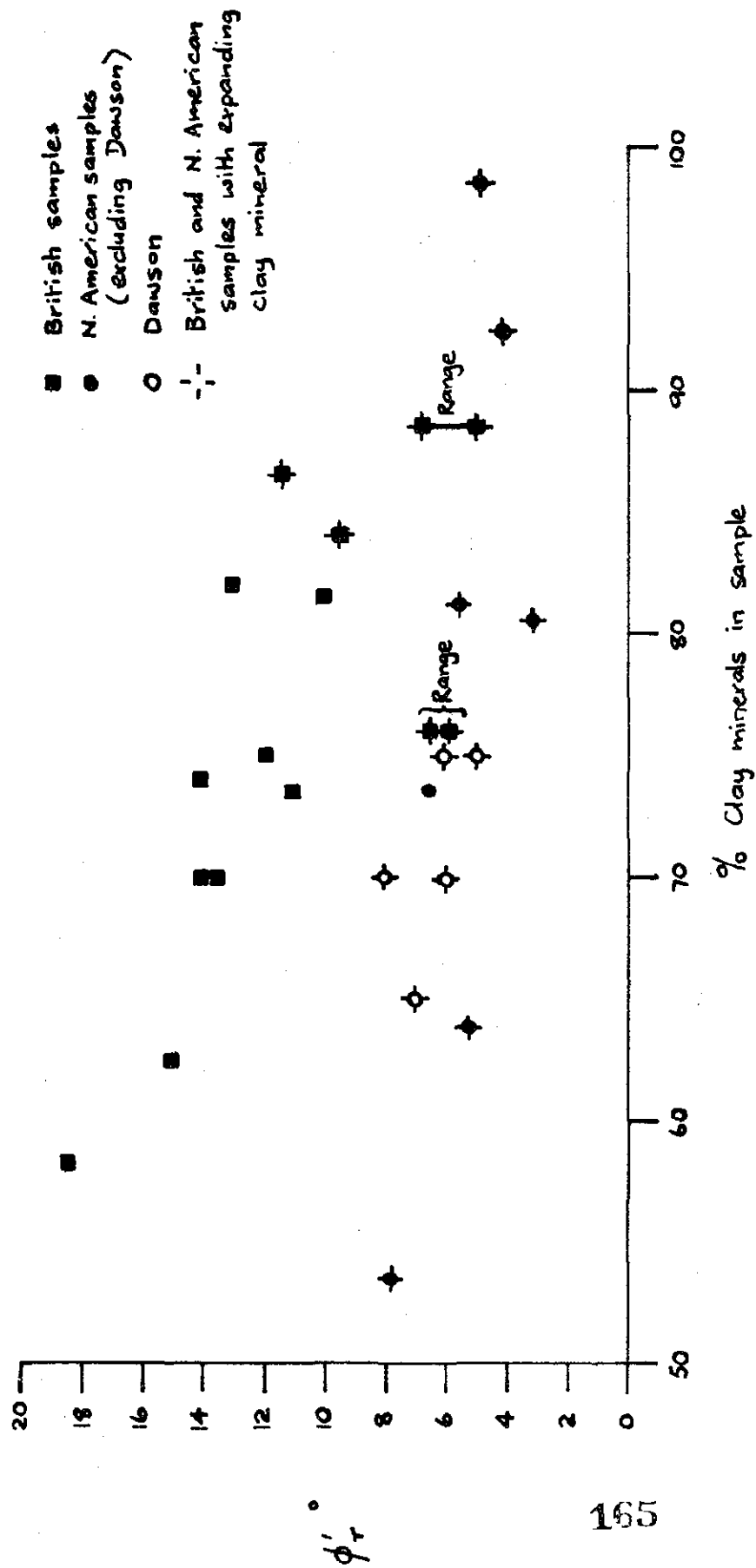
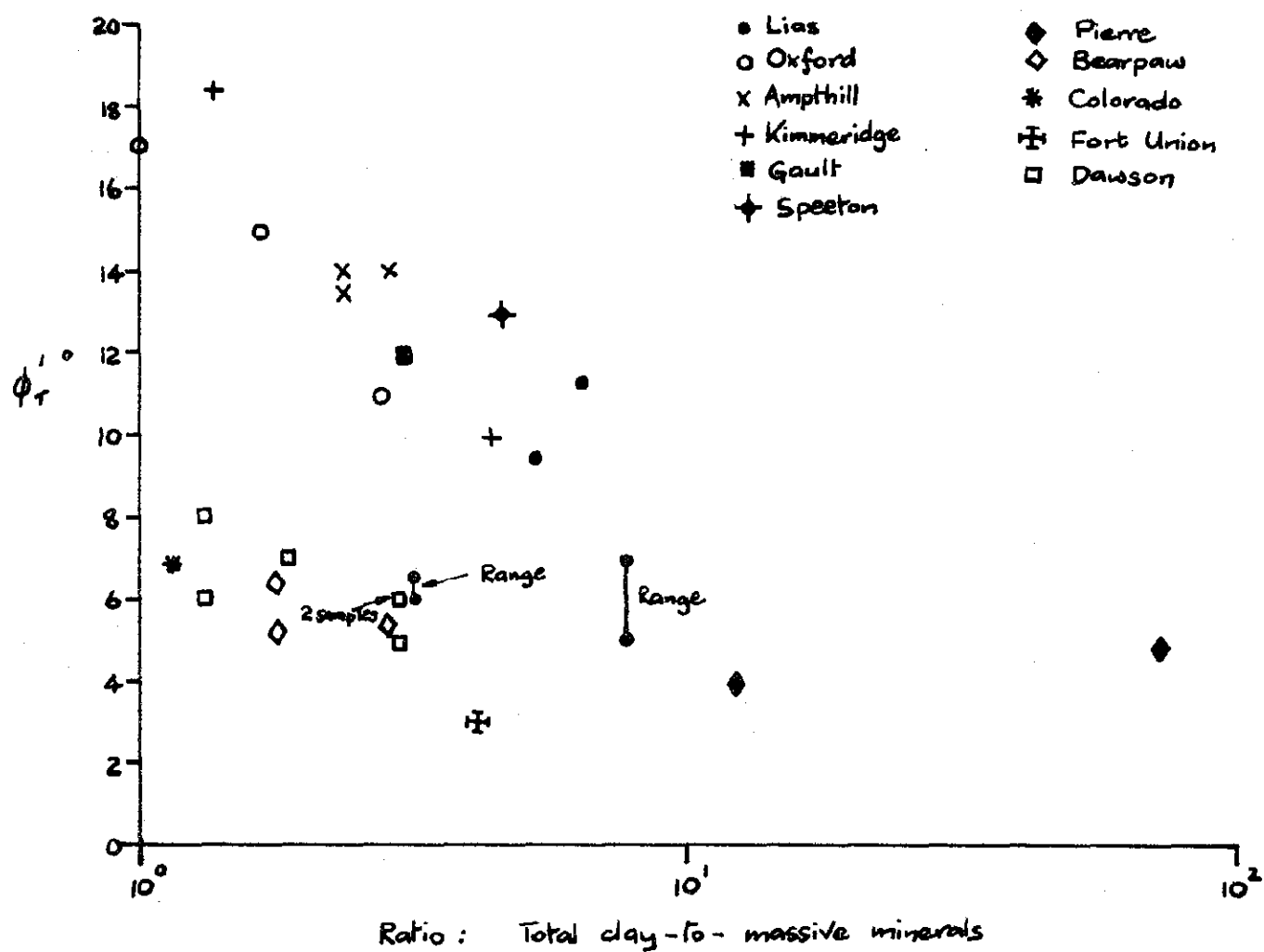
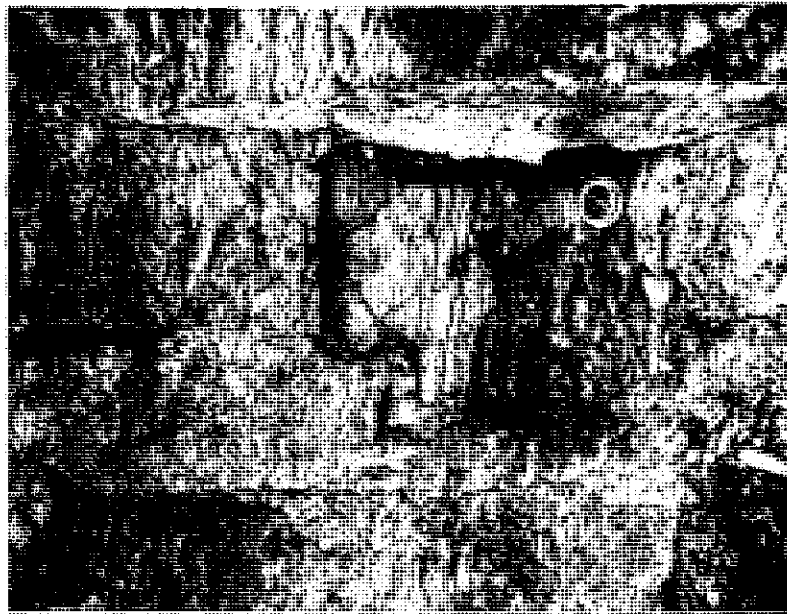


Figure 1.11. Influence of clay-to-massive mineral content upon the effective residual friction angle in both British and N. American samples







Reproduced from  
best available copy.

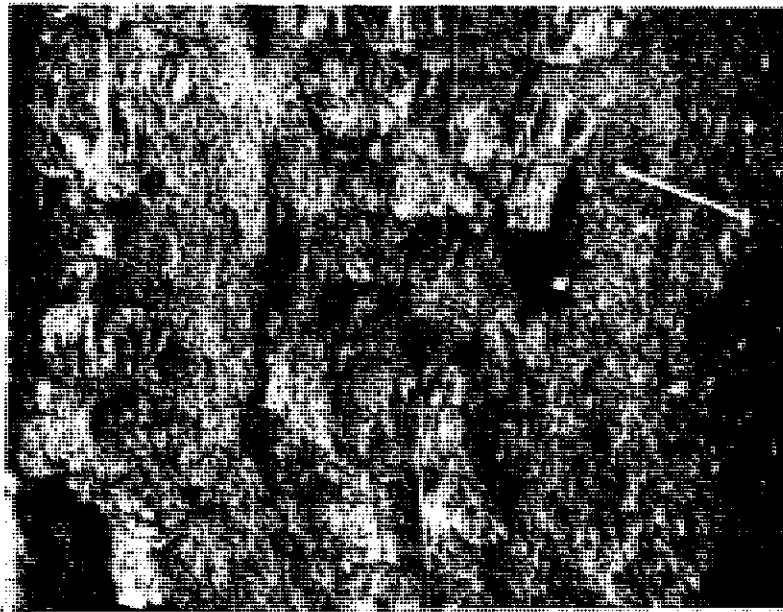


Plate 2.1.

Figure 2.1. Geological detail of Fox Hills and Golden Hill area in the Vale of Pickering, Yorkshire, England

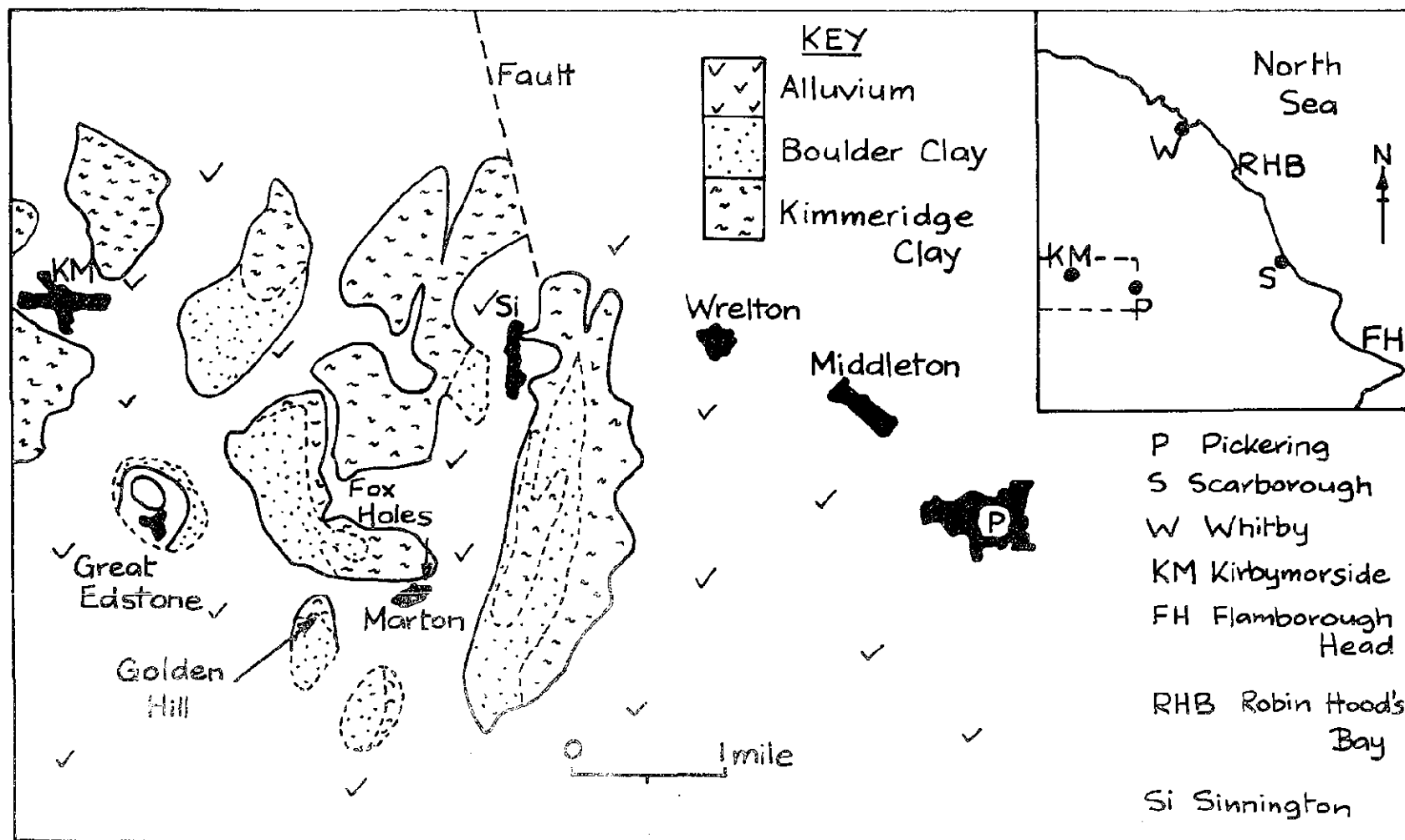


Figure 2.2. Fox Holes excavation, Marton, Yorks, England.

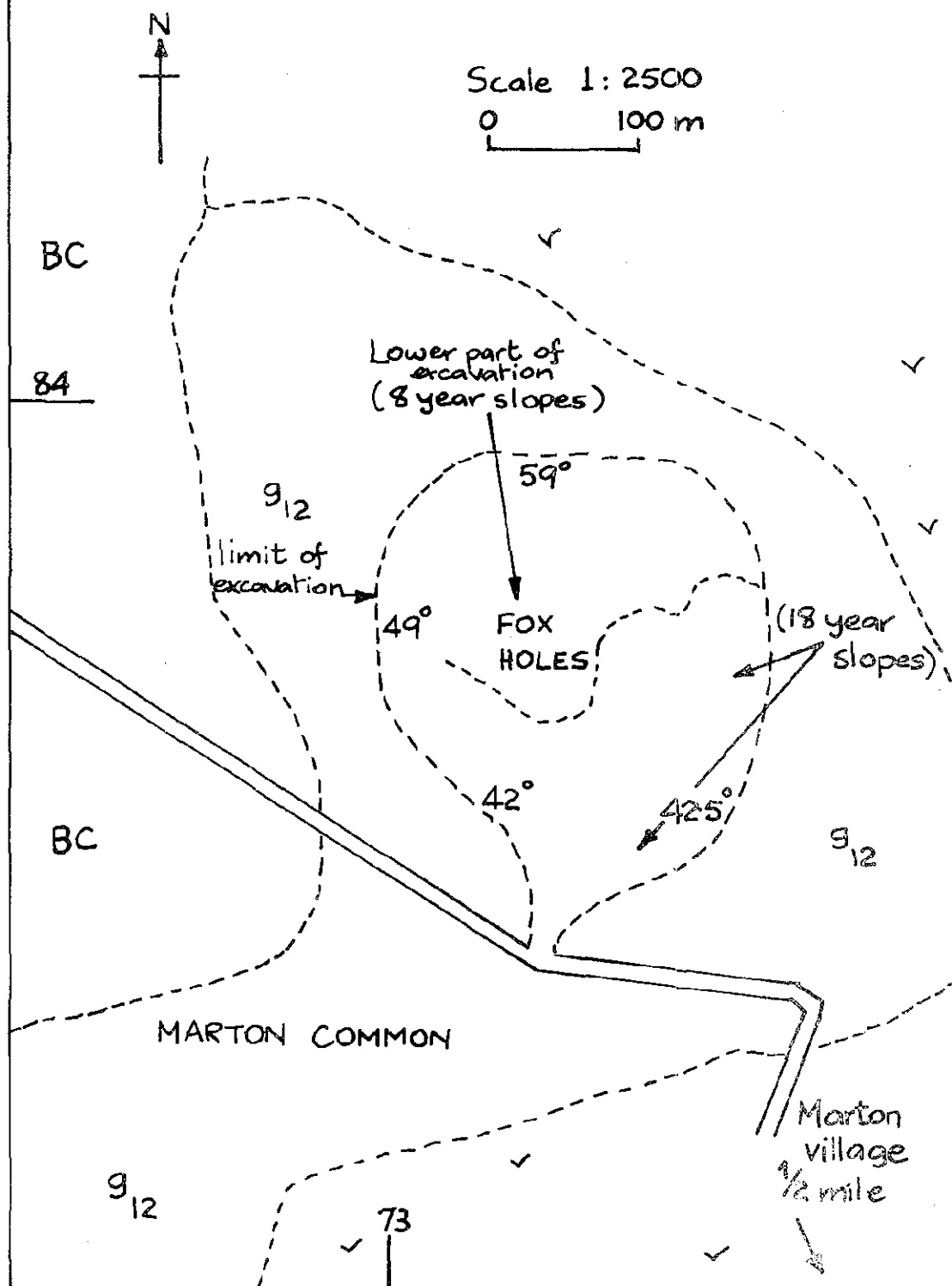
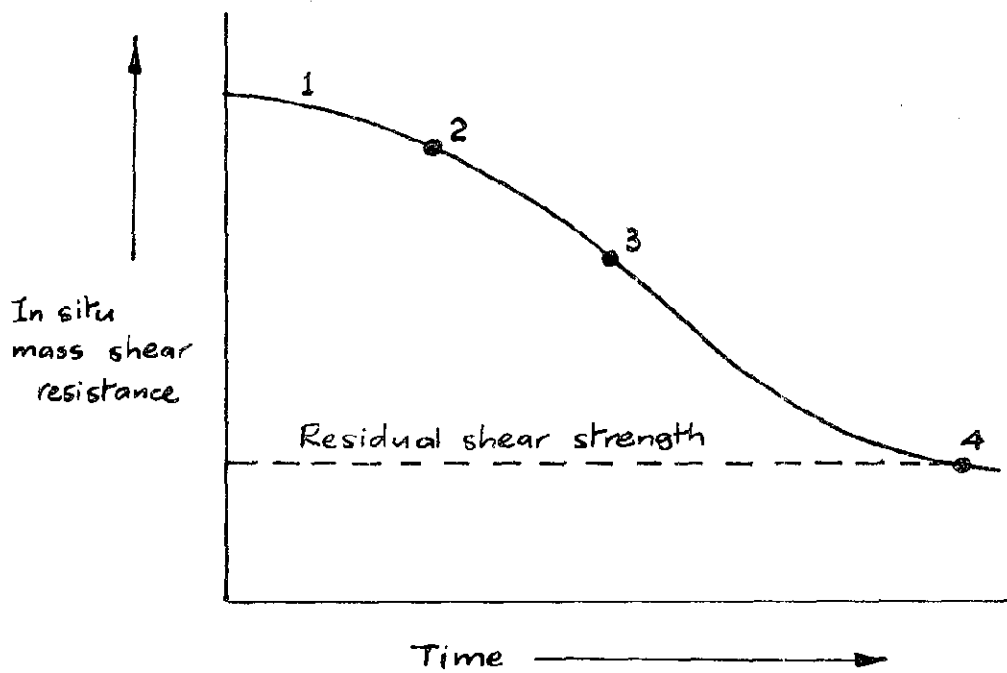




Figure 2.4. Initial, intermediate, and long-term stability conditions



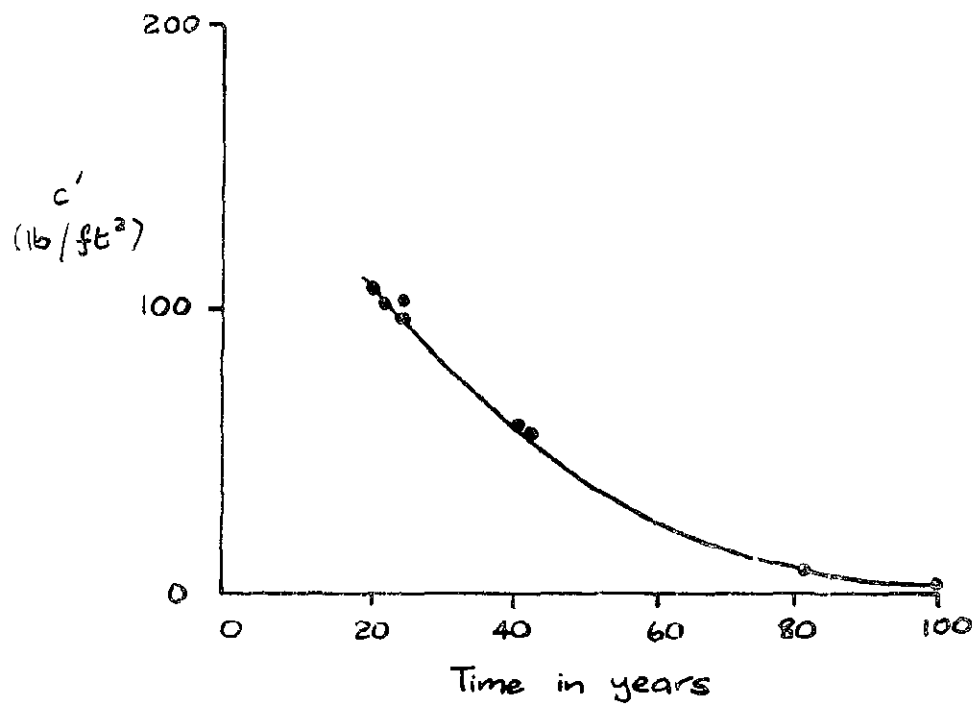


Figure 2.5. Strength reduction with time  
(after Skempton, 1969)

Figure 2.6. Golden Hill slopes in Kimmeridge Clay.

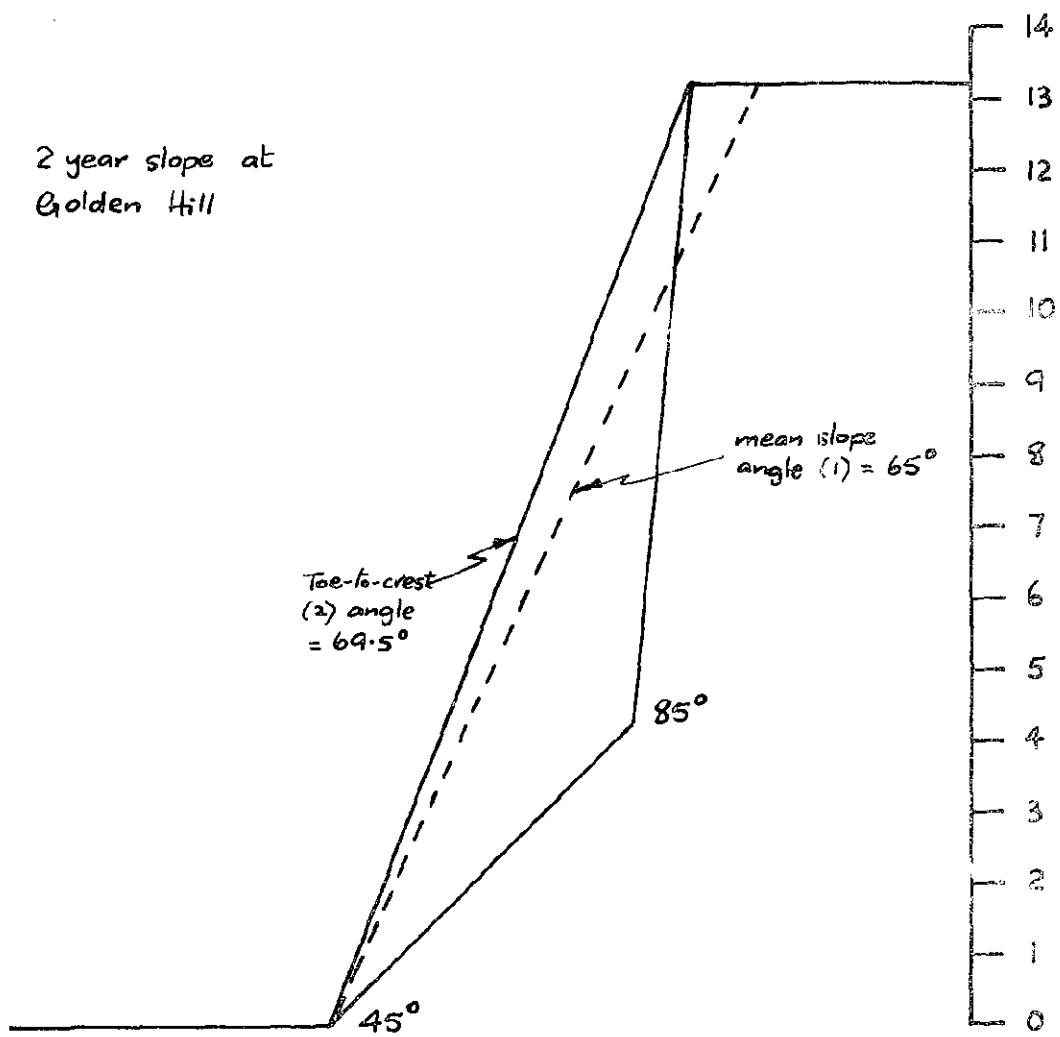
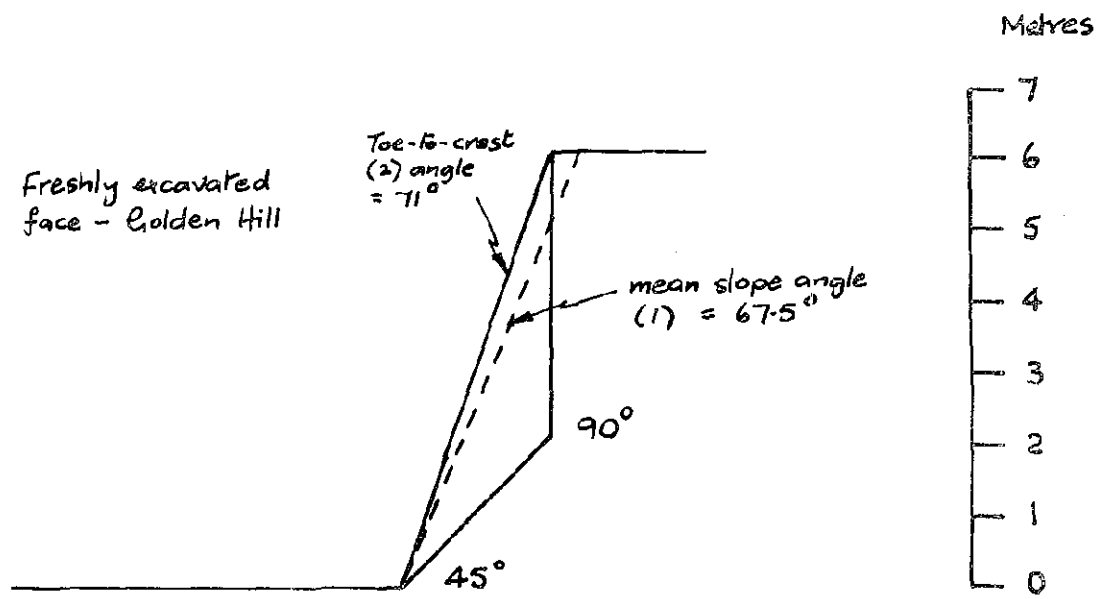


Figure 8.7. Fox-Holes 8 year slopes in Kimmeridge Clay

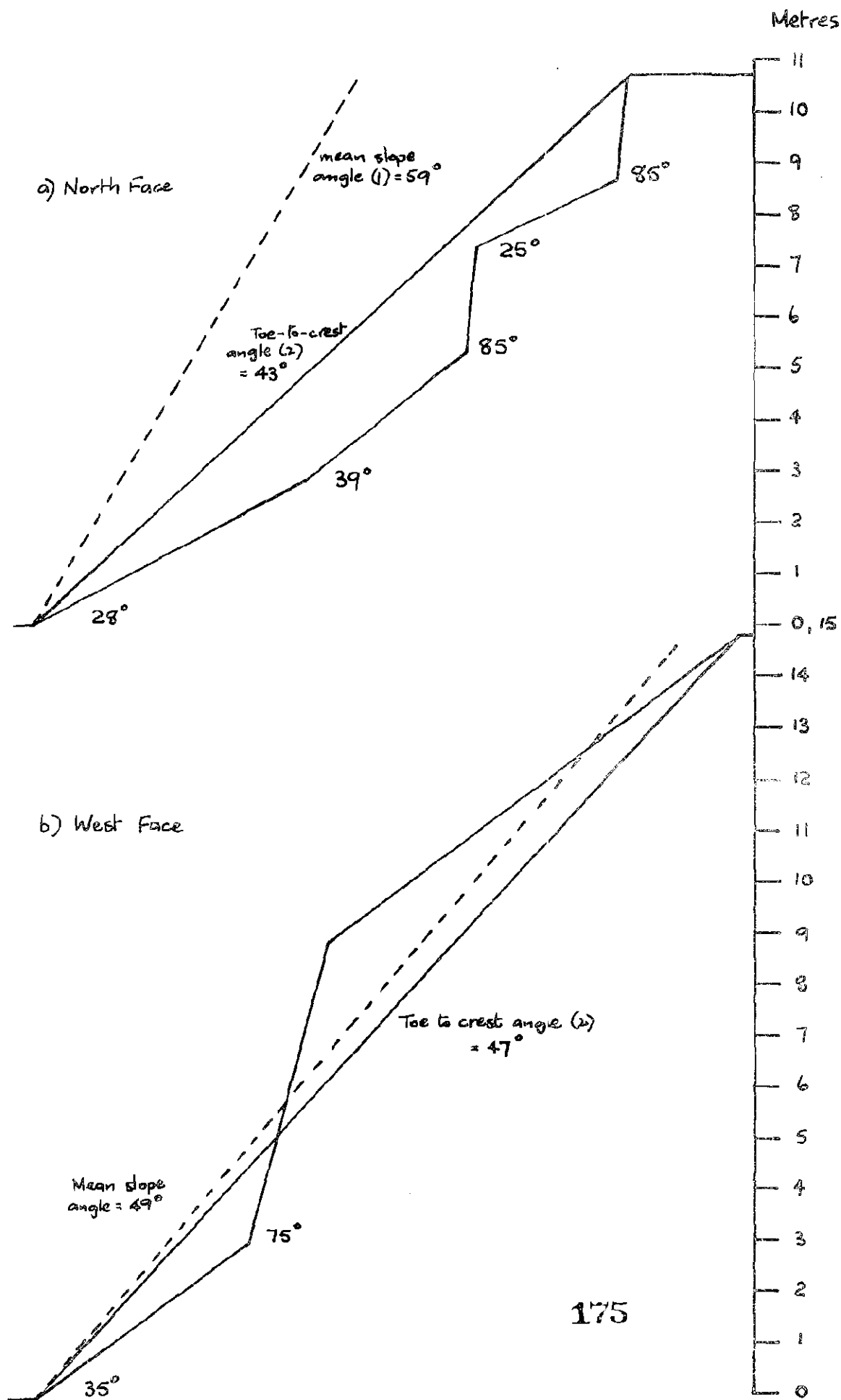




Figure 2.8. Fox Holes slopes in Kimmeridge Clay

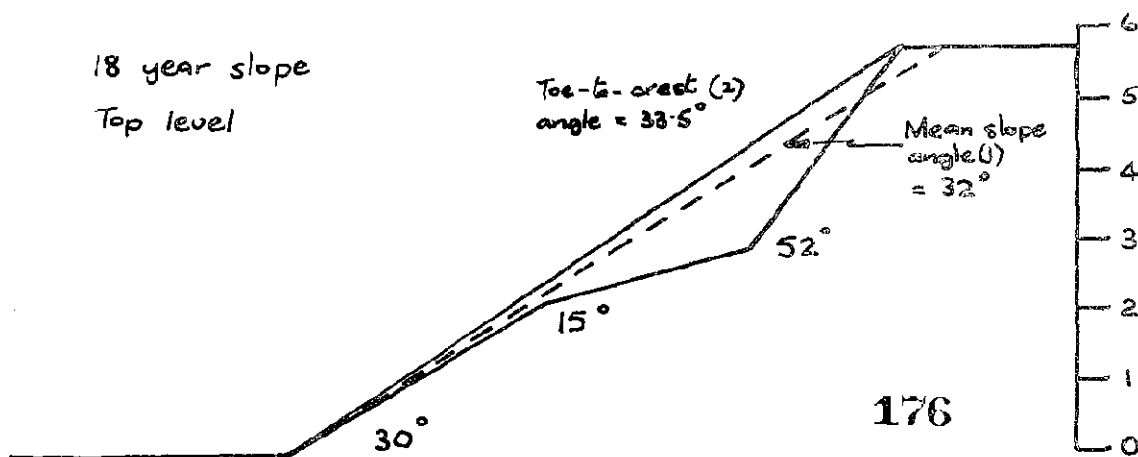
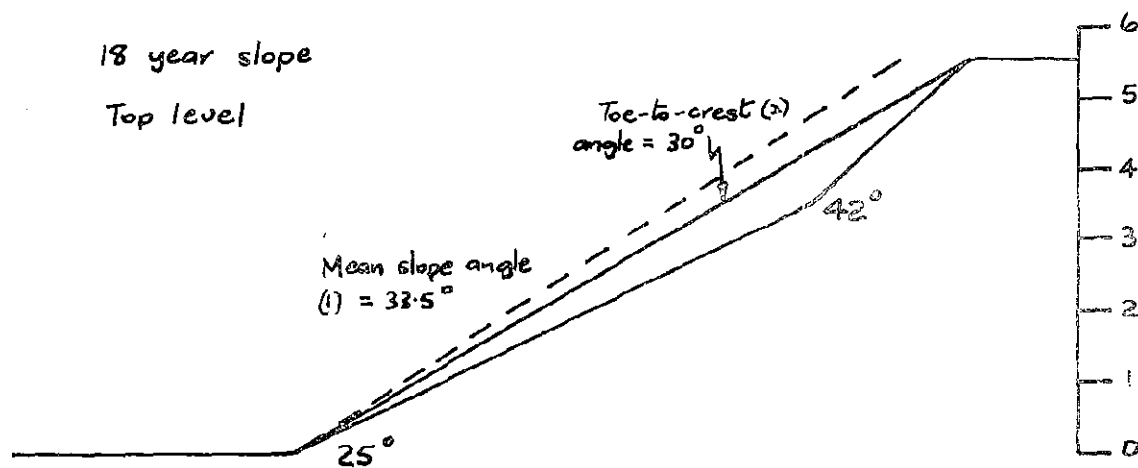
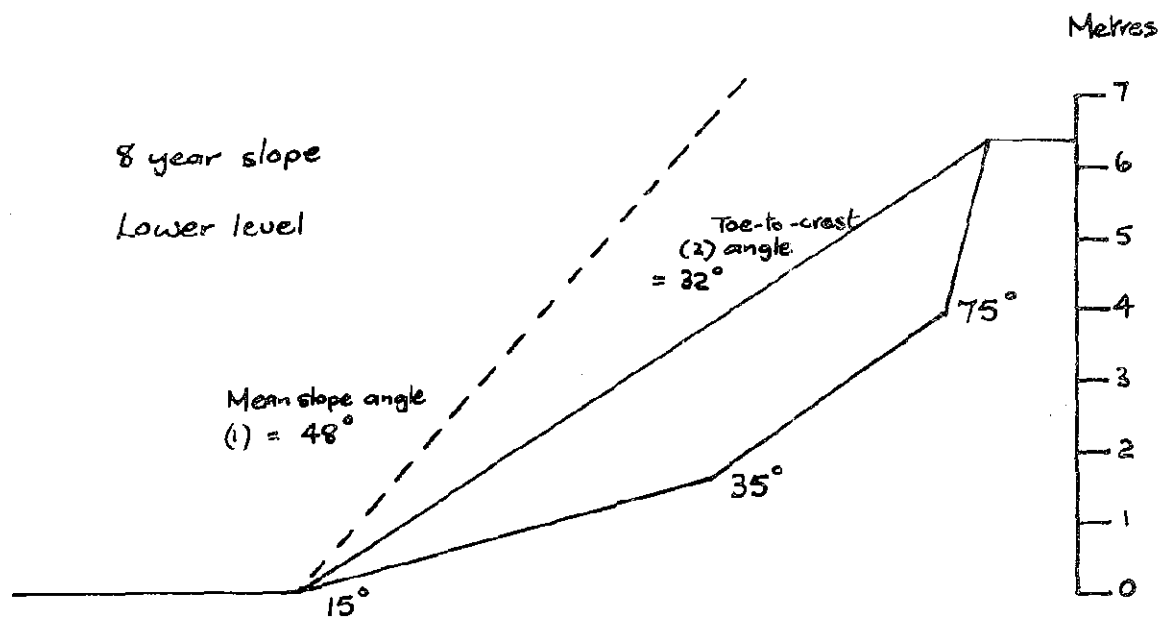
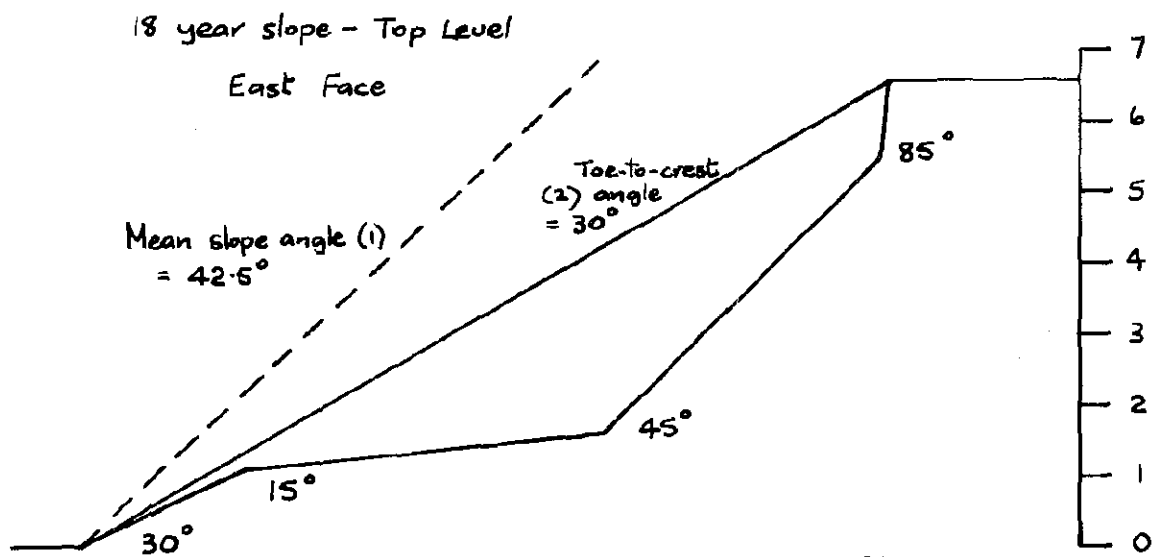
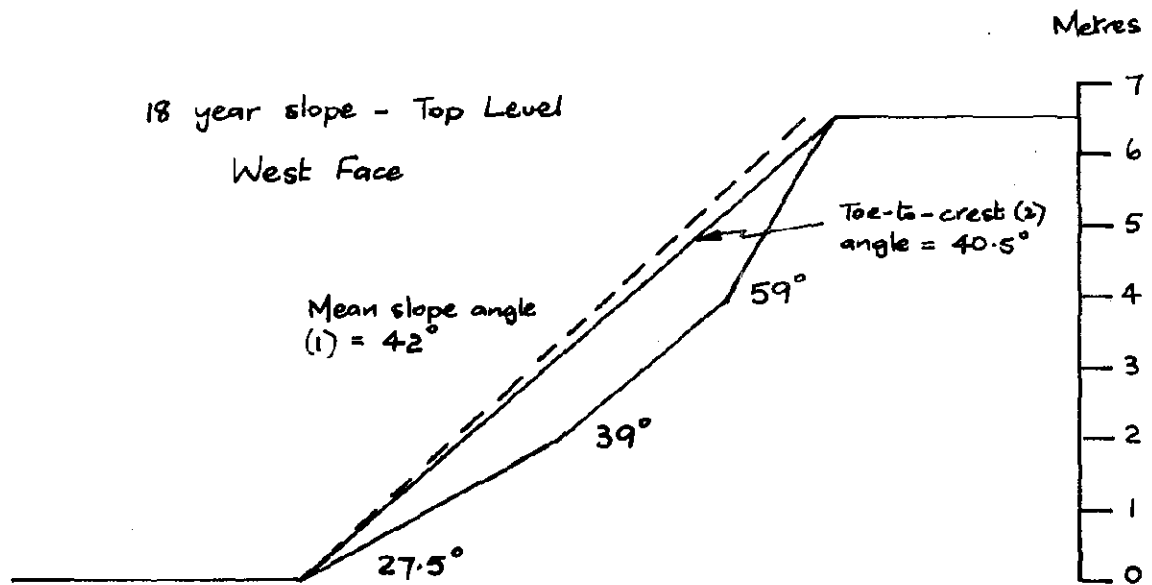
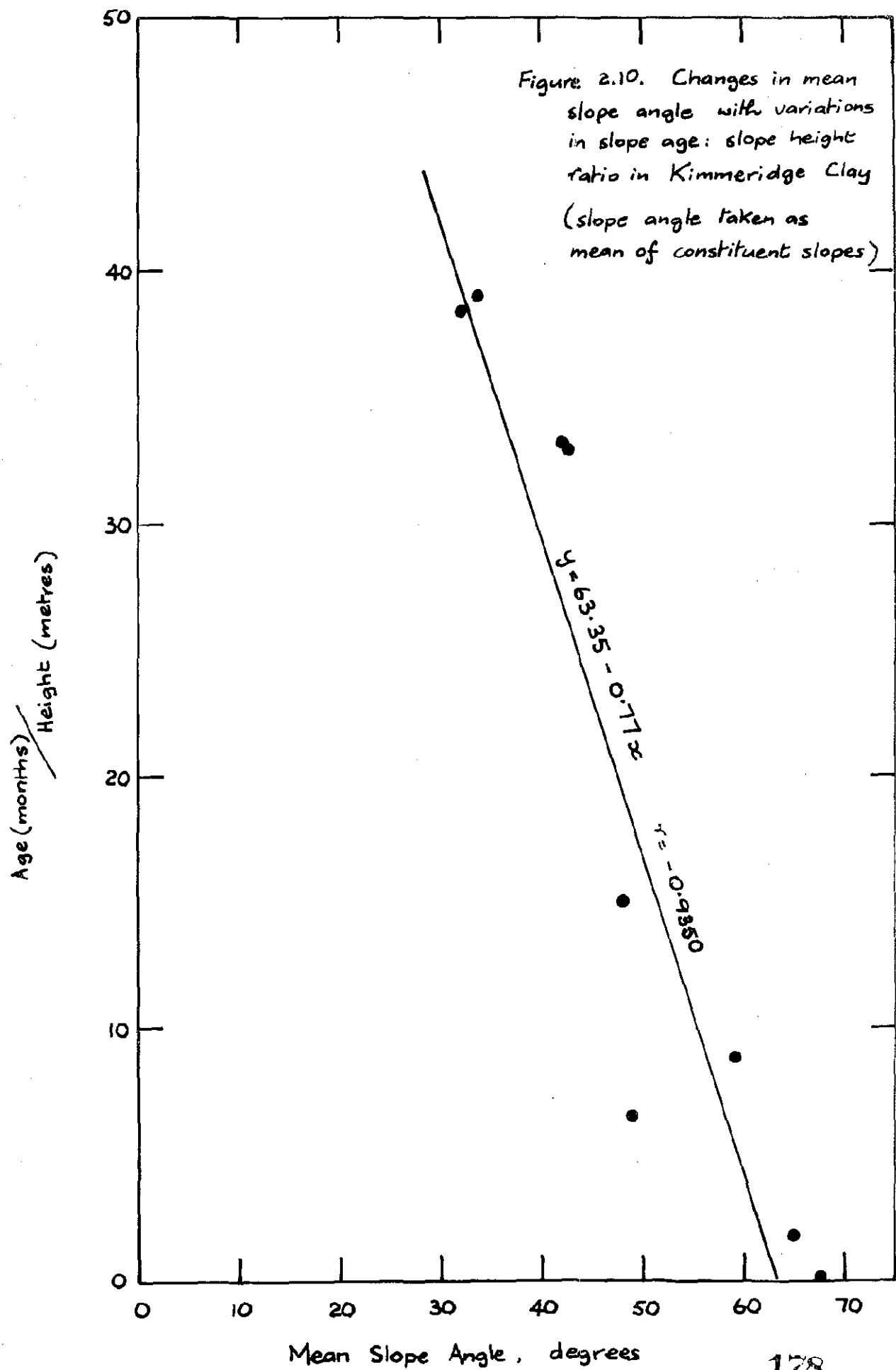


Figure 2.9. Fox Holes slopes in Kimmeridge Clay





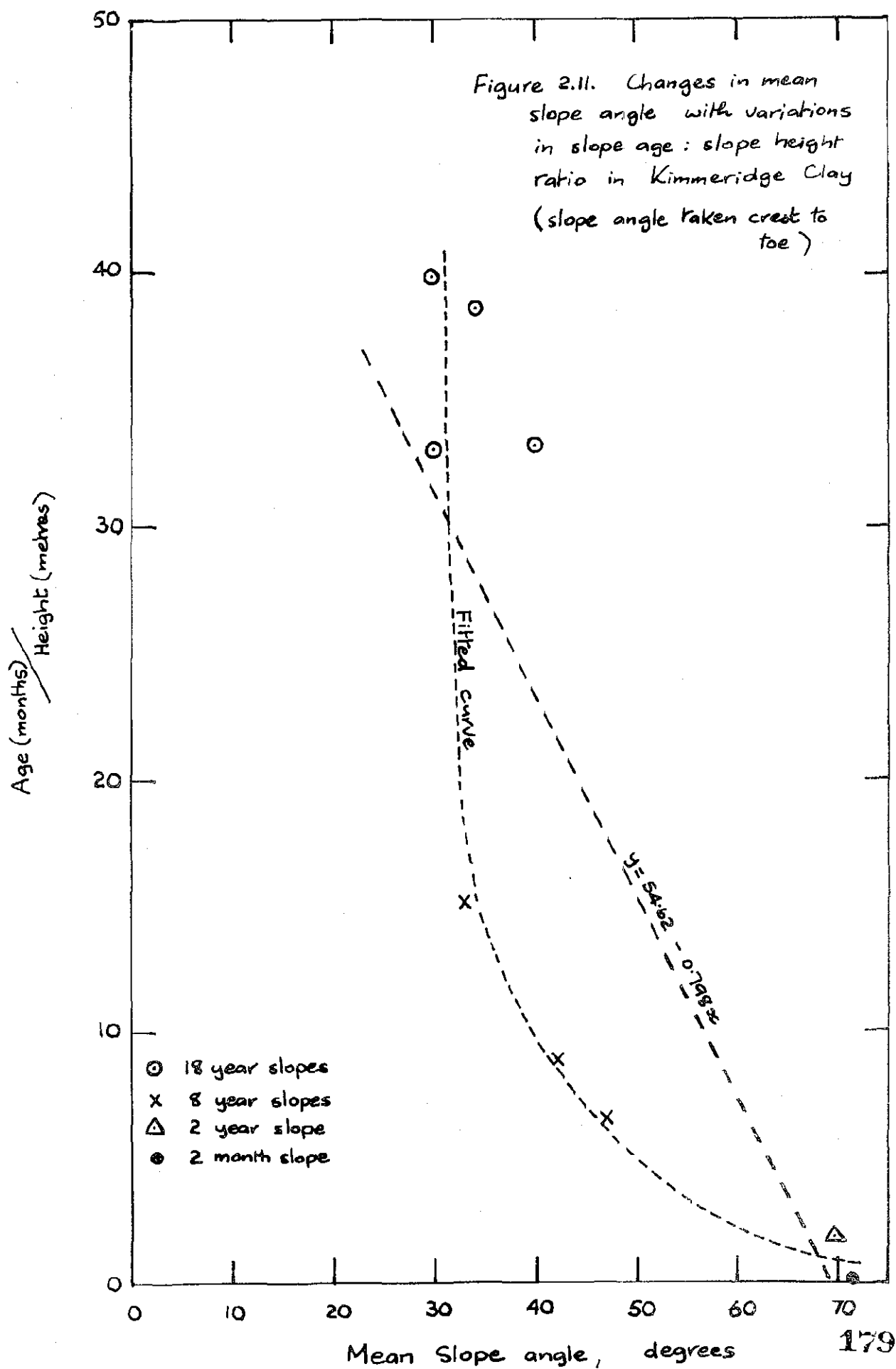


Figure 2.12. Slope height - angle relationships in the Kimmeridge Clay, Yorkshire, England.

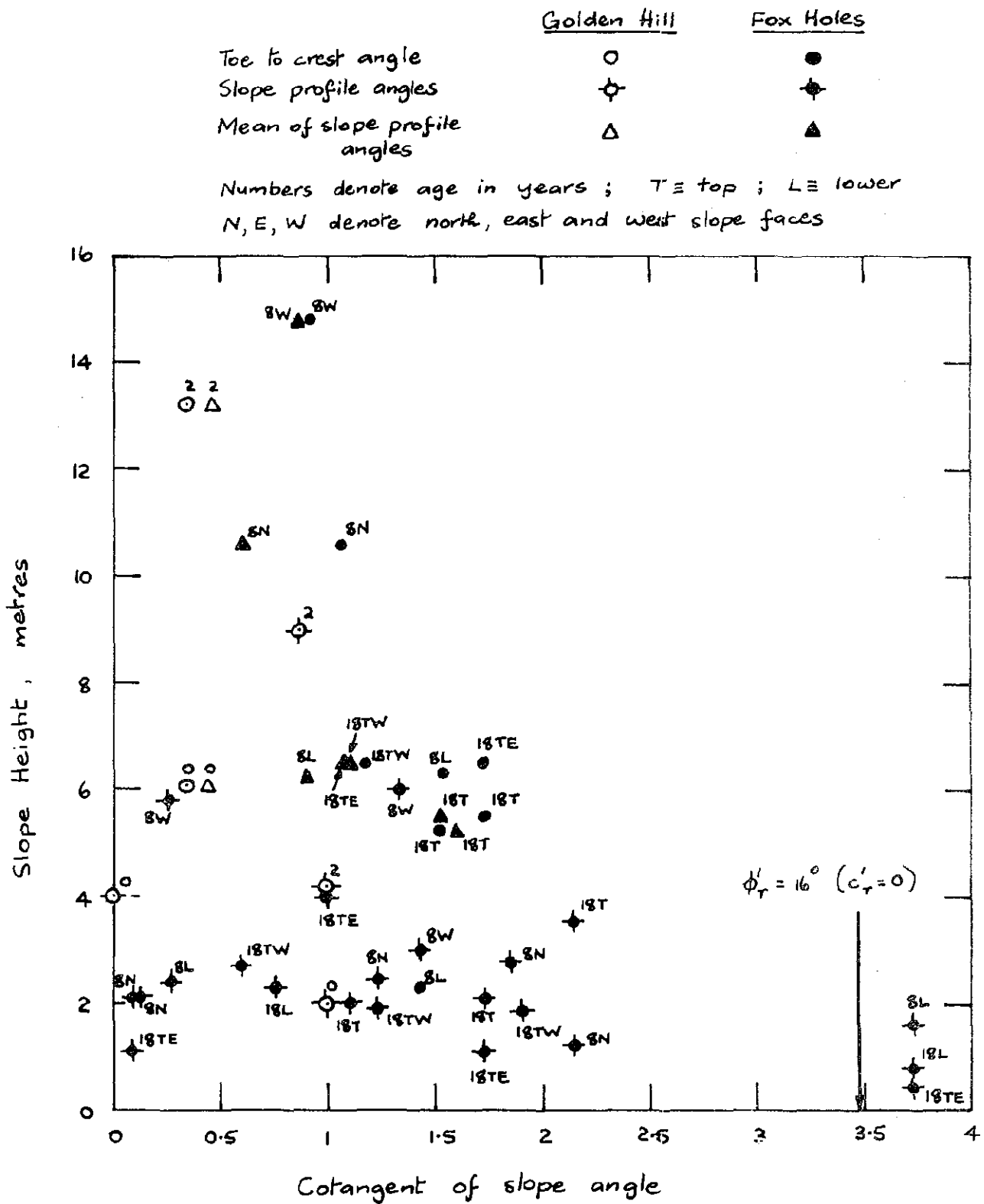


Figure 2.13 8 years slope, Fox Holes: slip-circle analysis.

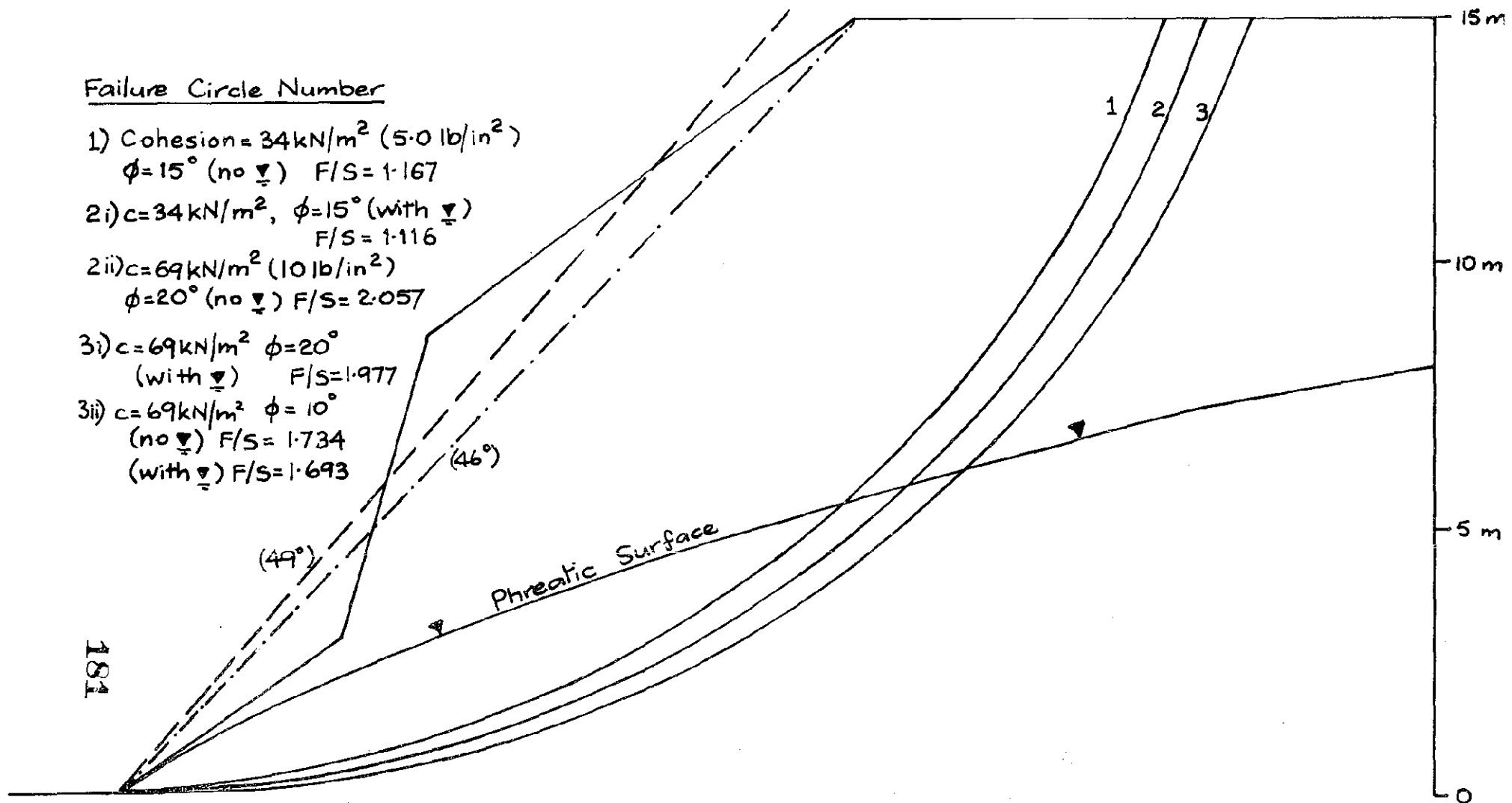


Figure 2.14.  $\frac{c'}{F}$  vs  $\frac{\phi'}{F}$  for 8 years slope  
at Fox Holes

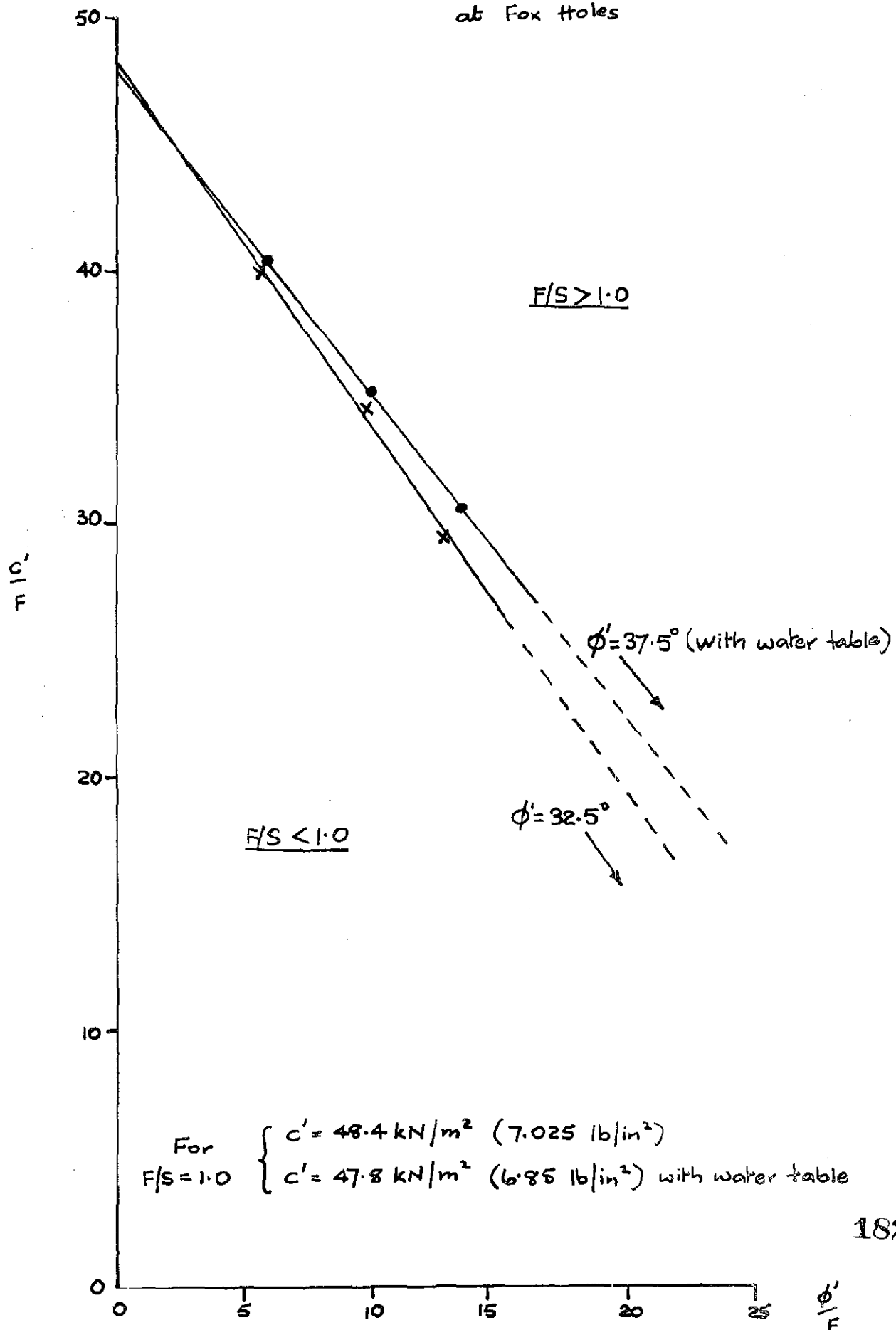


Figure 2-15 Analysis of Yorkshire Kimmeridge Clay stability using a plane strain condition such that  $\sigma_2 = 0.5(\sigma_1 + \sigma_3)$ ,  
15 metre slope, Anisotropic Shear Strain Energy Parameter

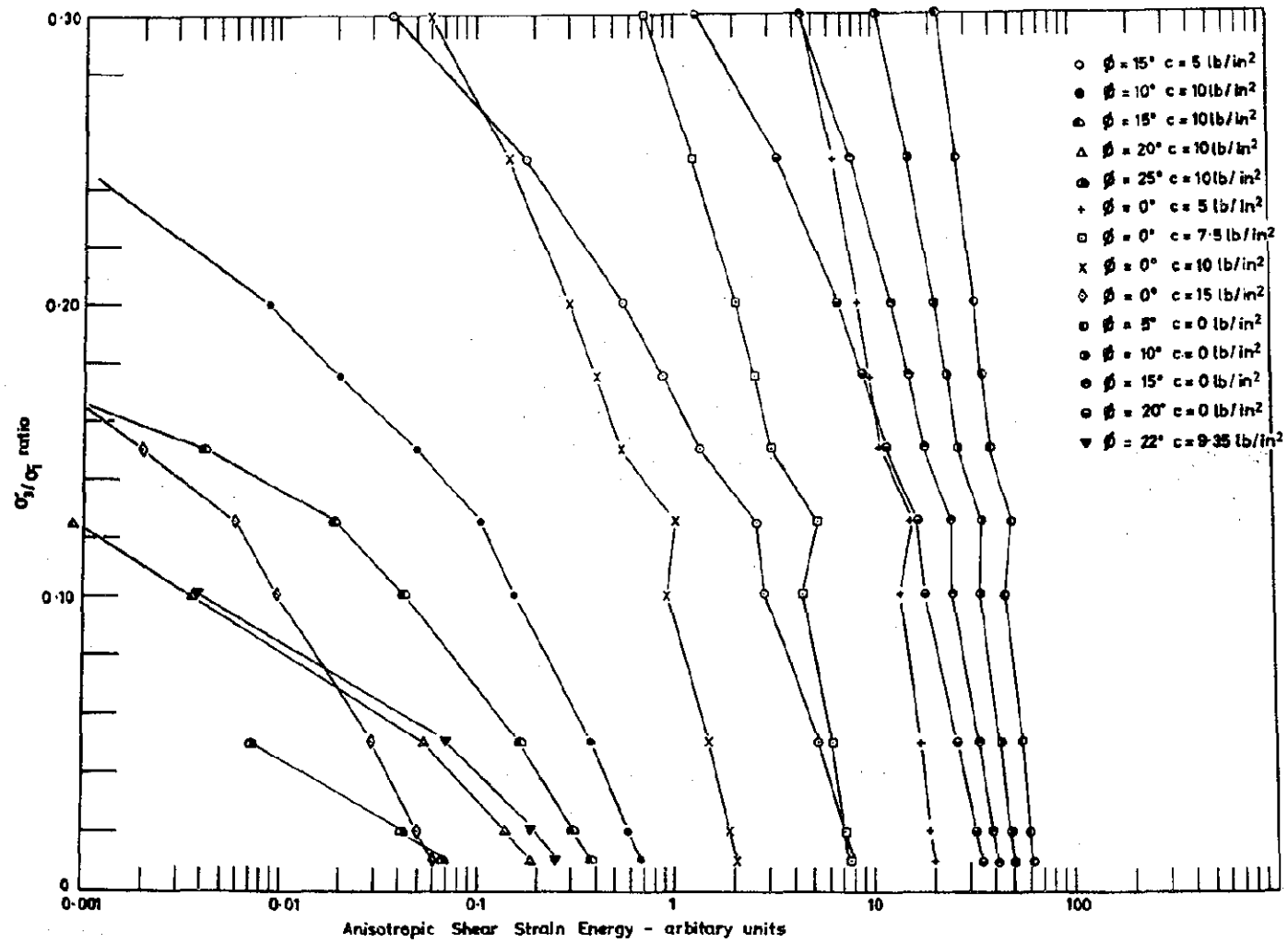




Figure 2-16 Analysis of Yorkshire Kimmeridge Clay stability using a plane strain condition such that  $\sigma_2 = 0.5(\sigma_1 + \sigma_3)$ ; 15 metre slope; Isotropic Shear Strain Energy Parameter

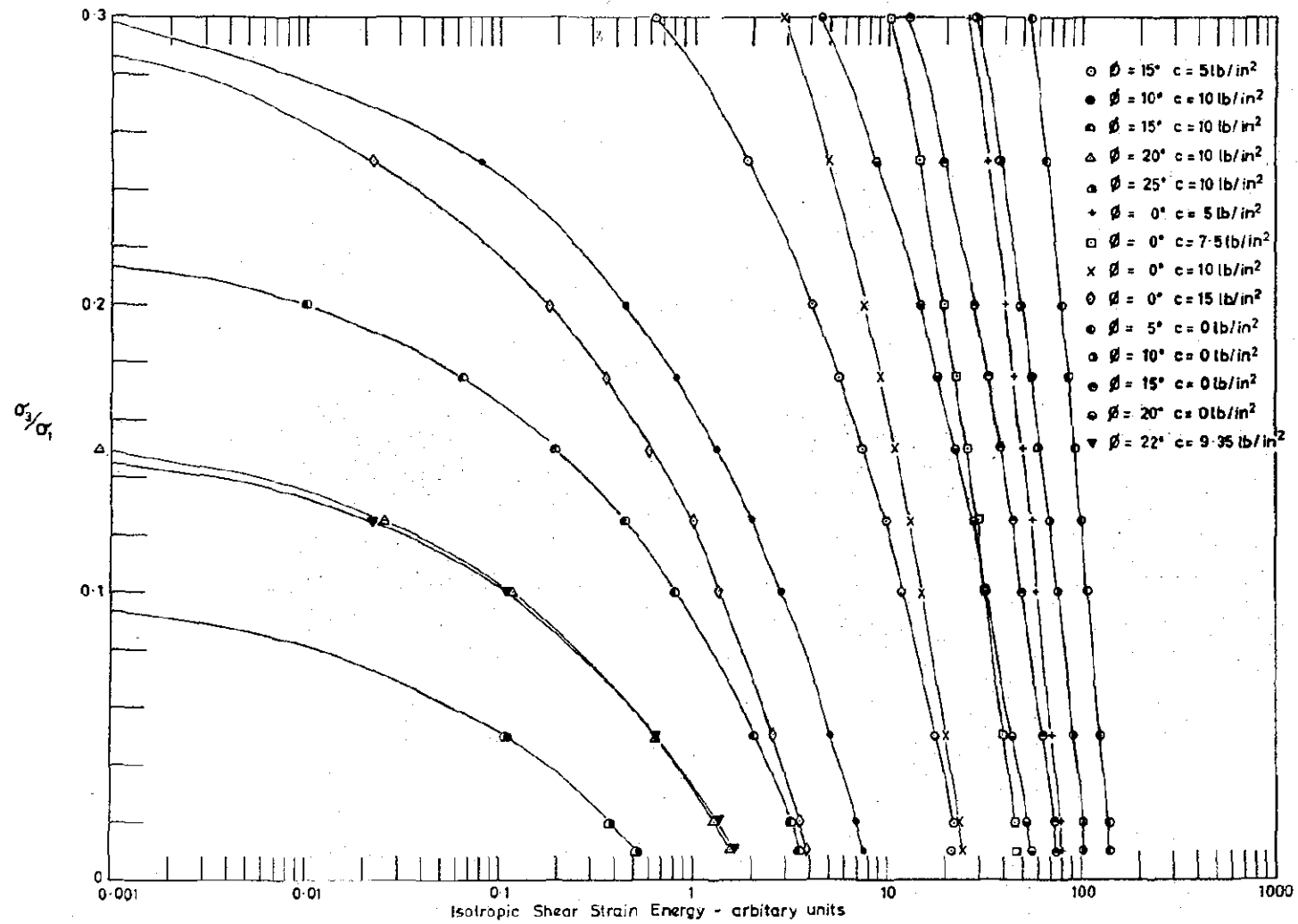


Figure 2-17 Kimmeridge Clay - Fox Holes, Yorkshire, England.  
Influence of magnitude of principal stress ratio upon the  
anisotropic shear strain energy index for a 15m high slope  
and for various  $c, \phi$  combinations across the discontinuities  
(computed for plane strain conditions throughout)

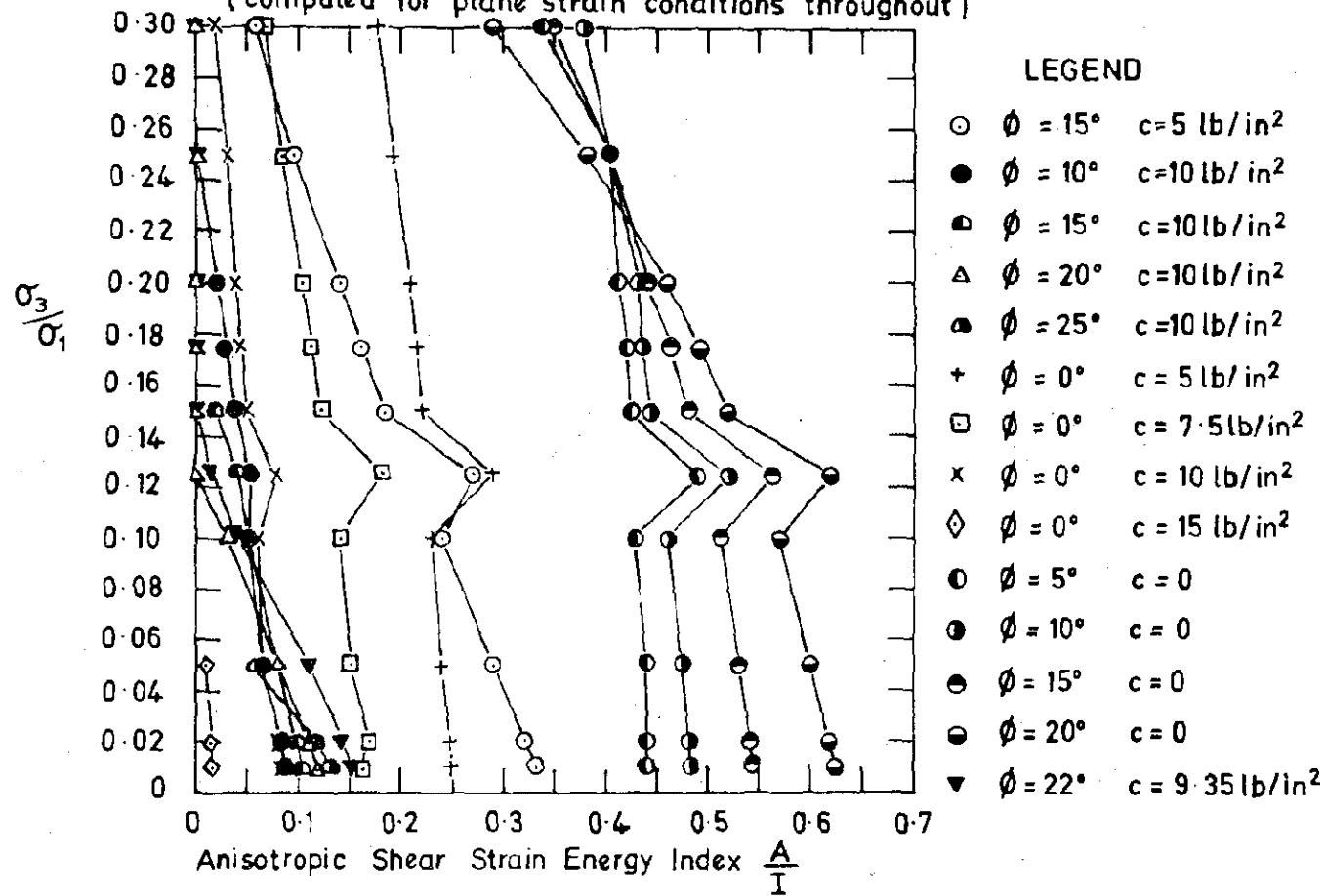


Figure 3.1.

# OXIDE / ALUMINA RATIOS

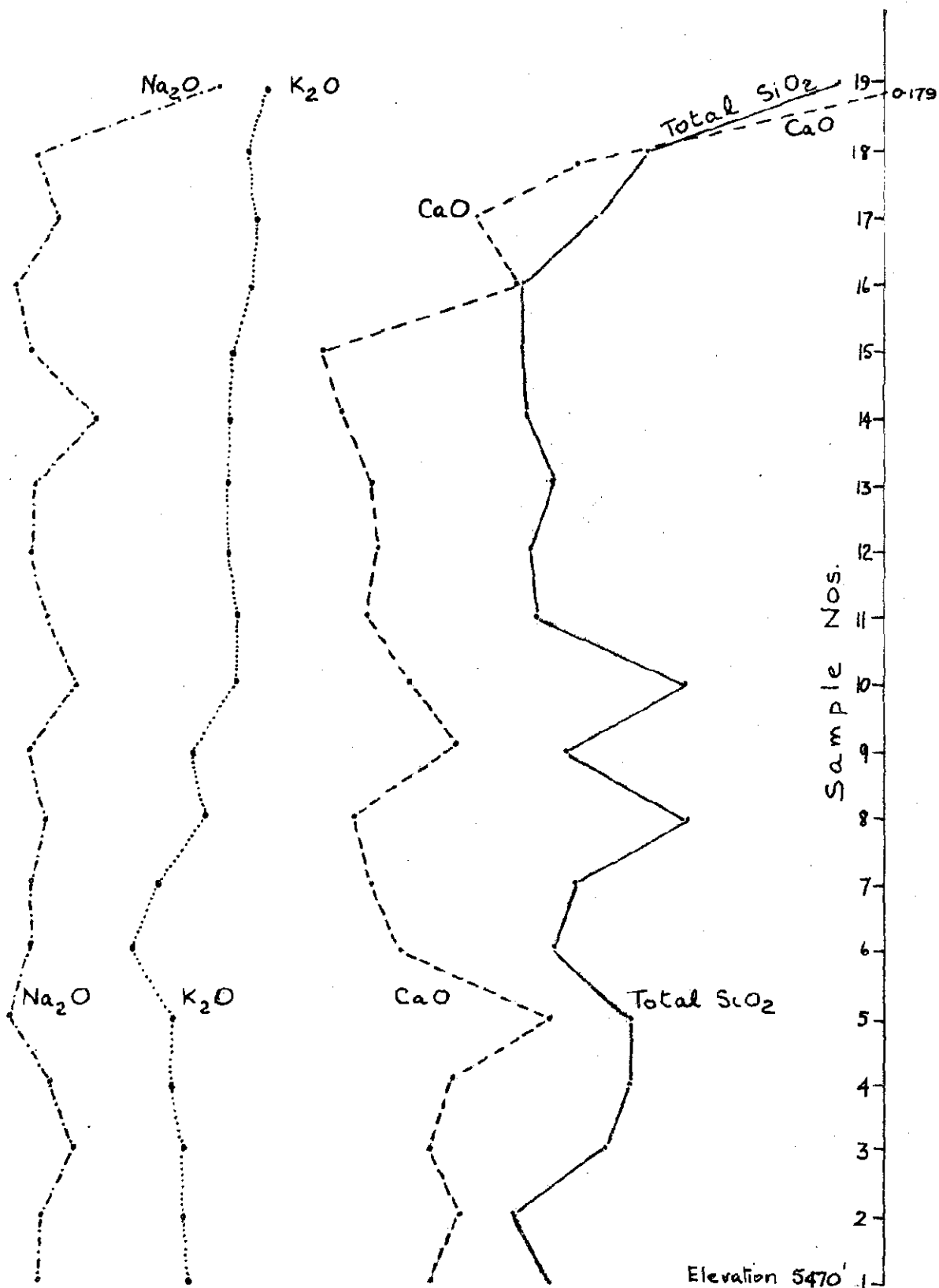
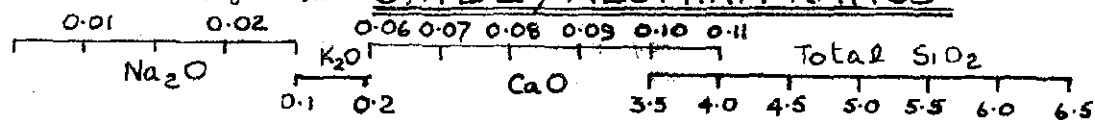


Figure 2.2. Print out of  $\tau/\sigma_n$  versus displacement for Dawson sample

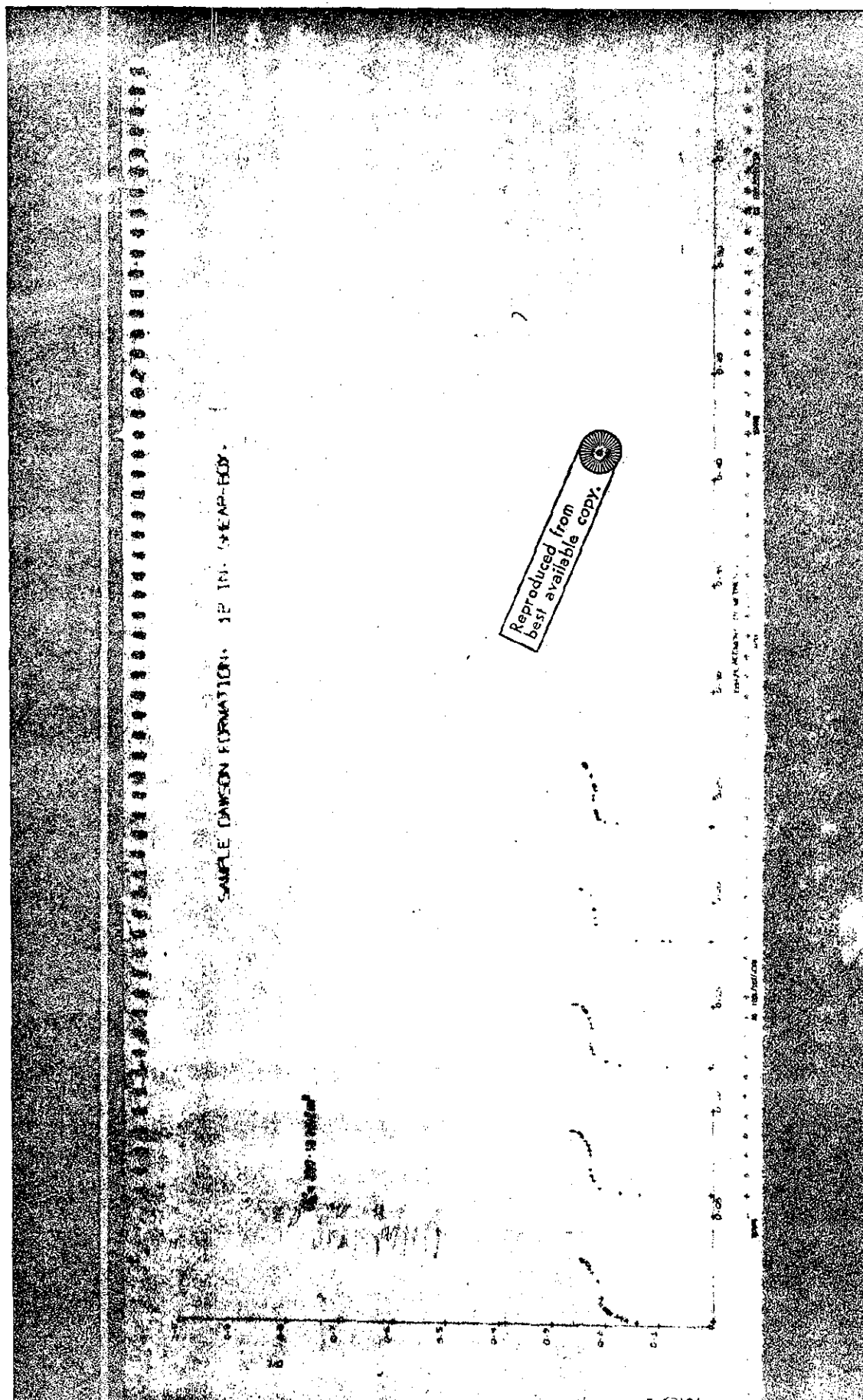


Figure 3.3.

SAMPLE 1T0 3, LITTLETON COLLIERY, STAFFS. 12 IN. SHEAR BOX.

$$\Delta \sigma_n = 211.5 \text{ kN/m}^2$$

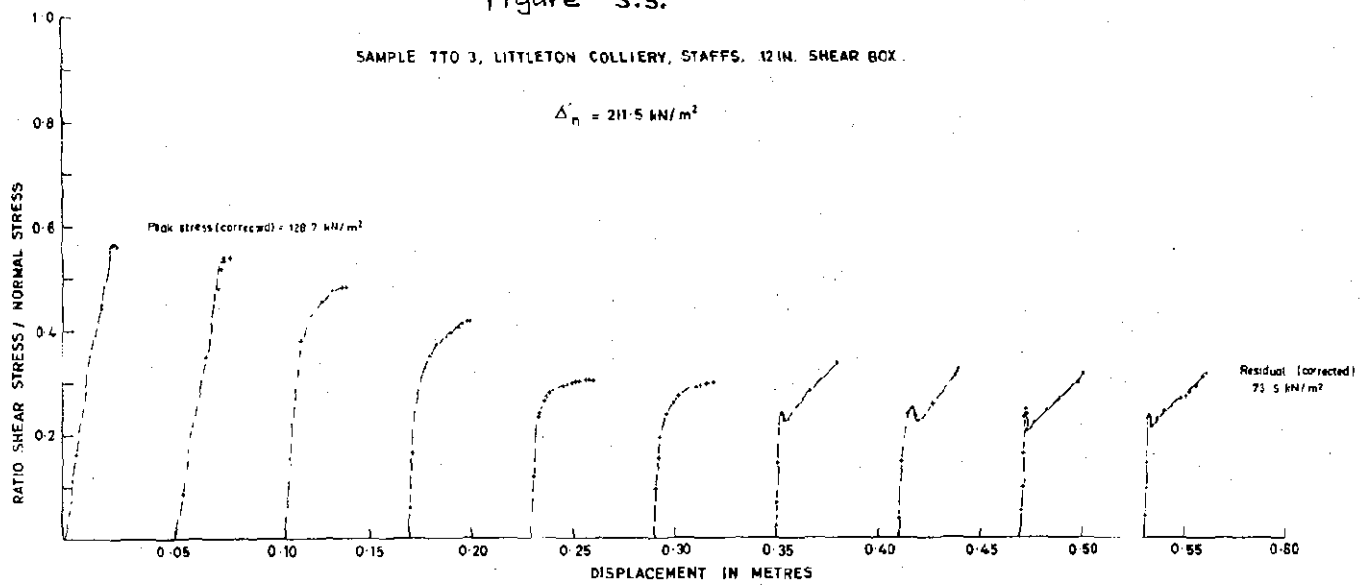


FIGURE 3.4.

12 in SHEAR-BOX TEST (PRE-LOADING)  
CHATFIELD SOFT SEAM

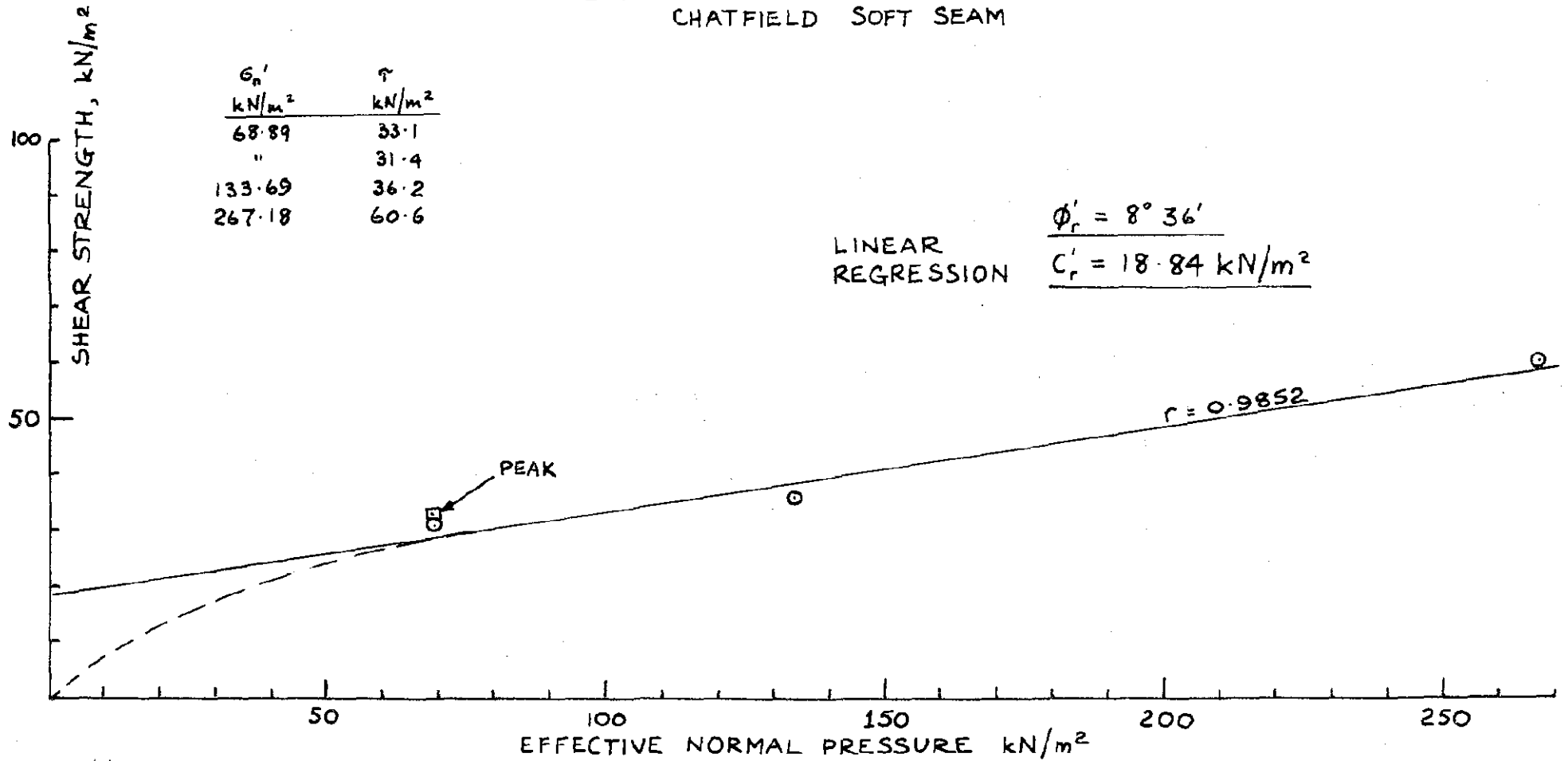


FIGURE 3.5

# 60 mm SHEAR-BOX RESULTS SILTY CLAY-SHALE CHATFIELD WEIR

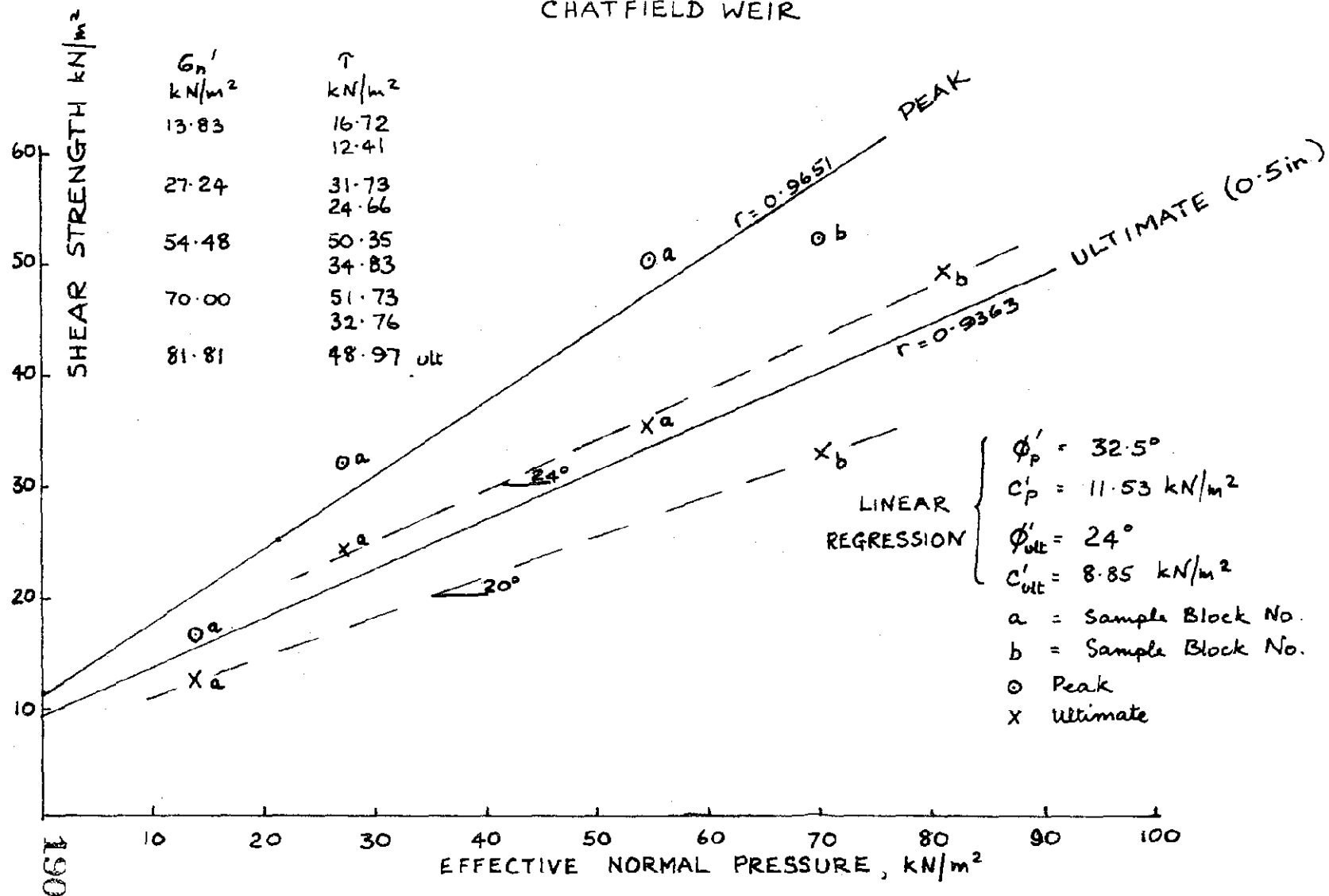


FIGURE 3.6.

DAWSON RESIDUALS, PROXIMATE  
MINERALOGY & LIMITS FROM DM No. PC-24  
VOL 2, 1968, PLATE 189, PLUS CLAY SEAM DATA.

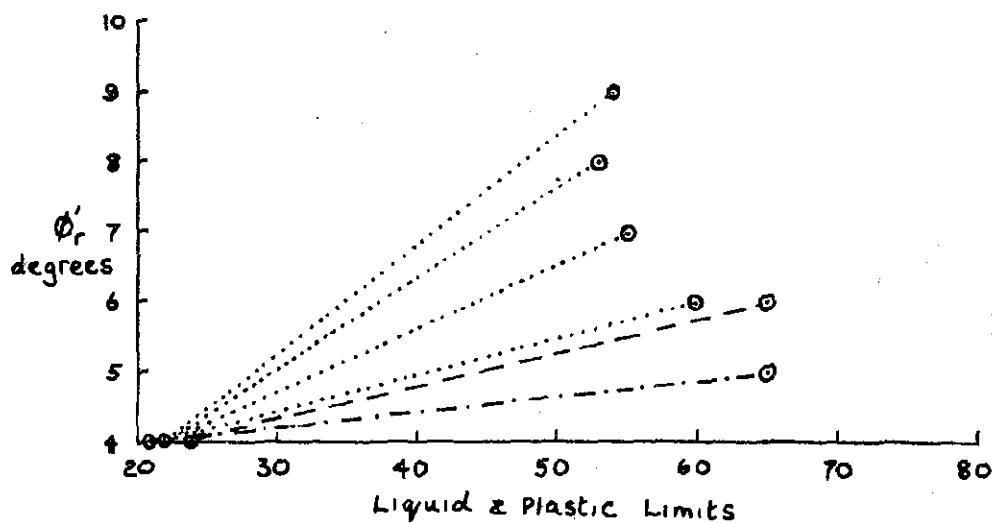
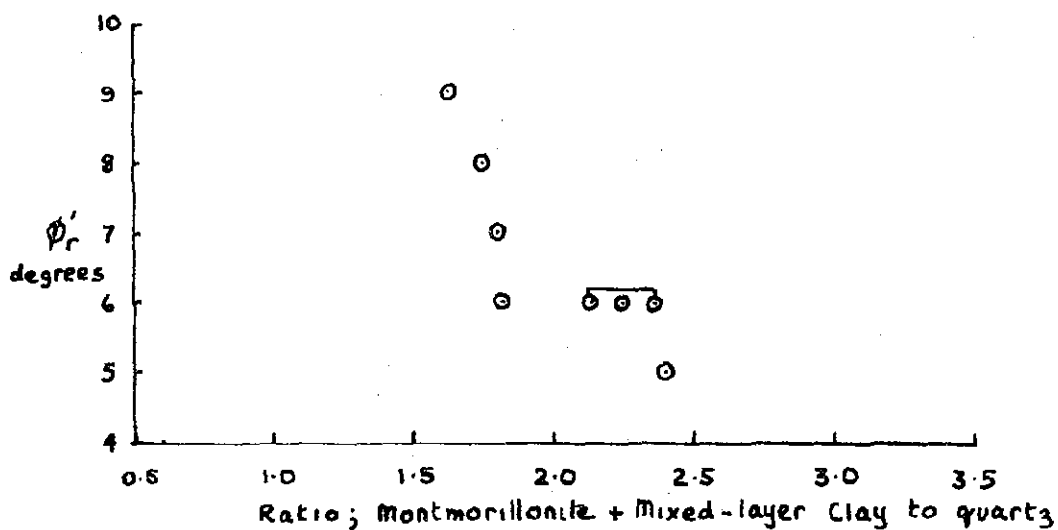
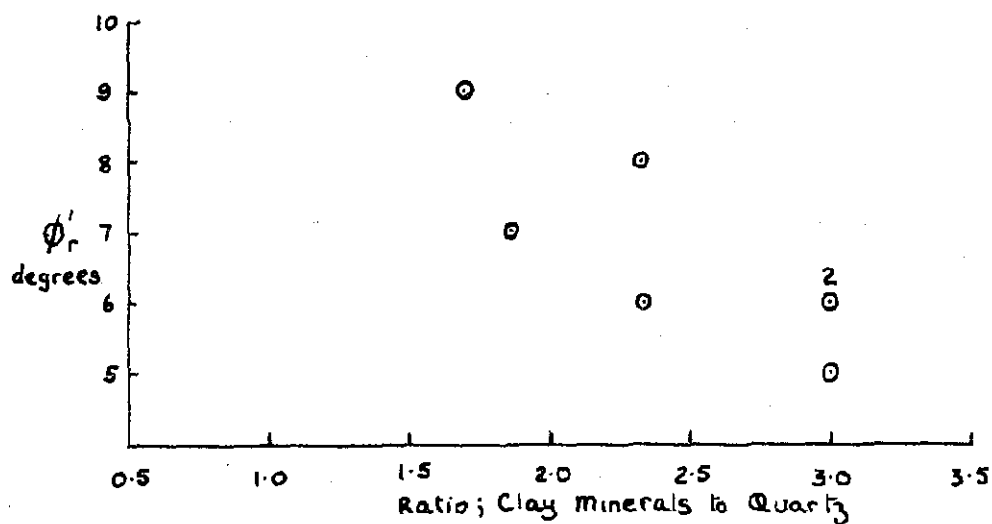
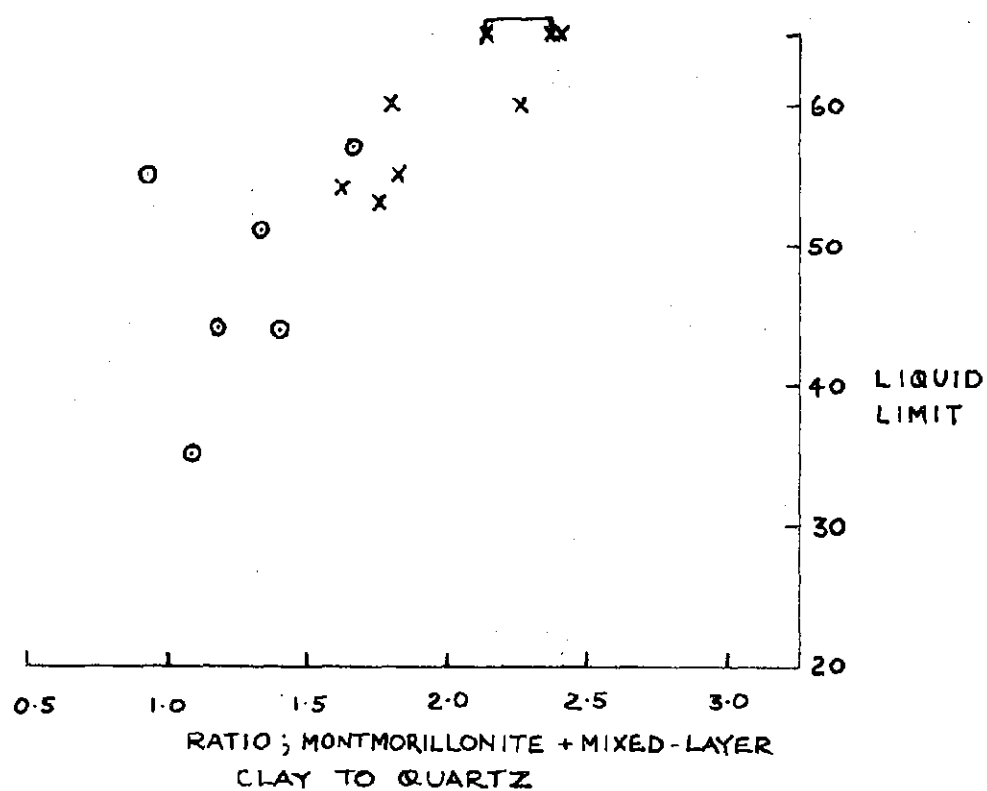
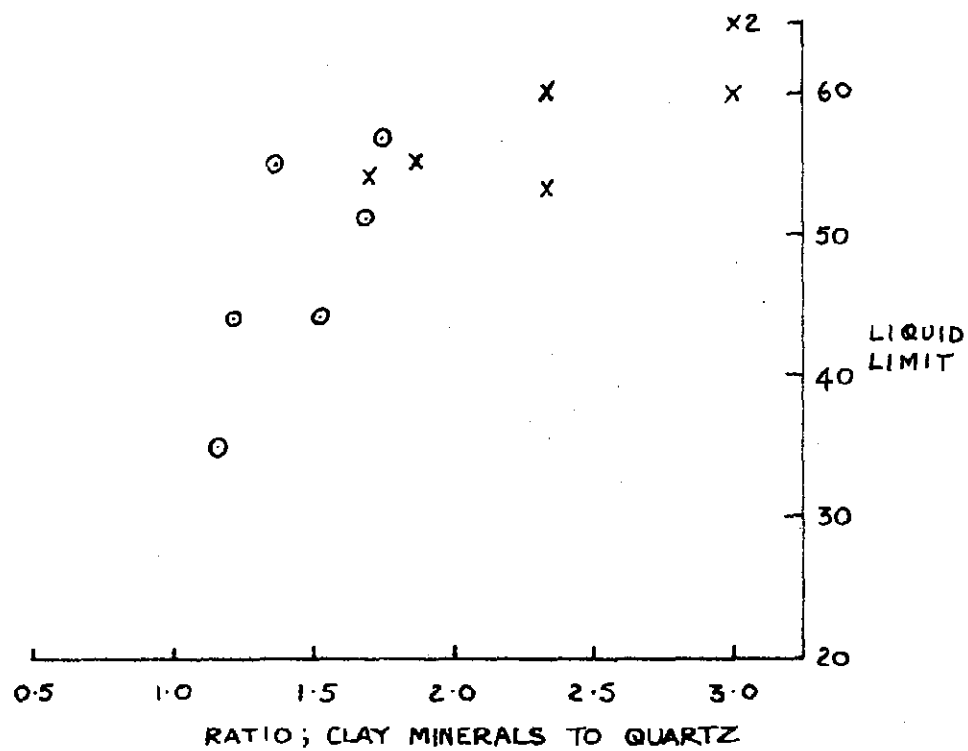




FIGURE 3.7.

RELATIONSHIP BETWEEN  
LIQUID LIMIT & MINERALOGY



X FROM D.M. NOPC-24, VOL 2, 1968, PLATE 189  
O TESTS AND ANALYSES CARRIED OUT IN DURHAM

CHATELAIN CAM CONTINUED SECTION SUTTERSTOCKS KEN ADRIAN  
 HEMISPHERE UPPER PROJECTION 16,000M CIRCLE  
 N: 4 U: 25,000  
 1.00 PER CENT AREA WINDOW USED

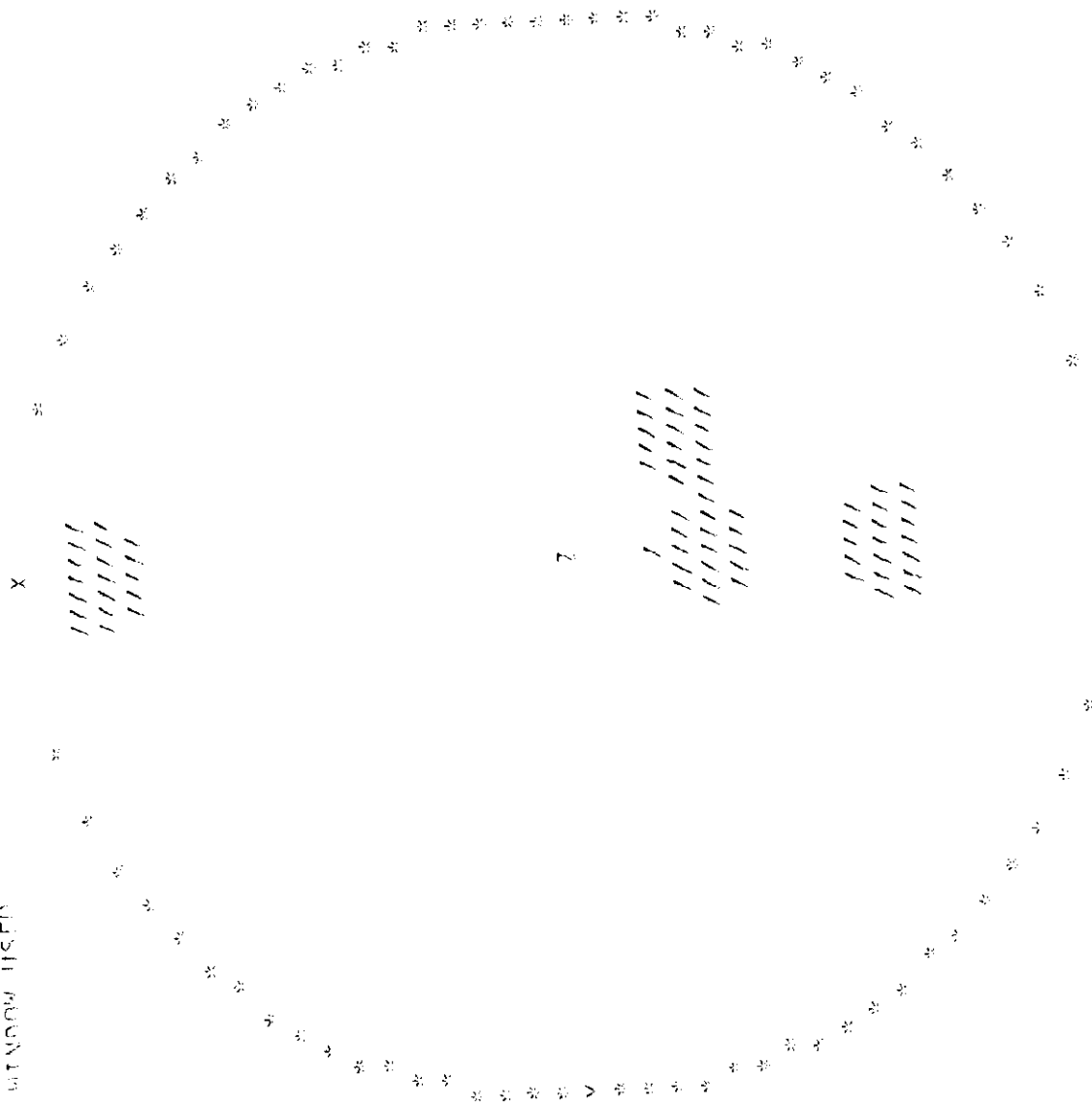


Figure 3.8.

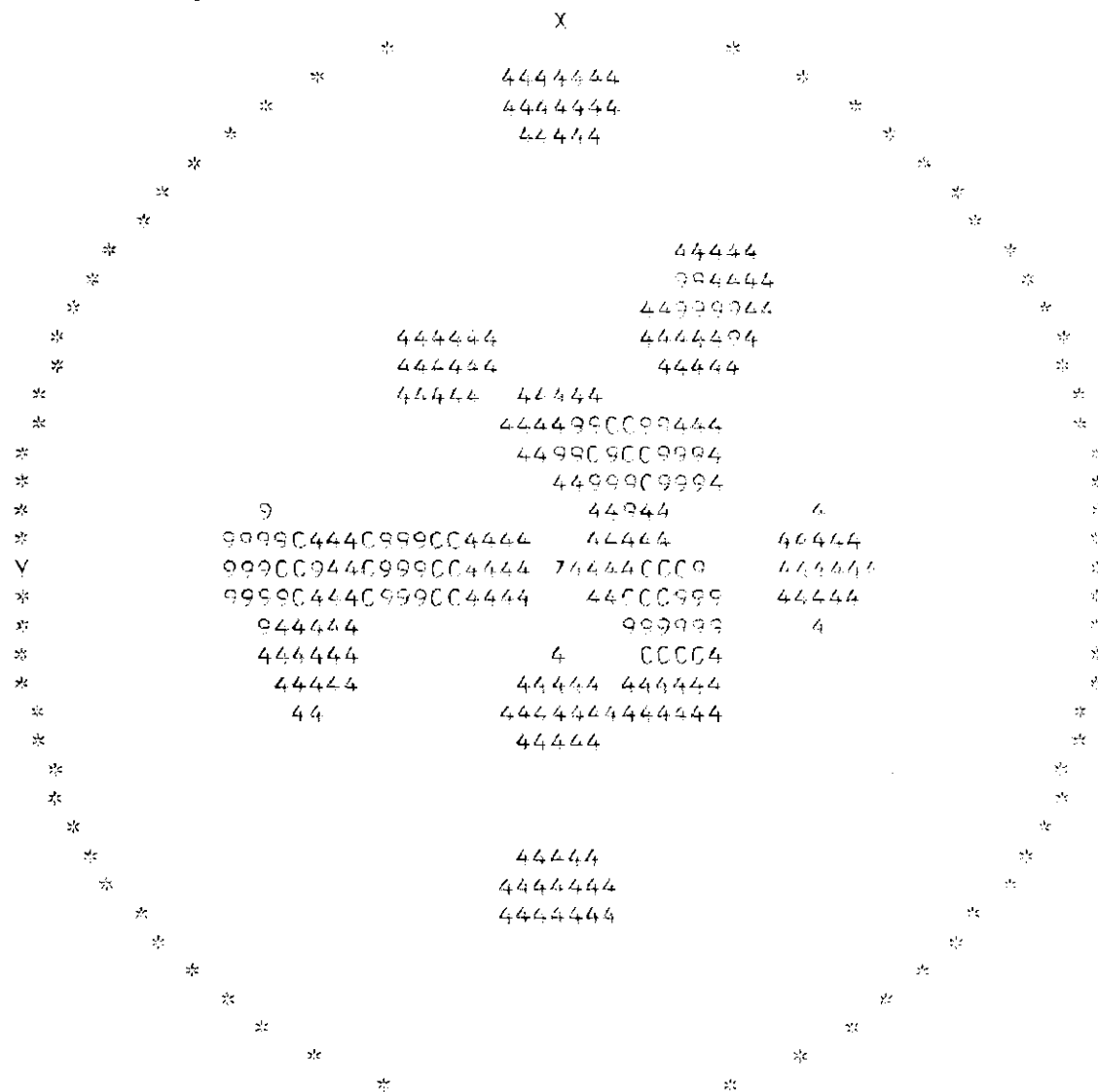
Reproduced from  
 best available copy.



[illegible][illegible]

CHATEFIELD DAM SPILLWAY AND WEIR SECTION SLICKENSIDES KEN ADRIAN  
 HEMISPHERE UPPER PROJECTION 16.00CM CIRCLE  
 N: 22 W: 4.545  
 1.00 PER CENT AREA WINDOW USED

Figure 3.11.



CHARACTER NAME: SOLI MAY 26/87  
 HEMISPHERE: UPPER DISSECTION 15,000 CYCLES  
 V: 42 W: 1,507  
 1.00 PER CENT AREA WINDOW HOOK

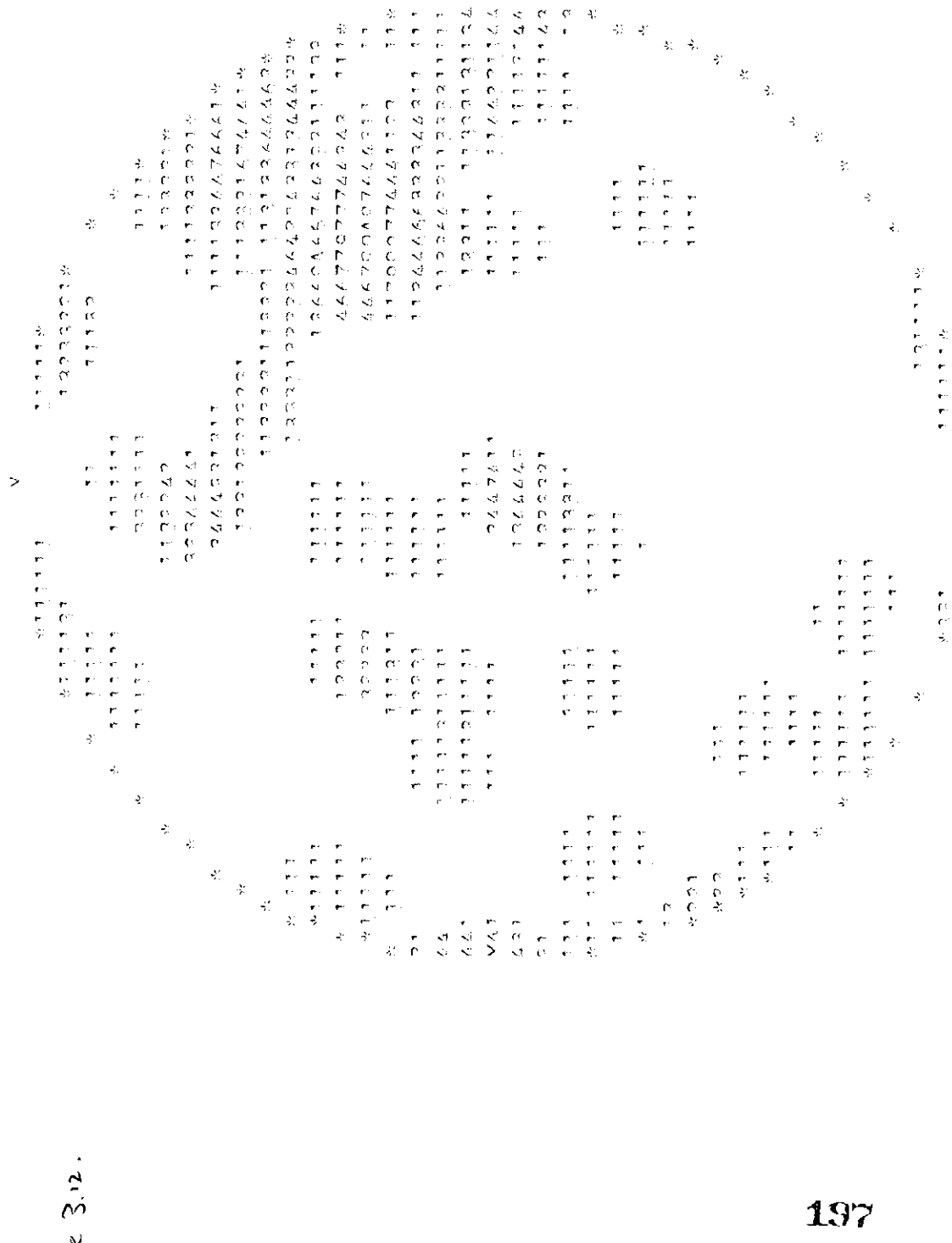



Figure 3.15.

[illegible]

[illegible]

Figure 3.16.



Reproduced from  
best available copy.

1



IN: 00000000  
TO: 00000000  
FROM: 00000000

RECEIVED 00000000  
TOTAL DISCOUNTS AND CENTS  
ON TOTAL DEDUCTIONS

DATE: 00/00/00

Figure 3.17.



Reproduced from  
best available copy.





CHART 1.000 TOTAL DISCONTINUITIES SURFACES ARE JOINTS FA/FT  
 HORIZONAL: 1.000 SURF CHINA 1.000 CIRC  
 N: 100 1.000  
 1.000 PER CIRC 1.000 SURF USED



Figure 320.

2. THE FOLLOWING INFORMATION IS FOR THE USE OF THE  
 OFFICE OF THE ATTORNEY GENERAL, AND IS NOT  
 TO BE RELEASED TO THE PUBLIC.

Figure 3.24

JOINTS IN DARK RED SANDSTONE NORTH BANK SAVAGE RIVER MARYLAND USA  
HEMISPHERE UPPER PROJECTION 16.00CM CIRCLE  
N: 25 W: 4.000  
1.00 PER CENT AREA WINDOW USED

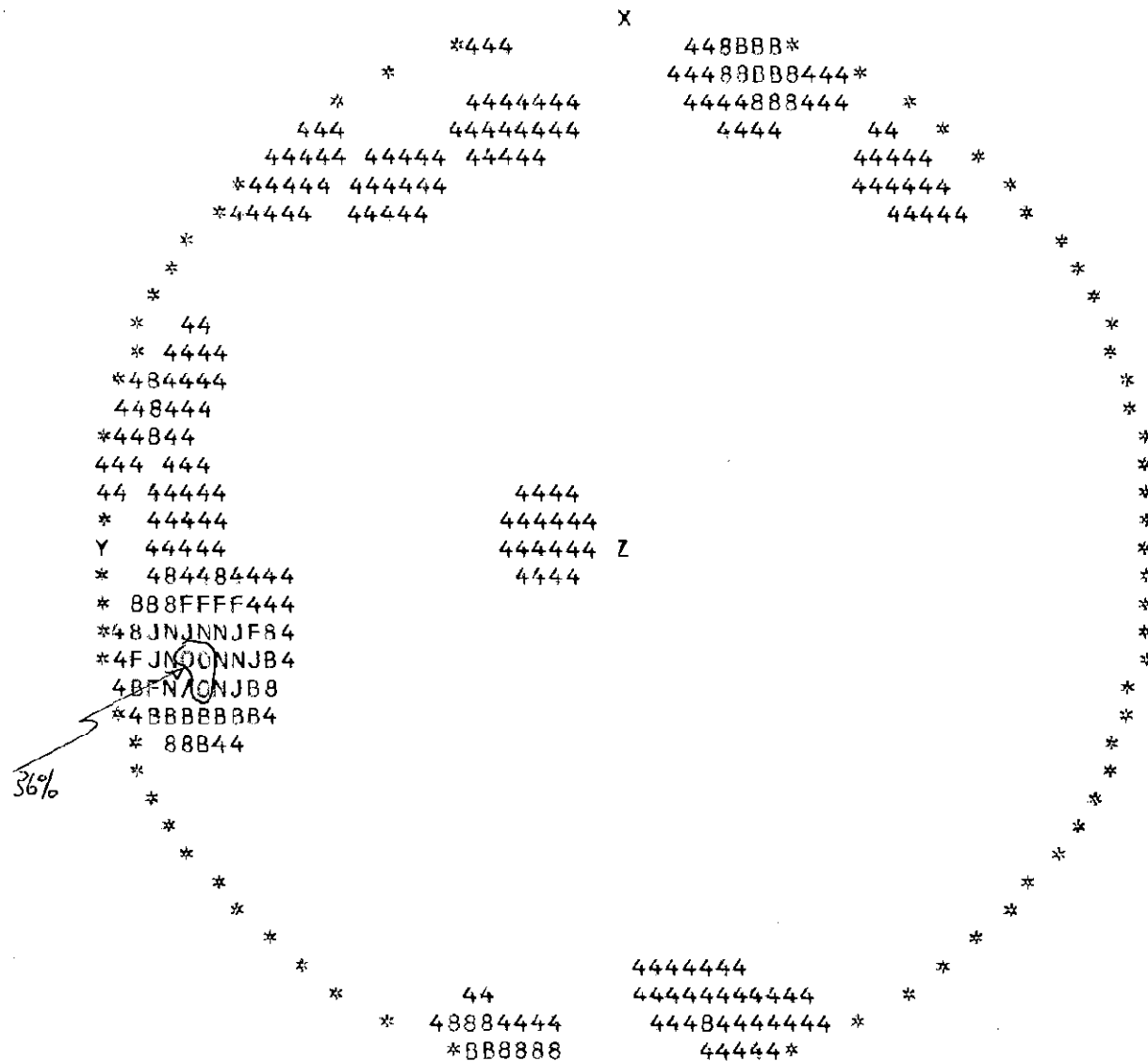


Figure 4.1.

PARTINGS IN SILTSTONE AND SHALE SOUTH BANK SAVAGE RIVER MARYLAND USA  
 HEMISPHERE UPPER PROJECTION 16.00CM CIRCLE  
 N: 4 W: 25.000  
 1.00 PER CENT AREA WINDOW USED

209

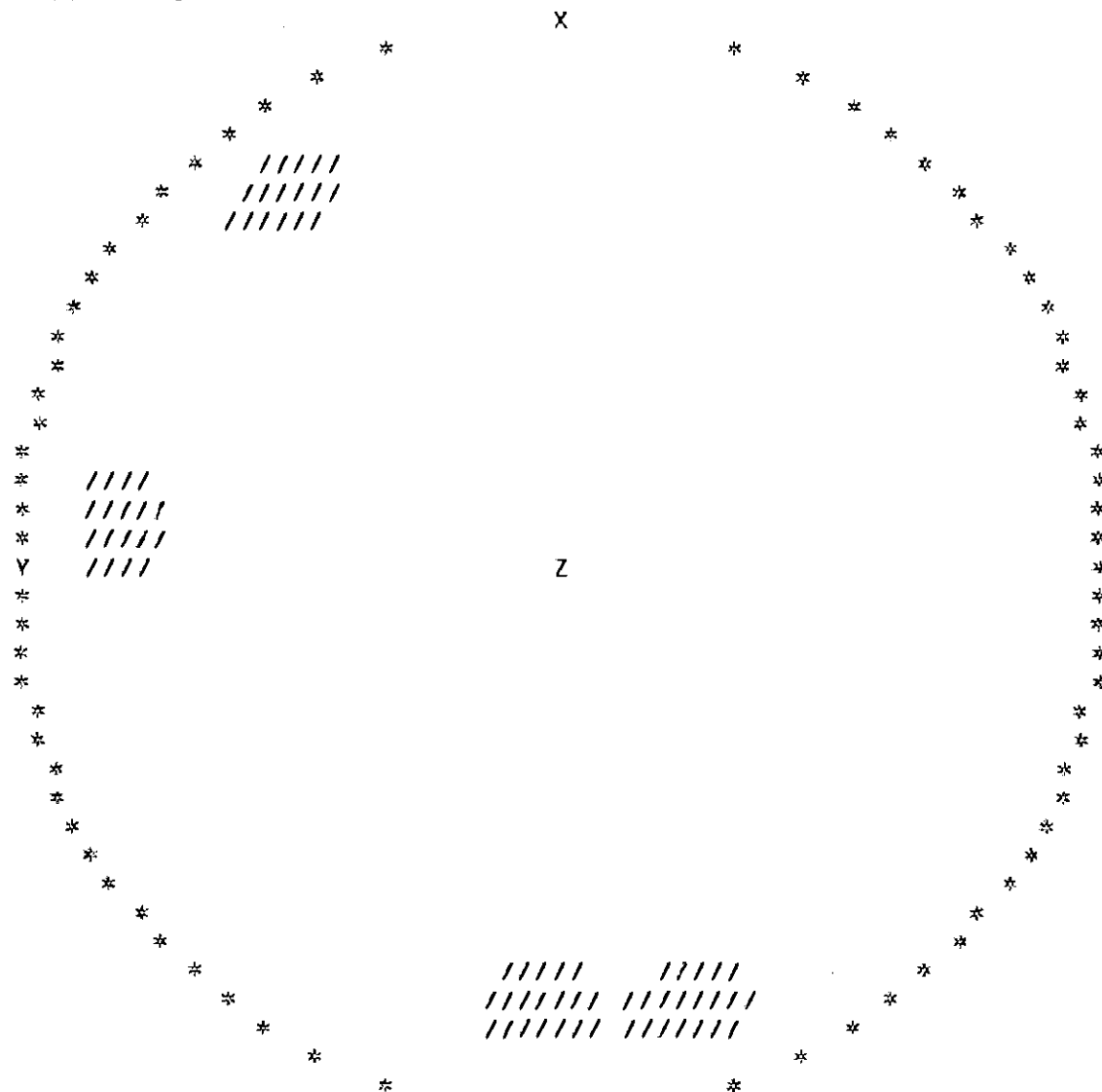
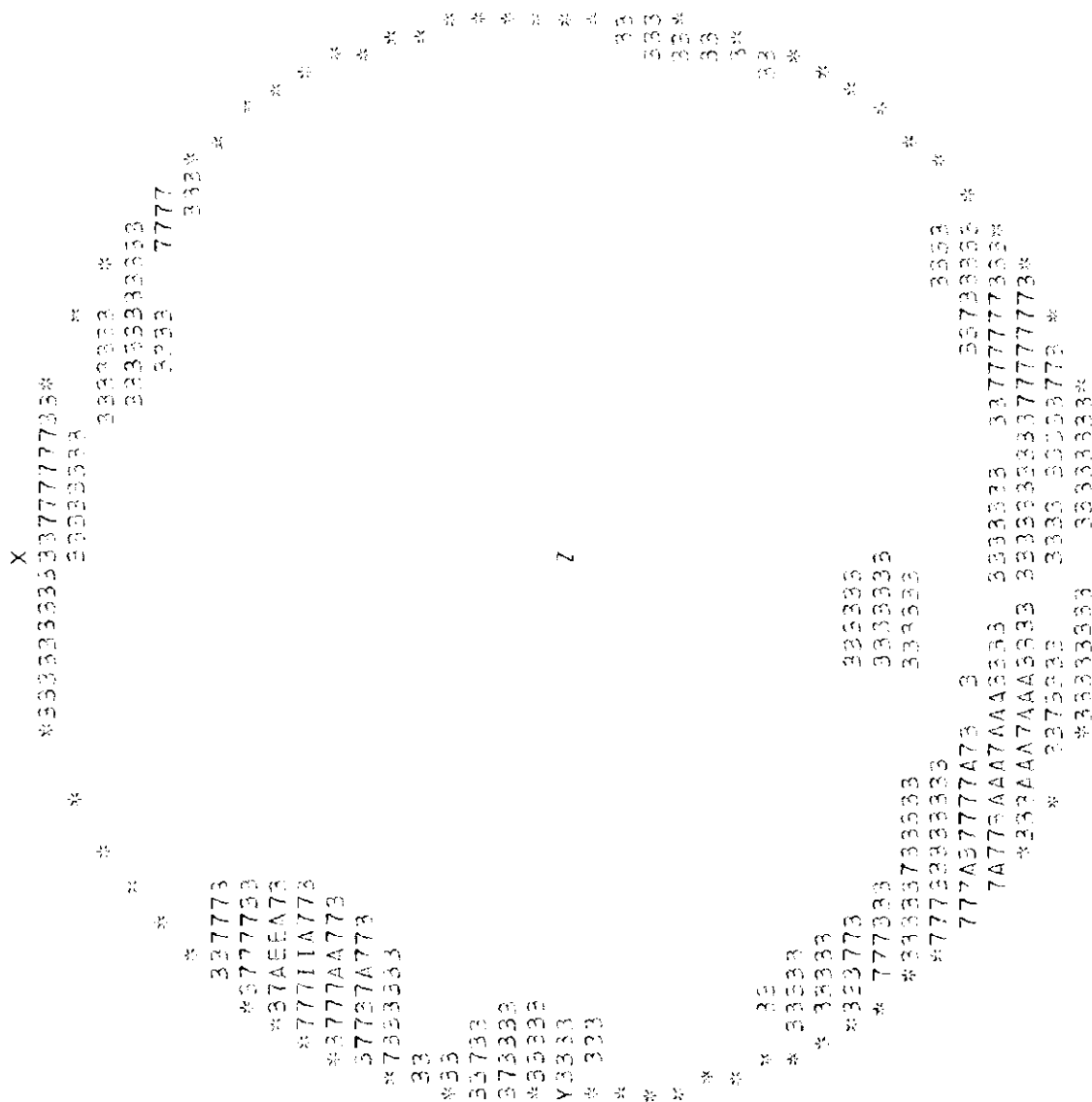


Figure 4.2.

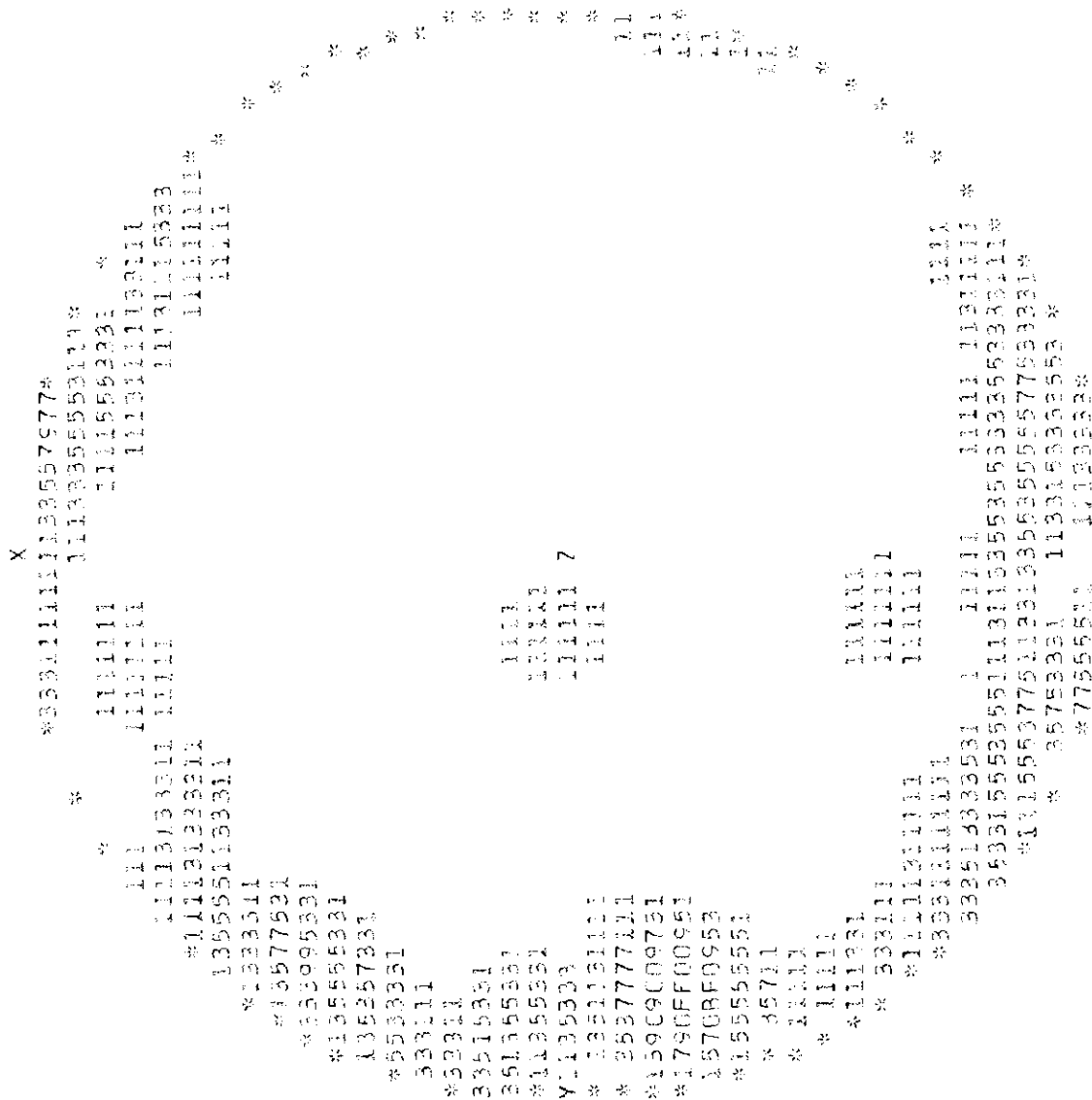




JOINTS IN BROWN FLAGGY SANDSTONE ROADSIDE WEST OF BLOOMINGTON KEYLAND  
 HEMISPHERE UPPER PROJECTION 3.6. 2004 CIRCLE  
 N: 26 W: 3.846  
 1.00 PER CENT AREA WINDOW USED



TOTAL JOINTS SAVAGE RIVER AND SANDSTONE AT SIDE ROUTE 235 MARYLAND  
 HEMISPHERE UPPER PROJECTION 16. JOCH CIRCLE  
 N: 55 W: 16816  
 1.00 PER CENT AREA WINDOW USED



JOINTS IN CLAYSTONE BETWEEN LR MAHONING AND BUFFALO SANDSTONES  
 HEMISPHERE UPPER PROJECTION 16.02CM CIRCLE  
 N: 31 W: 3,226  
 1.00 PER CENT AREA WINDOW USED

213

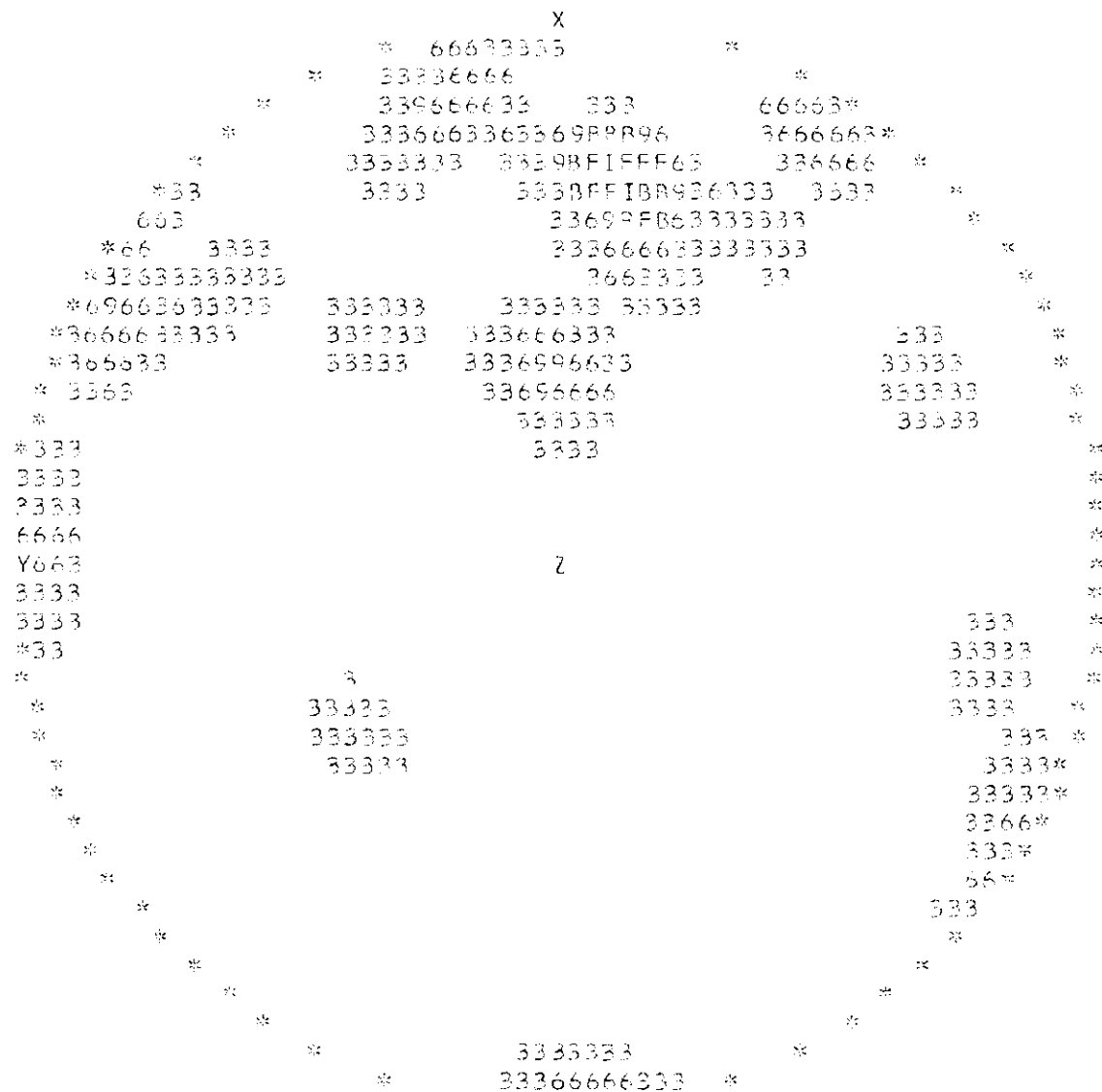


Figure 4.6

JOINTS IN LOWER MAHONING SANDSTONE BLOOMINGTON DANDITE MARYLAND USA  
 HEMISPHERE UPPER PROJECTION 16.90 CM CIRCLE  
 N: 30 W: 30.333  
 1.00 PER CENT AREA WINDOW USED

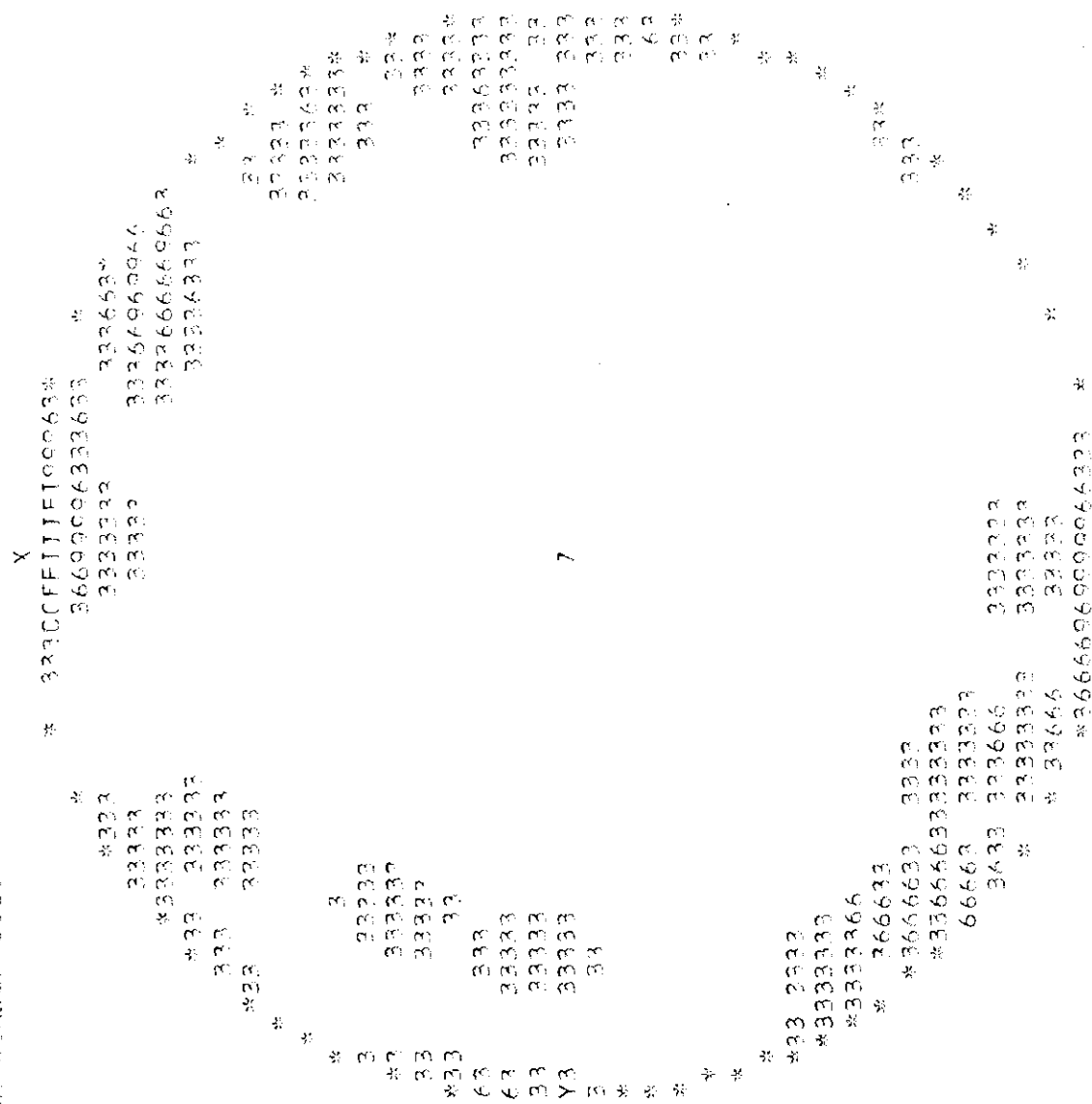
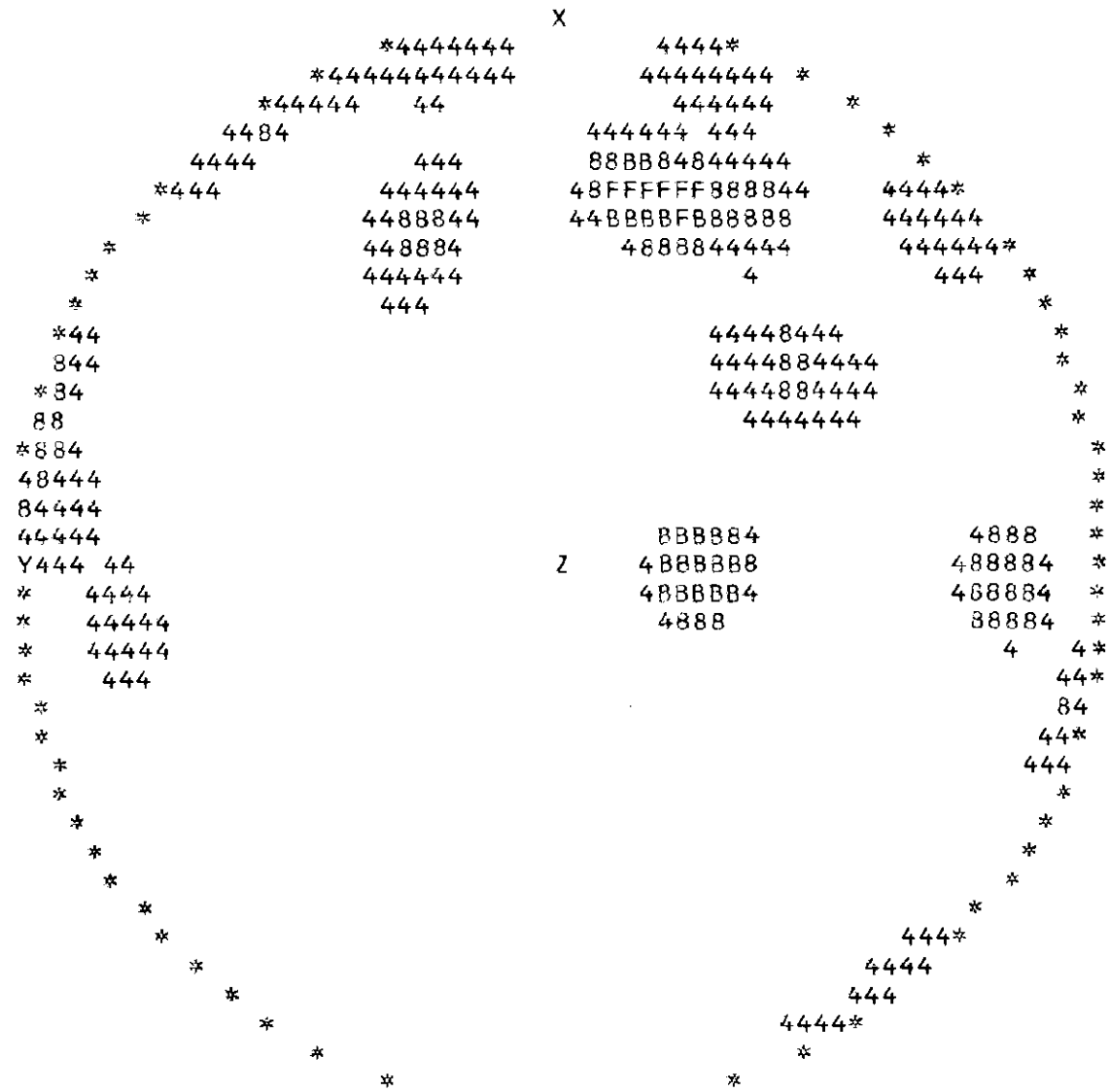


Figure 4.7.

JOINTS BELOW MAHONING SANDSTONE IN FLAGGY SILTSTONE CLAYSTONE  
 HEMISPHERE UPPER PROJECTION 16.00CM CIRCLE  
 N: 24 W: 4.167  
 1.00 PER CENT AREA WINDOW USED



215

Figure 4.8





BLOOMINGTON RESERVOIR POTOMAC RIVER U.S. CORPS OF ENGINEERS DATA  
 HEMISPHERE UPPER PROJECTION 16.7" OM CIRCLE  
 N: 84 W: 1.191  
 1.00 PER CENT AREA WINDOW USED

218

```

                                X
                                * 1111111 111233333*
                                *3111 11111243333*
                                #11111 44444*
                                11 113321
                                11 11112
                                * 11 11111*
                                2211111 1433
                                *3211111 1244*
                                *1112111 1112133*
                                *1111 11112334*
                                *32111 11122122*
                                3321 11121222
                                *221 1111 1112*
                                4321 22211 1111
                                *321 1222211111*
                                11 112222 11122
                                1 111 1112
                                1 123211 11 121
                                Y1122221 111 11
                                11222221 21111 *
                                112122111 112221111
                                211 1111 112332221
                                *1111 11111 11232422*
                                *111111111 111 23457754
                                *21111 11 11121479982*
                                12211 1123477900983
                                *121 133478000873*
                                *33 1111 2388889743*
                                *222 111111 1347878742*
                                *543111221111 2245577722*
                                443211111 1122221 1123225757432
                                *34322121222212233332211 1111223455441*
                                33222223355552234553311 111123223321
                                222355900975455544332 133243222
                                *478899895774554442 12233221*
                                *80A8084422442111 13333*
                                *33433421122222111 *
  
```

Figure 4.11



Figure 4.12.

